

**THE EFFECTS OF HYDROGEN SULFIDE (H₂S) ON THE
RELEASE OF INFLAMMATORY MEDIATORS FROM
MOUSE MACROPHAGES**

HUANG WEIHAO CALEB

(B. Sc (Hons)), National University of Singapore

A THESIS SUBMITTED

FOR THE DEGREE OF DOCTOR OF PHILOSOPHY

NUS GRADUATE SCHOOL FOR INTEGRATIVE

SCIENCES AND ENGINEERING

NATIONAL UNIVERSITY OF SINGAPORE

2017

Supervisors

Professor Philip Keith Moore, Main Supervisor
Associate Professor Shabbir Moochhala, Co-Supervisor

Examiners

Associate Professor Deng Lih Wen
Associate Professor Bian Jinsong
Professor Christoph Thiemermann, Queen Mary University London

DECLARATION

I hereby declare that the thesis is my original work and it has been written by me in its entirety. I have duly acknowledged all the sources of information which have been used in the thesis.

This thesis has also not been submitted for any degree in any university previously.



Huang Weihao Caleb

12/9/2017

PUBLICATIONS

Peer-reviewed articles

1. **Huang CW**, Peh MT and Moore PK. H₂S inhibits NLRP3 inflammasome activation in mouse macrophages.
Manuscript in preparation
2. **Huang CW**, Feng W, Peh MT, Peh K, Dymock BW and Moore PK. A novel slow-releasing hydrogen sulfide donor, FW1256, exerts anti-inflammatory effects in mouse macrophages and in vivo.
Pharmacol Res. 2016 Sep 27; 113(Pt A): 533-546

Book chapter

1. **Huang CW**, Moore PK. H₂S Synthesizing Enzymes: Biochemistry and Molecular Aspects.
Handb Exp Pharmacol. 2015;230: 3-25

International Conferences

1. **Caleb Huang**, Feng Wei, Brian William Dymock, Philip Keith Moore
85: Identification of novel hydrogen sulfide (H₂S) donors with controlled release rates that elicit anti-inflammatory effects in RAW264.7 cells.
Cytokine Vol 70, Issue 1, Nov 2014, Pages 48.
2. **Caleb W. Huang**, Meng Teng Peh, Philip Keith Moore
PP48 - The effect of exogenous hydrogen sulfide on LPS-induced markers of inflammation in CSE knockout and 3-MST knockdown RAW264.7 macrophages. *Nitric Oxide* Vol 47, Supplement, 1 May 2015, Pages S32
(3rd European Conference on the Biology of Hydrogen Sulfide H₂S 2015).

ACKNOWLEDGEMENTS

The completion of this thesis would not have been possible without the support, guidance and assistance of the many people whom I would like to gratefully acknowledge.

Professor Philip Moore, my supervisor, who has been tremendously encouraging towards me and supportive of this research. I thank him for his tutelage and the many insightful discussions, which has allowed me to grow as a research scientist. I would also like to thank my Thesis Advisory Committee chairperson, Professor Soong Tuck Wah, and the committee members Associate Professor Brian Dymock and Associate Professor Shabbir Moochhala for their invaluable comments and suggestions over the past four years.

To my friends Jason Tann and Wong RuiXiong from NGS, for the encouragements, numerous scientific discussions shared, as well as for the joy shared in journeying through graduate school together.

My appreciation also extends to my former laboratory colleagues Ng Li Theng, Dr. Tsai Chin Yi, David Ng and Liao Li Xiang. Especially so to Peh Meng Teng for her unconditional help with several experiments in this thesis, as well as Dr Mohamed Shirhan Bin Mohamed Atan for guiding me through the *in vivo* procedures.

The drug screening studies discussed in this thesis would not have been possible without the chemical synthesis and validation of the H₂S releasing compounds performed by Dr. Feng Wei from the group of Associate Professor Brian Dymock at the Department of Pharmacy, National University of Singapore. I am very grateful for their collaboration and tireless efforts in providing these compounds whenever it is required. I am also thankful to Dr Liang Dong for synthesizing the H₂S fluorescent probe used in this study, and Wisna Novera for her help in reconstituting the lyophilized probe.

I would also like to thank Dr. Paul Hutchinson and Guo Hui from the flow cytometry facility for their expertise and help in performing the cell sorting for the CRISPR-Cas9 experiments in this report. Also, special thanks to Lee Shu Ying and Wei An from the confocal microscopy unit for their kind assistance whilst I was using the confocal microscope.

Above all, I am very grateful to God and my family, whose unwavering support I have received extends well beyond the hours spent in the laboratory.

TABLE OF CONTENTS

PUBLICATIONS	ii
ACKNOWLEDGEMENTS	iii
SUMMARY	viii
LIST OF TABLES	ix
LIST OF FIGURES	x
LIST OF ABBREVIATIONS	xii
CHAPTER 1: INTRODUCTION	1
1.1 Hydrogen sulfide (H ₂ S)	1
1.1.1 Physical and chemical properties of H ₂ S.....	1
1.1.2 Endogenous sources of H ₂ S	2
1.1.3 Exogenous sources of H ₂ S	6
1.1.4 Catabolism of H ₂ S	8
1.1.5 Detection methods of H ₂ S.....	9
1.1.6 Other pharmacological tools and mouse knock-out models in H ₂ S research and their limitations	12
1.1.7 Recent advances in H ₂ S therapeutics	16
1.2 Inflammation	19
1.2.1 Role of macrophages and cytokines in inflammation – An overview	19
1.2.2 Molecular pathways involved in inflammatory mediator production and release from macrophages	21
1.2.3 Molecular targets of H ₂ S in inflammatory pathways	24
1.3 NLRP3 inflammasome	30
1.3.1 NLRP3 inflammasome in health and disease.....	30
1.3.2 Pyroptosis	34
1.3.3 Molecular mechanisms governing NLRP3 inflammasome activation.....	36
1.3.4 Effects of gasotransmitters on the NLRP3 inflammasome ..	40
1.4 Aims of Current Research	42

CHAPTER 2: MATERIALS & METHODS	44
2.1 Cell culture	44
2.2 Mice.....	44
2.3 Treatments on LPS-stimulated RAW264.7 macrophages	45
2.4 CRISPR plasmid synthesis and knock-down of genes	45
2.5 Preliminary screening of novel H ₂ S releasing drug compounds	46
2.6 <i>In vitro</i> microplate assay of H ₂ S in RAW264.7 cells using a fluorescent probe	46
2.7 Measurement of cell death	47
2.8 mRNA extraction, reverse transcription-polymerase chain reaction (RT-PCR) and quantitative real-time PCR (qPCR)	48
2.9 Cell cytoplasmic and nuclear extraction.....	49
2.10 Differentiation of bone marrow-derived macrophages (BMDMs) .	50
2.11 Flow cytometry	50
2.12 Inflammasome activation	50
2.13 ASC pyroptosome detection	51
2.14 Overexpression plasmid synthesis	52
2.15 Transfection.....	53
2.16 Immunofluorescence	54
2.17 ELISA	55
2.18 Immunoblot analysis	55
2.19 Co-immunoprecipitation	56
2.20 MitoTracker and MitoSOX Assay.....	57
2.21 Detection of mitochondrial DNA	58
2.22 Statistical analysis	58
CHAPTER 3: EFFECTS OF EXOGENOUS H₂S ON THE PRODUCTION OF PRO-INFLAMMATORY MEDIATORS IN CSE^{-/-} RAW264.7 MACROPHAGES	60
3.1 Exogenous H ₂ S (i.e. NaHS) reduces LPS-induced TNF α and IL-6 secretion from RAW264.7 macrophages	61
3.2 Generation of CSE ^{-/-} RAW264.7 macrophages using the CRISPR/Cas9 system.....	65

3.3 Effects of exogenous H ₂ S on LPS-stimulated CSE ^{-/-} RAW264.7 macrophages.....	70
3.4 Effect of the loss of CSE on phosphorylation of IκBα in RAW264.7 cells during LPS stimulation.....	75
3.5 Discussion.....	78

CHAPTER 4: A NOVEL SLOW-RELEASING HYDROGEN SULFIDE DONOR, FW1256, EXERTS ANTI-INFLAMMATORY EFFECTS IN MOUSE MACROPHAGES AND *IN VIVO* 85

4.1 Identification of a novel slow-releasing H ₂ S donor that exerts non-toxic, anti-inflammatory effects in LPS-stimulated RAW264.7 macrophages.....	86
4.2 FW1256 is a slow-releasing H ₂ S donor	91
4.3 FW1256 downregulated pro-inflammatory mediator release from LPS-stimulated RAW264.7 macrophages	93
4.4 NFκB activation is reduced in LPS-stimulated RAW264.7 macrophages treated with FW1256.....	99
4.5 FW1256 also downregulated pro-inflammatory mediator release from LPS-stimulated primary bone marrow derived macrophages (BMDMs).....	102
4.6 FW1256 downregulated pro-inflammatory mediator release in the LPS sepsis mouse model.....	105
4.7 Discussion.....	108

CHAPTER 5: H₂S INHIBITS NLRP3 INFLAMMASOME ACTIVATION IN MOUSE MACROPHAGES 113

5.1 The H ₂ S donor NaHS inhibits NLRP3 inflammasome-mediated IL-1β maturation in J774A.1 macrophages	114
5.2 Culture of primary BMDMs with L929 conditioned media	116
5.3 Exogenous H ₂ S inhibits NLRP3 inflammasome mediated IL-1β and IL-18 secretion in BMDMs	118
5.4 Exogenous H ₂ S inhibits NLRP3 inflammasome mediated IL-1β and caspase-1 maturation in BMDMs	121

5.5 NaHS and slow-releasing H ₂ S donors FW1256 and GYY4137 inhibits NLRP3 inflammasome activation in BMDMs	124
5.6 Exogenous H ₂ S inhibits NLRP3 inflammasome-mediated pyroptosome formation in BMDMs	126
5.7 The CSE inhibitor, DL-PAG, exacerbates NLRP3 inflammasome activation.....	130
5.8 Development and optimization of an <i>in vitro</i> NLRP3 inflammasome reconstitution system in HEK293T cells	133
5.9 Exogenous H ₂ S interferes with plasmid expression when administered concurrently during plasmid transfection	138
5.10 CSE overexpression inhibits IL-1 β secretion in the <i>in vitro</i> NLRP3 inflammasome reconstitution assay	140
5.11 Treatment of NLRP3 but not ASC with exogenous H ₂ S downregulates IL-1 β secretion in the <i>in vitro</i> NLRP3 inflammasome reconstitution assay.....	142
5.12 Exogenous H ₂ S disrupts NLRP3 – ASC protein protein interaction	146
5.13 Exogenous H ₂ S protects mitochondrial integrity and reduces mitochondrial ROS production in BMDMs during NLRP3 inflammasome activation.....	148
5.14 Exogenous H ₂ S does not affect cytoplasmic mitochondrial DNA levels in BMDMs during NLRP3 inflammasome activation.....	153
5.15 The slow-releasing H ₂ S donor GYY4137 reduces IL-1 β levels in LPS sepsis mice	155
5.16 Discussion	157
CHAPTER 6: OVERVIEW AND FUTURE PERSPECTIVES	167
6.1 Summary of findings	168
6.2 Future perspectives on the therapeutic applications of H ₂ S donors.....	171
6.3 Future perspectives on the intracellular signalling mediated by H ₂ S.....	176
REFERENCES	179

SUMMARY

Hydrogen sulfide (H₂S) is a gasotransmitter produced endogenously by enzymes cystathionine γ -lyase (CSE), cystathionine β -synthetase (CBS) and 3-Mercaptopyruvate sulfurtransferase (3-MST), or exogenously by H₂S-donor compounds. H₂S modulates the inflammatory response though no clear consensus exists regarding its pro- or anti-inflammatory effects. In this study, exogenous H₂S from NaHS and a novel slow H₂S-releaser, FW1256, reduced inflammatory mediators (TNF α , IL-6, NO, PGE₂, IL-1 β) produced from LPS-stimulated mouse macrophages. FW1256 inhibited NF κ B activation in these cells and reduced pro-inflammatory cytokine release in the LPS model of sepsis in the mouse. Using CRISPR-mediated gene editing, absence of CSE decreased iNOS and COX-2 expression in LPS-stimulated RAW264.7 cells, suggesting a differential role between exogenous and endogenous H₂S. H₂S from both NaHS and FW1256 also inhibited NLRP3 inflammasome activation in primary mouse macrophages, as evidenced by decreased IL-1 β and IL-18 secretion. In addition, NaHS decreased caspase-1 activation and reduced NLRP3 inflammasome mediated pyroptosome formation in these cells. Mechanistically, H₂S disrupted protein-protein binding in the NLRP3 inflammasome complex, preserved mitochondrial integrity and reduced mitochondrial reactive oxygen species (ROS) production in these cells. *In vivo*, GYY4137 reduced IL-1 β levels in LPS-treated mice. Altogether, this study shows that exogenous H₂S exerts anti-inflammatory effects in mouse macrophages via multiple molecular mechanisms.

LIST OF TABLES

Table 1.1 Proteins modified by S-sulfhydration.....	28
Table 1.2 Regulatory receptors of the inflammasomes and their agonists.....	33
Table 3.1 Predicted off target effects of CSE targeted sgRNA	67
Table 4.1 Chemical structures and properties of H ₂ S releasing compounds 1-11.....	88
Table 5.1 Previously reported In vitro NLRP3 inflammasome reconstitution assay conditions	136

LIST OF FIGURES

Figure 1.1 Pathways for H ₂ S biosynthesis in the cell.	5
Figure 1.2. Signaling pathway of inflammatory cytokine production by macrophages.	23
Figure 1.3 Current strategies for detecting protein sulfhydration.	29
Figure 1.4 Mechanisms of NLRP3 inflammasome activation	32
Figure 3.1 The fast-releasing H ₂ S donor NaHS exerts an anti-inflammatory effect in LPS stimulated RAW264.7 macrophages.....	64
Figure 3.2 Generation of CSE ^{-/-} RAW264.7 cells using the CRISPR/Cas9 system.	69
Figure 3.3 Effects of exogenous H ₂ S on LPS-stimulated wild-type and CSE ^{-/-} RAW264.7 macrophages.	74
Figure 3.4 Effects of the loss of endogenous H ₂ S producing enzymes on phosphorylation of IκBα in RAW264.7 cells during LPS stimulation.	77
Figure 4.1 Identification of novel H ₂ S releasing compounds: anti-inflammatory activity <i>in vitro</i> and toxicity.	90
Figure 4.2 FW1256 releases H ₂ S in a sustained manner in RAW264.7 cells.....	92
Figure 4.3. FW1256 reduces the production of inflammatory mediators from LPS-stimulated RAW264.7 macrophages.	98
Figure 4.4 Effects of FW1256 on the phosphorylation of IκBα in LPS-stimulated RAW264.7 macrophages.	100
Figure 4.5 FW1256 reduced the production of inflammatory mediators from LPS-stimulated bone marrow derived macrophages (BMDMs).	104
Figure 4.6 FW1256 reduced pro-inflammatory mediators in the mouse model of LPS induced septic shock.	107
Figure 5.1 The H ₂ S donor NaHS suppresses NLRP3 inflammasome mediated IL-1β maturation in J774A.1 macrophages.	115
Figure 5.2 L929 conditioned media differentiates mouse bone marrow cells into BMDMs.....	117
Figure 5.3 H ₂ S exerts an inhibitory effect on NLRP3 inflammasome mediated IL-1β and IL-18 secretion in BMDMs.	120

Figure 5.4 The H ₂ S donor NaHS exerts an inhibitory effect on NLRP3 inflammasome mediated IL-1 β and IL-18 secretion, and caspase-1 activation in BMDMs.	122
Figure 5.5 NaHS, FW1256 and GYY4137 induced Inhibition of IL-1 β and IL-18 from NLRP3 inflammasome activated BMDMs.	125
Figure 5.6 The H ₂ S donor NaHS inhibits NLRP3 inflammasome mediated pyroptosome formation in BMDMs.	127
Figure 5.7 DL-PAG exacerbates NLRP3 inflammasome mediated IL-1 β and IL-18 secretion, and caspase-1 activation in BMDMs.	131
Figure 5.8 In vitro NLRP3 inflammasome reconstitution assay in HEK293T cells.	136
Figure 5.9 Exogenous H ₂ S interferes with the <i>in vitro</i> NLRP3 inflammasome reconstitution assay in HEK293T cells.	139
Figure 5.10 CSE overexpression inhibits IL-1 β secretion in the <i>in vitro</i> NLRP3 inflammasome reconstitution assay.	141
Figure 5.11 Exogenous H ₂ S reacts with NLRP3 but not ASC in the <i>in vitro</i> NLRP3 inflammasome reconstitution assay.	144
Figure 5.12 Exogenous H ₂ S disrupts NLRP3-ASC protein protein binding.....	147
Figure 5.13 Exogenous H ₂ S decreased mitochondrial damage and mitochondrial ROS production induced during NLRP3 inflammasome activation.....	152
Figure 5.14 NaHS does not reduce cytoplasmic mtDNA in NLRP3 inflammasome activated BMDMs	154
Figure 5.15 GYY4137 reduced IL-1 β in the mouse model of LPS induced septic shock	156

LIST OF ABBREVIATIONS

3-MST	3-Mercaptopyruvate sulfurtransferase
ADT-OH	Anethole dithiolethione (ADT) -OH
AIM2	Absent in melanoma 2
AOAA	Aminooxyacetic acid
AP-1	Activator protein 1
AP39	(10-oxo-10-(4-(3-thioxo-3H-1,2-dithiol-5yl)phenoxy)decyl) triphenylphosphonium bromide
ASC	Apoptosis-associated speck-like protein with a caspase recruitment domain protein
ATP	Adenosine triphosphate
AVG	L-aminoethoxyvinylglycine
BAFFR	B-cell activating factor receptor
BBMTS	S-4-bromobenzyl methanethiosulfonate
BCA	Beta-cyanoalanine
BMDMs	Bone marrow derived macrophages
CAPS	Cryopyrin-associated periodic syndrome
CAT/AAT	Cysteine aminotransferase/aspartate aminotransferase
CBS	Cystathionine β -synthetase
CHH	O-(carboxymethyl) hydroxylamine hemihydrochloride
CO	Carbon monoxide
COX-2	Cyclooxygenase-2
CRISPR-Cas9	Clustered regularly interspaced short palindromic repeats-Cas 9(CRISPR-associated 9)
CSE	Cystathionine γ -lyase
DADS	Diallyl disulfide
DAMP	Damage-associated molecular patterns
DATS	Diallyl trisulfide
DL-PAG	DL-propargylglycine
DTT	Dithiothreitol
GABA-T	4-aminobutyrate aminotransferase

GSH	Glutathione
GGY4137	Morpholin-4-ium-4-methoxyphenyl(morpholino)phosphinodithioate
HS-	Anionic sulfide
H ₂ S	Hydrogen sulfide
HDR	Homologous-directed repair
IFI16	IFN γ -inducible protein 16
IFN γ	Interferon γ
IKK	I κ B kinase
iNOS	Inducible nitric oxide synthase
IRAK	Interleukin-1 receptor-associated kinase
LPS	Lipopolysaccharide
LRR	Leucine rich repeats
LT β R	Lymphotoxin- β receptor
MAPK	Mitogen-activated protein kinase
MMTS	Methyl methanethiosulfonate
MyD88	Myeloid differentiation primary response gene 88
NADH	Nicotinamide adenine dinucleotide
NADPH	Reduced nicotinamide adenine dinucleotide phosphate
Na ₂ S	Sodium sulfide
NaHS	Sodium hydrosulfide
NF κ B	Nuclear factor kappa-light-chain-enhancer of activated B cells
NLR	Nucleotide-binding oligomerization domain (NOD)-like receptor
NLRP	NOD-, Leucine rich repeats (LRR)-, and pyrin domain-containing
NHEJ	Non-homologous end joining
NO	Nitric oxide
NSAID	Nonsteroidal anti-inflammatory drug
PAMP	Pathogen-associated molecular pattern
PGE ₂	Prostaglandin E ₂
PI	Propidium iodide

PLP	Pyridoxal-5'-phosphate
PRR	Pattern recognition receptor
PYCARD	PYD and CARD domain containing protein
PYHIN	Pyrin and HIN domain-containing protein
RANK	Receptor activator of nuclear factor κ B
ROS	Reactive oxygen species
RP-HPLC	Reverse phase high-performance liquid chromatography
S^{2-}	Sulfide
SNAP	S-Nitroso-N-Acetyl-D,L-Penicillamine
$S_2O_3^{2-}$	Thiosulfate
SO_3^{2-}	Sulfite
SO_4^{2-}	Sulfate
TAK	TGF- β activated kinase
TGF- β	Transforming growth factor β
TLR	Toll-like receptor
TNF α	Tumour necrosis factor α
TRAF	TNF receptor associated factor
TRIF	TIR-domain-containing adaptor-inducing interferon
Tx-NaHS	Time expired NaHS
VDCC	Voltage-dependent calcium channel

CHAPTER 1: INTRODUCTION

1.1 Hydrogen sulfide (H₂S)

Hydrogen sulfide (H₂S) is a gas found ubiquitously in nature. From sulfur springs to lagoons and marshes, it is produced as a by-product of decomposition of organic material caused by sulfate-reducing bacteria in the absence of oxygen, and is known to be a toxic environmental hazard (Beauchamp et al., 1984). H₂S exerts most probably its toxic effects by binding to cytochrome oxidase in the mitochondria, hence preventing the conversion of molecular oxygen to water, thereby inhibiting mitochondrial function by impeding adenosine triphosphate (ATP) generation (Reiffenstein et al., 1992). Despite its toxicity, H₂S is now gaining acceptance as the third biologically active endogenous gasotransmitter -- after its counterparts nitric oxide (NO) and carbon monoxide (CO) (Wang, 2014; Łowicka and Bełtowski, 2007). These gasotransmitters are endogenous gaseous molecules that can act as messengers in signalling pathways.

1.1.1 Physical and chemical properties of H₂S

H₂S is a colourless gas that is flammable and with the distinctive smell of rotten eggs. It is soluble in polar as well as non-polar solvents and is lipid soluble. Hence, it readily penetrates biological lipid membranes (Mathai et al., 2009). As H₂S is a weak acid that ionizes in polar solvents with a pK_a value of 6.9 for the anionic sulfide (HS⁻) and >12 for S²⁻ in solvents at physiological pH, approximately two-thirds of total H₂S dissociates into the anionic sulfide (HS⁻) and hydrogen ions (H⁺) (Kabil et al., 2014). The remaining one-third remains in the un-dissociated form.

1.1.2 Endogenous sources of H₂S

H₂S is produced endogenously by three 'H₂S synthesizing enzymes' namely cystathionine γ -lyase (CSE), cystathionine β -synthetase (CBS) and 3-mercaptopyruvate sulfurtransferase (3-MST). CSE and CBS are pyridoxal-5'-phosphate (PLP) dependent and utilize homocysteine, L-cysteine and cystathionine as substrates whilst 3-MST is non-PLP dependent and uses 3-mercaptopyruvate as substrate (Shibuya et al., 2009a; Steegborn et al., 1999). 3-MST, in conjunction with aspartate aminotransferase (AAT), which has cysteine aminotransferase (CAT) activity, can also generate sulfane sulfur which when reduced, releases H₂S (Shibuya et al., 2009b). The enzymatic pathways for H₂S biosynthesis in the cell are many and are depicted in Figure 1.1.

The initial clue suggesting H₂S may be of biological relevance was the finding that endogenous sulfides are present in the mammalian brain (Goodwin et al., 1989; Warenycia et al., 1989). Thereafter, H₂S was found to be produced from L-cysteine in mammalian brain, catalysed by the enzyme CBS, which is highly expressed in the hippocampus (Abe and Kimura, 1996). More than a decade later, the presence of H₂S producing activity in the brains of CBS^{-/-} mice prompted the discovery of a novel H₂S producing pathway regulated by 3-MST and CAT (Shibuya et al., 2009b).

CSE and CBS are both cytosolic enzymes while 3-MST is located inside the mitochondria. However under circumstances when intracellular calcium level is increased, CSE in smooth-muscle cells can translocate into mitochondria (Fu et al., 2012), suggesting that the intracellular compartmentalization of H₂S-generating enzymes may be fluid. It was widely

accepted that CBS is predominantly found in cells of the nervous system (Abe and Kimura, 1996), while CSE is present in peripheral tissues as a smooth muscle relaxant (Hosoki et al., 1997). However, cumulative evidence has indicated that CBS is present in many other organs such as the kidney (Sen et al., 2009), intestine (Martin et al., 2010), pancreas (Kaneko et al., 2006) and placenta (Guzmán et al., 2006). It is positively regulated by S-adenoxylmethionine, which allosterically activates CBS. Conversely, CBS activity is downregulated by both NO and CO (Taoka and Banerjee, 2001). CSE is found in a diverse number of organs and tissues. It is expressed in the vasculature (Hosoki et al., 1997), liver, kidney (Kabil et al., 2011), brain (Diwakar and Ravindranath, 2007) and uterus (Patel et al., 2009). Although CSE and CBS are both present in a number of these organs, CSE is more abundant than CBS in the murine kidney and liver, whilst CBS is more abundant than CSE in the murine brain. Interestingly, at high substrate concentrations, CBS was the major source of H₂S production in the kidney and brain *in vitro* (Kabil et al., 2011). Like CBS and CSE, 3-MST is present in the liver, kidney, vasculature and brain and produces H₂S and bound sulfane sulfur (Nagahara et al., 1998; Shibuya et al., 2009b). However unlike CBS and CSE which are present in the cytoplasm, 3-MST is in addition found in mitochondria as well (Nagahara et al., 1998). The synthesis of H₂S by 3-MST requires the substrate 3-mercaptopyruvate, which can either be produced by the metabolism of L-cysteine and α-ketoglutarate by the enzyme cysteine aminotransferase (CAT, or known as aspartate aminotransferase), or from D-cysteine by the enzyme D-amino acid oxidase (DAO). DAO and 3-MST are localized to peroxisomes and

mitochondria respectively, and together, the 3-MST/DAO pathway produces H₂S by the interaction of both organelles (Shibuya et al., 2013).

Endogenous H₂S can also be produced non-enzymatically. Red blood cells supplemented with sulfur and glucose, containing electron carriers NADH, NADPH and reduced glutathione (GSH), spontaneously react with sulfur to produce H₂S (Searcy and Lee, 1998). Iron-sulfur cluster-containing proteins carrying Fe₂S₂, Fe₃S₄ or Fe₄S₄ clusters are also a source of non-enzymatically generated H₂S. Such proteins include ferredoxins and 'Rieske' proteins amongst others (Beinert et al., 1997). In addition, H₂S can be released from bound sulfur in the presence of reducing agents like glutathione from persulfides in cells such as neurons and astrocytes (Ishigami et al., 2009).

1.1.3 Exogenous sources of H₂S

Exogenous H₂S donors which generate what may be referred to as 'pharmacological' H₂S have been used extensively to evaluate the effect of H₂S both in cells and animal disease models. Beyond their use as simple research tools, the recognition of the potential beneficial effects of such donors, has prompted the incremental development of novel and more potent H₂S-based therapeutics (Wallace and Wang, 2015). These donors can be separated into two main classes depending on the speed with which they release H₂S and their chemical characteristics *viz.* 'fast' and 'slow' H₂S donors.

As a highly flammable, explosive and a toxic gas, H₂S administration in the gaseous form presents severe safety issues. In the literature, the widely accepted means of administering H₂S is therefore via H₂S releasing compounds. Very commonly used and especially in the early stages of H₂S research, are inorganic sulfide salts such as sodium hydrosulfide (NaHS), Na₂S₂O₃ and Na₂S (Bhatia et al., 2008; Dufton et al., 2012; Li et al., 2005; Zhang et al., 2010). When dissolved in an aqueous solution, these compounds release an immediate and large bolus of H₂S over a period of seconds to minutes (Whiteman et al., 2010). Hence, these compounds are referred to as 'fast' H₂S releasers. Cells exposed to H₂S from these compounds would be expected to 'experience' a high concentration of H₂S over a short period of time. This is in sharp contrast to cells exposed to 'physiological' H₂S generated from natural substrates endogenously. Nonetheless, the use of these compounds may also have advantages. For example, fast H₂S releasers have simple chemical structures and are thus straightforward to synthesise. Any biological effects produced by these compounds will almost certainly be mediated by H₂S

which is not always the case with more complex donors. As such, fast H₂S releasers are often useful in proof-of-concept experiments demonstrating that H₂S can elicit a particular biological effect.

Conversely, 'slow' H₂S releasers are compounds that generate H₂S in a sustained and controlled manner, lasting a period of hours to days. These synthetic compounds contain a H₂S-donating moiety, hybridized to a parental small molecule structure, and will release H₂S in a manner that is more likely to mimic conditions in which cells are typically exposed to endogenous H₂S. A very widely used slow H₂S releaser is GYY4137 (morpholin-4-ium-4-methoxyphenyl (morpholino) phosphinodithioate) (Li et al., 2008). GYY4137 has been shown to exhibit anti-inflammatory effects both *in vitro* and *in vivo*. It is anti-inflammatory in a rat model of endotoxic shock (Li et al., 2009), anti-atherosclerotic in high fat fed apolipoprotein E^{-/-} mice (Liu et al., 2013), and exhibits vasodilator and antihypertensive activity (Li et al., 2008). New H₂S releasing phosphordithioates based on the structure of GYY4137, have also been synthesized and characterized and found to have antiproliferative activity against cancer cells (Feng et al., 2015).

Besides the sulfide salts and synthetic H₂S releasing compounds, H₂S sources stemming from natural origins have also been used in H₂S research. These include diallyl disulfide (DADS) and diallyl trisulfide (DATS) which are derived from garlic and sulforaphan, erucin and iberin which are found in vegetables like broccoli, wasabi, mustard and horseradish (Bełtowski, 2015; Kashfi and Olson, 2013). Although DADS and DATS have been characterized *in vitro* and *in vivo* (Benavides et al., 2007) the characterization of sulforaphan, erucin and iberin is still far from complete.

1.1.4 Catabolism of H₂S

The catabolism of H₂S in the body is of utmost importance given that H₂S is a toxic gas. H₂S is eliminated from the body via the lungs and faeces, while its metabolites are removed in the urine. Three metabolic pathways govern the catabolism of H₂S: oxidation, alkylation and reactions with disulfide- or metallo- bearing proteins (Beauchamp et al., 1984), with oxidation being the main catabolic pathway.

As a reducing species, H₂S is easily oxidized. Using Na₂³⁵S, it has been shown that the rate of sulfide oxidation differed between organs. In rat lung, sulfide (S²⁻) was oxidized slowly to thiosulfate (S₂O₃²⁻), while in rat kidney, sulfide was oxidized to sulfate (SO₄²⁻) with thiosulfate as an intermediate. Whereas in the rat liver, sulfide was rapidly oxidized and converted also completely to sulfate, with thiosulfate and sulphite as intermediates (Bartholomew et al., 1980). The mitochondrial sulfide oxidation pathway involves oxidation of thiosulfate to sulfate, in a glutathione-dependent manner. This process is governed by three enzymatic activities catalysed by (1) sulfide quinone oxidoreductase found on the inner mitochondrial membrane, which converts sulfide to persulfides and transfers electrons to the ubiquinone pool; (2) sulfur dioxygenase which oxidizes persulfide to sulfite (SO₃²⁻); and (3) sulfur transferase, which links a persulfide to sulfite, creating thiosulfate (Hildebrandt and Grieshaber, 2008). Upon oxidation, the final metabolites of H₂S are sulfate, thiosulfate, sulfite and persulfide.

1.1.5 Detection methods of H₂S

Due to its chemical properties, the accurate measurement of H₂S has proved to be a considerable challenge. For a detection method to be employed readily and widely, it has to be easy to use and have a high level of specificity and sensitivity. To date, several methods have been used for sulfide detection in solutions as well as biological systems.

Measuring sulfide concentrations using sulfide-ion microelectrodes has been carried out in biological samples (Chang et al., 2010; Chen et al., 2005; Whiteman et al., 2010). As this method involves the use of a glass pH electrode with electrodes which measure S²⁻, maintaining a constant pH during the course of measurements as well as establishing the standard curve under identical conditions, is crucial for obtaining reproducible data. In some studies, such probes have detected H₂S in concentrations as low as nanomole per mg of protein (Chang et al., 2010) and low micromolar range of H₂S in serum (Chen et al., 2005). The use of such electrodes has the added advantage that they do not require sulfide derivatization and hence can measure free sulfide concentrations. However, for some electrode surfaces with the Ag⁺/Ag₂S system, sulfide measurements may be complicated by the presence of thiols (Nagy et al., 2014).

A second very common method is the methylene blue assay. Here, sulfide is chemisorbed by zinc acetate and converted into zinc sulfide. Upon contact with the oxidizing agent ferric chloride in a strong acid solution, it reacts with N,N-dimethyl-p-phenylnediamine to give a methylene blue dye, which is then measured spectrophotometrically at an absorbance wavelength of 670nm. The concentration of H₂S is then determined from an established standard

curve derived from different concentrations of NaHS. Although easy to carry out, a drawback of this method is that the extreme acidic conditions required not only measure free H₂S but also release sulfide from acid-labile pools such as sulfur present in iron-sulfur proteins (Johnson et al., 2005), and bound sulfane sulfur pools such as thiosulfate, persulfide, polysulfides. These are all present endogenously in biological systems (Beinert et al., 1997; Kimura, 2014; Searcy and Lee, 1998). The acidic conditions may also release sulfide from slow-releasing H₂S donors thereby leading to issues interpreting released H₂S levels when such donors have been used. Whilst the methylene blue method has its shortcomings and the absolute values may not be accurate, the relative difference comparing between biological groups may provide an indication as to whether an experimental treatment has resulted in a modulation of H₂S levels.

Detection of minute amounts of H₂S in biological samples with a 2 nM limit of detection (Shen et al., 2015) can also be achieved using the monobromobimane method followed by reverse phase high-performance liquid chromatography (RP-HPLC). This method requires the derivatization of H₂S with monobromobimane to form sulfide-dibimane. Sulfide-dibimane is then separated by RP-HPLC and analysed by fluorescence detection (Shen et al., 2011). While the monobromobimane method is highly sensitive and can be modified to measure other forms of sulfide such as acid-labile sulfur and bound sulfane sulfur, the procedures are complex and several caveats must be kept in mind to prevent inaccurate readings. Examples include the deoxygenation of all solutions prior to preparation of sulfide samples as well as ensuring that pH, time, oxygen tension and volatilization are all well controlled when performing

the chemical derivatization reaction of H₂S with monobromobimane (Shen et al., 2015).

In recent years, the use of H₂S sensitive fluorescent probes has been increasingly adopted by research groups as this approach is both highly selective and sensitive to H₂S (Feng and Dymock, 2015). For this approach to be applied in different biological situations, the probe must exhibit rapid reactivity with H₂S, be selective and sensitive for H₂S over, for example, thiols and anions, be cell permeable if measurements of intracellular H₂S are required, be non-toxic towards cells and also chemically stable. The mechanism of action by which these probes react with H₂S are: (1) nucleophilic substitution-cyclization reaction (Peng et al., 2014); (2) reduction of aromatic azide probes to produce a fluorescent product (Lin et al., 2013); or (3) de-complexing of a metal group from a non-fluorescent probe in response to H₂S thereby activating its fluorescence (Wu et al., 2014a).

In this project, we have used a near-infrared-fluorescent H₂S probe belonging to the third class of probe using a copper(II)-cyclen complex which acts as a reaction centre for H₂S and as a quencher for BODIPY (boron-dipyrromethene) based fluorophores. This probe was characterized and was found to have a detection limit of 80 nM H₂S in a chemical system. In addition, the assay was sufficiently sensitive to detect endogenous H₂S in HEK293 cells overexpressed with CSE, as well as *in vivo* in mice injected with Na₂S, making it a useful tool for detecting H₂S release in biological systems (Wu et al., 2014a).

1.1.6 Other pharmacological tools and mouse knock-out models in H₂S research and their limitations

The effect of exogenous H₂S in a biological system can be assessed using H₂S donors whilst the response to endogenous H₂S can be monitored by overexpressing H₂S producing enzymes in cells. Another approach is the use of inhibitors of H₂S synthesizing enzymes. Inhibitors of both CSE and CBS are readily available commercially. Examples of CSE inhibitors include DL-propargylglycine (PAG) which inhibits CSE irreversibly by interfering with the accessibility of substrate to the active site of the enzyme (Sun et al., 2009), β-cyanoalanine (BCA) which inhibits CSE reversibly (Pfeffer and Ressler, 1967) and L-aminoethoxyvinylglycine (AVG). Aminoxyacetic acid (AOAA) has been shown previously to be a specific inhibitor of CBS (d'Emmanuele di Villa Bianca et al., 2009; Oh et al., 2006; Roy et al., 2012) while trifluoroalanine and hydroxylamine are inhibitors of both CSE and CBS. O-(carboxymethyl) hydroxylamine hemihydrochloride (CHH) also inhibits CBS. Whilst L-aspartate can inhibit the production of H₂S by 3-MST indirectly by inhibiting cysteine aminotransferase/aspartate aminotransferase (CAT/AAT) (Akagi, 1982), only very recently has the discovery of several 3-MST inhibitors by means of high-throughput screening been reported (Hanaoka et al., 2017).

One area of concern with regard to the use of several of these inhibitors is poor selectivity. For example, PAG binds to the pyridoxal 5'-phosphate (PLP) binding site of the CSE enzyme. Thus, it may affect other PLP-dependant enzymes. AOAA, an often stated selective inhibitor of CBS, has been reported also to inhibit human CSE in experiments using recombinant human CSE and CBS. In this work, AOAA was surprisingly a more potent inhibitor of CSE than

of CBS (Asimakopoulou et al., 2013). As an inhibitor of PLP-dependent enzymes, AOAA like PAG, has also been found to inhibit PLP-dependent enzymes such as 4-aminobutyrate aminotransferase (GABA-T) (WALLACH, 1961) and aspartate aminotransferase (Kauppinen et al., 1987).

Research into the biological effects of nitric oxide (NO) has been aided by the use of a range of so called 'NO scavengers' which bind to and hence inactivate NO (Barakat et al., 2014; Harbrecht, 2006; Queiroz et al., 2014). Unfortunately, very few H₂S scavengers have been reported and are not commonly used in research of H₂S in biological systems. Vitamin B_{12a}, also known as hydroxocobalamin, is one such compound which does sequester H₂S dissolved in a cell free solution of PBS or saline (Van de Louw and Haouzi, 2013). *In vivo*, hydroxocobalamin is an effective antidote against H₂S poisoning in mice and prevents NaHS-induced hepatocyte cytotoxicity (Truong et al., 2007). Hence, vitamin B_{12a} may currently be the only option when it comes to scavenging H₂S under experimental conditions.

Besides the use of pharmacological tools, mouse knock-out models have been very useful in studying the role of H₂S synthesizing enzymes in disease models *in vivo*. The majority of studies using H₂S synthesizing enzyme knock out models have been performed in CSE^{-/-} mice. CSE^{-/-} mice were first reported to exhibit reduced H₂S levels in blood serum and vessels. These mice displayed an age-dependent development of hypertension and exhibited reduced endothelium-dependent vasorelaxation responses thereby providing evidence that endogenous H₂S regulates vasodilation and blood pressure (Yang et al., 2008). CSE^{-/-} mice fed with an atherogenic paigen-type diet developed early fatty streak lesions in the aortic root and had increased

cholesterol and low-density lipoprotein cholesterol amongst other markers for atherosclerosis. The accelerated atherosclerosis in these mice was halted by treatment with NaHS. This highlights the importance of the endogenous CSE/H₂S pathway in controlling atherosclerosis (Mani et al., 2013). Other than its role in the cardiovascular system, CSE^{-/-} mice reportedly display abnormal hindlimb clasping and clenching similar to that of mouse models of Huntington's disease. Subsequent exploration into the disease model revealed that depletion of CSE in Huntington's disease tissues could have mediated the disease pathophysiology (Paul et al., 2014).

As compared to the CSE^{-/-} mouse, the CBS^{-/-} mouse model has been less extensively studied. CBS deficiency is a cause of homocystinuria (HCU), characterized by very high levels of blood plasma homocysteine. In patients with CBS deficiency, symptoms such as skeletal abnormalities, mental retardation and thrombosis are commonplace (Sachdev, 2005; Yap et al., 2000). 90% of CBS^{-/-} mice fed with a standard laboratory diet died before 1 month of age due to severe hepatopathy and growth retardation (Hamelet et al., 2007; Watanabe et al., 1995). In CBS^{-/-} mice fed with standard A04 rodent chow enriched in choline chloride which is vital for their survival, these mice displayed lung fibrosis and air space enlargement (Hamelet et al., 2007). Due to the semi-lethal phenotype, studying the effects of CBS deficiency in health and disease in adult mice, has been considered generally impractical for many years. However, an experimental substitute for CBS^{-/-} mice has been recently reported. This mouse model of classical homocystinuria has the mouse *cbs* gene inactivated and has low-level expression of the human *cbs* transgene under the promoter of the human *cbs* promoter. Such mice exhibit mild hepatopathy but

do not incur neonatal death with approximately 90% of the mice living for at least 6 months (Maclean et al., 2010). Such a model may be a useful alternative to the previous CBS^{-/-} mouse model to study the longer term effects of CBS deficiency into adulthood.

Lastly, only lately has it been possible to produce 3-MST^{-/-} mice (Nagahara, 2013). This mouse model was subsequently instrumental in the discovery that 3-MST is required for the production of hydrogen polysulfides (H₂S_n) and H₂S from 3-mercaptopyruvate in the brain of wild-type mice (Kimura et al., 2015).

1.1.7 Recent advances in H₂S therapeutics

Understanding the importance of H₂S in inflammatory conditions has led to an increased effort in discovering H₂S donors with greater potency. Specifically, development of H₂S releasing hybrids and H₂S donors that can preferentially target certain cell types or organelles have gained traction in recent years.

Non-steroidal anti-inflammatory drugs (NSAIDs) are an effective mainstay in treating the symptoms of inflammatory conditions. However, a harmful side effect stemming from the use of NSAIDs is gastric mucosal bleeding. By combining the anti-inflammatory effect of both NSAIDs and H₂S, NSAID-H₂S releasing hybrids have been formulated. This is achieved by synthesizing NSAIDs with an anethole dithiolethione (ADT)-OH, a H₂S releasing moiety. Stemming from this concept, the H₂S-releasing derivative of the NSAID diclofenac (S-diclofenac) was synthesized and found to inhibit lipopolysaccharide (LPS)-induced inflammation in rats with significantly reduced gastric toxicity as compared to diclofenac (Li et al., 2007). In the model of carrageenan-induced hindpaw oedema in rats, S-diclofenac displayed greater potency in reducing inflammation and likewise caused markedly reduced gastrointestinal damage as compared to diclofenac (Sidhapuriwala et al., 2007; Wallace et al., 2007). Reduced gastrointestinal toxicity was also seen in another H₂S-releasing hybrid, S-aspirin (Sparatore et al., 2009), while S-naproxen (ATB-346) hastened the healing of gastric ulcers in rats, and was found to be more effective than naproxen in downregulating leukocyte infiltration and cyclooxygenase-2 (COX-2) activity in these rats (Wallace et al., 2010). In rats with ligature-induced periodontitis, ATB-346 inhibited pro-

inflammatory cytokine levels and alveolar bone loss in these mice, while preventing gastric mucosa damage (Herrera et al., 2015). Such examples highlight the possibility of combining the therapeutic potential of H₂S with present day drugs used to treat inflammatory conditions.

It was previously established that H₂S donors reduce mitochondria-induced cell death response and maintain mitochondrial integrity (Elrod et al., 2007; Módis et al., 2013; Suzuki et al., 2011). With this in mind, a mitochondrial-targeted H₂S donor, AP39, was designed to provide a more specific and targeted response intracellularly. When used in nanomolar concentrations, AP39 was shown to increase H₂S levels within the mitochondria of endothelial cells, conferred cytoprotective effect and attenuated the loss of cellular bioenergetics in these cells when subjected to oxidative stress (Szczesny et al., 2014). Following from this study, others have demonstrated the efficacy of AP39 in animal models. AP39 improved the neurological outcome after cardiac arrest in mice (Ikeda et al., 2015), displayed protective effects against renal ischemia-reperfusion injury in rats (Ahmad et al., 2016b), preserved mitochondrial function in APP/PS1 mice and neurons, thereby protecting against Alzheimer's disease (Zhao et al., 2016), and also showed protective effects in a mouse model of burn injury (Ahmad and Szabo, 2016).

There has been much evidence documenting the efficacy of H₂S donors used in basic research in cells and animals over the years. However, evidence for the safety of such donors in humans remain scarce and the push towards the use of H₂S donors for therapy in humans still remains a challenge. One such H₂S donor that has made its way into clinical trials is a H₂S prodrug, SG1002. In preclinical studies, SG1002 protected against pressure overload-

induced heart failure by reducing ventricular remodelling and dysfunction in mice (Kondo et al., 2013). The H₂S prodrug also attenuated high fat diet-induced cardiac dysfunction in mice (Barr et al., 2015). Subsequently when SG1002 underwent Phase I clinical trials, it was reported that oral ingestion of SG1002 was safe and well tolerated by both healthy patients and patients with heart failure. SG1002 also increased blood H₂S levels and circulating NO bioavailability (Polhemus et al., 2015). Given the promising findings gleaned from the Phase I trial, this novel H₂S donor warrants further study in a larger subsequent clinical trial.

1.2 Inflammation

1.2.1 Role of macrophages and cytokines in inflammation – An overview

Inflammation is a host defence mechanism whereby tissues of the body respond to an injury or invading foreign agent with the aim of repairing structure and function. In this process, the immune system seeks to eradicate the invading foreign agent in order to achieve tissue homeostasis. This is characterized by a cascade of signals leading to the immediate recruitment of innate immune cells such as neutrophils (Kolaczkowska and Kubes, 2013) and macrophages (Mosser and Edwards, 2008) to the site of injury. Upon recruitment to the site of injury and, acting in concert with neutrophils, macrophages serve as a first line of defence against viral, parasitic and bacterial infections. The main role of the neutrophil is to eliminate the foreign body by phagocytosis and kill it by means of reactive oxygen species (ROS) or antibacterial proteins inside the phagosome (Kolaczkowska and Kubes, 2013). While macrophages similarly eliminate pathogens by phagocytosis followed by lysosomal inactivation, macrophages also secrete mediators that have antimicrobial effects or immune regulatory functions that can initiate cell to cell communication.

Macrophages have long been known to be found in all tissues in mammals (Okabe and Medzhitov, 2016), and may be derived from circulating monocytes or embryonic progenitors that are present before birth in developing tissues, such as the yolk sac and fetal liver (Ginhoux and Guilliams, 2016). Depending on their activation status, macrophages serve different functions. On one extreme, classically activated macrophages (M1 macrophages) occurs when naïve macrophages detect stimuli like LPS, interferon- γ (INF- γ) and

tumor-necrosis factor (TNF). On the other hand, polarization of naïve macrophages to the alternatively activated macrophages (M2 macrophages) occur in response to interleukin-4 (IL-4), transforming growth factor β (TGF- β) and IL-13 (Weisser et al., 2013).

While the role of M2 macrophages involve angiogenesis, debris scavenging and tissue remodelling – activities associated with the resolution of inflammation, the M1 macrophage release several pro-inflammatory cytokines such as interferon- γ (IFN γ), tumour-necrosis factor (TNF), IL-6, IL-1 β , IL-18, IL-23, anti-microbial effectors like nitric oxide (NO), prostaglandin E₂ (PGE₂), and chemokines such as CCL15, CCL20, CXCL9, CXCL10 and CXCL11 that induce chemotaxis of neighbouring immune cells to the site of infection (Mosser and Edwards, 2008). These pro-inflammatory cytokines are proteins which cause cell death of neighbouring cells and trigger the activation of other immune cells. Together, these inflammatory mediators secreted from classically activated macrophages initiate the inflammatory cascade.

1.2.2 Molecular pathways involved in inflammatory mediator production and release from macrophages

Macrophages sense and determine what are considered to be danger signals via pattern recognition receptors (PRR) such as toll-like receptors (TLRs) that are present on both the cell surface and intracellularly. Pathogen-associated molecular patterns (PAMPs) and damage-associated molecular patterns (DAMPs) bind to TLRs eliciting an acute inflammatory molecular signaling cascade (Medzhitov and Horng, 2009). LPS, which is found on the outer membrane of Gram-negative bacteria, is a PAMP which is very commonly used to induce inflammation and a strong immune response both *in vitro* and *in vivo* experimentally. Once LPS binds to TLR4, the intracellular domain of TLR4 interacts with the adaptor protein myeloid differentiation primary response gene 88 (MyD88) and TIR-domain-containing adaptor-inducing interferon- β (TRIF) separately. MyD88 recruits TNF receptor associated factor 6 (TRAF6) and members of the interleukin-1 receptor-associated kinase (IRAK) family leading to the oligomerization and self-ubiquitination of TRAF6. MyD88 also recruits TAB2 and TAB3, which, in turn, activates TGF- β activated kinase 1 (TAK1). TAK1 phosphorylates I κ B kinase β (IKK β) to activate the IKK complex, resulting in the degradation of I κ B α and thereby causing activation of nuclear factor kappa-light-chain-enhancer of activated B cells (NF κ B), which is defined as translocation of the p50-RelA (or p50-p65) dimer into the nucleus to bind to DNA and elicit transcription of pro-inflammatory cytokines (Vallabhapurapu and Karin, 2009). Simultaneously, TAK1 activates the mitogen-activated protein kinase (MAPK) cascades leading to activation of transcription factor activator protein 1 (AP-1) which also binds to the DNA in the nucleus and triggers

production of cytokine genes (Takeuchi and Akira, 2010). This is referred to as the "classical or canonical NF κ B pathway". In the non-canonical pathway, the protein p100 undergoes processing, thereby allowing the p52-RelB dimer to translocate into the nucleus to initiate the transcription of downstream genes. This pathway regulates biological functions such as lymphoid organogenesis, B-cell survival and maturation and dendritic cell activation. Unlike the canonical pathway which is activated by TLRs, the activation of the non-canonical pathway is triggered by a subset of TNF receptors such as B-cell activating factor receptor (BAFFR), CD40, lymphotoxin- β receptor (LT β R) and receptor activator of nuclear factor κ B (RANK) (Sun, 2011).

Cytokines that are transcribed upon activation of the NF κ B pathway include TNF α (Collart et al., 1990; Shakhov et al., 1990), IL-6 (Libermann and Baltimore, 1990) and IL-1 β (Hiscott et al., 1993). The gene regulation of COX-2 and inducible nitric oxide synthase (iNOS), enzymes which synthesise PGE₂ and NO respectively, are also known to be upregulated by activation of the NF κ B pathway (Tak and Firestein, 2001). Activation of the NF κ B pathway can also be triggered by the binding of TNF α and IL-1 β to TNF and IL-1 receptors respectively, which are present on the cell surface (Lawrence, 2009). In addition, expression of IL-6 gene is also induced in response to TNF α and IL-1 β (Libermann and Baltimore, 1990). Hence, the molecular control of NF κ B and cytokine expression is complex since auto-regulatory loops exist.

The control of the production of inflammatory cytokines, via NF κ B activation or otherwise, is crucial since aberrant inflammatory cytokine signalling can cause uncontrolled inflammation and cell death, contributing to inflammatory diseases such as rheumatoid arthritis, atherosclerosis,

inflammatory bowel disease and systemic inflammatory response syndrome among many other conditions (Tak and Firestein, 2001).

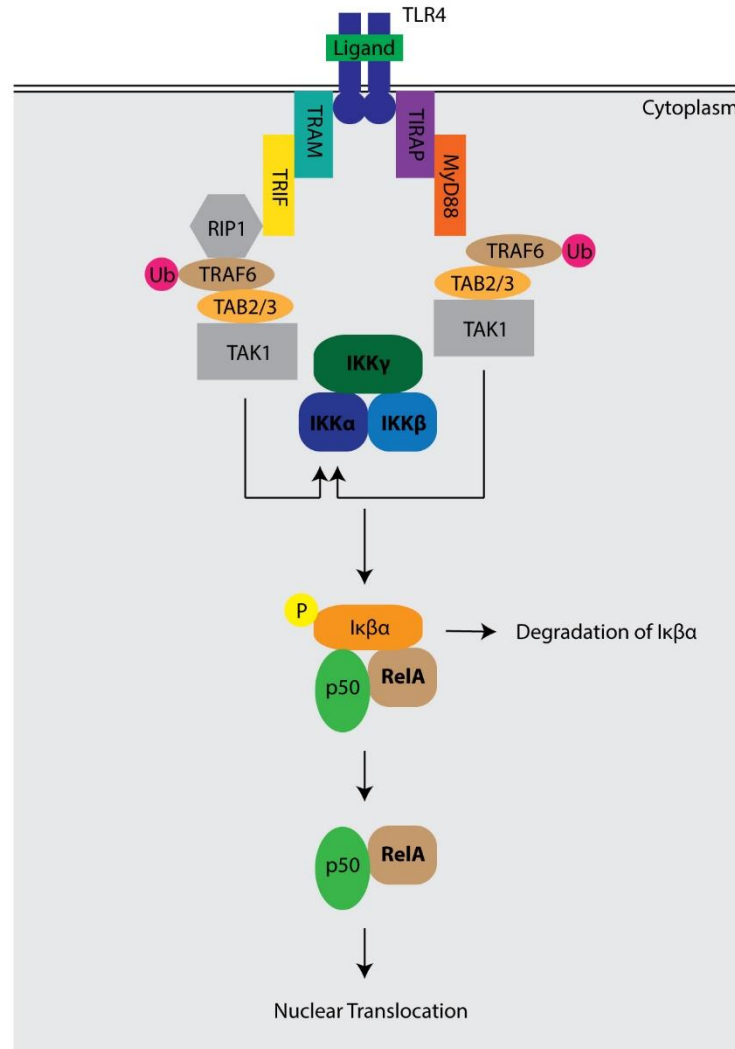


Figure 1.2. Signaling pathway of inflammatory cytokine production by macrophages.

Binding of LPS to TLR4 activates a signalling cascade that results in the downstream phosphorylation of IκBα. This eventually leads to its degradation, which frees the p50-ReIα (NFκB) dimer, which subsequently translocates into the nucleus to initiate the transcription of pro-inflammatory cytokines.

Adapted from (Medzhitov and Horng, 2009)

1.2.3 Molecular targets of H₂S in inflammatory pathways

The interaction of H₂S with membrane ion channels accounts for many of the cellular effects of H₂S. The first reported molecular target for H₂S was the K_{ATP} channel, activation of which causes vasorelaxation (Zhao et al., 2001). Voltage-dependent calcium channels (VDCCs) are also targets for H₂S in several cell types, albeit differing in effect in different cell types. For example, H₂S inhibits L-type VDCC currents in rat cardiomyocytes (Zhang et al., 2012) and mouse pancreatic β -cells (Tang et al., 2013) whereas in neurons, the Cav3.2 T-type VDCC is conversely activated by both exogenous and endogenous H₂S (Maeda et al., 2009; Sekiguchi et al., 2014).

With respect to intracellular inflammatory pathways, H₂S decreases the activation of several transcription factors including NF κ B (Oh et al., 2006) and STAT3 (Li et al., 2008), which control the synthesis of a plethora of downstream pro-inflammatory cytokines and chemokines which contribute to inflammation. NaHS inhibits I κ B α degradation and thus prevents NF κ B from translocating into the nucleus (Pan et al., 2011). The slow-releasing H₂S donor, GYY4137, also reduced NF κ B activation in LPS-stimulated mouse macrophages and Cocksackie virus B3-infected rat cardiomyocytes (Whiteman et al., 2010; Wu et al., 2015). In another study in macrophages *in vitro*, LPS upregulated the expression of CSE and subsequently H₂S formation through the toll-like receptor-4/p38 and NF κ B pathways (Zheng et al., 2013).

Apart from transcription factors, H₂S also affects kinases including those of the p38 MAPK pathway. H₂S attenuates LPS-induced p38 MAPK phosphorylation in BV-2 microglial cells resulting in an anti-inflammatory effect in LPS-stimulated microglial and astrocytes (Hu et al., 2007). An anti-apoptotic

effect of H₂S in human polymorphonuclear leukocytes has also been associated with inhibition of p38 MAPK (Rinaldi et al., 2006).

Similar to the NO-mediated, S-nitrosylation, H₂S can trigger S-sulfhydration of cellular proteins (Mustafa et al., 2009). This may be a natural mechanism by which H₂S alters protein and enzyme functions within the cell. In this process, sulfur from H₂S is added to the thiol groups of cysteine residues to yield a hydropersulfide (-S-SH) moiety (Mustafa et al., 2011). Proteins with the -S-SH group exhibit increased enzyme activity when compared with base cysteines with sulfur in the thiol state. This enhanced activity may translate to an altered state of biological activity. S-sulfhydration affects numerous proteins. The earliest proteins noted to be sulfhydrated by H₂S were glyceraldehyde 3-phosphate dehydrogenase and β -actin (Mustafa et al., 2009). Since then, many other proteins have been found to be sulfhydrated and their functions modulated in this way (Table 1).

To date, three common methods of detecting S-sulfhydration have been used. These are the modified biotin-switch assay and the maleimide assay (Mustafa et al., 2009), as depicted in Figure 1.2. In the modified biotin-switch assay, methyl methanethiosulfonate (MMTS) is used to bind and block free thiols (-SH) and not persulfides (-S-SH). The unreacted persulfides are then conjugated to biotin-HDPD before being immunoprecipitated by streptavidin-coupled beads, which can then be detected and quantified by immunoblotting with an antibody against the protein of interest (Paul and Snyder, 2015). However, the chemical basis for this method has been questioned (Zhang et al., 2014a) as a study has shown that both thiols and persulfides have similar reactivity towards MMTS (Pan and Carroll, 2013). In this study, the authors

reacted MMTS with glutathione persulfide (GSSH) and papain persulfide before analysing the reaction products by mass spectrometry. They detected an increase in the molecular mass of the byproduct that could either be due to MMTS modification (-S-SCH₃) or oxidation of thiols and persulfides to thiosulfate (-SO₃⁻). As the difference in molecular mass between the -S-SCH₃ and -SO₃H group are almost non-distinguishable (difference of only about 2Da), the authors synthesized an analogue of MMTS, S-4-bromobenzyl methanethiosulfonate (BBMTS), which would produce a larger mass change resulting from the thio-BBMTS adduct (+200Da). The reactivity of BBMTS was tested and found to be comparable to that of MMTS. Repeating the reaction between protein persulfides (GSH persulfide, papain persulfide and glutathione peroxidase 3 persulfide) with BBMTS, the authors observed strong mass spectrometry peaks corresponding to persulfide derivatives and concluded that protein persulfides reacts with MMTS and BBMTS reagents.

In the maleimide assay, maleimide which binds selectively with thiol groups irrespective of sulfhydrylation status of the protein of interest, is used. In this method, the protein of interest is isolated by means of immunoprecipitation. Thereafter, treatment of the immunoprecipitated protein with maleimide conjugated with a fluorescent dye enables the protein to be labelled at all sulfhydryl groups. An advantage of using maleimide is that nitrosylated or oxidized groups would not be detected. Next, treatment of the fluorescent-maleimide labelled protein with dithiothreitol (DTT) would cause the cleaving of disulfide bonds from sulfhydrated proteins, but not unmodified ones. Subsequent separation of the fluorescently labelled protein using SDS-PAGE followed by the quantitation of the fluorescent intensity before and after DTT

treatment using an image analyser would indicate the extent of sulfhydrylation of the protein (Paul and Snyder, 2015).

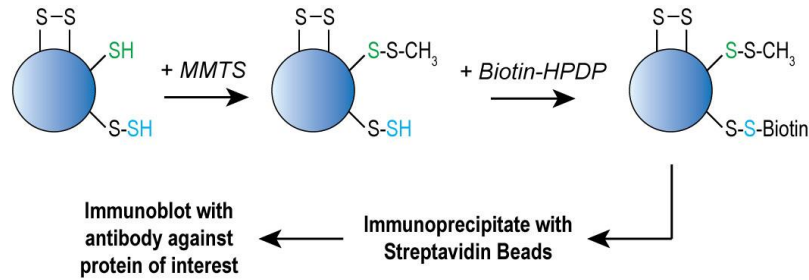
The detection of S-sulfhydrylation in proteins by the red maleimide assay requires the use of the reducing agent DTT. However, there is a lack of clarity on the unspecificity of DTT, such that it can also reduce disulfide bonds in addition to persulfide bonds (Zhang et al., 2014a). As such, a third method known as the tag-switch method was developed as an alternative for the detection of S-sulfhydrylation in proteins. In this method, methylsulfonyl benzothiazole (MSBT) is first used to block and form adducts on all free thiols (-SH) and persulfides (-SSH) in the protein of interest. As these two types of adducts have different reactivity towards nucleophiles, the adduct formed from thiols (-S-MBST) would be unreactive. The adduct formed from the persulfide (-S-S-MBST) can instead react with a cyanoacetate-based CN-biotin compound, hence 'switching the tag' from the persulfide adduct (-S-S-MBST) to the biotin tag (-S-CN-biotin). With the biotin tag, the presence of persulfides on the protein of interest can be detected by streptavidin tagged with a fluorophore (Park et al., 2015).

Table 1.1 Proteins modified by S-sulphydration

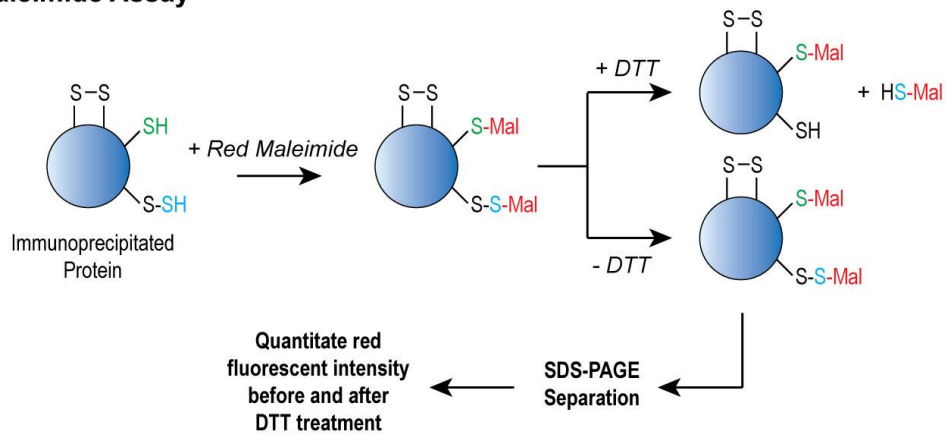
Modified Proteins	References
Glyceraldehyde 3-phosphate dehydrogenase	(Mustafa et al., 2009)
β -Actin	(Mustafa et al., 2009)
Protein Tyrosine Phosphatase 1B (PTP1B)	(Krishnan et al., 2011)
Kir6.1 subunit of ATP-sensitive potassium channel	(Mustafa et al., 2011)
p65 subunit of NF κ B	(Sen et al., 2012)
Parkin	(Vandiver et al., 2013)
Keap1	(Yang et al., 2013)
MEK1	(Zhao et al., 2014)
p66Shc	(Xie et al., 2014)
TRP channels	(Liu et al., 2014)
Pyruvate carboxylase	(Ju et al., 2015)
α subunit (ATP5A1) of ATP synthase	(Modis et al., 2016)
Transcription factor Specificity Protein 1 (SP1)	(Saha et al., 2016)

Adapted from (Paul and Snyder, 2015)

Modified Biotin-Switch Assay



Maleimide Assay



$$\% \text{ sulfhydrated protein} = \frac{\text{Red fluorescent intensity of protein before DTT treatment} - \text{Red fluorescent intensity of protein after DTT treatment}}{\text{Total level of protein (input)}} \times 100\%$$

Figure 1.3 Current strategies for detecting protein sulfhydration.

Illustration depicting a protein with disulfide bonds (S-S), unmodified cysteine (-SH) and hydropersulfide moiety (-S-SH), treated with methyl methanethiosulfonate (MMTS), red maleimide (-Mal) and dithiothreitol (DTT). The formula for quantitating sulfhydrated proteins using the maleimide assay is shown in the lower panel.

1.3 NLRP3 inflammasome

1.3.1 NLRP3 inflammasome in health and disease

Although the transcription and translation of IL-1 β and IL-18 are downstream of NF κ B activation, both IL-1 β and IL-18 within the cell exist as non-secreted pro-forms. For them to be proteolytically cleaved and activated as the secreted form, caspase-1, which is produced in cells as a catalytically inactive zymogen is required. Secreted IL-1 β and IL-18 are potent pyrogens which, when released systemically, initiate numerous downstream cascades and affect many other immune cells. IL-1 β generates systemic and local responses to infection and injury by causing fever via COX-2 enzyme induction. IL-1 β also activates lymphocytes and promotes leukocyte infiltration at sites of infection and injury. Dysregulation of IL-1 β genetics can be found in patients with periodic fever syndrome or in cryopyrin associated periodic syndrome (CAPS), an autoinflammatory syndrome (Sims and Smith, 2010). IL-18 also has wide systemic effects by inducing IFN- γ production which then increases natural killer cells, CD8+ T cell and macrophage activity, as well as upregulating iNOS enzyme and IgG2 production from plasma B cells (Dinarello, 2009; Sims and Smith, 2010). Due to the widespread systemic effects of IL-1 β and IL-18, regulation of its release needs to be tightly controlled.

For IL-1 β and IL-18 to be released in their active secretable forms, proteolytic processing by the inflammasome complex is required. The inflammasomes are multimeric protein complexes that comprise an inflammasome sensor molecule, an adaptor protein encoded by the PYD and CARD domain containing (*PYCARD*) gene which is common to all types of inflammasomes and is also known as the apoptosis-associated speck-like

protein with a caspase-recruitment domain protein (ASC), and pro caspase-1, which is cleaved from its immature (pro-) form to a catalytic active form (p20/p10) also upon the formation of the inflammasome (Martinon et al., 2002). Co-localization of these 3 components results in the triggering of the inflammasome complex and subsequent activation of caspase-1.

The activation of the NLRP3 inflammasome requires two signals (Fig 1.3). The first signal, known as the priming signal, is mediated by NF κ B which, through stimulation of TLRs, pro-IL-1 β , pro-IL-18 and the nucleotide-binding oligomerization domain (NOD)-like receptor (NLR) sensor molecule of the inflammasome, are transcribed and subsequently translated. The priming signal also induces the deubiquitination of NLRP3 by the deubiquitinating enzyme BRCC3, which is required for NLRP3 inflammasome activation (Guo et al., 2015; Py et al., 2013) However, it is the second signal which ultimately switches on the inflammasome, and this is triggered by a plethora of substances or agonists that are present during tissue damage or an infection (summarised in Table 1.2) with different substances activating specific nucleotide-binding oligomerization domain receptors or in short, NLR sensor molecules. These include the NLRP1 (NOD-, Leucine rich repeats (LRR)-, and pyrin domain-containing 1), NLRP3, NLRP6, NLRP7, NLRP12 or NLRC4 which is also known as IPAF. Two other inflammasomes that do not contain NLR but instead contain the pyrin and HIN domain-containing protein (PYHIN) include absent in melanoma 2 (AIM2) and IFN γ -inducible protein 16 (IFI16) (Latz et al., 2013).

The best characterized inflammasome is the NLRP3 inflammasome. This is activated by a wide range of stimuli and is implicated in an array of

diseases including bacterial infection (Mariathasan et al., 2006), gout (Martinon et al., 2006), atherosclerosis (Düwell et al., 2010), Alzheimer's disease (Heneka et al., 2013), asbestosis (Hillegass et al., 2013) and diabetes (Jourdan et al., 2013).

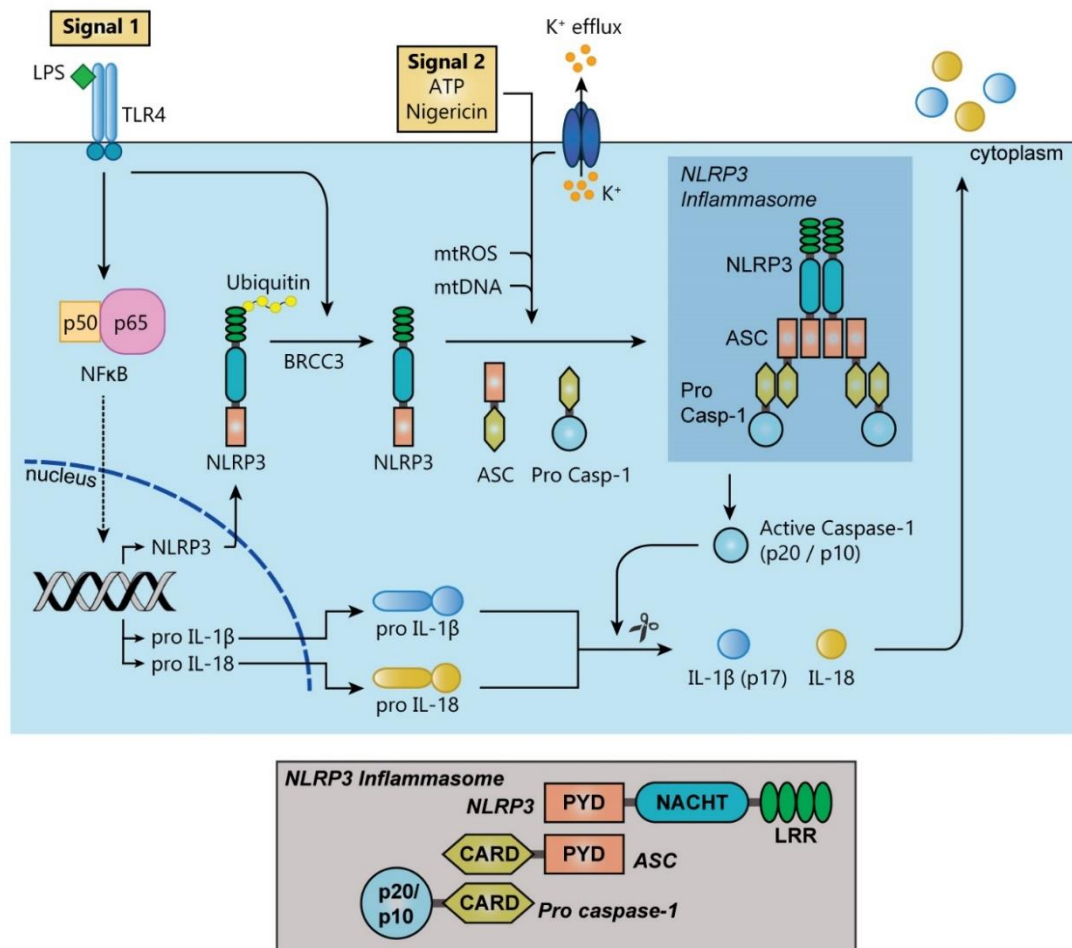


Figure 1.4 Mechanisms of NLRP3 inflammasome activation

NLRP3 inflammasome activation requires two signals. The first priming signal involves an NFκB activating signal triggered by stimuli such as lipopolysaccharide (LPS) activating Toll-like receptor 4 (TLR4), leading to the transcription and translation of NLRP3, pro IL-1β and pro IL-18. The priming signal also induces deubiquitination of NLRP3 by BRCC3. The second activating signal is initiated by NLRP3 agonists such as extracellular ATP and the pore-forming toxin, nigericin. These agonists provide a second signal in the form of mitochondrial reactive oxygen species (mtROS), mitochondrial DNA (mtDNA) in the cytoplasm and K⁺ efflux. Activation of the NLRP3 inflammasome leads to maturation of pro caspase-1 into active caspase-1. Active casase-1 then cleaves pro IL-1β and pro IL-18, thereby releasing IL-1β and IL-18 out of the cell. The NLRP3 inflammasome comprises of the NLRP3, ASC and pro caspase-1 proteins. LRR, leucine-rich repeat; NACHT, nucleotide-binding and oligomerization domain; PYD, pyrin; CARD, caspase recruitment domain.

Table 1.2 Regulatory receptors of the inflammasomes and their agonists

Agonist	NOD-like Receptor (NLR) / PYHIN	Disease/Condition/Functions	References
Muramyl dipeptide (MDP)	NLRP1	Bacterial infections	(Faustin et al., 2007)
Anthrax Toxin	NLRP1	<i>Bacillus anthracis</i> infections	(Levinsohn et al., 2012)
ATP	NLRP3	Extracellular ATP in cancer, graft-versus-host disease, hypersensitivity, sterile inflammation	(Mariathasan et al., 2006)
		Extracellular ATP from apoptotic and necrotic cells as a 'danger signal'	
Nigericin	NLRP3	Microbial toxin from <i>Streptomyces hygroscopicus</i>	(Mariathasan et al., 2006)
β Amyloid	NLRP3	Alzheimer's disease	(Heneka et al., 2013)
Asbestos	NLRP3	Asbestosis	(Hillegass et al., 2013)
Alum	NLRP3	Aluminium adjuvants	(Franchi and Núñez, 2008)
Cholesterol	NLRP3	Cardiovascular disease	(Düwell et al., 2010)
Silica	NLRP3	Silicosis	(Peeters et al., 2013)
Monosodium Urate Crystals	NLRP3	Gout	(Martinon et al., 2006)
Microbial metabolites	NLRP6	Maintenance of bacterial homeostasis in the gut	(Levy et al., 2017)
Microbial acylated lipopeptides	NLRP7	<i>Mycoplasma</i> spp. infections	(Khare et al., 2012)
<i>Yersinia pestis</i>	NLRP12	Bubonic plagues	(Vladimer et al., 2012)
<i>Salmonella</i> or <i>Pseudomonas</i>	NLRC4 / IPAF	Bacterial infections	(Franchi et al., 2012)

Double stranded DNA (dsDNA)	AIM2	Virus infection, cytoplasmic DNA	(Fernandes-Alnemri et al., 2009)
Herpesvirus (KSHV)	IF16	Kaposi sarcoma	(Kerur et al., 2011)

1.3.2 Pyroptosis

Besides converting IL-1 β and IL-18 from the pro-form to the active secreted form, the inflammasome has also been implicated in an inflammatory and programmed form of cell death known as pyroptosis (Fernandes-Alnemri et al., 2007; Sharma and Kanneganti, 2016). During pyroptosis, the cell membrane ruptures and release intracellular pro-inflammatory contents into the microenvironment (Bergsbaken and Cookson, 2007; Chen et al., 1996). This is in contrast to apoptosis, in which the cell membrane remains intact during blebbing, thus resulting in a non-inflammatory form of cell death. Active caspase-1 is central to initiating pyroptosis as it forms ion-permeable pores in the plasma membrane (Fink and Cookson, 2006). Although caspase-1 activation is linked to the maturation of IL-1 β and IL-18, it is still not clear whether all cells in which the inflammasome is activated, undergo pyroptotic cell death (Duprez et al., 2009). During pyroptosis, a pyroptosome is formed. This occurs when there is oligomerization of the adaptor protein ASC to form a supramolecular assembly of ASC which recruits and activates pro-caspase-1 (Fernandes-Alnemri and Alnemri, 2008; Fernandes-Alnemri et al., 2007). This can be visualized as an ASC speck, one per cell.

Beyond pyroptosis, it was reported that the NLRP3 inflammasome, upon activation of caspase-1, oligomerizes and is released from macrophages (Baroja-Mazo et al., 2014). These speck-like particles trigger caspase-1

activation extracellularly and intracellularly during phagocytosis by macrophages in the vicinity. The presence of such ASC particles in the serum of patients with cryopyrin-associated periodic syndromes (CAPS) further supports the claim that pyroptosis perpetuates inflammation beyond inflammasome-mediated secretion of IL-1 β and IL-18. Another study (Franklin et al., 2014) showed that inflammasome activation triggered ASC polymerization to form ASC specks. However, these specks, when released after pyroptotic cell death, could also trigger further maturation of IL-1 β extracellularly. Uptake of extracellular ASC specks by macrophages augmented the inflammation by inducing lysosomal damage, nucleation of soluble ASC and activation of IL-1 β in recipient cells. These findings implicate the ASC speck as, not only an inflammatory mechanism found intracellularly, but also, potentially as a form of cell-to-cell communication.

In light of these findings, the ASC speck is likely to be an inflammatory signal causing pyroptosis and initiating IL-1 β secretion from the host macrophage as well as the recipient macrophage when it is released from the cell. However, it remains unclear whether the previously described pyroptososome is indeed the inflammasome or whether the two entities are distinct and independent of each other.

1.3.3 Molecular mechanisms governing NLRP3 inflammasome activation

NLRP3 is the best characterized inflammasome sensor protein. Many molecular mechanisms governing its activation have been proposed to date. Despite the numerous studies performed, the exact role of each suggested mechanism remains inconclusive, and perhaps multiple mechanisms may be concurrently activated leading to caspase-1 maturation and subsequently, IL-1 β and IL-18 secretion. Moreover, determining which mechanism precedes or acts independently of the other has proved to be a great challenge and is still a matter of contention. While there is consensus that activation of the NLRP3 inflammasome requires two separate signals, reports in recent years have highlighted the role of post-transcriptional modification of both signal 1 and 2 to be pivotal events in NLRP3 inflammasome activation (Ghonime et al., 2014; Juliana et al., 2012; Py et al., 2013).

Two very commonly used inducers of the NLRP3 inflammasome are adenosine triphosphate (ATP) and the bacterial toxin, nigericin. Extracellular ATP, which physiologically is derived from neighbouring injured cells, binds to the purinoceptor P2X₇. Upon binding of ATP, the cation channel opens leading to cell depolarization. Nigericin, a potassium ionophore activates NLRP3 by a mechanism involving pannexin-1 dependent potassium (K⁺) efflux (Mariathasan et al., 2006). Lysosomal membrane damage caused by phagocytosis of particulate matter such as amyloid β , silica crystals and aluminium salts, leading to the release of cathepsin B into the cytosol has also been linked to NLRP3 inflammasome activation (Halle et al., 2008; Hornung et al., 2008). Extracellular calcium ions (Ca²⁺) have previously been shown to be an NLRP3 activator (Lee et al., 2012). However, a recent study provided

contrary evidence to this, showing that the Ca^{2+} influx which occurs when the NLRP3 inflammasome is activated occurs downstream of the caspase-1 activation cascade. Moreover, these authors found that the increased cytosolic Ca^{2+} induced by Ca^{2+} ionophore was not a sufficient signal for NLRP3 inflammasome (Katsnelson et al., 2015). In trying to find a model to unify the seemingly different stimuli governing NLRP3 inflammasome activation, it was proposed that K^+ efflux is the common trigger governing NLRP3 inflammasome stemming from ATP, nigericin, cathepsin B and Ca^{2+} signaling (Muñoz-Planillo et al., 2013), re-affirming similar findings described in an earlier study done in 1994 (Perregaux and Gabel, 1994).

The involvement of mitochondria in NLRP3 inflammasome activation has also received much attention. In a landmark paper, the role of the mitochondria in NLRP3 inflammasome activation was first established (Zhou et al., 2011). Thereafter, different groups have advanced the idea that reactive oxygen species (ROS) derived from mitochondrial perturbations (mtROS) or otherwise due to various 'signal 2' stimuli lead to the activation of the NLRP3 inflammasome. mtROS was shown to induce NLRP3-dependent lysosomal damage leading to inflammasome activation (Heid et al., 2013). The plasma membrane cation channel TRPM2 and the tripartite-motif protein 30 (TRIM30) have also been found to regulate NLRP3 inflammasome activation by modulating ROS production (Hu et al., 2010; Zhong et al., 2013). More recently, resveratrol was shown to suppress mitochondrial damage and thereby inhibited the activation of the NLRP3 inflammasome (Chang et al., 2015). NF κ B, while being a key activator for inflammation, impairs inflammation by restricting

inflammasome activation via the elimination of damaged mitochondria, specifically by the NF κ B-p62-mitophagy pathway (Zhong et al., 2016).

In contrast, some have suggested that ROS production in the process of NLRP3-triggered inflammation falls upstream of NLRP3 induction, and not during activation (Bauernfeind et al., 2011; Won et al., 2015). Others have also failed to replicate experiments involving the activation of the NLRP3 inflammasome by mtROS (Muñoz-Planillo et al., 2013; Won et al., 2015) as shown by Zhou et al. (Zhou et al., 2011), hence casting doubt on the veracity of previously published data.

Lastly, mitochondrial DNA (mtDNA) linked to disrupted mitochondria integrity have also been implicated in the activation of the NLRP3 inflammasome. The depletion of autophagic proteins lead to the build-up of dysfunctional mitochondria and cytosolic mtDNA in the cytoplasm. It has been reported that the cytoplasmic accumulation of mtDNA depended on NLRP3 inflammasome and mtROS (Nakahira et al., 2011). In another study, oxidized mtDNA released from bone marrow derived macrophages (BMDMs) stimulated with LPS and ATP bound to and localized with NLRP3, thereby activating the NLRP3 inflammasome. Moreover, mtDNA deficient macrophages in this study did not secrete IL-1 β despite being stimulated with NLRP3 inflammasome activators, strongly suggesting that oxidized mtDNA activates the NLRP3 inflammasome (Shimada et al., 2012).

The molecular mechanisms governing NLRP3 inflammasome activation are complex. In the last decade, various studies have implicated K⁺ efflux, Ca²⁺ influx, mtROS and mtDNA as molecular events behind the 'signal 2' ATP or nigericin stimulus. However, conflicting opinions as to whether some or all of

these mechanisms are essential for inflammasome activation still exists. Hence, successfully integrating all these signals together to achieve a unifying model should be the next goal for a clearer understanding of how the NLRP3 inflammasome is activated.

1.3.4 Effects of gasotransmitters on the NLRP3 inflammasome

Nitric oxide (NO), which is produced by the enzyme inducible nitric oxide synthase (iNOS), was the first gasotransmitter reported to inhibit NLRP3 inflammasome activation (Hernandez-Cuellar et al., 2012). The authors observed S-nitrosylation of the NLRP3 protein in macrophages treated with the NO donor S-Nitroso-N-Acetyl-D,L-Penicillamine (SNAP), and hence suggested that this post-translational modification may have accounted for the observed inhibition of NLRP3 inflammasome activation. When considering the role of NO in affecting mtROS production induced by LPS and ATP, the authors found that SNAP only modestly reduced mtROS production. Thus, they effectively dismissed the reduction in mtROS as the mechanism of action (Hernandez-Cuellar et al., 2012). In a later study, the effects of NO in controlling NLRP3 inflammasome activation in a mouse model of tuberculosis was described. These authors reported that NO inhibited the assembly of the NLRP3 inflammasome due to thiol nitrosylation of NLRP3 (Mishra et al., 2013). Subsequently, NO was shown to inhibit NLRP3 activation in macrophages both *in vitro* and in a mouse model of LPS-induced septic shock (Mao et al., 2013). While the involvement of mtROS presented in this work contrasts with a previous study (Hernandez-Cuellar et al., 2012), it is important to note that the conclusions derived in (Hernandez-Cuellar et al., 2012) was based on the effects of exogenous NO on NLRP3 inflammasome activation whereas the conclusions in (Mao et al., 2013) derive from the study of endogenous NO.

The second and final gasotransmitter reported to have an antagonistic effect on NLRP3 inflammasome activation is carbon monoxide (CO). CO, which is produced endogenously as a byproduct of heme oxygenase-1 (HO-1)

catalysed heme catabolism inhibits mitochondrial ROS production, reduced mitochondrial membrane potential and translocation of mitochondrial DNA to the cytoplasm in macrophages stimulated with LPS and ATP. This was concurrent with the inhibition of NLRP3 inflammasome mediated caspase-1 activation, and IL-1 β and IL-18 secretion (Jung et al., 2015) .

1.4 Aims of Current Research

It is becoming increasingly clear that endogenous H₂S plays multiple roles in the inflammatory process. However, whether exogenous H₂S generated by either fast or slow H₂S donor drugs, exhibits anti-inflammatory activity and can thence be used therapeutically remains unclear. Numerous factors likely determine the overall effect of H₂S donors in inflammation. These include the dose and timing of administration of the donor as well as the choice of H₂S donor. Thus, a 'fast releasing donor' will lead to large but transient increases in concentrations of H₂S within the body whilst a 'slow-releasing donor' will expose cells to much lower concentrations of the gas over a more prolonged time period. Considerations such as these will likely be critical in determining whether an H₂S donor exacerbates or dampens inflammation.

Classically activated macrophages play a key role in initiating the inflammatory cascade via secretion of a multitude of pro-inflammatory mediators. As such, the initial aim of the present research was to determine whether H₂S, generated by a 'fast releasing' donor inhibits or promotes the release of pro-inflammatory mediators (TNF α , IL-6, PGE₂ and NO) from macrophages in cell culture. Thereafter, using a CRISPR approach to knock down the H₂S synthesizing enzyme, CSE, in macrophages, we sought to investigate the significance of CSE in regulating the release of pro-inflammatory mediators from macrophages and determining whether exogenous H₂S was able to reverse the effect.

The current literature supports the possibility that slow-releasing H₂S donors are anti-inflammatory and therapeutically compatible. Thus, a further aim of this work was to screen and subsequently characterize novel slow H₂S-

releasing donors exhibiting anti-inflammatory properties in activated macrophages and in intact animals *in vivo*.

The NLRP3 inflammasome activation pathway has received much attention and scrutiny by immunologists in the last decade. It is now clear that the NLRP3 inflammasome is a crucial 'gatekeeper' of IL-1 β and IL-18 secretion in a wide range of sterile and non-sterile inflammatory conditions. Moreover, other gasotransmitters including CO and NO have recently been found to exert some form of control over the activation of the NLRP3 inflammasome. The final aim of the current research was therefore to investigate whether H₂S also affects the function of the NLRP3 inflammasome and if so, the molecular mechanism by which it acts.

CHAPTER 2: MATERIALS & METHODS

2.1 Cell culture

RAW264.7, J774A.1 and HEK293T cells from the American Type Culture Collection (ATCC) were cultured in Dulbecco's Modified Eagle's Medium (DMEM) (Gibco) supplemented with 10% v/v heat inactivated fetal bovine serum (FBS) (Gibco), L-glutamine (4mM), sodium pyruvate (1mM), HEPES buffer (20mM) (Hyclone), penicillin (100 U/ml) and streptomycin (100µg/ml). RAW264.7 and J774A.1 cells were cultured in non-tissue culture treated petri dishes (Biomed) and HEK293T cells were cultured in tissue culture treated dishes (NUNC). All cell lines were maintained at 37°C in a 5% CO₂ humidified environment.

2.2 Mice

Male C57BL/6 mice (20-25g, 6-10 weeks) were maintained in the Comparative Medicine Department of this University. All animal experiments were approved by the Institutional Advisory Care and Use Committee (IACUC) of the National University of Singapore (protocol numbers 108/11 and R14-1388). Mice were killed by exposure to an increasing concentration of CO₂. Blood was obtained by cardiac puncture, collected in plasma separator tubes with lithium heparin (BD microtainer) and centrifuged (5000 rpm, 10 min, 4°C) to prepare plasma which was stored at -80°C for cytokine analysis. Peritoneal cavities of mice were lavaged with 5ml ice cold sterile PBS and centrifuged to remove any cells. The lavage fluid was stored at -80°C for subsequent cytokine analysis.

2.3 Treatments on LPS-stimulated RAW264.7 macrophages

RAW264.7 cells were seeded in 24-well cell culture treated plates (NUNC) at a density of 2×10^5 cells per well or in 6 well cell culture treated plates at a density of 1×10^6 cells per well in DMEM supplemented with 10% v/v FBS the day before the experiment was carried out. Cells were pretreated with NaHS (200 μ M or 500 μ M) (Sigma-Aldrich Ltd.) 30 min prior to a 6 h stimulation with lipopolysaccharide (1 μ g/ml) from *E. coli* (0111:B4) (Sigma-Aldrich Ltd.) with or without 2 additional doses of NaHS (200 μ M or 500 μ M) at subsequent 2 h intervals. Time expired NaHS (tx-NaHS) was prepared by dissolving NaHS in cell culture media and left exposed to air in a sterile environment overnight. In some experiments, vitamin B_{12a} (Sigma-Aldrich Ltd.) was added into the cell culture media together with the H₂S releasing compound.

2.4 CRISPR plasmid synthesis and knock-down of genes

The CRISPR plasmid pSpCas9(BB)-2A-GFP (PX458) (Ran et al., 2013) was purchased from Addgene (plasmid #48138). PX458 was linearized with *BbsI* fast restriction digest enzyme (Thermo Scientific Ltd.). Guide RNAs (gRNAs) were designed by the CRISPR Design Tool (crispr.mit.edu) and commercially synthesized (AITbiotech). The forward and reverse sgRNAs were annealed in CutSmart™ buffer (New England Biolabs) by incubation in a 95°C water bath and left to cool till room temperature. Annealed sgRNA and the linearized plasmid was ligated with T4 DNA ligase (Thermo Scientific Ltd.) for 2 h at 22°C. Resulting plasmids were sequenced to ensure successful ligation. RAW264.7 cells were then transfected with 2.5 μ g of CRISPR plasmid using Lipofectamine 3000 (Life Technologies Ltd.) in accordance to the manufacturer's protocol. 24

h after transfection, GFP positive cells were sorted with MoFlo™ cell sorter (Beckman Coulter) into single colonies in a 96-well cell culture treated plate (NUNC). Single colonies that grew were expanded and screened for CSE using immunoblotting. The sequence of the sgRNA used is Mouse CSE: 5'-GCAATGGAATTCTCGTGCCG -3'.

2.5 Preliminary screening of novel H₂S releasing drug compounds

RAW264.7 cells were seeded in 96 well cell culture treated plates (NUNC) at a density of 3.5×10^4 cells per well in DMEM supplemented with 10% FBS the day before experiments were carried out. Cells were treated with varying concentrations of test compounds 30 min prior to a 24 h stimulation with lipopolysaccharide (1µg/ml) from *E. coli* (0111:B4) (Sigma-Aldrich Ltd.). Test compounds were dissolved in dimethyl sulfoxide (DMSO) (Sigma-Aldrich Ltd.) at a final concentration of 0.5% v/v. Subsequent experiments utilised a vehicle control at an identical concentration (v/v). Supernatant was collected for analysis by ELISA thereafter.

2.6 *In vitro* microplate assay of H₂S in RAW264.7 cells using a fluorescent probe

Lyophilized H₂S fluorescent probe (A near infrared (NIR)-fluorescent probe based on a Cu²⁺-cyclen complex linked to a NIR light-emitting BODIPY fluorophore) (Wu et al., 2014a) was prepared by reconstitution in dichloromethane (100µl) by mixing with DoTaP (Avanti polar lipids, Inc.) liposome. Argon gas was used to evaporate the mixture followed by removal of organic solvent with a vacuum pump. The probe was then dissolved in

deionized water and diluted in cell culture media for use. RAW264.7 cells (5×10^5) were plated in a 96 well culture plate overnight. The fluorescent probe ($20\mu\text{M}$) was added and cells were incubated (3 h, 37°C), washed with phosphate buffered saline (PBS) and exogenous H_2S donors added at the indicated concentrations indicated in results section. Fluorescence was read at ex620/em680 using a Synergy H1 microplate reader (Biotek).

2.7 Measurement of cell death

Cell death was quantitated by the MTT assay kit (Sigma-Aldrich Ltd.). Briefly, 5×10^4 RAW264.7 or BMDM cells were plated in a 96 well tissue culture treated plate overnight. The next day, the cells were treated with varying concentrations of H_2S donors (as indicated in the results section) with or without LPS ($1\mu\text{g/ml}$). Thereafter, supernatant was removed and cells were washed once with sterile PBS before the MTT assay was performed on the cells in accordance with the manufacturer's protocol. Briefly, MTT was added to fresh cell culture media at a final concentration of 10% v/v. $100\mu\text{l}$ of this mixture was added to each 96-well and incubated for 3 h at 37°C . Following which, $100\mu\text{l}$ of MTT solubilization solution was added to each 96-well and mixed well by pipetting up and down. Data was obtained by spectrophotometrically measuring the absorbance at 570nm. Background absorbance was measured at 690nm and subtracted from the 570nm measurement.

2.8 mRNA extraction, reverse transcription-polymerase chain reaction (RT-PCR) and quantitative real-time PCR (qPCR)

RAW264.7 cells treated with FW1256 (200 μ M, 30 min) followed by LPS (1 μ g/ml, 24 h) were washed with ice cold PBS and incubated with TRIzol reagent (Invitrogen). Total RNA was extracted using Aurum Total RNA Mini Kits (Bio-Rad). Briefly, cells were lysed with 1ml TRIzol for 5 min at room temperature and mixed with chloroform (200 μ M, 5 min) at room temperature, before being centrifuged (12,000 g, 15 min, 4°C). Following centrifugation, the aqueous phase was recovered without disturbing the interface. An equal amount of 70% ethanol v/v was added to the aqueous phase and passed through the RNA binding column via centrifugation (14,000 g, 1 min). Contaminating genomic DNA was removed by incubating the column with DNase I (15 min, room temperature). The column was then washed with high and low stringency wash buffers, before RNA was eluted from the column. 1 μ g of total RNA was reverse-transcribed into cDNA using an iScript cDNA Synthesis kit (Bio-Rad), according to the manufacturer's protocol. Relative quantitative real-time PCR was performed by administering 3 μ l of cDNA, 2 μ l of primers and 5 μ l of the reaction mix buffer from the Power SYBR Green PCR master mix kit (Life Technologies). The amplification reaction was performed using a ViiA7 qPCR thermal cycler (Applied Biosystem). The thermocycling parameters were 50°C (2 min), 95°C (10 min) followed by 40 cycles of 95°C (15 sec), 60°C (1 min) and 95°C (15 sec). Expression values were determined by 2- $\Delta\Delta$ CT equation and normalized with GAPDH housekeeping gene. Samples prepared without RNA served as negative controls. The primers used were:

Mouse iNOS FP 5'-GGCAGCCTGTGAGACCTTTG-3',

mouse iNOS RP 5'-GCATTGGAAGTGAAGCGTTTC-3',
mouse COX-2 FP 5'-TTGAAGACCAGGAGTACAGC-3',
mouse COX-2 RP 5'-GGTACAGTTCCATGACATCG-3',
mouse IL-1 β FP 5'-GCCCATCCTCTGTGACTCAT-3',
mouse IL-1 β RP: 5'-TTGAAGAGAACCTGGGAGTA-3',
mouse GAPDH FP 5'-TGCACCACCAACTGCTTAGC-3',
mouse GAPDH RP 5'-GCATGGACTGTGGTCATGAG-3'

2.9 Cell cytoplasmic and nuclear extraction

Cytoplasmic and nuclear extracts from PBS-washed RAW264.7 cells were separated using the MinuteTM cytoplasmic and nuclear extraction kit (Invent Biotechnologies) according to the manufacturer's protocol, before being used for immunoblot analysis as described in section 2.18. Briefly, cells were washed with PBS before being lysed on ice for 5 min with cytoplasmic extraction buffer. The cell extract was vortexed for 15 sec before being centrifuged (14,000 g, 5 min, 4°C). The supernatant (cytosolic fraction) was transferred to a new tube while the pellet which contains the nucleus was resuspended with nuclear extraction buffer. The resuspended pellet was vortexed for 15 sec followed by incubation on ice for 1 min. This was repeated 4 times. Following which, the resuspended pellet was transferred to a pre-chilled filter cartridge with collection tube (provided in the kit) and centrifuged (14,000 g, 30 sec, 4°C). The filter cartridge was discarded while the eluent containing the nuclear fraction was stored in -80°C for further analysis.

2.10 Differentiation of bone marrow-derived macrophages (BMDMs)

Bone marrow cells were flushed from the tibia and femur bones of male C57BL/6 mice of age 6-10 weeks old in a sterile environment. Bone marrow cells were differentiated into macrophages in non-cell culture treated petri dishes (Biomedica) using DMEM containing 10% FBS supplemented with 10% v/v conditioned media from L929 mouse fibroblast for 6 days, with a change of media on day 3 (Mishra et al., 2013).

2.11 Flow cytometry

Cells were gently scrapped from cell culture plates after treatment as indicated in the results section and centrifuged (1500 rpm, 5 min, 4°C) before being resuspended in 300 µl of PBS supplemented with FCS (1% v/v) and PI (0.075mg/ml) (Sigma-Aldrich Ltd.). The data was acquired with LSR-Fortessa (BD Biosciences) and analyzed using FlowJo analytical software (TreeStar).

2.12 Inflammasome activation

J774A.1 cells or BMDMs were seeded in 96-well or 6-well cell culture treated plates at a density of 5×10^4 cells or 2×10^6 cells per well respectively in DMEM supplemented with 10% v/v FBS the day before experiments were carried out. BMDMs were stimulated with LPS (1µg/ml) for 4 h. Freshly prepared NaHS (Sigma-Aldrich Ltd.) or time-expired NaHS (tx-NaHS) was added at the indicated dose (200, 400 or 600µM, 30 min) before ATP (5mM) (Sigma-Aldrich Ltd.) or nigericin (10µM) (Sigma-Aldrich Ltd.) was added for 30 min or 1 h respectively. After inflammasome activation, supernatant was collected for

analysis by ELISA, and cells were lysed on ice for immunoblotting as indicated in section 2.18 of the materials & methods.

2.13 ASC pyroptosome detection

BMDMs were seeded in 6-well plates at 2×10^6 cells per well overnight and treated with LPS (1 μ g/ml) for 4 h the next day. Next, freshly prepared NaHS (Sigma-Aldrich Ltd.) or time expired NaHS (tx-NaHS) (600 μ M) was added for 30 min before ATP (5mM) (Sigma-Aldrich Ltd.) was added for another 30 min. The cells were gently scraped on ice and pelleted by centrifugation (1500 rpm, 5 min, 4°C) before being resuspended in 500 μ l cold lysis phosphate-buffered saline (PBS) containing HEPES-KOH (20mM, pH 7.5), KCl (150mM), 1% v/v Triton-X, PMSF (0.1mM) with protease and phosphatase inhibitors. Cells were lysed by shearing 10 times through a 21-gauge needle and the lysates were centrifuged (5000 g, 10min, 4°C). The resultant pellets were washed twice with 500 μ l PBS and finally resuspended in 500 μ l PBS. Resuspended pellets were cross-linked with freshly prepared disuccinimidyl suberate (2mM, 30 min, room temperature) (Sigma-Aldrich Ltd.) and then centrifuged (5000 g, 10min, 4°C). The cross-linked pellets and lysates were resuspended in 30 μ l of laemmli sample buffer with 10% v/v β -mercaptoethanol, boiled for 5 min at 95°C, before being resolved by 10% SDS-PAGE and immunoblotted using anti-mouse ASC antibodies.

2.14 Overexpression plasmid synthesis

Mouse BMDMs treated with LPS (1µg/ml, 24 h) were washed with ice cold PBS and incubated with TRIzol reagent (Invitrogen). Total RNA was extracted using Aurum Total RNA Mini Kits (Bio-Rad). Total RNA was reversed-transcribed into cDNA using the GoScript Reverse Transcription System (Promega) according to the manufacturer's instructions. cDNA of mouse IL-1β, NLRP3, ASC, Caspase-1 and CSE were cloned from mouse BMDM mRNA with the following forward (FP) and reverse (RP) primer sequences, using the Q5 Hot Start High-Fidelity DNA Polymerase (New England BioLabs), according to the manufacturer's instructions. Briefly, a PCR mixture containing 25ng template DNA and 1X Q5 Hot Start High-Fidelity master mix was carried out using a final concentration of 0.5µM forward and reverse primers. Mouse IL-1β FP 5'-ATACGAGCTAGCATGGCAACTGTTCCTGAA-3', mouse IL-1β RP 5'-AGCATAGCGGCCGCTTAGGAAGACACGGATTC-3', mouse NLRP3 FP 5'-ATACGAGCTAGCATGACGAGTGTCCTGTTGC-3', mouse NLRP3 RP 5'-AGCATAGCGGCCGCCTACCAGGAAATCTCGAA-3', mouse ASC FP 5'-ATACGAGCTAGCATGGGGCGGGCACGAGAT-3', mouse ASC RP 5'-AGCATAGCGGCCGCTCAGCTCTGCTCCAGGTC-3', mouse Caspase-1 FP 5'-ATACGAGCTAGCATGGCTGACAAGATCCTG-3', mouse Caspase-1 RP 5'-AGCATAGCGGCCGCTTAATGTCCCGGAAGA-3', mouse CSE FP 5'-ATACGAGCTAGCATGCAGAAGGACGCCTCT-3', mouse CSE RP 5'-AGCATAGCGGCCGCTTAAGGGTGCGCTGCCTT-3'.

The overexpression plasmid pcDNA3.1(+) and cloned inserts were digested with *NheI*-HF and *NotI*-HF (New England BioLabs) (16 h, 37°C) before being ligated using T4 DNA ligase (Thermo Scientific) (2 h, 22°C).

To synthesize the HA-tagged NLRP3 overexpression plasmid, the HA epitope (YPYDVPDYA) was inserted into the N-terminus region of NLRP3 in the pcDNA3.1(+)-NLRP3 overexpression plasmid using the Q5 Site-Directed Mutagenesis Kit (New England BioLabs). Briefly, a PCR containing 25ng template DNA and 1X Q5 Hot Start High-Fidelity master mix was carried out using a final concentration of 0.5 μ M forward and reverse primers. HA-NLRP3 FP 5'-GCCGGATTATGCGACGAGTGTCCGTTGCAAG-3', HA-NLRP3 RP 5'-ACATCATACGGATACATGCTAGCCAGCTTGGG-3'. Thereafter, the PCR product was incubated (5 min, room temperature) in a mixture of 1X Kinase, Ligase & DpnI (KLD) reaction buffer and enzyme mix (New England BioLabs) according to the manufacturer's protocol. Sequences of all constructs were verified by DNA sequencing (ATBiotech).

2.15 Transfection

HEK293T cells were seeded in 12-well cell culture treated plates at a density of 2.5×10^5 cells per well, or in 6-well cell culture treated plates at a density of 1.0×10^6 cells per well 1 day before transfection. For the *in vitro* inflammasome-reconstitution assay, HEK293T cells were seeded in 12-well cell culture treated plates coated with poly-D-lysine (Sigma-Aldrich Ltd.). Transfection was carried out with a total DNA concentration of 1 μ g per well, using Lipofectamine 3000 (Invitrogen) according to the manufacturer's instructions. Briefly, 50 μ l of Opti-MEM medium (Gibco) containing 1 μ g DNA and 2 μ l P3000 reagent was mixed with 50 μ l of Opti-MEM medium containing 2 μ l Lipofectamine 3000 reagent, and incubated (5 min, room temperature) before being added to the cell culture.

2.16 Immunofluorescence

BMDMs were plated on sterile coverslips in 6-well plates at 2×10^6 cells per well overnight and treated with LPS (1 μ g/ml) for 4 h the next day. Freshly prepared NaHS (600 μ M) (Sigma-Aldrich Ltd.) was added for another 30 min before nigericin (10 μ M) (Sigma-Aldrich Ltd.) was added for another 1 h. Cells were then rinsed twice with PBS before being fixed with 4% w/v paraformaldehyde dissolved in PBS (20 min, room temperature). After 3 rinses with PBS, cells were permeabilized with 0.1% w/v saponin (Sigma-Aldrich Ltd.) and dissolved in PBS (30 min, room temperature). Cells were then blocked with 10% v/v FBS (30 min, room temperature) before being incubated with anti-mouse ASC (1:200) in blocking solution (1 h, room temperature), and then rinsed 3 times with 0.1% w/v saponin dissolved in PBS. Thereafter, cells were incubated with a FITC-conjugated anti-mouse secondary antibody (3:100) in blocking solution (1 h, room temperature). Cells were rinsed a further 3 times before being mounted on microscope slides with Fluoroshield™ mounting medium with DAPI (Sigma-Aldrich Ltd.) and visualized under the Olympus FluoView FV1000 (Olympus, Japan) laser scanning confocal microscope or the BX51 Olympus immunofluorescent microscope. Images were captured with the Olympus FluoView FV1000 confocal microscope using a 60x/1.00 water objective, with 488nm Argon ion and 543nm HeNe Green laser as the excitation source.

2.17 ELISA

Cytokines in culture supernatant, blood plasma and peritoneal lavage fluid was measured by ELISA using commercially available kits. Mouse TNF α (88-7324 from eBioscience), mouse IL-6 (88-7064 from eBioscience), mouse IL-1 β (88-7013 from eBioscience), mouse IL-18 (BMS618 from eBioscience), nitrate/nitrite assay (DN-006 from Kamiya Biomedical Company) and prostaglandin E₂ Express EIA kit (500141 from Cayman Chemical) were used in accordance with the manufacturer's protocol. Absorbance was read with an EON Biotek microplate reader at absorbance values as indicated in the manufacturer's protocol.

2.18 Immunoblot analysis

Cells were lysed in lysis buffer comprising of EDTA (5mM), containing inhibitors against serine, cysteine and aspartic acid proteases, amino-peptidases and metalloproteases (Halt™ Protease Inhibitor Cocktail), phosphatase inhibitors (Halt™ Phosphatase Inhibitor Cocktail) and 1% v/v Triton-X 100 in Tris buffered saline (TBS) on ice. The suspension was next centrifuged (14,000g, 5 min, 4°C) and homogenates collected. Protein concentration was quantified using the Bradford assay (Bio-Rad Ltd.). Whole cell lysates were resuspended in loading sample buffer (Laemmli buffer) with 10% v/v β -mercaptoethanol, boiled for 5 min at 95°C before being separated by 10% or 15% v/v SDS-PAGE. Separated proteins were transferred onto PVDF membranes (Bio-Rad Ltd.) prior to incubation (1 h, room temperature) with blocking buffer (TBS containing 5% v/v skim milk and 0.1% v/v Tween-20). Membranes were incubated (overnight, 4°C) with anti-mouse NLRP3 (Cryo-2 from Adipogen), ASC (AL177 from Adipogen),

Caspase-1 (p20 Casper-1 from Adipogen), IL-1 β (AF-401-NA from R&D Systems), iNOS (AB3523 from Abcam Ltd.), COX-2 (AB15191 from Abcam Ltd.), phospho-IkBa (#9246 from Cell Signaling), IkBa (#9242 from Cell Signaling), CSE (AB136604 from Abcam Ltd.), HA-Tag (6E2 from Cell signalling) or β -actin (Sigma-Aldrich) with gentle agitation. The next day, immunoblots were washed with TBS containing 0.1% v/v Tween-20 and incubated (1 h, room temperature) with secondary antibodies donkey anti-goat goat HRP (Santa Cruz Ltd.), anti-mouse IgG HRP or goat anti-rabbit IgG HRP (Thermo Scientific Pierce Ltd.) with gentle agitation. The immunoreactive bands were visualized using chemiluminescent reagent (Merck Millipore Ltd.) and exposed to X-ray film. Blots were scanned and quantified using ImageJ software.

2.19 Co-immunoprecipitation

HEK293T cells were seeded in 6-well cell culture treated plates (NUNC) at a density of 1.5×10^6 per well in DMEM supplemented with 10% v/v FBS the day before experiments were carried out. Cells were transfected with 1 μ g of HA-NLRP3 expression vector using Lipofectamine 3000 (Invitrogen) according to the manufacturer's instructions. 24 h later, cells were treated with NaHS (600 μ M, 30 min) followed by a change of media. Thereafter, cells were transfected with 1 μ g of ASC expression vector. After a subsequent 24 h incubation, transfected cells were lysed by passing through a 25G needle ten times in a hypotonic lysis buffer (20mM HEPES pH 7.4, 10mM KCl, 1mM EDTA) containing inhibitors against serine, cysteine and aspartic acid proteases, amino-peptidases and metalloproteases (Halt™ Protease Inhibitor Cocktail).

Cell lysates were centrifuged (10,000 g, 15min, 4°C). Supernatant was diluted 1:1 with a 2X immunoprecipitation buffer (100mM Tris pH 7.8, 300mM NaCl, 0.2% v/v Triton-X, 10mM EDTA). Equal protein concentrations of lysates (1mg protein) were immunoprecipitated using anti-HA magnetic beads (Pierce) (overnight, 4°C) on a mechanical rotator. The magnetic beads were then washed three times with 1X immunoprecipitation buffer (50mM Tris pH 7.8, 150mM NaCl, 0.1% v/v Triton-X, 5mM EDTA), and eluted with 0.1M glycine, pH 2.0 (5 min, room temperature). Magnetic beads were separated and supernatant was collected and neutralized with 1M Tris, pH 8.5. Samples were resuspended in loading sample buffer (Laemmli buffer) with 10% v/v β -mercaptoethanol, boiled for 5 min at 95°C before being separated by 15% v/v SDS-PAGE and immunoblotted with the indicated antibodies.

2.20 MitoTracker and MitoSOX Assay

Mitochondrial mass was measured by staining LPS primed BMDMs with MitoTracker Red CMXRos and MitoTracker Green (25nM, 15 min, 37°C) (Invitrogen) followed by ATP (5mM, 30 min) treatment. For detection of mitochondrial ROS, BMDMs stimulated with LPS and ATP were stained with MitoSOX Red mitochondrial superoxide indicator (5 μ M, 20 min, 37°C). Cells were washed twice with cell culture media and resuspended in a FACs buffer (1% v/v FBS in PBS) for FACs analysis. Data was acquired with LSR-Fortessa (BD Biosciences) and analyzed using FlowJo analytical software (TreeStar).

2.21 Detection of mitochondrial DNA

BMDMs were seeded in 6-well cell culture treated plates (NUNC) at a density of 2.0×10^6 per well in DMEM supplemented with 10% FBS the day before experiments were carried out. Cells were lysed by passing through a 25G needle ten times in a buffer (250mM sucrose, 20mM HEPES pH 7.4, 10mM KCl, 2mM MgCl₂, 1mM EDTA) containing protease inhibitors (Halt™ Protease Inhibitor Cocktail). Cell lysates were centrifuged (10,000 g, 15min, 4°C) for the production of a supernatant corresponding to the cytosolic fraction, of which, DNA was isolated with the Isolate II Genomic DNA kit (Bioline) according to the manufacturer's instructions. For detection of mtDNA, qPCR was carried out using the specific primers for the representative genes listed below. The thermocycling parameters were 50°C (2 min), 95°C (10 min) followed by 40 cycles of 95°C (15 sec), 60°C (1 min) and 95°C (15 sec). Expression values were determined by $2^{-\Delta\Delta CT}$ equation and normalized with 18S housekeeping gene. Samples prepared without RNA served as negative controls. The primers used were mouse cytochrome c oxidase I FP 5'-GCCCCAGATATAGCATTCCC-3', mouse cytochrome c oxidase I RP 5'-GTTTCATCCTGTTCTGCTCC-3', 18S FP 5'-TAGAGGGACAAGTGGCGTTC-3', 18S RP 5'-CGCTGAGCCAGTCAGTGT-3'.

2.22 Statistical analysis

All results were analyzed using GraphPad Prism 5 software package. Data are presented as the mean \pm SEM or mean \pm SD of at least three separate experiments, unless otherwise noted. Statistical comparisons between the different treatments were performed using one-way analysis of variance

(ANOVA) for multiple groups, followed by Dunnett's post-hoc evaluation applied to grouped data to test the probability of significant differences among treatments, or the Mann-Whitney *U* test for comparison between two groups. A *P* value of less than 0.05 was considered significant.

**CHAPTER 3: EFFECTS OF EXOGENOUS H₂S ON THE
PRODUCTION OF PRO-INFLAMMATORY MEDIATORS IN
CSE^{-/-} RAW264.7 MACROPHAGES**

3.1 Exogenous H₂S (i.e. NaHS) reduces LPS-induced TNF α and IL-6 secretion from RAW264.7 macrophages

In preliminary experiments, the ability of exogenous H₂S to affect the release of inflammatory mediators from activated macrophages was assessed. RAW264.7 cells were pre-treated with NaHS (500 μ M) for 30 min prior to LPS (1 μ g/ml) stimulation for a further 24 h. NaHS significantly decreased TNF α ($P < 0.05$) but not IL-6 concentrations after 24 h (Fig 3.1A). Since H₂S, released from NaHS, has been shown in multiple reports to be short lived (Lee et al., 2011; Li et al., 2008; Whiteman et al., 2010) we hypothesized that a greater inhibition of pro-inflammatory cytokine release could be achieved by increasing the exposure time of RAW264.7 cells to NaHS. As such, the duration of LPS stimulation was shortened to 6 h while the frequency of exposure of cells to NaHS was increased to 3 times. To this end, two concentrations of NaHS (200 μ M or 500 μ M) were added to LPS-stimulated RAW264.7 macrophages using two separate treatment regimens. Pre-treating macrophages with either NaHS (200 μ M or 500 μ M) for 30 min prior to LPS (1 μ g/ml) stimulation for a further 6 h caused a concentration-dependent decrease in TNF α and IL-6 secretion as compared to cells treated with LPS alone only ($P < 0.001$) (Fig. 3.1B). Increasing the frequency of NaHS administration from 1 to 3 exposures further diminished the release of both TNF α ($P < 0.01$) and IL-6 ($P < 0.05$) (Fig 3.1B). An identical concentration of time-expired NaHS (tx-NaHS) was used as a negative control. Tx-NaHS did not reduce TNF α or IL-6 secretion from LPS-stimulated RAW264.7 cells (Fig. 3.1C). To ensure that the reduced cytokine release was not due to cell death, an MTT assay was performed on LPS-stimulated RAW264.7 cells treated with varying doses/frequencies of

administration of NaHS. No significant change in cell viability was noted regardless of dose or exposure time of cells to NaHS (Fig. 3.1D). Together, these data suggest that H₂S released from NaHS downregulate the secretion of TNF α and IL-6 from LPS-stimulated RAW264.7 cells in a dose-dependent manner.

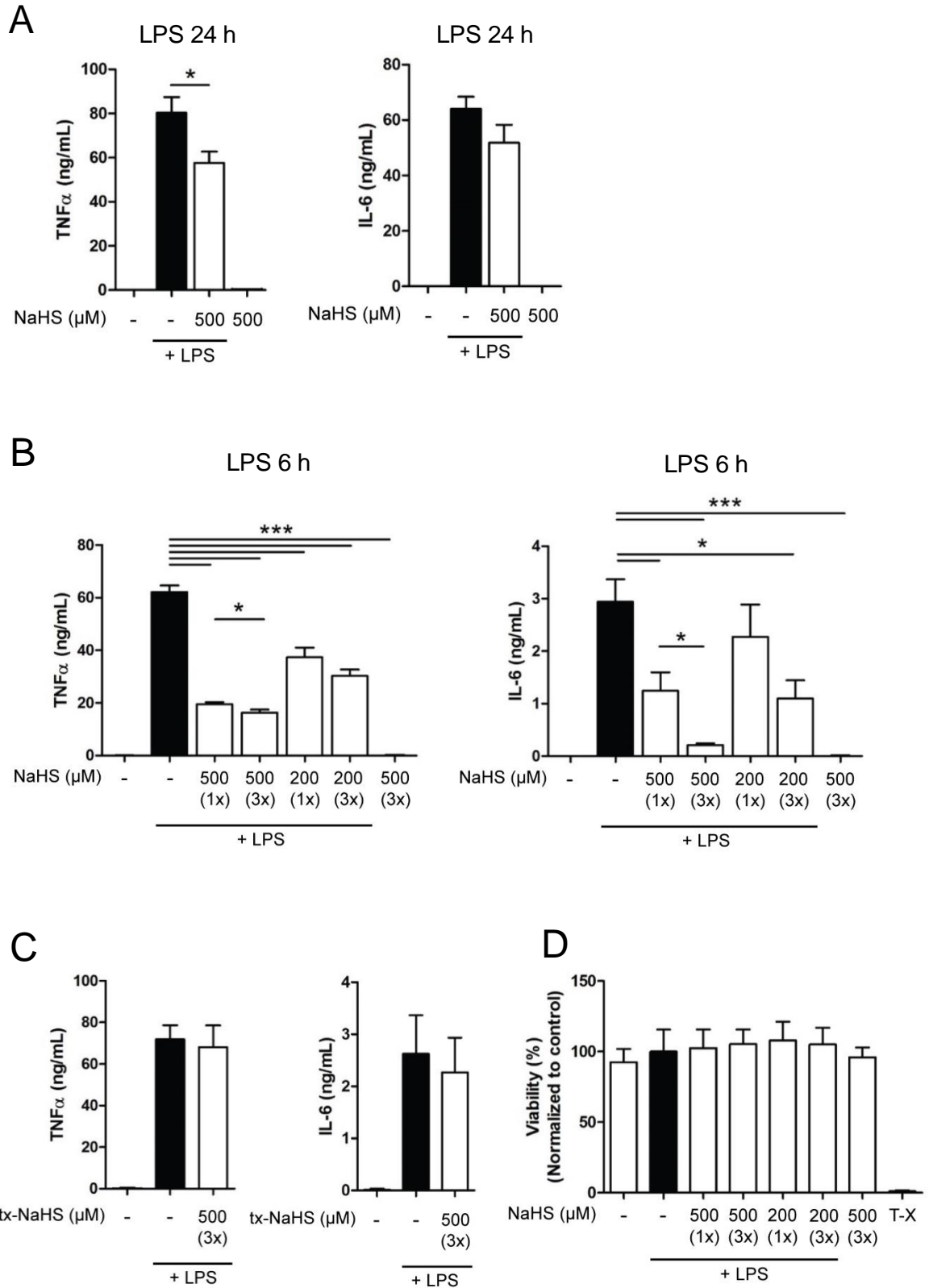


Figure 3.1 The fast-releasing H₂S donor NaHS exerts an anti-inflammatory effect in LPS stimulated RAW264.7 macrophages.

(A) Reduction of inflammatory cytokine (TNF α & IL-6) generation in LPS (1 μ g/ml, 24 h) RAW264.7 macrophages following 30 min pre-treatment with NaHS (500 μ M).

(B) Dose dependent reduction of secreted inflammatory cytokine (TNF α & IL-6) in LPS-stimulated (1 μ g/ml, 6 h) RAW264.7 macrophages with 30 min pre-treatment of NaHS (200 μ M or 500 μ M) (1x); or with 30 min pre-treatment of NaHS (200 μ M or 500 μ M) followed by 2 additional exposures to NaHS (200 μ M or 500 μ M) at subsequent 2 h intervals (3x).

(C) Production of inflammatory cytokines in LPS-stimulated (1 μ g/ml, 6 h) RAW264.7 macrophages following 30 min pre-treatment with time expired NaHS (500 μ M) (tx-NaHS 500 μ M) followed by 2 additional doses of tx-NaHS (500 μ M) at subsequent 2 hour intervals (3x).

(D) Toxicity of different doses of NaHS on LPS-stimulated (1 μ g/ml, 6 h) RAW264.7 macrophages, determined by the MTT assay. 1% Triton-X (T-X) was used as a positive control.

* $P < 0.05$, ** $P < 0.01$, *** $P < 0.001$. Data in **A** is representative of 2 repeated experiments (mean \pm SD, n=4, Mann-Whitney U test, 2-tailed), and **B-D** is from 3 repeated experiments (mean \pm SEM, n=3, one-way ANOVA with Dunnett's post-test against controls).

Fig 3.1B-D are reproduced from (Huang et al., 2016a)

3.2 Generation of CSE^{-/-} RAW264.7 macrophages using the CRISPR/Cas9 system

Since exogenous H₂S inhibited LPS-evoked TNF α and IL6 generation by LPS-challenged macrophages, it was of interest to determine whether naturally occurring i.e. endogenous H₂S may have the same effect. To this end, CSE was permanently deleted in RAW264.7 cells using the clustered regularly interspaced short palindromic repeats Caspase 9 (CRISPR-Cas9) system. By way of explanation, the single-guide RNA (sgRNA) targeting mouse CSE was ligated into the CRISPR-Cas9 plasmid (Fig. 3.2A). Guided to the CSE gene by the sgRNA, Cas9 cuts the DNA on both strands and causes double stranded breaks (DSB). Depending on the accuracy of the DNA-repair mechanism of non-homologous end joining (NHEJ), random insertion or deletion (indel) mutations may occur, resulting in the formation of a premature stop codon, hence permanently silencing the gene. In the presence of a repair template, precise editing alternatively can occur via the high-fidelity homologous-directed repair (HDR) (Ran et al., 2013) (Fig. 3.2B).

The CSE sgRNA used in this study was designed to target exon 1 of the CSE gene with the purpose of creating a premature stop codon upstream of the gene. Using the recommended online CRISPR design tool (<http://tools.genome-engineering.org>) (Ran et al., 2013), a recommended 20 base pair sgRNA sequence was generated along with 3 predicted offsite targets that reside in other genes, and summarized in Table 3.1. As none of these 3 genes are known to regulate the expression of pro-inflammatory mediators directly, this sgRNA against CSE was selected and cloned into the CRISPR/Cas9 plasmid.

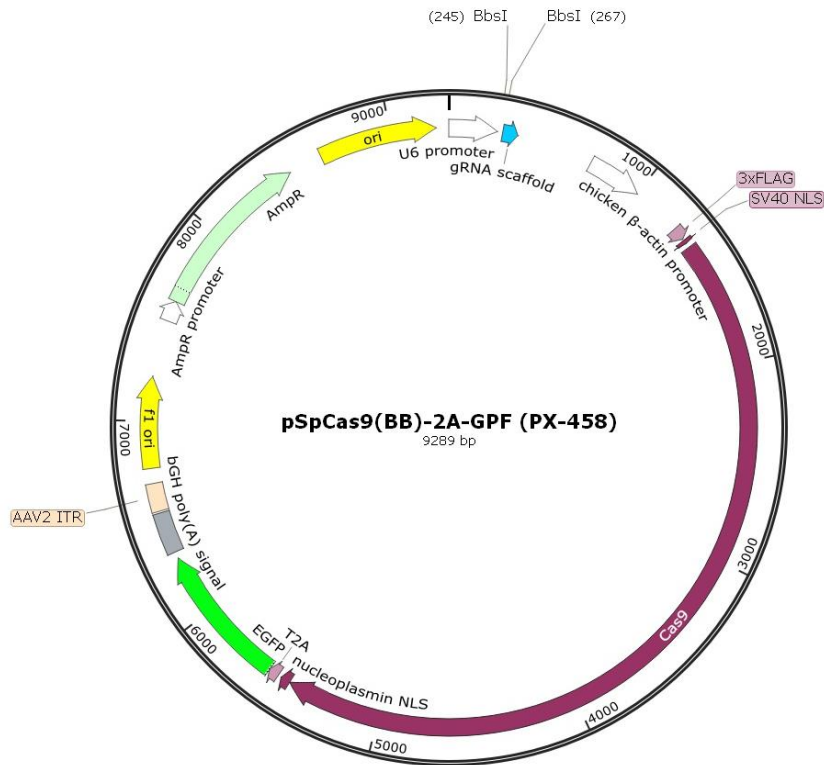
Wild type (WT) RAW264.7 cells were transfected with either the empty vector (Cas9) or CSE sgRNA before single cells were sorted for GFP expression 24 h after transfection. The single cells were then expanded and screened for CSE expression. As CSE expression is upregulated in macrophages upon LPS-stimulation, screening for CSE knockdown clones were determined by immunoblotting for the CSE antigen 24 h after stimulation with LPS (1µg/ml) (Fig 3.2C). CSE expression of 3 representative knockout clones, with or without LPS stimulation are shown in Fig 3.2D. The absence of any upregulation of CSE, which was otherwise seen in wild-type and Cas9 RAW264.7 control cells after 24 h LPS-stimulation, confirmed the knock-down of CSE in the CSE^{-/-} cells (Fig 3.2D).

In the present study, only CSE was knocked out in RAW264.7 cells. It was previously reported that RAW264.7 cells do not contain CBS mRNA and protein (Zhu et al., 2010). As such, the protein expression of CBS was compared against liver lysates of wild-type C57BL/6 mice. As seen in Fig 3.2E, immunoblot staining of RAW264.7 lysates with CBS antibody revealed a band lower in molecular weight as compared to the band seen in the liver lysates. The predicted molecular weight of CBS is 61kDa, which is greater than the band detected in the RAW264.7 cell lysates. Hence, it was decided not to attempt to knock out CBS in RAW264.7 cells in the present study. In addition to CSE, attempts were also made to knock down 3-MST in RAW264.7 cells. However due to an oversight in the design of the sgRNA against 3-MST, an intron in the 3-MST gene was edited. Although a 3-MST partially knocked-down (3-MST^{+/-}) RAW264.7 clone was obtained, the data for this cell line was disregarded in this thesis.

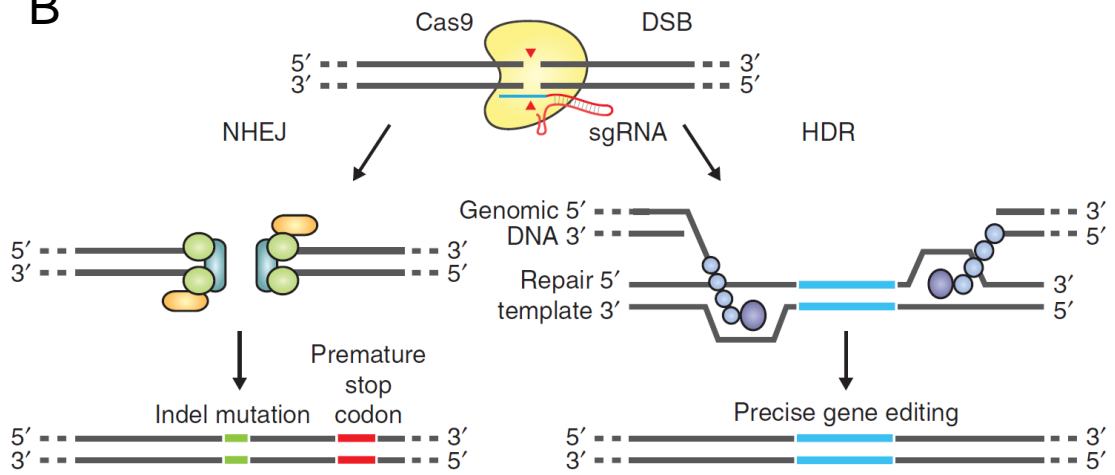
Table 3.1 Predicted off target effects of CSE targeted sgRNA

No.	Predicted Off Target Gene	Known function(s) of Gene	Ref
1	FAM65a	Golgi reorientation during cell migration	(Mardakheh et al., 2016)
2	Heat Shock Protein 4	Cell migration, spermatogenesis, cardiac hypertrophy and fibrosis, association with poor outcomes of HBV-related early-stage hepatocellular carcinoma, and gastric and colorectal cancers	(Wu et al., 2011), (Held et al., 2011), (Mohamed et al., 2012), (Yang et al., 2015), (Jo et al., 2016)
3	Zinc Finger Protein 219	Central nervous system development in zebrafish	(Lien et al., 2013)

A



B



Reproduced from (Ran et al., 2013)

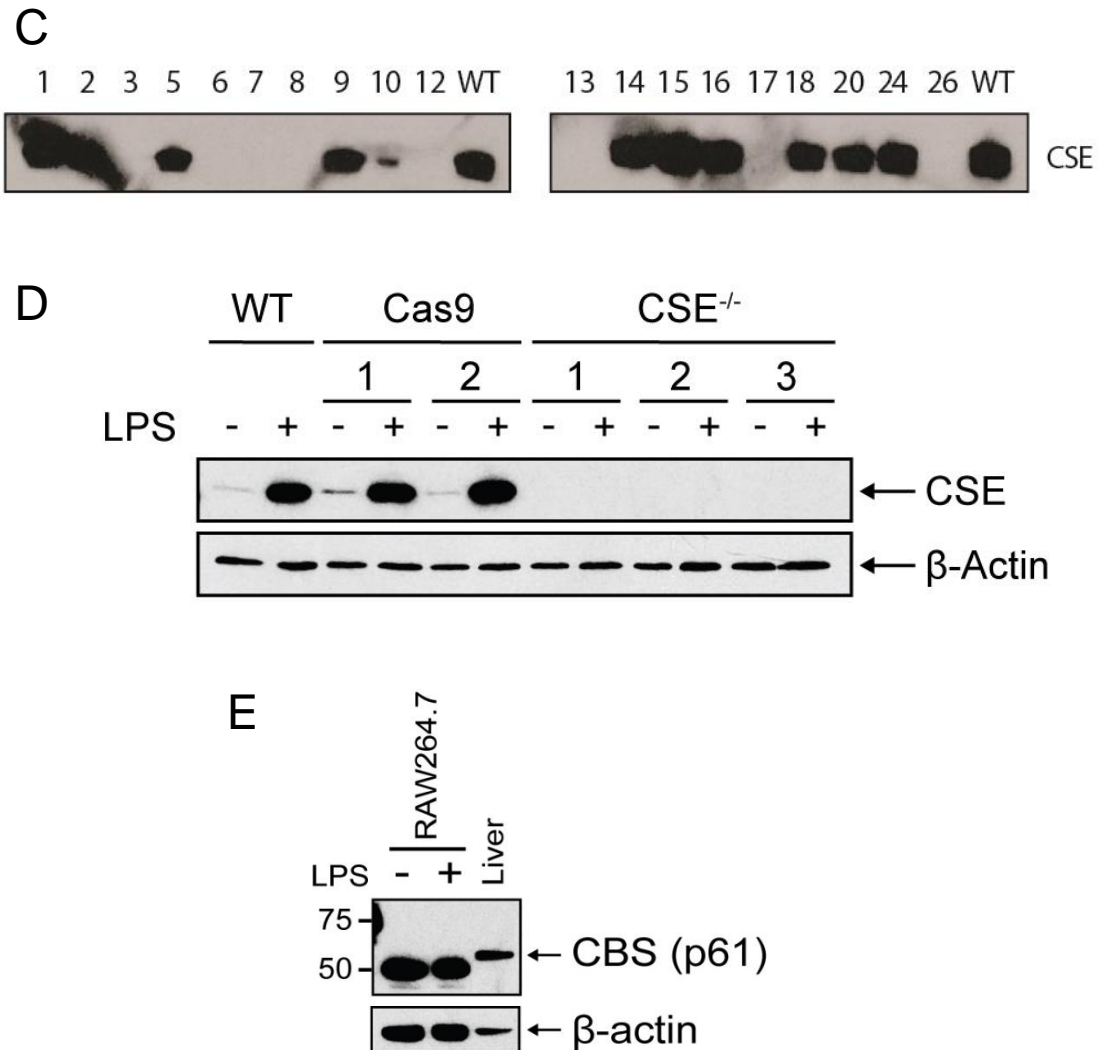


Figure 3.2 Generation of CSE^{-/-} RAW264.7 cells using the CRISPR/Cas9 system.

(A) Plasmid map of the CRISPR/Cas9 plasmid PX-458 (Addgene). sgRNA against mouse CSE was ligated into the plasmid following digestion with the *BbsI* enzyme.

(B) Mechanism of action by which the CRISPR/Cas9 system elicits gene editing and knockout of a gene.

(C) CSE expression in different clones of RAW264.7 cells transfected with the CRISPR/Cas9 plasmid encoding the sgRNA against CSE, after stimulation with LPS (1µg/ml, 24 h). Numbers denote clone numbers and WT indicate wild-type RAW264.7 cells.

(D) CSE expression levels of expanded single clones of wild-type (WT) RAW264.7 cells, two representative clones of empty vector transfected RAW264.7 cells (Cas9) and three representative clones of CSE specific sgRNA transfected RAW264.7 cells (CSE^{-/-}), stimulated with or without LPS (1µg/ml, 24h).

(E) Immunoblot analysis of CBS expression in C57BL/6 mouse liver lysates and RAW264.7 cell lysates stimulated with or without LPS (1µg/ml, 24h).

Data is from 1 experiment.

Immunoblots in **C-E** are from 1 experiment.

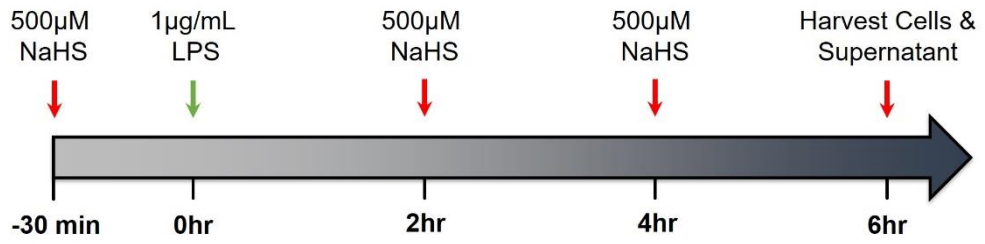
3.3 Effects of exogenous H₂S on LPS-stimulated CSE^{-/-} RAW264.7 macrophages

Secreted TNF α and IL-6 from 3 clones of CRISPR-mediated knockout cells were assessed 6 h post LPS-stimulation and compared against control cells (Cas 9) (Fig 3.3A). The data indicated that the knockout of CSE did not significantly affect the secretion of TNF α and IL-6 in these RAW264.7 cells (Fig 3.3B). As 3 doses of NaHS (500 μ M) at 2 hourly intervals over a span of 6 h previously reduced TNF α and IL-6 secretion from LPS-stimulated RAW 264.7 cells most drastically (Fig 3.1B), the same dosing regimen of NaHS was applied to the knockout cell lines (Fig 3.3A). To ascertain if the loss of CSE would affect the response of LPS-stimulated RAW264.7 cells to exogenous H₂S, CSE^{-/-} cells were treated with NaHS. It was hypothesized that the lack of endogenous H₂S may sensitize the cell towards exogenous H₂S thereby resulting in a greater downregulation of LPS-induced TNF α and IL-6 secretion as compared to wild-type cells. At this dose and frequency of treatment, NaHS reduced IL-6 secretion in both LPS-stimulated control and CSE^{-/-} cells to a similar extent (Fig 3.3B), suggesting that the loss of CSE did not sensitize the cell towards exogenous H₂S. However, NaHS significantly reduced TNF α secretion from only 1 out of the 3 clones (clone 2) of CSE^{-/-} cells stimulated with LPS, which effect was not observed in control cells (Fig 3.3B).

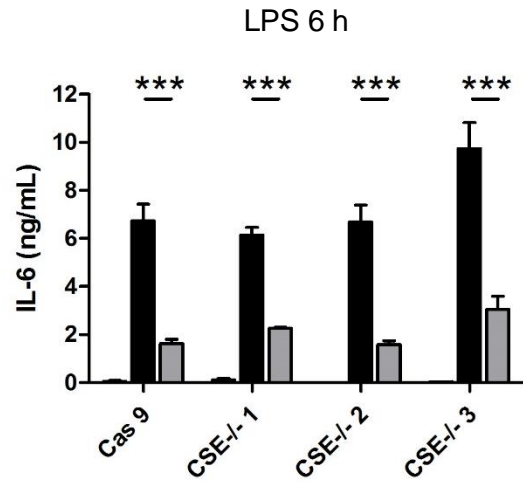
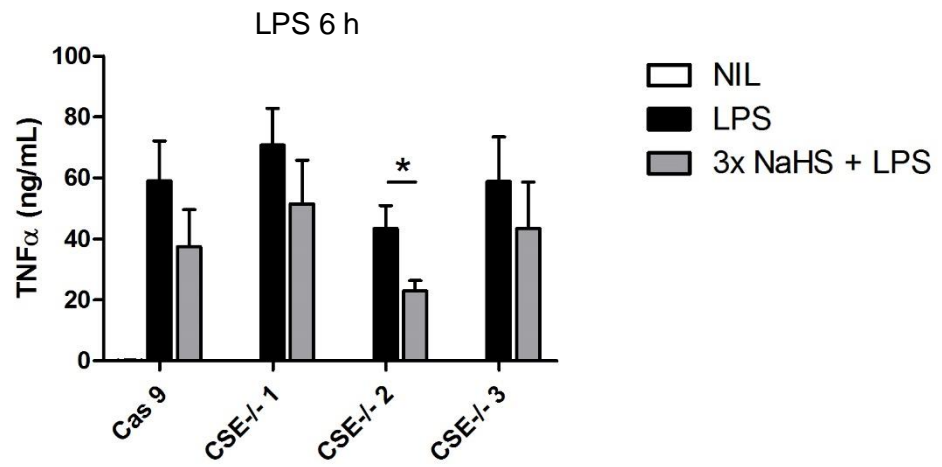
In addition to secreted pro-inflammatory mediators, the expression of enzymes that control the production of pro-inflammatory mediators was also assayed in CSE^{-/-} RAW264.7 cells derived from a single sampled clone, with or without NaHS treatment. Inducible nitric oxide synthase (iNOS) and cyclooxygenase-2 (COX-2) are known to be strongly upregulated by pro-

inflammatory stimuli such as LPS, and control the production of nitric oxide (NO) and prostaglandin-E2 (PGE₂) respectively. Apart from these 2 enzymes, expression of pro IL-1 β was also measured (Fig 3.3C). Immunoblotting of iNOS revealed non-specific bands. Of the 3 bands, the upper 2 bands are likely the result of non-specific staining due to the presence in both lysates of cells that were stimulated with or without LPS. Conversely, in the lowest of the 3 bands, iNOS was only detected in the lysates of LPS-stimulated cells. Assaying secreted IL-1 β in the supernatant by means of ELISA was not performed as IL-1 β maturation and secretion requires the activation of the inflammasome, which RAW264.7 cells lack (Pelegriin et al., 2008). The loss of CSE resulted in a significant decrease in iNOS ($P < 0.05$) and COX-2 ($P < 0.01$) expression, but not pro IL-1 β , in response to 6 h LPS-stimulation. NaHS reduced only pro-IL-1 β levels in control (Cas9) and CSE^{-/-} cells, but did not affect iNOS and COX-2 expression levels (Fig 3.3D). Collectively, the data suggest that loss of CSE selectively downregulate iNOS and COX-2 expression in LPS-stimulated RAW264.7 cells and did not affect the cell's sensitivity towards exogenous H₂S with respect to inhibiting the production of pro-inflammatory mediators.

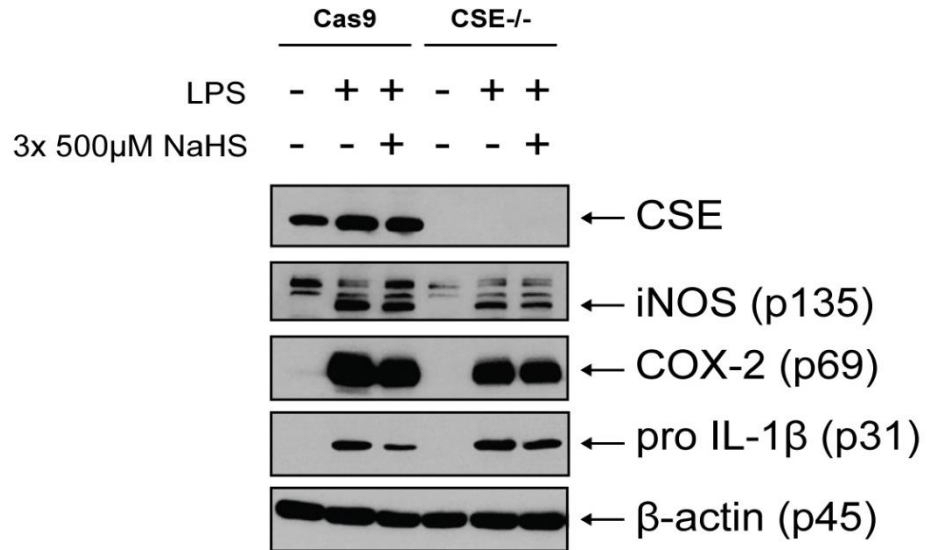
A



B



C



D

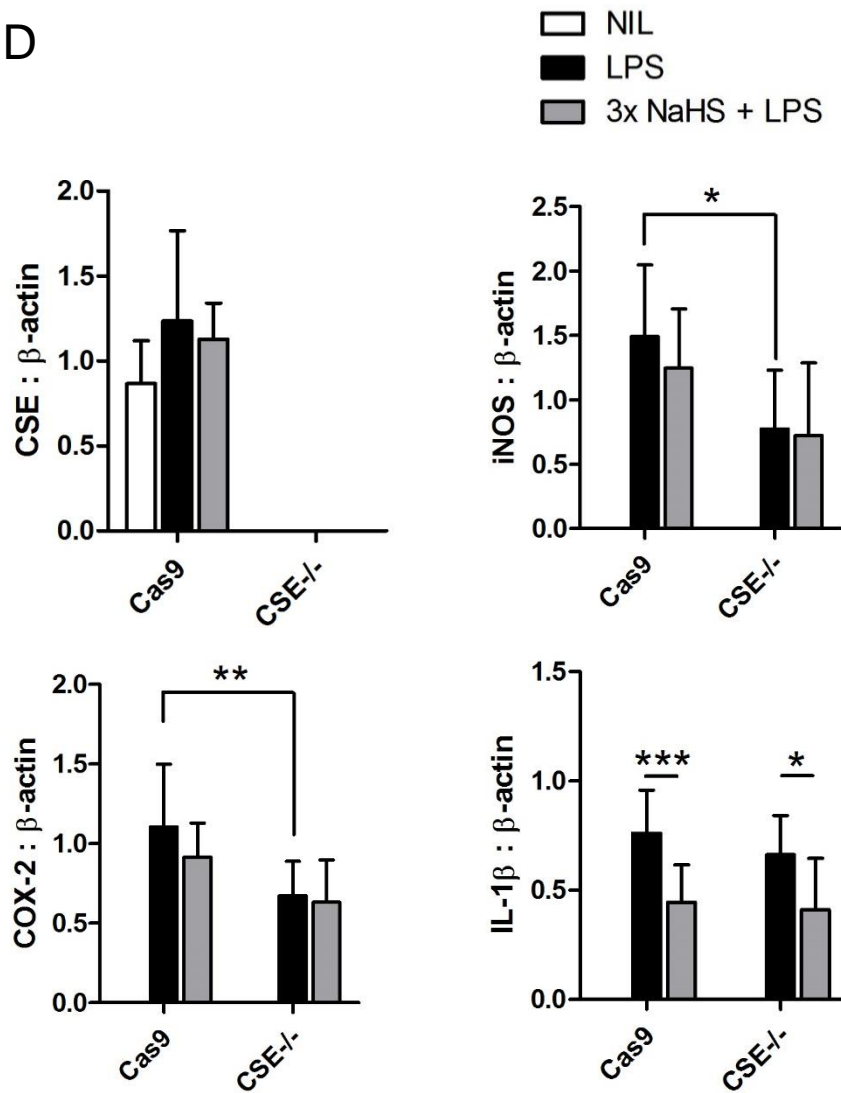


Figure 3.3 Effects of exogenous H₂S on LPS-stimulated wild-type and CSE^{-/-} RAW264.7 macrophages.

(A) Dosing regimen of RAW264.7 cells with LPS and NaHS.

(B) Production of inflammatory cytokines (TNF α and IL-6) in LPS-stimulated (1 μ g/ml, 6 h) empty vector transfected (Cas9) and 3 clones of CSE knockout (CSE^{-/-}) RAW264.7 macrophages with NaHS (500 μ M, 30 min), followed by 2 additional doses of NaHS (500 μ M) at subsequent 2 h intervals (3X). (Mean \pm SEM, n=3).

(C) Representative immunoblot of CSE, pro-IL-1 β , iNOS and COX-2 in RAW264.7 cells as treated in **A**.

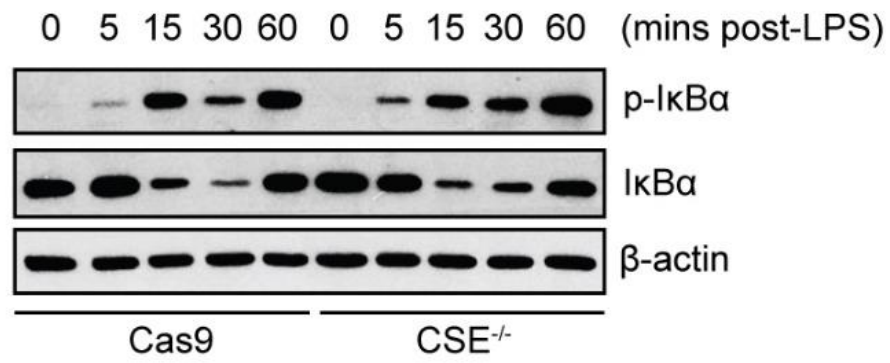
(D) Quantification of IL-1 β , COX-2, iNOS and CSE from immunoblots as treated in **C**.

* $P < 0.05$, *** $P < 0.001$. Data in **B** is from 3 repeated experiments (mean \pm SEM, n=3, Mann-Whitney U test). Immunoblot in **C** is representative of 4 repeated experiments (CSE immunoblot), 8 repeated experiments (pro IL-1 β immunoblot), and 9 repeated experiments (iNOS & COX-2 immunoblot). Data in **D** is from 4-9 repeated experiments as indicated for **C** (mean \pm SD, n=4-9, Mann-Whitney U test, 2-tailed).

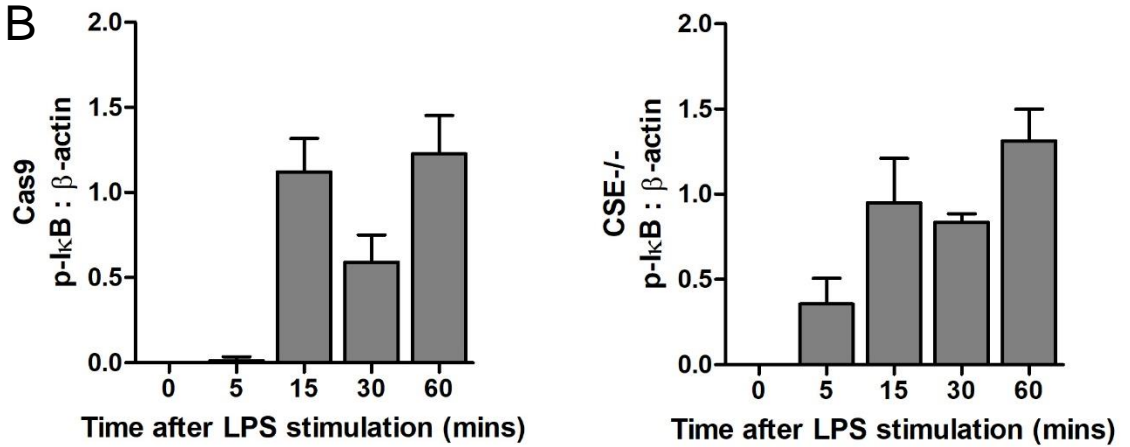
3.4 Effect of the loss of CSE on phosphorylation of I κ B α in RAW264.7 cells during LPS stimulation

Since the loss of CSE affected the expression of iNOS and COX-2, we next assessed whether corresponding changes in NF κ B, a critical transcription factor that has been shown to be a regulator of both iNOS (Aktan, 2004) and COX-2 (Kim et al., 2007; Rafi et al., 2007) gene expression, were apparent in LPS-challenged CSE^{-/-} cells. The phosphorylation of I κ B α is a key event preceding the translocation of NF κ B from the cytoplasm into the nucleus, thereby initiating NF κ B activation. Accordingly, changes in phospho-I κ B α (p-I κ B α) and I κ B α expression over a span of 60 min after LPS-stimulation in control cells (Cas9) and CSE^{-/-} cells were monitored (Fig 3.4A). Measurement of p-I κ B α levels was carried out within 60 min after LPS-stimulation as NF κ B functions as a fast messenger, evidenced by reports showing that the peak of LPS-induced nuclear p65 accumulation in macrophages occurs within the first 60 min (Neacsu et al., 2015; Sharif et al., 2007). In both control (Cas9) and CSE^{-/-} cells, p-I κ B α expression peaked at 15 min post LPS-stimulation, before decreasing at the 30 min time-point, and re-emerging at 60 min after LPS-stimulation. I κ B α levels conversely decreased to its lowest expression level 30 min after LPS-stimulation, before re-emerging at 60 min post LPS-stimulation. No significant difference for both p-I κ B α and I κ B α levels were apparent between control and CSE^{-/-} cells (Fig 3.4). The re-emergence of I κ B α and p-I κ B α at the 60 min post LPS-stimulation time-point is likely to be part of the negative feedback mechanism of NF κ B activation (Vallabhapurapu and Karin, 2009). In this pathway, NF κ B activation leads to the synthesis of I κ B α , which sequesters p50/65 dimers, preventing further binding to the DNA.

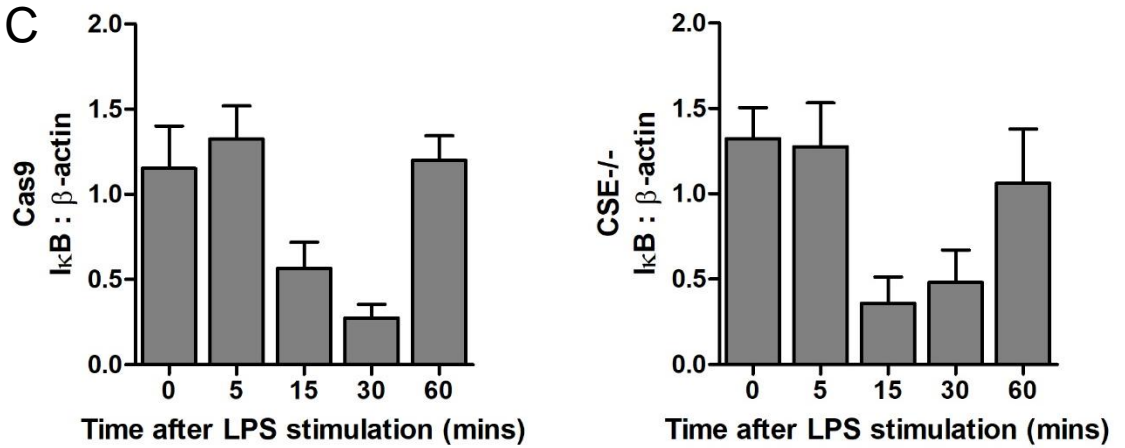
A



B



C



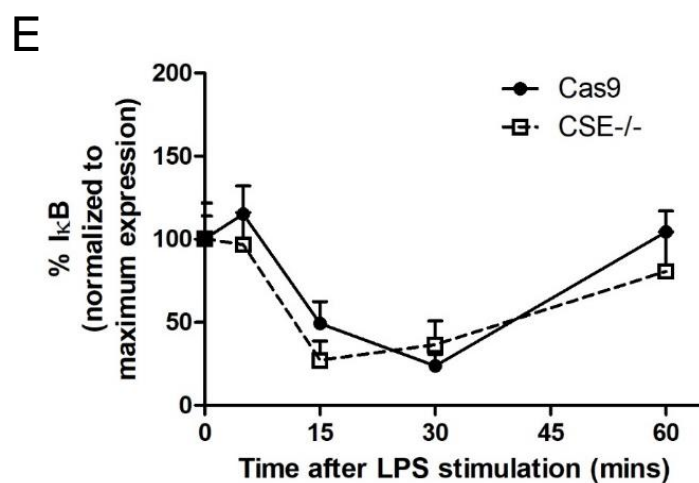
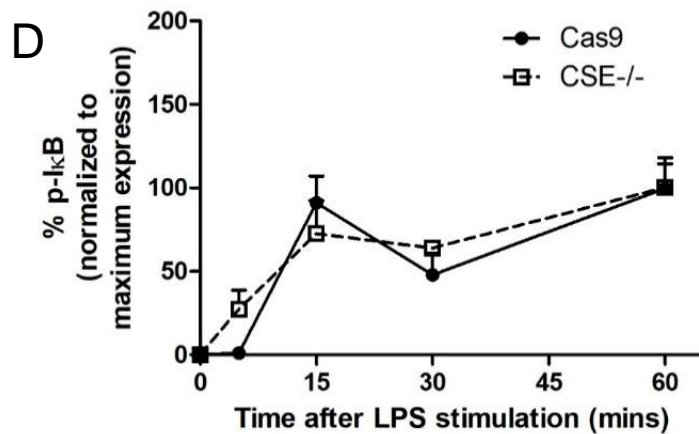


Figure 3.4 Effects of the loss of endogenous H₂S producing enzymes on phosphorylation of IκBα in RAW264.7 cells during LPS stimulation.

(A) Immunoblot analysis of phosphorylated-IκBα (p-IκBα) and IκBα in empty vector transfected (Cas9) and CSE^{-/-} RAW264.7 cells that were stimulated with LPS (1μg/ml) for 0, 5, 15, 30 and 60 min.

(B) Expression of p-IκBα (c.f. actin); and

(C) IκBα (c.f. actin), in LPS stimulated RAW264.7 cells at 0, 5, 15, 30 and 60 min, as treated in **A**.

(D & E) Change of p-IκBα and IκBα expression levels for Cas9 and CSE^{-/-} RAW264.7 cells, as shown in **B** and **C**. Expression levels are normalized to the maximum expression level for each cell line, over the period of up to 60 min (mean and SD).

Immunoblot in **A** is representative of 3 repeated experiments. Data in **B** to **D** is from 3 repeated experiments.

3.5 Discussion

The study of macrophages deficient in H₂S producing enzymes can be achieved either through the generation of CSE^{-/-} mice (Yang et al., 2008), or by using siRNA to transiently knockdown these enzymes (Badieli et al., 2013). For the purpose of the present experiments, the first approach is likely to be optimal since macrophages can be obtained from the bone marrow or peritoneum of these mice. The latter approach is more challenging as macrophages being professional phagocytes, contain degradative enzymes that disrupt nucleic acid integrity making transfection inefficient (Zhang et al., 2009). In addition, as innate immune cells with the function of sensing foreign entities such as RNA viruses, the introduction of siRNA may unintentionally activate cytoplasmic RNA sensors such as RIG-I, MDA5, TLR3 and TLR8 in these cells (Wu and Chen, 2014). This may then trigger unwanted downstream immune responses. While CSE^{-/-}, CBS^{-/-} or 3-MST^{-/-} knockout mice are an ideal resource to study macrophages devoid of these enzymes, generating double or triple knockout mice poses a significant challenge. Hence to study macrophages lacking any of the known H₂S producing enzymes, we opted to generate such cells using CRISPR gene editing technology wherein the generation of stable cell lines with single and double gene knockouts are possible.

In the present study, CBS was not attempted to be knocked-out as RAW264.7 cells were reported not to express CBS. Although not done in this study, the measurement of CBS activity can be performed by means of liquid chromatography mass spectrometry (LC-MS/MS) (Smith et al., 2012). As CBS catalyzes the reaction between homocysteine and serine to form cystathionine, briefly, this method requires the mixing of cell extracts with the CBS cofactors

pyridoxal-phosphate (PLP) and S-adenosylmethionine (SAM), serine and L-homocysteine. [D₄]-cystathionine would also be added in the mixture as an internal standard. After incubation at 37°C at 4 h, the sample would be analysed by LC-MS/MS, and CBS activity would then be calculated by dividing the measured cystathionine concentration by the incubation time (4 h) and the protein concentration used. Another possible method is to transfect macrophages with a CBS targeted siRNA, and observe for the presence of CBS. As the transfection efficiency of macrophages is poor, this method will require a co-transfection of the siRNA with a GFP plasmid as a positive control.

The role of endogenous H₂S producing enzymes in the production of endogenous H₂S has been extensively studied (Huang and Moore, 2015). However, whether endogenous H₂S is pro- or anti-inflammatory remains uncertain (Wallace and Wang, 2015; Whiteman and Winyard, 2011). Having established that exogenous H₂S downregulated pro-inflammatory cytokine release from LPS-stimulated wild-type RAW264.7 cells, we made use of the stable CSE^{-/-} RAW264.7 cell line to study whether these cells would respond differently (c.f. wild-type cells) to exogenous H₂S. Three independent clones of CRISPR generated CSE^{-/-} cells were first isolated by random sampling. Assaying multiple clones was performed in order to exclude the possibility that any observed effects were clone specific thereby producing false results. The loss of CSE did not affect LPS induced TNF α and IL-6 secretion, and pro IL-1 β levels (Fig 3.3B - D), but significantly decreased iNOS and COX-2 at the protein level (Fig 3.3C & D). This data is at odds with an earlier study in which CSE was knocked down in RAW264.7 cells by siRNA silencing. In that study, the authors observed that RAW264.7 cells treated with CSE siRNA secreted less

TNF α (approximately 1.4 times lower), IL-6 (approximately 5.5 times lower), IL-1 β (approximately 3 times lower) and MCP-1 in response to 24 h LPS-stimulation. The authors also reported an increase in iNOS mRNA expression (approximately 2 times higher) in CSE siRNA treated cells (c.f. control cells) (Badiei et al., 2013). While there is no definitive evidence in the present study to explain this discrepancy, we reason that a CRISPR mediated permanent knockout of the CSE gene may be considered a more efficient approach as compared to an siRNA knockdown approach, which mechanistically causes a transient knockdown of CSE at the mRNA transcript level. Hence, we are inclined to consider the data from the present study to be more indicative of the role of CSE in controlling the release of these inflammatory mediators under the present experimental conditions. A recent study examined the effects of LPS on the production of inflammatory mediators in mice with CSE deficiency. As compared to wild-type mice, IL-6 and IL-1 β levels in the blood plasma of CSE^{-/-} mice after LPS injection (6 h) did not differ significantly from control mice, which is consistent with that observed in CSE^{-/-} macrophages in the present study. TNF α levels in the blood plasma of LPS challenged CSE^{-/-} mice were however slightly reduced (approximately 1.5 times lower) as compared to LPS challenged wild-type mice, thereby differing from what was observed in the present study (Ahmad et al., 2016a). One important aspect to note is that whilst macrophages are key producers of inflammatory mediators, other immune cell types such as dendritic cells (Blanco et al., 2008) and lymphoid cells (Klose and Artis, 2016) amongst others produce these mediators as well. Hence, whilst the absence of CSE in macrophages *in vitro* did not change its response to LPS in the aspect of inflammatory mediator production, the same may not be true for

the other immune cell types. Therefore, what has been observed with respect to macrophages may not be completely representative of what occurs *in vivo* in the mouse model of LPS induced septic shock.

Since exogenous H₂S from NaHS downregulated the release of TNF α and IL-6 from LPS-stimulated wild-type RAW264.7 cells (Fig 3.1B), it was reasoned that the absence of CSE might alter the extent of pro-inflammatory mediator inhibition exerted by exogenous H₂S. Evidence of such a phenomenon could shed light on the possible difference in function between endogenous and exogenous H₂S in regulating inflammatory mediator production, and how the absence of an endogenous H₂S producing enzyme (CSE) might affect the response of macrophages to exogenous H₂S. In a mouse model of renal ischemia/reperfusion injury, exogenous H₂S from NaHS rescued CSE^{-/-} mice from the injury and mortality associated with renal ischemia, as evidenced by a decrease in DNA damage in cells and an increase in the proliferation of cells (c.f. untreated CSE^{-/-} mice) (Bos et al., 2013). This suggested that exogenous H₂S could compensate for the loss of endogenous H₂S. A similar relationship between exogenous H₂S and endogenous H₂S was also reported in a mouse model of atherosclerosis, whereby treatment of CSE^{-/-} mice with NaHS reversed the accelerated atherosclerosis development during a 12 week atherogenic paigen-type diet in CSE^{-/-} mice (Mani et al., 2013). However to the best of our knowledge, no study has reported the effects of exogenous H₂S on LPS-stimulated CSE^{-/-} macrophages to date. The present work revealed that loss of CSE in RAW264.7 cells did not significantly affect the sensitivity of cells to exogenous H₂S with respect to inhibition of release of pro-inflammatory mediators (Fig 3.3). Although NaHS significantly decreased

TNF α secretion from LPS-stimulated CSE^{-/-} clone 2 but not in control cells (Fig 3.3B), this downregulation was absent in the other 2 clones of CSE^{-/-} RAW264.7 (ie. Clone 1 and 3). When performing the experiments, greater variation between replicates and experiments for TNF α was observed as compared to IL-6, hence resulting in larger error bars. As such, more replicates need to be carried out to ascertain whether the observed anomaly in CSE^{-/-} clone 2 can be repeated. Taking into consideration the effect of NaHS on release of other pro-inflammatory mediators and enzymes (ie. IL-6, IL-1 β , COX-2 and iNOS), the absence of a difference between the inhibitory effects of NaHS in reducing these mediators both in control and CSE^{-/-} cells stimulated with LPS strongly suggests that the loss of CSE did not affect the sensitivity of these cells to exogenous H₂S, with respect to pro-inflammatory mediator production.

In the present study, CRISPR-mediated knock-out of CSE in RAW264.7 cells did not significantly change TNF α and IL-6 secretion (cf. control cells). It is perhaps possible that a compensatory mechanism exists within these cells, such that the loss of CSE resulted in the upregulation of H₂S produced by other H₂S producing enzymes (ie. 3-MST, or CBS if it is present in RAW264.7 cells). Further experiments may be useful to determine the expression and activity levels of these enzymes in CSE^{-/-} RAW264.7 cells.

Since loss of CSE did not significantly change TNF α and IL-6 secretion as compared to control RAW264.7 cells, it was not surprising that no significant difference in NF κ B activation was apparent between these cells. As NF κ B activation occurs within the first 60 min after toll-like receptor activation in macrophages (Neacsu et al., 2015; Sharif et al., 2007), the biomarker for NF κ B activation, cytoplasmic p-I κ B α and I κ B α , was measured and quantified at 4

time-points up to 60 min after LPS-stimulation (Fig 3.4). Having ruled out NFκB activation under the present experimental conditions, the decrease in iNOS and COX-2 expression suggests that CSE deficiency in RAW264.7 cells affected the activation of other molecular pathways regulating iNOS and COX-2 expression levels. Besides NFκB, the regulation of iNOS gene induction in RAW264.7 macrophages is also under the control of interferon regulatory factor-1 (IRF-1) and signal transducer and activator of transcription-1α (STAT-1α) (De Stefano et al., 2006). Likewise, COX-2 gene transcription in macrophages is also controlled by activator protein 1 (AP-1) (Harper and Tyson-Capper, 2008), cAMP-response element binding protein (CREB) (Eliopoulos et al., 2002), and the p38-MAP kinase pathway (Rafi et al., 2007), in addition to NFκB. As such, CSE deficiency may alter the expression and/or binding of these transcription factors to the promoters of iNOS and COX-2 gene. Further studies are hence required to investigate the role of H₂S in regulating these transcription factors.

In conclusion, we show here, for the first time, that CSE was permanently knocked out in RAW264.7 mouse macrophages using the CRISPR gene-editing tool, thereby generating a stable CSE^{-/-} cell line. The loss of CSE did not affect TNFα and IL-6 secretion or pro IL-1β upregulation in these cells (c.f. control cells) in response to LPS stimulation. Absence of CSE decreased iNOS and COX-2 expression after LPS stimulation via a mechanism of action not involving NFκB activation. In addition, the absence of CSE did not affect the downregulation of inflammatory mediators from these cells in response to exogenous H₂S. Altogether, these findings suggest that CSE may be redundant in the regulation of several pro-inflammatory mediators in mouse macrophages,

and that its absence does not critically affect anti-inflammatory effects exerted by exogenous H₂S.

**CHAPTER 4: A NOVEL SLOW-RELEASING HYDROGEN
SULFIDE DONOR, FW1256, EXERTS ANTI-INFLAMMATORY
EFFECTS IN MOUSE MACROPHAGES AND *IN VIVO***

4.1 Identification of a novel slow-releasing H₂S donor that exerts non-toxic, anti-inflammatory effects in LPS-stimulated RAW264.7 macrophages

In an attempt to identify novel, slow-releasing H₂S donors with anti-inflammatory effects, 11 H₂S releasing compounds were screened for their ability to reduce TNF α and IL-6 secretion from LPS-stimulated RAW264.7 macrophages. These compounds were synthesized by Dr Feng Wei from the department of Pharmacy, NUS, in the laboratory of Professor Brian Dymock. The chemical structures of these compounds were derived from GYY4137 as either direct analogues, by substitution of side chains with diamino groups, or by cyclisation (Huang et al., 2016a). Compounds were selected on the basis of their structural diversity, low molecular weights and a wide range of cLogPs (calculated logP value of a compound). For reference, a low logP value indicates high hydrophilicity and enhanced permeability across cell membranes suggesting better absorption. Based on the Lipinski rule of 5 (Lipinski et al., 2001), compounds with cLogP values lesser than 5 have a higher probability of being well absorbed by cells and hence predictive of drug-like properties.

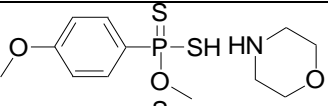
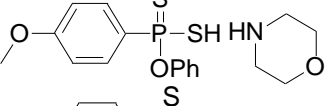
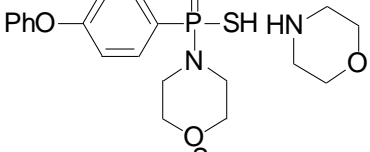
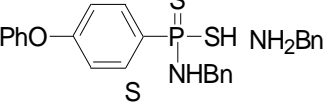
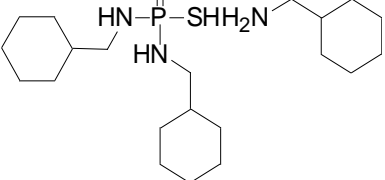
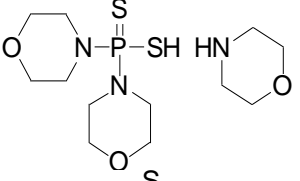
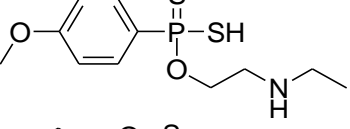
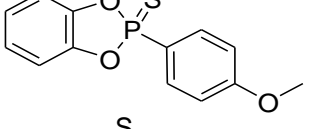
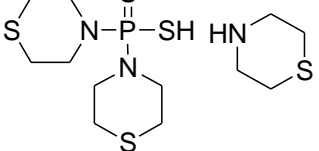
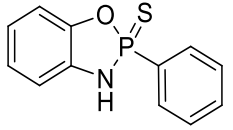
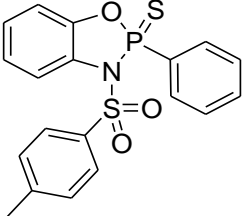
All 11 compounds are known to be slow-releasing H₂S donors as their H₂S release rates were previously quantified in cell free media (Feng et al., 2015). The chemical structures and properties of the H₂S releasing compounds **1-11** are as shown in Table 4.1.

None of these compounds are water soluble and hence they were dissolved in DMSO. Preliminary control experiments were therefore undertaken to determine a suitable concentration of DMSO which would not affect the release of pro-inflammatory cytokines from LPS-stimulated RAW264.7

macrophages. By pre-treating RAW264.7 macrophages with various concentrations of DMSO followed by 24 h of LPS stimulation (1µg/ml), it was determined that 0.5% v/v was the maximal concentration of DMSO in the reaction mixture that would not affect TNFα secretion from these cells (Fig 4.1A). All compounds used in this study were therefore dissolved in DMSO at this concentration.

All 11 H₂S donors were screened for their ability to reduce formation of pro-inflammatory cytokines in RAW264.7 cells stimulated with LPS (1µg/ml) for 24 h (Whiteman et al., 2010). Whilst a single exposure to NaHS (500µM) reduced the release of TNFα and IL-6 by about 1.5 fold, compounds **4** and **10**, at the same concentration, diminished TNFα secretion by approximately 2500 and 4 times respectively and additionally reduced IL-6 secretion by approximately 40,000 and 120 times (Fig 4.1B). Compound **4** and **10** are hereinafter referred to as FW1131 and FW1256. Since both compounds appeared to have significant effects on cytokine generation, their effect on cell toxicity was determined. Perhaps not surprisingly, FW1131 was clearly toxic towards macrophages (Fig 4.1C) whilst FW1256 was not toxic as determined by both PI staining (Fig 4.1C), and the MTT assay (Fig 4.1D). In addition to being non-toxic, FW1256 possessed a logP value of 3.4 which is less than 5, and a molecular weight 247.02 which is less than 500, thereby fulfilling criteria from the Lipinski rule of 5. FW1256 was therefore characterized further in this study.

Table 4.1 Chemical structures and properties of H₂S releasing compounds 1-11.

#	Structure	MW (parent)	cLogP
1		321.4	3.1
2		383.47	4.5
3		438.54	6.1
4 (FW1131)		478.61	7.3
5		433.70	7.1
6		355.46	1.8
7		291.05	2.8
8		278.26	4.5
9		403.05	3.9
10 (FW1256)		247.02	3.4
11		401.40	5.6

Reproduced from (Huang et al., 2016a)

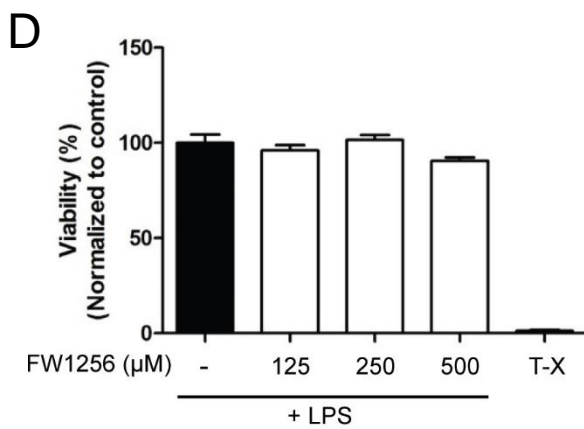
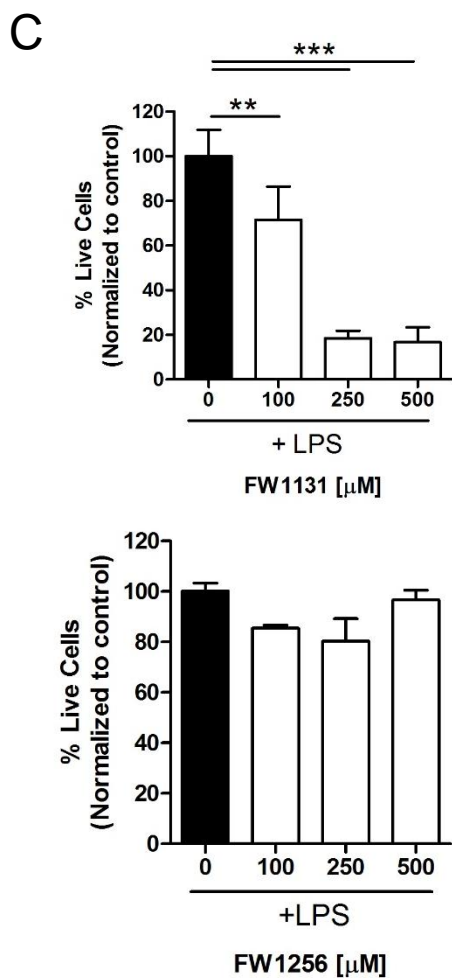
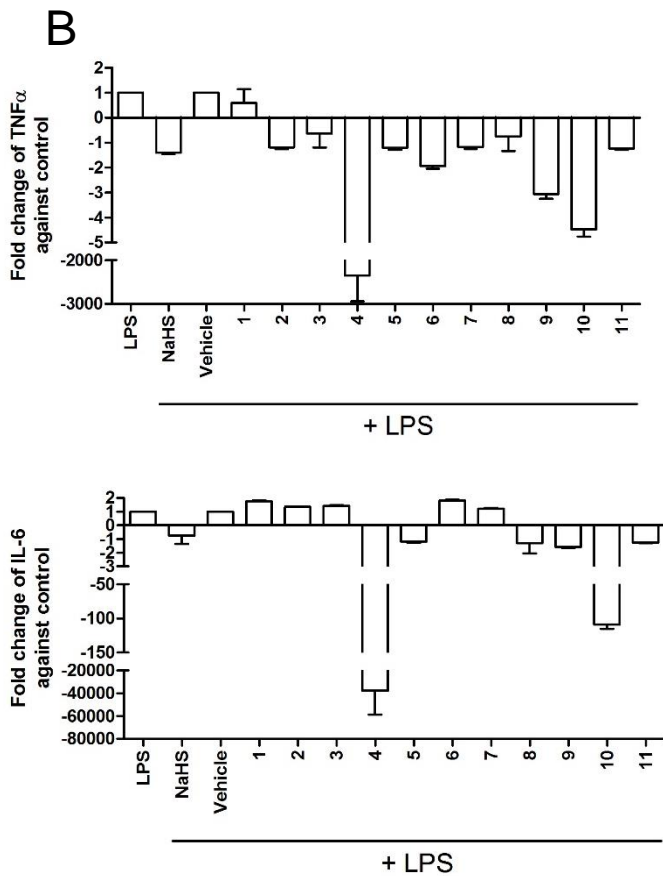
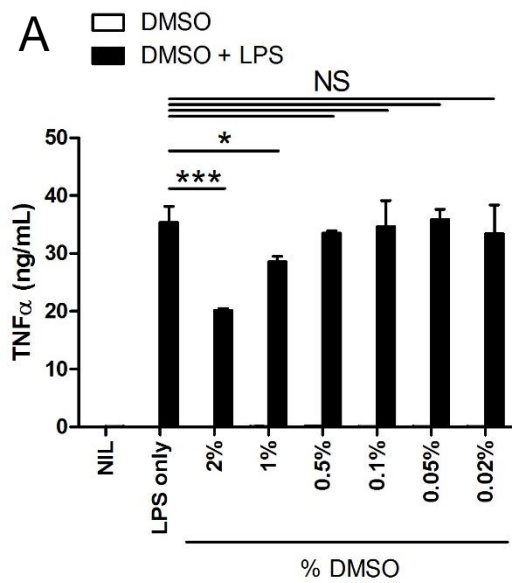


Figure 4.1 Identification of novel H₂S releasing compounds: anti-inflammatory activity *in vitro* and toxicity.

(A) Effects of DMSO on the secretion of TNF α in LPS-stimulated RAW264.7 cells (1 μ g/ml, 24 h).

(B) Screen of 11 novel slow-releasing H₂S donors (500 μ M) against RAW264.7 macrophages stimulated with LPS (1 μ g/ml, 24 h) for ability to inhibit release of pro-inflammatory cytokines.

(C) Drug-induced cytotoxicity of FW1131 and FW1256. Cells were pretreated for 30 min (various concentrations) with test compounds before stimulation with LPS (1 μ g/ml, 24 h). Toxicity was determined by propidium iodide (PI) staining.

(D) Drug-induced cytotoxicity of FW1256 on RAW264.7 cells pretreated for 30 min (various concentrations) with FW1256 before stimulation with LPS (1 μ g/ml, 24 h). Toxicity was determined by the MTT assay. Mean \pm SEM. 1% Triton-X (T-X) was used as a positive control.

NS denotes not significant, * $P < 0.05$, ** $P < 0.01$, *** $P < 0.001$.

Data in **A** is from 1 experiment (mean \pm SD, n=3, one-way ANOVA with Dunnett's post-test against controls). Data from **B** is representative of 2 separate experiments (mean \pm SD, n=4). Data from **C** is from 1 experiment (FW1131), and 2 repeated experiments (FW1256) (mean \pm SD, n=3-4, one-way ANOVA with Dunnett's post-test against controls). Data from **D** is from 3 repeated experiments (mean \pm SEM, n=3, one-way ANOVA with Dunnett's post-test against controls).

Reproduced from (Huang et al., 2016a)

4.2 FW1256 is a slow-releasing H₂S donor

To establish the kinetics of H₂S release from FW1256, a recently reported H₂S fluorescent probe (a near infrared (NIR)-fluorescent probe based on a Cu²⁺-cyclen complex linked to a NIR light-emitting BODIPY fluorophore) (Wu et al., 2014a) was used to measure intracellular H₂S in LPS-stimulated and non-stimulated RAW264.7 cells after treatment with FW1256. The probe was first encapsulated in liposomes before being taken up by RAW264.7 cells. The cells were then washed with cell culture media, treated with FW1256 with or without LPS and fluorescent readings taken over a period of 24 h.

As expected the entire 'payload' of H₂S was released from NaHS within the first hour. Fluorescence of these cells continued to remain high for the next 24 h, with or without LPS-stimulation (Fig 4.2A & B). Conversely, macrophages challenged with LPS or control, unchallenged cells, treated with FW1256 showed increasing intensity of fluorescence over the next 24 h (Fig 4.2C & D) indicating that FW1256 is indeed a slow (c.f. NaHS) H₂S releaser. Whilst a strict comparison of the rate of release of H₂S from these two compounds was not possible due to the explosive nature of H₂S release from NaHS, NaHS released its entire 'payload' of H₂S within 30 min, while FW1256 released its entire 'payload' only after 22 hr. The presence of LPS did not affect the release of H₂S from either NaHS or FW1256.

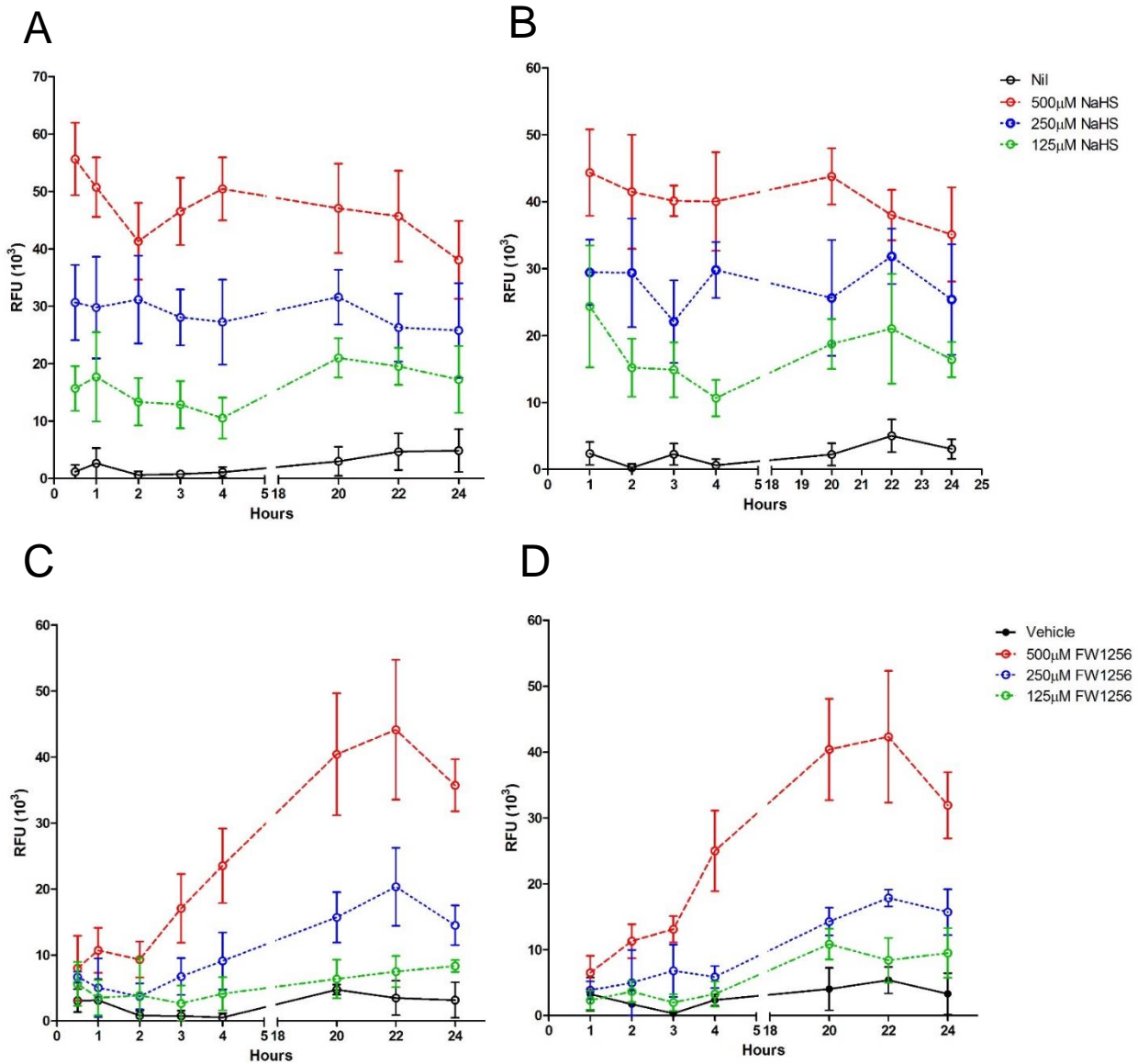


Figure 4.2 FW1256 releases H₂S in a sustained manner in RAW264.7 cells. RAW264.7 cells were incubated with a fluorescent H₂S probe (20 μ M) for 3 h at 37°C before being treated with varying concentrations of H₂S donors. **(A)** NaHS without LPS; **(B)** NaHS with LPS; **(C)** FW1256 without LPS, and **(D)** FW1256 with LPS. Data is from 2 repeated experiments (mean \pm SD, n=6).

Reproduced from (Huang et al., 2016a)

4.3 FW1256 downregulated pro-inflammatory mediator release from LPS-stimulated RAW264.7 macrophages

A characteristic hallmark of inflammation is the presence of pro-inflammatory mediators released from macrophages when these sentinel cells detect sterile tissue damage and foreign pathogens. To examine the anti-inflammatory effect of FW1256 on LPS-stimulated macrophages, secreted TNF α , IL-6, PGE₂ and NO from LPS-stimulated RAW264.7 macrophages were measured with or without FW1256 treatment. FW1256 concentration dependently inhibited the secretion of all of these mediators from LPS-stimulated RAW264.7 cells (Fig 4.3A). The half maximal inhibitory concentrations (IC₅₀) of TNF α , IL-6, PGE₂ and NO are 61.2 μ M, 11.7 μ M, 2.55 μ M and 34.6 μ M respectively, with the corresponding 95% confidence interval (CI) indicated in Fig 4.3B.

As the synthesis of NO and PGE₂ is mediated by the enzymes iNOS and COX-2, the effect of FW1256 on mRNA transcription of iNOS and COX-2 was first measured using quantitative PCR (qPCR). IL-1 β mRNA levels were also measured in the present study as a study has shown that RAW264.7 cells do not secrete IL-1 β due to the absence of a functional inflammasome, which is required for IL-1 β maturation and subsequent secretion (Pelegriin et al., 2008). Treatment of RAW264.7 cells with FW1256 (200 μ M) followed by LPS stimulation for 24 h significantly downregulated mRNA transcription of COX-2 (P < 0.01), iNOS (P < 0.05) and IL-1 β (P < 0.001) (Fig 4.3C). Consistent with the observation at the mRNA level, downregulation of these mediators at the protein level was further confirmed by immunoblotting for pro IL-1 β , COX-2 and iNOS (Fig 4.3D).

To determine whether the H₂S released from FW1256 was responsible for downregulating formation of pro-inflammatory mediators, the H₂S scavenger vitamin B_{12a} (hydroxocobalamin) was used together with FW1256 in equimolar concentrations. Vitamin B_{12a} has been shown previously to decrease H₂S concentration (c.f. H₂S in PBS only or H₂S in CoCl₂ containing buffer) in a cell free buffered solution of H₂S (Van de Louw and Haouzi, 2013). In addition, vitamin B_{12a} has been suggested as an antidote against H₂S poisoning as it prevented NaHS-induced mouse lethality and cytotoxicity (Truong et al., 2007). It was proposed that vitamin B_{12a} formed a complex with H₂S thereby reducing Co³⁺ in the vitamin B_{12a} core to Co⁺. In the process, H₂S is oxidized to sulfate (Truong et al., 2007). Together, these data suggest that vitamin B_{12a} is an H₂S scavenger. Under the current experimental conditions, vitamin B_{12a} reversed the anti-inflammatory effect of FW1256 without directly affecting the secretion of TNF α or IL-6 from LPS-stimulated RAW264.7 macrophages (Fig 4.3E) thereby supporting the hypothesis that the inhibitory effect of FW1256 on pro-inflammatory release under these conditions was indeed due to the H₂S moiety.

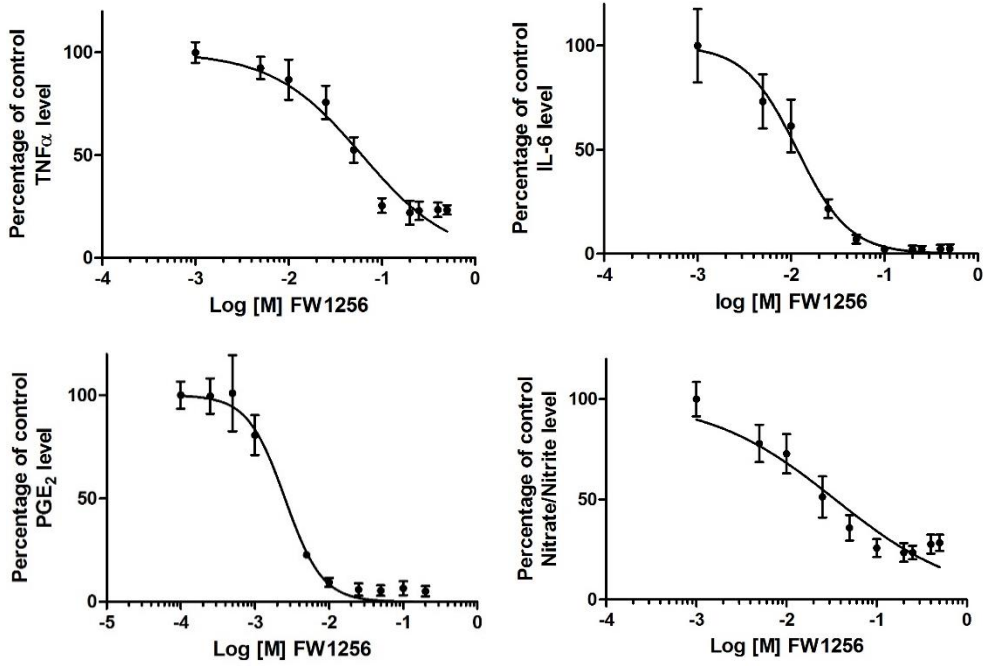
To determine whether FW1256 had efficacy in downregulating pro-inflammatory mediators when administered after LPS stimulation, secreted TNF α and IL-6 levels were compared between RAW264.7 macrophages that were treated with FW1256 30 min either before or after LPS stimulation. Treating cells with FW1256 after LPS stimulation was as effective as treating cells with FW1256 before LPS stimulation (Fig 4.3F), suggesting potential translational potential.

Finally, FW1256 was compared against NaHS and another slow H₂S releasing compound, GYY4137. FW1256, but not GYY4137, inhibited TNF α

and IL-6 release from RAW264.7 cells stimulated with LPS for 24 h when these 2 compounds were given at concentrations of 75 μ M and 15 μ M (similar to the IC₅₀s of FW1256 to inhibit TNF α and IL-6 release respectively in these cells). A much higher concentration of NaHS (500 μ M) was unable to downregulate TNF α and IL-6 levels from RAW264.7 cells stimulated with LPS for 24 h (Fig 4.3G). Although RAW264.7 cells treated with NaHS (500 μ M, 30 min) prior to LPS-stimulation (1 μ g/ml, 6 h) downregulated TNF α and IL-6 secretion (Fig 3.1B), identical NaHS treatment on RAW264.7 cells prior to LPS-stimulation (1 μ g/ml, 24 h) did not affect TNF α and IL-6 secretion (Fig 4.3G). A plausible reason is that NaHS being a fast H₂S donor would have dissipated to a greater extent after 24 h (cf. 6 h). This may well result in less reduction of cytokines in Fig 4.3G (24 h LPS) c.f. Fig 3.1B (6 h LPS). Likewise, treatment of RAW264.7 cells with GYY4137 (75 μ M or 15 μ M, 30min) prior to LPS-stimulation (1 μ g/ml, 24 h) did not downregulate TNF α and IL-6 secretion, unlike in cells treated with identical concentrations of FW1256 (Fig 4.3G). This may be attributed to the lower rate of release of H₂S from GYY4137 as compared to FW1256.

Together, this data strongly suggests that FW1256 has a higher efficacy and potency (c.f. GYY4137 and NaHS) in reducing pro-inflammatory mediator generation from RAW264.7 cells stimulated with LPS over a duration of 24 h.

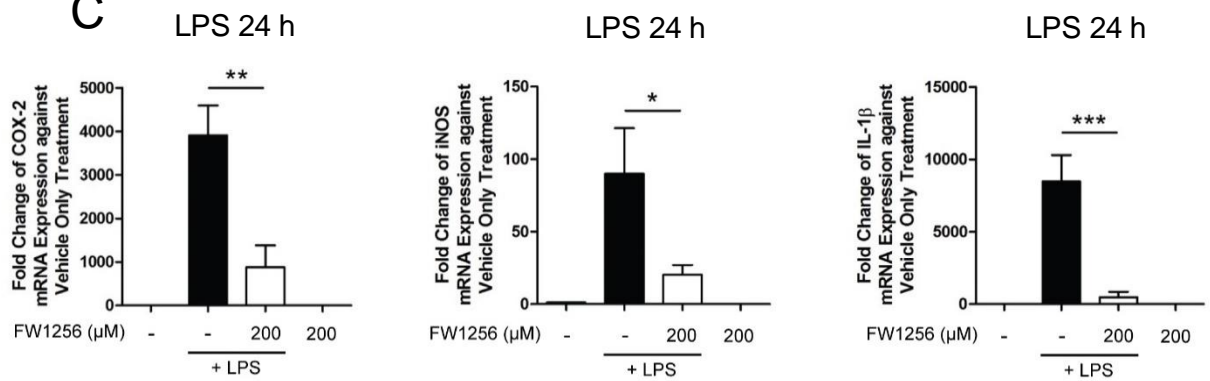
A



B

	TNF α	IL-6	PGE $_2$	NO
IC $_{50}$ FW1256 (μ M)	61.2	11.7	2.55	34.6
95% CI (μ M)	47.0 – 79.7	8.9 – 15.3	1.8 – 3.6	23.0 – 51.9

C



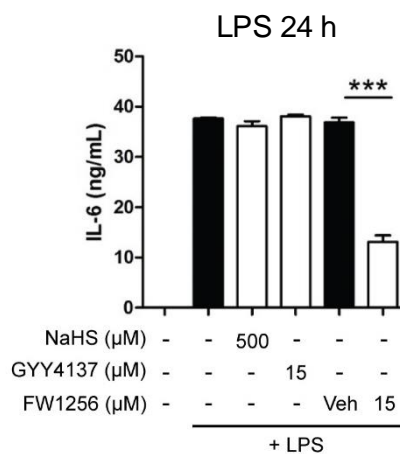
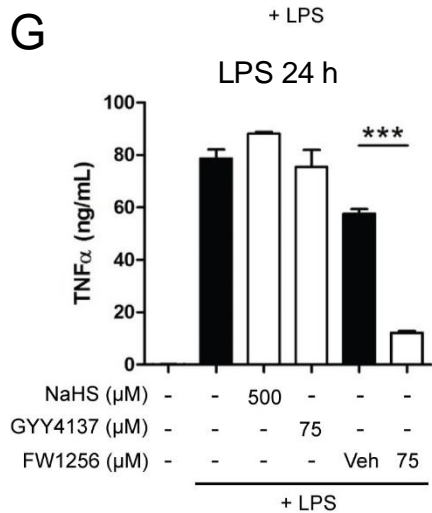
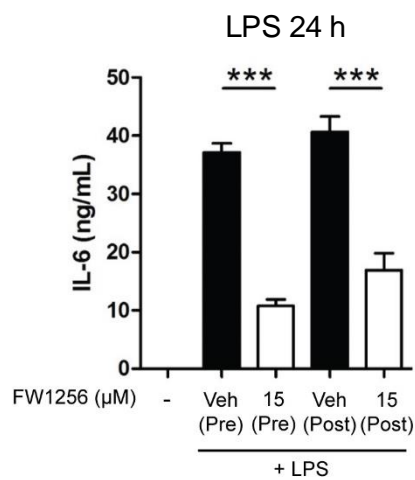
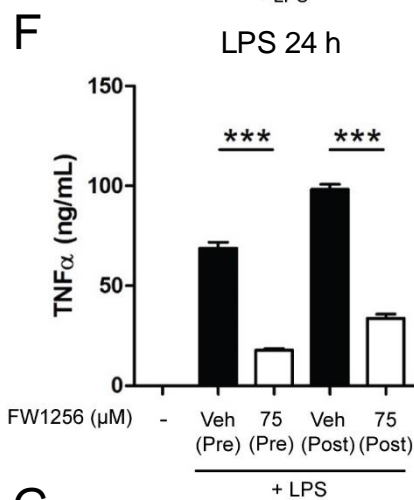
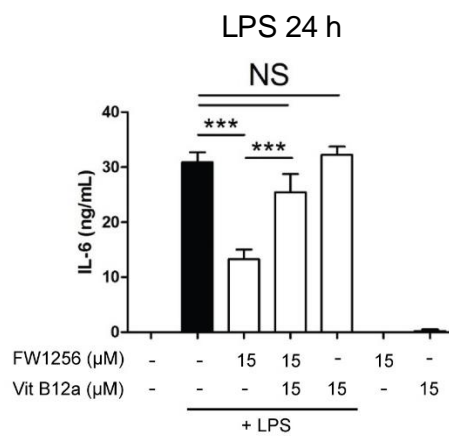
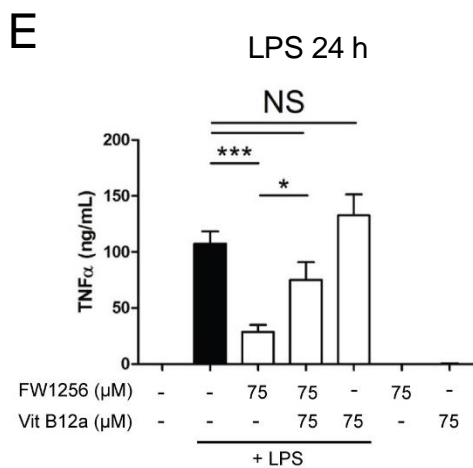
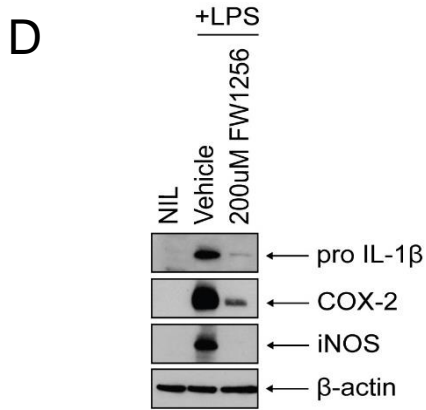


Figure 4.3. FW1256 reduces the production of inflammatory mediators from LPS-stimulated RAW264.7 macrophages.

(A) Dose dependent inhibition of inflammatory cytokines and mediators from RAW264.7 macrophages pretreated 30 min with various doses of FW1256 before stimulation with LPS (1µg/ml, 24 h). Nonlinear regression analysis was performed for dose response curves, and the curve of Log [M] FW1256 versus the normalized response is presented.

(B) IC₅₀ of FW1256 in reducing inflammatory cytokines and mediators in LPS-stimulated RAW264.7 cells as treated in **A**.

(C) mRNA expression of IL-1β, iNOS and COX-2 in RAW264.7 cells pretreated with FW1256 (200µM) for 30 min before stimulation with LPS (1µg/ml, 24 h).

(D) Immunoblot analysis of pro-IL-1β, iNOS and COX-2 in RAW264.7 cells as treated in **C**.

(E) TNFα and IL-6 secretion from LPS stimulated RAW264.7 macrophages treated with FW1256, with or without co-treatment with the H₂S scavenger vitamin B_{12a} (hydroxocobalamin).

(F) TNFα and IL-6 secretion from RAW264.7 macrophages treated with vehicle (Veh), or FW1256 30 min before (pre) or 30 min after (post) stimulation with LPS (1µg/ml, 24 h).

(G) TNFα and IL-6 secretion from RAW264.7 macrophages pretreated 30 min with H₂S releasing compounds or vehicle (Veh), before stimulation with LPS (1µg/ml, 24 h).

P* < 0.05, *P* < 0.01, ****P* < 0.001. Data in **A** is from 4 repeated experiments (mean ± SEM, n=4), **C**, **E-G** is from 3 repeated experiments (mean ± SEM, n=3, one-way ANOVA with Dunnett's post-test against controls). Immunoblot in **D** is representative of 3 repeated experiments.

Reproduced from (Huang et al., 2016a)

4.4 NF κ B activation is reduced in LPS-stimulated RAW264.7 macrophages treated with FW1256

A key activator that regulates the transcription of pro-inflammatory mediators TNF α , IL-6, IL-1 β , COX-2 and iNOS is the transcription factor NF κ B. H₂S has previously been shown to inhibit NF κ B activation in RAW264.7 macrophages challenged with LPS (Oh et al., 2006). Hence, the effect of FW1256 on NF κ B activation was assessed. NF κ B activation is marked by the degradation of I κ B α , which is a protein that sequesters NF κ B in the cytoplasm. The degradation of I κ B α is preceded by its phosphorylation, mediated by upstream activation of TLRs. Without I κ B α binding, NF κ B would subsequently translocate into the nucleus and activate the transcription of pro-inflammatory mediators.

Phosphorylation of I κ B α is an event which happens within minutes of TLR activation and is also an indicator of NF κ B activation. To determine if FW1256 inhibited NF κ B activation, phosphorylation of I κ B α was assessed in whole cell lysates of these cells stimulated with LPS at intervals between 5 to 60 min (Fig. 4.4A). As compared to untreated cells, FW1256 (200 μ M), reduced phosphorylation of I κ B α at 30 min and 60 min post LPS-stimulation ($P < 0.05$) (Fig 4.4B). To confirm that NF κ B activation was indeed reduced in FW1256 treated cells, nuclear fractionation was carried out on these cells 60 min after LPS-stimulation. The NF κ B p65 subunit present in the nuclear fraction of these cells was quantitated and was significantly reduced when compared to control cells ($P < 0.01$) (Fig 4.4C & D). These findings indicate that FW1256 inhibited NF κ B activation, as evidenced by a reduction in the phosphorylation of I κ B α in

the cytoplasm, as well as reduced p65 translocation into the nucleus of LPS-stimulated RAW264.7 cells.

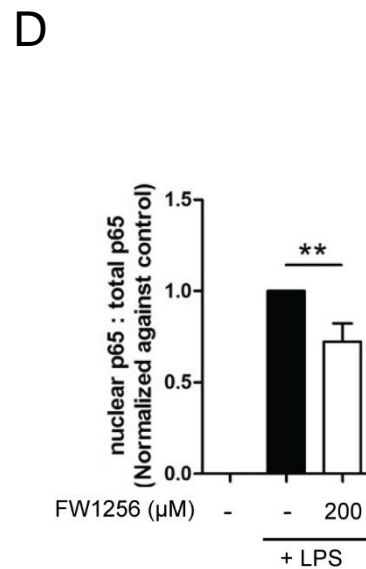
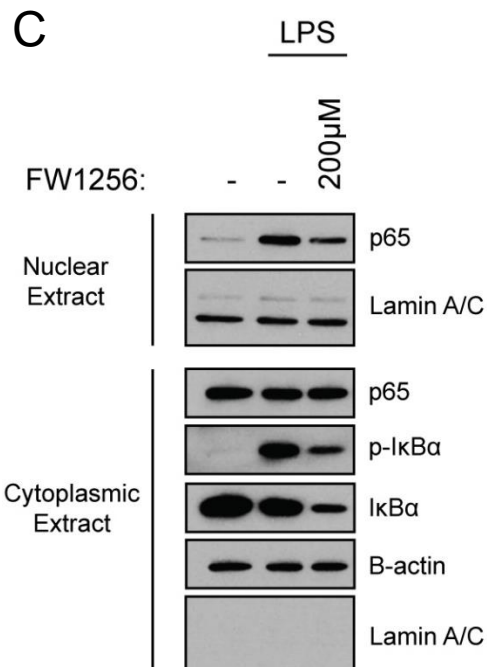
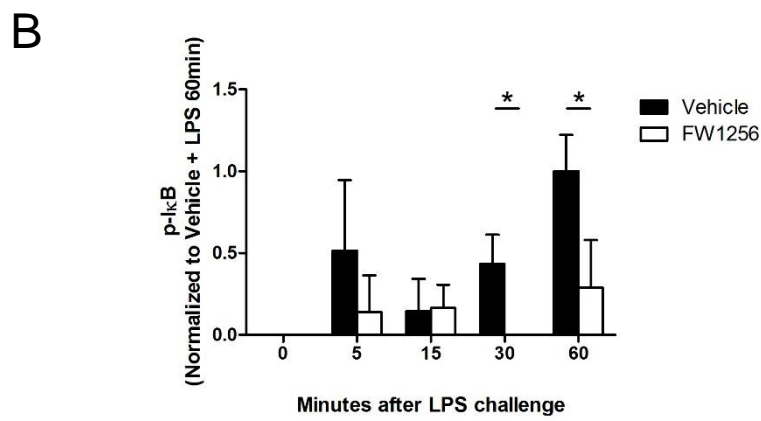
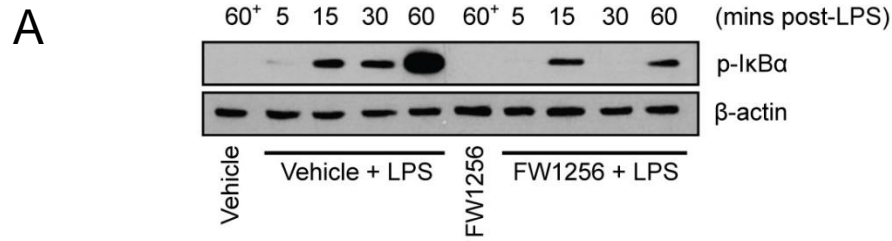


Figure 4.4 Effects of FW1256 on the phosphorylation of I κ B α in LPS-stimulated RAW264.7 macrophages.

(A) Representative immunoblot of phosphorylated I κ B α (p-I κ B α) in RAW264.7 cells pretreated with FW1256 (200 μ M, 30min) before stimulation for 5, 15, 30 and 60 min with LPS (1 μ g/ml). + denotes no LPS added.

(B) Expression of p-I κ B α (c.f. actin, normalized to vehicle + LPS 60 min group) in LPS stimulated RAW264.7 cells as treated in **A**. (mean \pm SD, Mann-Whitney *U* test).

(C) Representative immunoblot of nuclear p65, cytoplasmic p65, p-I κ B α and I κ B α in RAW264.7 cells that were pretreated with FW1256 (200 μ M, 30 min) before stimulation with LPS (1 μ g/ml, 60 min).

(D) Expression of nuclear p65 (c.f. nuclear + cytoplasmic p65) in LPS stimulated RAW264.7 cells as treated in **C**.

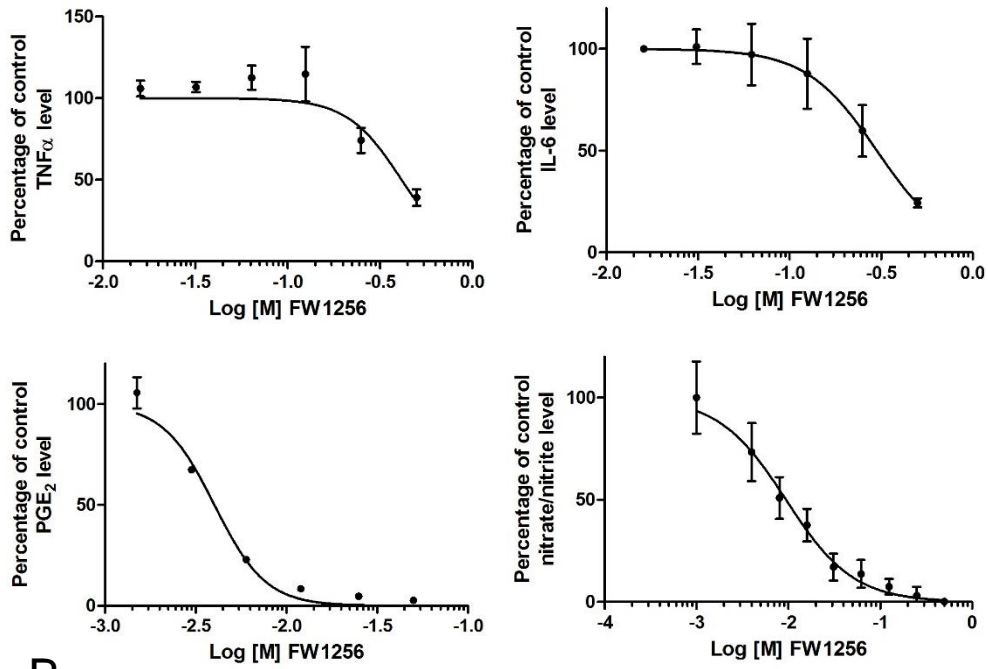
* $P < 0.05$, ** $P < 0.01$. Immunoblots in **A** and **C** are representative of 3 repeated experiments. Data in **B** and **D** is from 3 repeated experiments as indicated for **A** and **C** (mean \pm SD, $n=3$, Mann-Whitney *U* test).

Reproduced from (Huang et al., 2016a)

4.5 FW1256 also downregulated pro-inflammatory mediator release from LPS-stimulated primary bone marrow derived macrophages (BMDMs)

Primary cells taken directly from an *in vivo* source have very few population doublings as compared to immortalised cell lines. As such, primary cells are exposed to lesser selection pressure and are genetically more heterogeneous, and thus may be more representative of the *in vivo* state as compared to immortalised cell lines. We therefore examined whether the downregulation of pro-inflammatory mediators by FW1256 in RAW264.7 cells was also apparent in primary macrophages. BMDMs were pre-treated with varying concentrations of FW1256 prior to stimulation with LPS. Similar to results obtained using RAW264.7 cells, FW1256 also concentration dependently reduced pro-inflammatory cytokine and mediator release from BMDMs (Fig 4.5A), albeit with lesser potency. The IC₅₀s for inhibiting formation of TNF α , IL-6, PGE₂ and NO were 414.9 μ M, 300.2 μ M, 4 μ M and 9.5 μ M respectively, with the corresponding 95% confidence intervals indicated in Fig 4.5B. As a comparison with RAW264.7 cells, the IC₅₀ for inhibiting the release of TNF α and IL-6 in BMDMs is approximately 6.8 and 25.7 times higher respectively. Similar to RAW264.7 cells, FW1256 was not cytotoxic to BMDMs in the presence or absence of LPS (Fig 4.5C), as evidenced by the MTT assay.

A



B

	TNF α	IL-6	PGE ₂	NO
IC ₅₀ FW1256 (μ M)	414.9	300.2	4	9.5
95% CI (μ M)	321.6 – 535.3	225.1 – 400.3	3.6 – 4.5	8.3 – 10.8

C

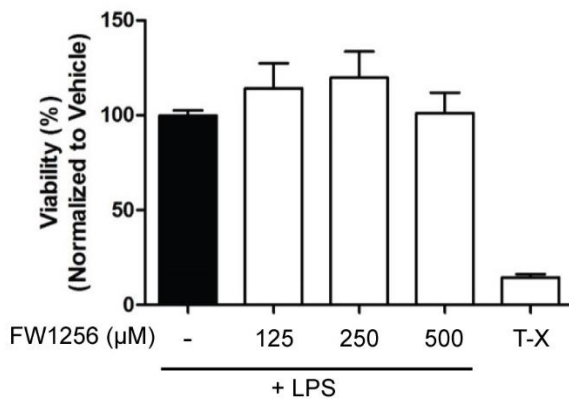


Figure 4.5 FW1256 reduced the production of inflammatory mediators from LPS-stimulated bone marrow derived macrophages (BMDMs).

(A) Dose dependent inhibition of inflammatory cytokines and mediators from BMDMs pretreated 30 min with various doses of FW1256 before stimulation with LPS (1 μ g/ml, 24 h) by FW1256. Nonlinear regression analysis was performed for dose response curves, and the curve of Log [M] FW1256 versus the normalized response is presented. All data points are represented as mean \pm SEM, n=3, except for the NO dose response curve, mean \pm SD, n=6-8.

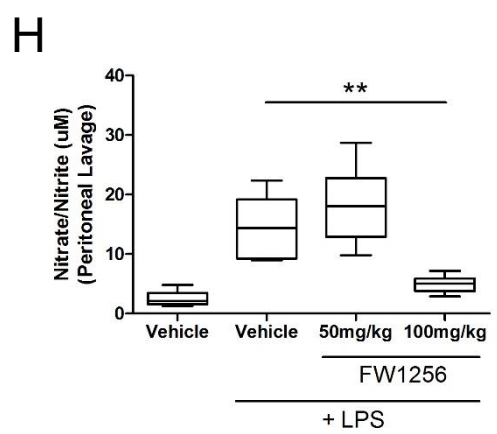
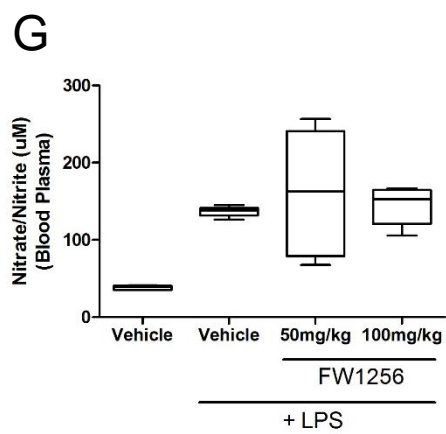
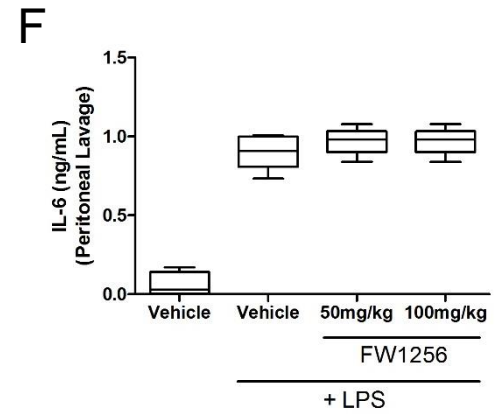
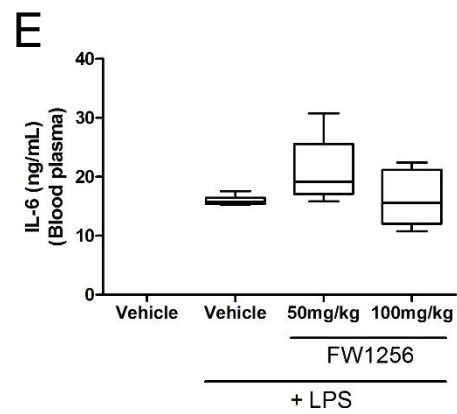
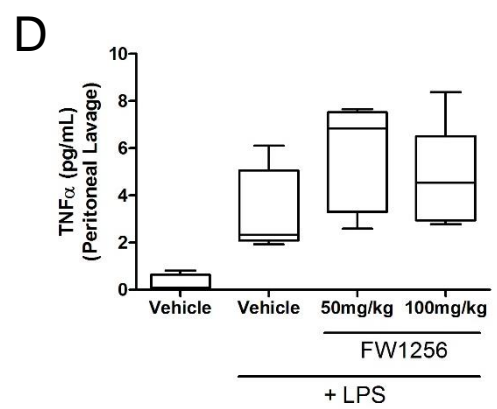
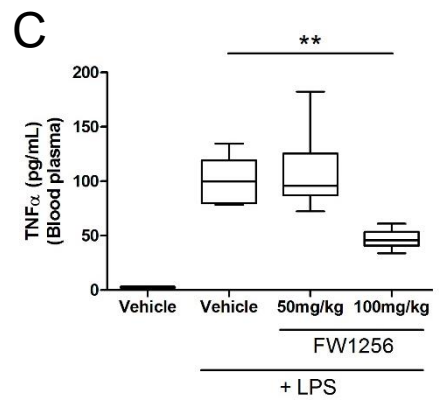
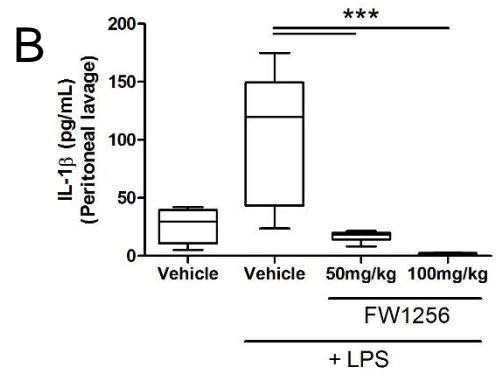
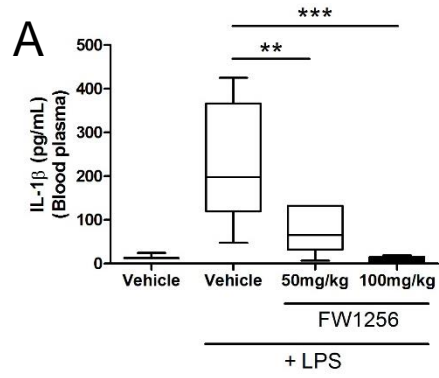
(B) IC₅₀ of FW1256 in reducing inflammatory cytokines and mediators in LPS stimulated BMDMs as treated in **A**.

(C) Toxicity of different doses of FW1256 on LPS (1 μ g/ml) stimulated BMDMs, determined by the MTT assay. 1% Triton-X (T-X) was used as a positive control. Data in **A** (TNF α , IL-6 & PGE₂) is from 3 repeated experiments (mean \pm SEM, n=3), and NO from 2 repeated experiments (mean \pm SD, n=6-8). Data in **C** is from 3 repeated experiments (mean \pm SEM, n=3).

Reproduced from (Huang et al., 2016a)

4.6 FW1256 downregulated pro-inflammatory mediator release in the LPS sepsis mouse model

Having established that FW1256 is able to downregulate pro-inflammatory mediator release both in the RAW264.7 macrophage cell line and in primary mouse BMDMs, the effect of FW1256 (50mg/kg & 100 mg/kg, i.p.) was next assessed *in vivo*, in an LPS model of sepsis in the mouse. To this end, mice were injected with FW1256 (100mg/kg) 30 min before injection of LPS (10mg/kg, i.p.) and killed 6 h thereafter. This timing is the maximal approved duration stipulated in the IACUC protocol under which authority these experiments were conducted. Significantly lower levels of IL-1 β were detected both in blood plasma ($P < 0.01$ and 0.001) and peritoneal lavage ($P < 0.001$) of FW1256-treated mice compared to control animals (Fig 4.6A & B). As compared to control mice, TNF α in the blood plasma, PGE $_2$ in the peritoneum, and nitrate/nitrite levels in the peritoneum were also significantly reduced when mice were treated with a higher dose of FW1256 (ie. 100mg/kg but not 50mg/kg) (Fig 4.6C, 4.6H & I). FW1256 however did not reduce IL-6 levels in these LPS sepsis mice. Together, these data suggest that FW1256 is effective in limiting pro-inflammatory mediator release *in vivo* during systemic infection in mice.



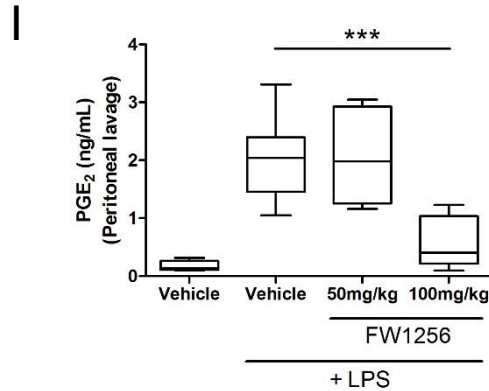


Figure 4.6 FW1256 reduced pro-inflammatory mediators in the mouse model of LPS induced septic shock.

- (A) IL-1 β levels at 6 h in the blood plasma;
- (B) IL-1 β levels at 6 hours in the peritoneal lavage;
- (C) TNF α levels at 6 h in the blood plasma;
- (D) TNF α levels at 6 h in the peritoneal lavage;
- (E) IL-6 levels at 6 h in the blood plasma;
- (F) IL-6 levels at 6 h in the peritoneal lavage;
- (G) nitrate/nitrite levels at 6 h in the blood plasma;
- (H) nitrate/nitrite levels at 6 hours in the peritoneal lavage;
- (I) PGE₂ levels at 6 h in the peritoneal lavage, after intraperitoneal (i.p.) injection with LPS (10mg/kg of body weight), with or without 1 hour i.p. injection of FW1256 (100mg/kg of body weight) prior to LPS injection.

* $P < 0.05$, ** $P < 0.01$, *** $P < 0.001$ (Box and whiskers plot showing median with the 25th and 75th percentiles, whiskers represent smallest and largest values, one-way ANOVA with Dunnett's post-test against controls, n=4-7 mice per group).

Partially reproduced from (Huang et al., 2016a)

4.7 Discussion

The positive effects of exogenous H₂S (i.e. H₂S donor compounds) in diseases with an inflammatory component has been demonstrated in numerous *in vivo* studies in the past decade. Such conditions include but are not limited to hypertension (Cacanyiova et al., 2016), osteoarthritis (Burguera et al., 2016), gastrointestinal disorders (Farrugia and Szurszewski, 2014), cancer (Elsheikh et al., 2014; Lee et al., 2011), renal damage (Lin et al., 2016), myocardial infarction (Karwi et al., 2016) and myocardial fibrosis (Meng et al., 2015). Some of the manifestations of inflammation in these diseases include potential activation of immune cells, fever, swelling, loss of function and pain which conditions are regulated at least in part by the release of pro-inflammatory mediators and cytokines from macrophages (Zhang and An, 2007). Seeking to target macrophages and reduce the release of pro-inflammatory mediators from these cells may therefore be a strategy to limit the extent of inflammation and the associated undesirable symptoms.

Whilst there is a general consensus about the benefits of exogenous H₂S in alleviating symptoms of inflammation as seen in animal models (Wallace et al., 2015), the toxicity of H₂S at high concentrations and its short lifespan due to volatility create significant challenges in the translation of H₂S releasing donors from experimental tools to therapeutic agents. One strategy which may help to overcome these shortcomings is the development of slow-releasing H₂S donors, which release H₂S in small amounts over a prolonged period of time instead of a single large bolus very rapidly. This might be crucial as many inflammatory diseases are chronic and occur over extended time periods. Assuming that H₂S is indeed anti-inflammatory in humans then H₂S releasing

donors which deliver their payload slowly may be advantageous in the clinic. The slow-releasing H₂S donor, GYY4137, has previously been shown to be more potent and more efficient in inhibiting the release of pro-inflammatory mediators from LPS-stimulated RAW264.7 cells, as compared to the fast-releasing H₂S donor, NaHS (Whiteman et al., 2010). Such findings offer support to the principle that slow-releasing H₂S donors have greater potential for therapeutic purposes c.f. fast-releasing H₂S donors. In the present study, we demonstrated that, in the absence of toxicity, the downregulation of pro-inflammatory mediator release from LPS-stimulated RAW264.7 cells by the fast-releasing H₂S donor, NaHS, was greater when administered at a higher concentration and frequency (Fig 3.1). This finding supports the possibility that exposure of macrophages to a smaller concentration of H₂S but over a longer duration is more efficient in limiting pro-inflammatory cytokine release compared to a single large bolus of H₂S. Consistent with these observations, a recent study by Rios *et al.* (Rios et al., 2015) showed that NaHS reduced TNF α and IL-6 secretion from the LPS-challenged human macrophage cell line, THP-1.

Screening of a panel of novel slow-releasing H₂S donors was carried out at an initial concentration of 500 μ M. This concentration was chosen as a starting point based on a previous study in which the potency of GYY4137 in downregulating the release of pro-inflammatory mediators from LPS-stimulated RAW264.7 macrophages was assessed and compared against NaHS (Whiteman et al., 2010). In this study, GYY4137 at the dose of 500 μ M inhibited the release of TNF α , IL-6, PGE₂, nitrite and IL-1 β from LPS-stimulated RAW264.7 macrophages to the largest extent. The panel of H₂S donors

screened in the current work belonged to the same class of H₂S donors (ie. slow-releasing H₂S donors). In addition, since the chemical structures of the novel slow-releasing H₂S donors used in the present study were derived from GYY4137 as either direct analogues, by substitution of side chains with diamino groups, or by cyclisation, we conjectured that any observable anti-inflammatory properties (if any) would be prevalent at a similar concentration.

Using a 2,6-dansyl azide H₂S sensitive fluorescent probe, FW1256 was previously shown to release 77.6% of its available sulfur over a period of 72 h at 37°C in a cell free buffer system (77.6µM ± 1.1 H₂S detected from a solution of FW1256 (100µM) after 72 h, 37°C) (Feng et al., 2015). In a comparison with GYY4137 (1mM) over 72 h at 22°C, FW1256 (1mM) released more H₂S c.f. GYY4137 (approximately 150µM H₂S released from FW1256 as compared to approximately 5µM H₂S released from GYY4137) (Feng et al., 2015). In the present study, the kinetics of H₂S release from FW1256 after delivery into RAW264.7 macrophages by DOTAP liposomes over a period of 24 h was determined using a different H₂S sensitive fluorescent probe as reported in (Wu et al., 2014a). Unlike the 2,6-dansyl azide probe, this probe has been shown to capture H₂S and fluoresce intracellularly. FW1256 released its H₂S 'payload' gradually over the course of 24 h (Fig 4.2C & D). NaHS conversely released its entire payload of H₂S within the first hour (Fig 4.2A & B).

Besides downregulating the inflammatory mediators TNFα and IL-6, FW1256 also reduced both NO release and iNOS expression at the mRNA and protein level (Fig 4.3A - D). This is consistent with other studies showing similar activity of H₂S gas (Oh et al., 2006), GYY4137 (Whiteman et al., 2010), and

diallyl trisulfide (DATS) (Liu et al., 2006), which provides a source of H₂S when metabolized by glutathione in red blood cells (Benavides et al., 2007).

Mechanistically, the anti-inflammatory effect of H₂S has previously been linked to the inhibitory effect it exerts over NFκB (Oh et al., 2006). Other studies also showed that GYY4137 reduced LPS-induced NFκB activation *in vitro* (Whiteman et al., 2010) and *in vivo* (Li et al., 2009). Similarly, diallyl trisulfide (DATS) also suppressed activation of NFκB in LPS-stimulated RAW264.7 cells (Lee et al., 2015). Hence, we hypothesized that FW1256 exerted an inhibitory effect on NFκB, thereby contributing to the downregulation of pro-inflammatory mediators. By assessing cytoplasmic phosphorylated-IκB levels and further substantiating this data with translocated nuclear p65 levels, it was confirmed that FW1256 inhibited NFκB activation in LPS-stimulated RAW264.7 cells (Fig 4.4). Nonetheless, it must also be noted that as there are numerous adaptor proteins and kinases upstream of p65 and IκBα in the TLR4/NFκB activation signaling pathway such as MyD88, TIRAP, TRIF, TRAM, TBK1, TRAF6 and the IκB kinase complex (IKKα, IKKβ and NEMO) (Vallabhapurapu and Karin, 2009), the possibility of H₂S interacting with one of these proteins and thereby inhibiting subsequent downstream NFκB activation is likely. In the present study, the molecular mode of action by H₂S on these other proteins were not examined and remains as potential protein targets to be studied.

When comparing IC₅₀ values of FW1256 that inhibit release of pro-inflammatory mediators from primary BMDMs and the RAW264.7 macrophage cell line, it was clear that, except for NO and PGE₂, the potency of FW1256 against BMDMs differed from that of the RAW264.7 cells. FW1256 was comparatively very poor in inhibiting the release of TNFα and IL-6 in LPS-

stimulated BMDMs as compared to RAW264.7 macrophages (Fig 4.3B and 4.5B). Hence when tested in the LPS sepsis mouse model, it was perhaps not surprising that there was no significant reduction of IL-6 in the blood plasma and peritoneum of these mice as compared to the control group. However, FW1256 did significantly reduce secretion of other pro-inflammatory mediators including IL-1 β , TNF α , nitrate/nitrite and PGE₂ in the LPS sepsis mice 6 h after LPS challenge. Whilst the dose of 50mg/kg of FW1256 was sufficient to reduce IL-1 β levels in the blood plasma and peritoneum, doubling the dose to 100mg/kg further reduced TNF α , NO and PGE₂ levels (Fig 4.6). Although the exact reasons behind the disparity of efficacy between primary macrophages and a cell line was not determined in this study, it is conceivable that the degree of H₂S penetration through the cell membrane differs between BMDMs and RAW267.4 cells. In addition, whether the donors are taken up into the cell prior to the release of H₂S intracellularly or whether the release of H₂S occurs extracellularly prior to its diffusion across the cell membrane also remains an unanswered question.

In conclusion, FW1256, a novel slow-releasing H₂S donor, was found to exert anti-inflammatory effects against mouse macrophages by diminishing the secretion of inflammatory mediators via NF κ B inhibition. Such effects were also apparent when FW1256 was tested in an LPS sepsis mouse model. FW1256 might be used as a slow H₂S-releasing tool to study how H₂S affects biological systems. In addition, the chemical structure of FW1256 could also be further modified to enhance its solubility, permeability and metabolic stability for further improvement of its drug-like properties.

**CHAPTER 5: H₂S INHIBITS NLRP3 INFLAMMASOME
ACTIVATION IN MOUSE MACROPHAGES**

5.1 The H₂S donor NaHS inhibits NLRP3 inflammasome-mediated IL-1 β maturation in J774A.1 macrophages

The release of IL-1 β from macrophages requires a 'priming' step by TLR activation followed by activation of the NLRP3 inflammasome. Previous studies have shown that NLRP3 inflammasome activation in macrophages causes maturation of pro IL-1 β (31 kDa) producing cleaved IL-1 β (17 kDa) which is subsequently secreted out of the cell. This response can be achieved by treating macrophages with LPS (4 h) followed by ATP (5mM, 30 min) (Perregaux and Gabel, 1994). To study the effect of NaHS on NLRP3 inflammasome activation aside from its effect on the 'priming' step by LPS, J774A.1 macrophages were first primed with LPS (1 μ g/ml, 4 h) and then treated with NaHS (30 min) followed by addition of ATP to induce NLRP3 inflammasome activation. In the presence of increasing concentrations of NaHS, the maturation of pro IL-1 β was inhibited in a concentration dependent manner (Fig 5.1). To determine that this inhibitory effect was due to H₂S released from NaHS, time-expired NaHS (tx-NaHS) at the highest concentration studied (600 μ M) was used as a negative control. Unlike NaHS, tx-NaHS, at the same concentration, did not inhibit maturation of pro IL-1 β (Fig 5.1). This strongly suggested that H₂S, released from NaHS, inhibits NLRP3 inflammasome activation in mouse macrophages.

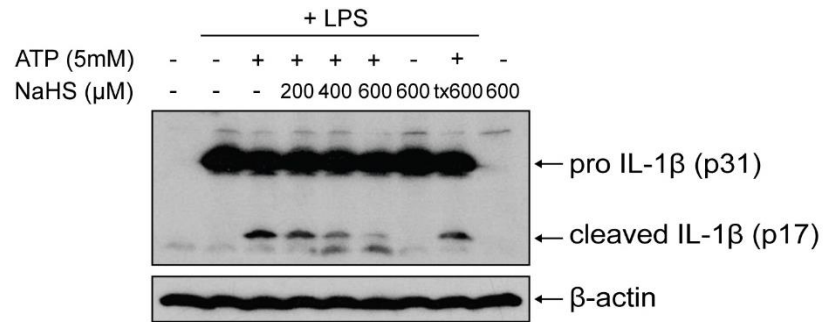


Figure 5.1 The H₂S donor NaHS suppresses NLRP3 inflammasome mediated IL-1 β maturation in J774A.1 macrophages.

Immunoblot analysis of pro- and cleaved IL-1 β in J774A.1 primed with LPS (1 μ g/ml, 4 h) followed by treatment with varying concentrations of NaHS (0, 200, 400 or 600 μ M, 30 min) or time-expired NaHS (tx-NaHS) (600 μ M, 30min), before stimulation with ATP (5mM, 30 min). Immunoblot is representative of 2 repeated experiments.

5.2 Culture of primary BMDMs with L929 conditioned media

One aim of this study was to evaluate the effect of NaHS on NLRP3 inflammasome activation in primary mouse macrophages instead of a cell line. For this work, the conditions required for the differentiation of BMDMs from bone marrow cells in culture were different from those employed for the cell line. Thus, DMEM supplemented with conditioned media from L929 mouse fibroblasts, was used to differentiate and culture BMDMs from mouse bone marrow cells. This procedure is well established in the literature. Media from the L929 cell line contains macrophage colony-stimulating factor (M-CSF), which is essential for BMDM derivatization. However, the use of both 10% v/v L929 (Weischenfeldt and Porse, 2008) and 20% v/v L929 (Mishra et al., 2013) conditioned media has been reported. To determine which percentage would be sufficient for the differentiation process, mouse bone marrow cells from the femurs and tibias of mice were cultured in 10% v/v or 20% v/v L929 conditioned media for 7 days, with a change of media on day 4. Using flow cytometry, BMDMs were stained with antibody against the F4/80 antigen, which is expressed by the majority of mature macrophages (Austyn and Gordon, 1981), and compared with expression in the J774A.1 cells. Culture of bone marrow cells with either 10% v/v or 20% v/v L929 conditioned media led to complete differentiation as indicated by the expression of F4/80 on BMDMs, which was comparable to that of the J774A.1 cell line (Fig 5.2). Hence, the lower concentration of 10% v/v L929 conditioned media (10%) was used for all subsequent experiments.

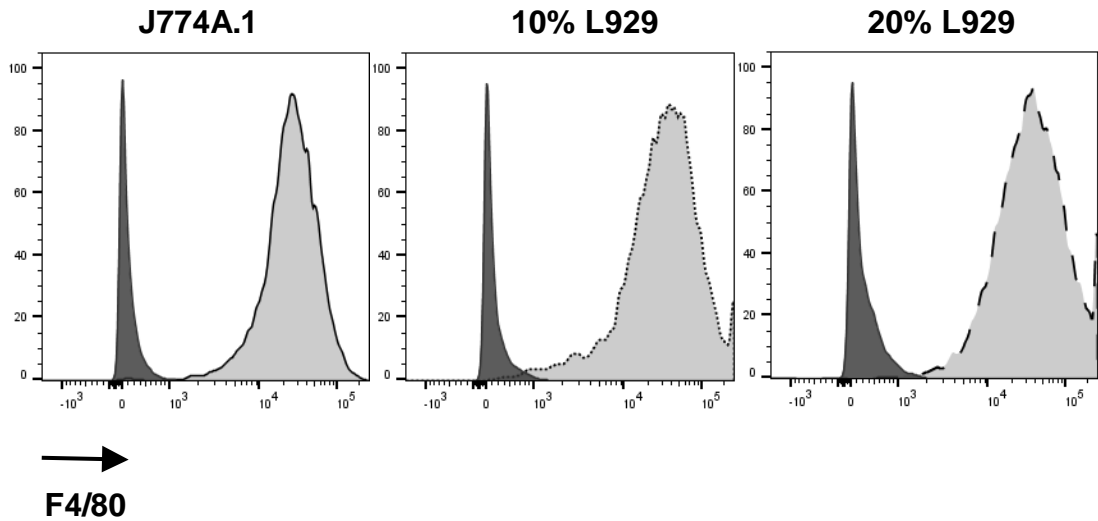


Figure 5.2 L929 conditioned media differentiates mouse bone marrow cells into BMDMs.

Flow cytometry histograms of J774A.1 cells and bone marrow cells cultured in either 10% or 20% L929 conditioned media, stained with the antibody against the F4/80 antigen. Stained cells (light grey histograms) were compared to unstained cells (dark grey histograms).

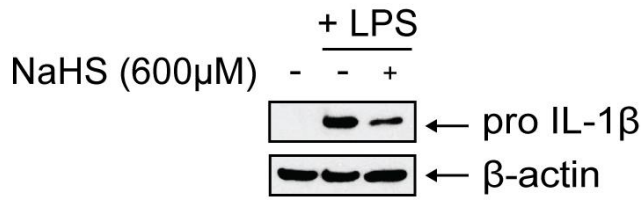
Data is from 1 experiment.

5.3 Exogenous H₂S inhibits NLRP3 inflammasome mediated IL-1 β and IL-18 secretion in BMDMs

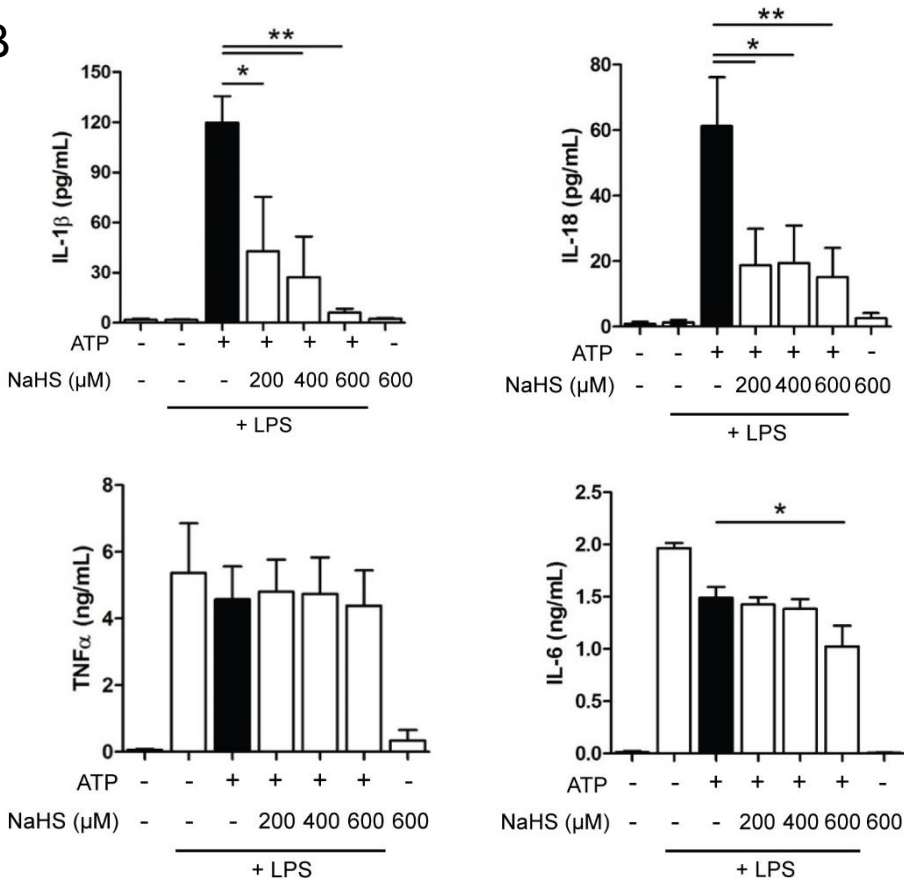
To further investigate whether H₂S inhibits NLRP3 inflammasome activation in primary mouse macrophages, BMDMs were primed with LPS (4 h) and treated with varying concentrations of NaHS (30 min), before activation of the NLRP3 inflammasome by ATP (30 min). Treatment of cells with NaHS was conducted only after LPS priming, as pre-treating cells with NaHS prior to LPS stimulation downregulates pro IL-1 β levels in these cells (Fig 5.3A). In the presence of NaHS administered after LPS priming, IL-1 β and IL-18 secretion were inhibited ($P < 0.01$) (Fig. 5.3B). Conversely, secretion of TNF α and IL-6, which relies on toll-like receptor signalling but not NLRP3 inflammasome activation, was unaffected. This was the case with the exception of IL-6 secretion at the maximal concentration of NaHS (600 μ M). At this concentration, NaHS caused a significant decrease in IL-6 secretion ($P < 0.05$) (Fig. 5.3B). To substantiate these findings, another widely reported NLRP3 inflammasome activator, nigericin, was used. Similar to data obtained with ATP stimulation, NaHS inhibited nigericin induced IL-1 β ($P < 0.001$) and IL-18 ($P < 0.05$) secretion without affecting either TNF α or IL-6 secretion (Fig 5.3C).

A second hallmark of NLRP3 inflammasome activation is activation of caspase-1. Activation of caspase-1 occurs when pro caspase-1 (45 kDa) is degraded to form a cleaved, mature form of caspase-1 (20 kDa). Treatment of LPS-primed BMDMs with the pan caspase inhibitor Z-VAD-FMK (10 μ M) prior to ATP or nigericin stimulation inhibited the secretion of IL-1 β , thereby strongly suggesting that activation of caspase-1 is required for the secretion of IL-1 β (Fig 5.3D).

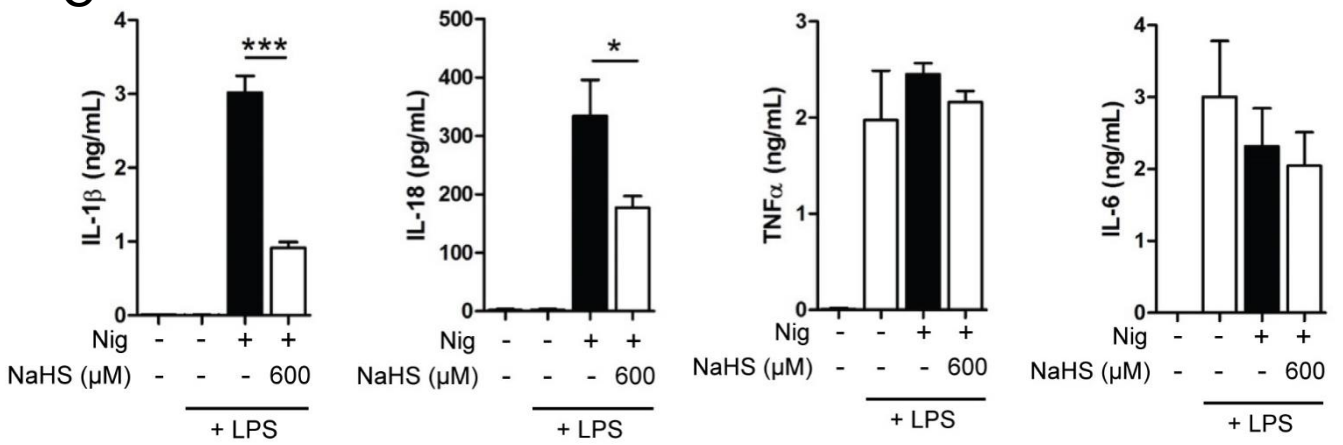
A



B



C



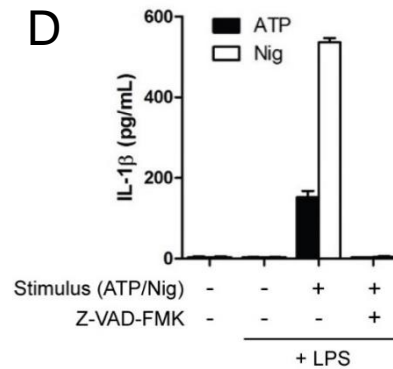


Figure 5.3 H₂S exerts an inhibitory effect on NLRP3 inflammasome mediated IL-1 β and IL-18 secretion in BMDMs.

(A) Immunoblot analysis of lysates from BMDMs treated with NaHS (600 μ M, 30 min) prior to stimulation with LPS (1 μ g/ml, 4 h). Data is from 3 repeated experiments.

(B) Inflammatory cytokines secreted (IL-1 β , IL-18, TNF α and IL-6) from BMDMs primed with LPS (1 μ g/ml, 4 h) followed by treatment with varying concentrations of NaHS (0, 200, 400 or 600 μ M, 30 min), before stimulation with ATP (5mM, 30 min).

(C) Inflammatory cytokines secreted (IL-1 β , IL-18, TNF α and IL-6) from BMDMs primed with LPS (1 μ g/ml, 4 h) followed by treatment with NaHS (600 μ M, 30 min), before stimulation with nigericin (10 μ M, 1 h).

(D) Secreted IL-1 β from BMDMs primed with LPS (1 μ g/ml, 4 h), followed by treatment with the pan caspase inhibitor Z-VAD-FMK (10 μ g/ml, 30 min), before stimulation with either ATP (5mM, 30min) or nigericin (10 μ M, 1 h).

* $P < 0.05$, ** $P < 0.01$, *** $P < 0.001$. Immunoblot in **A** is representative of 3 repeated experiments. Data in **B-D** is from 3 - 5 repeated experiments (mean \pm SEM, n=3-5, one-way ANOVA with Dunnett's post-test against controls).

5.4 Exogenous H₂S inhibits NLRP3 inflammasome mediated IL-1 β and caspase-1 maturation in BMDMs

Secreted IL-1 β exists as the cleaved, mature form of IL-1 β (17 kDa) (Perregaux and Gabel, 1994). Having observed that H₂S reduced IL-1 β secretion from BMDMs as detected by ELISA (Fig 5.3B & C), it was not surprising that H₂S also reduced cleaved IL-1 β in the lysates of BMDMs primed with LPS and stimulated with either ATP or nigericin, as detected by immunoblotting (Fig 5.4A & C). Tx-NaHS did not reduce cleaved IL-1 β expression (Fig 5.4A & C) thereby suggesting H₂S mediates the inhibitory effect of NaHS. In addition, NaHS also significantly reduced cleaved caspase-1 (20 kDa) levels in the lysates of these cells ($P < 0.001$) (Fig 5.4A – D). As expected, tx-NaHS did not inhibit the activation of caspase-1 to form cleaved caspase-1 (Fig 5.4A - D).

To rule out the possibility that inhibition of IL-1 β and IL-18 secretion, as well as the maturation of IL-1 β and IL-18 by NaHS, was due to cell death, an MTT assay was performed on cells treated with the highest concentration of NaHS (600 μ M). At this concentration, NaHS did not cause cell death (Fig 5.4E). Altogether, these data suggest that exogenous H₂S, released from NaHS, inhibits the activation of the NLRP3 inflammasome in BMDMs in the absence of cell toxicity.

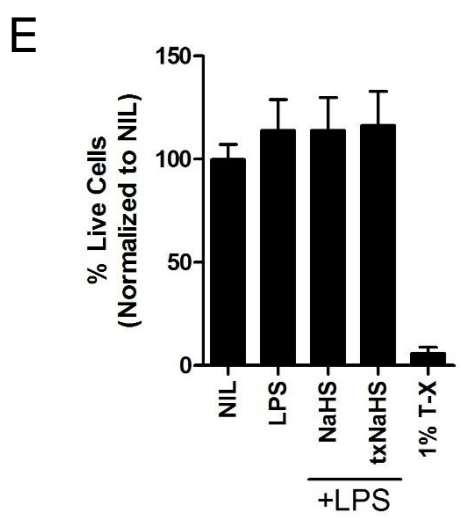
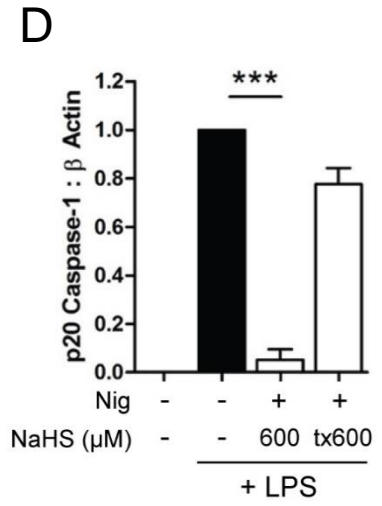
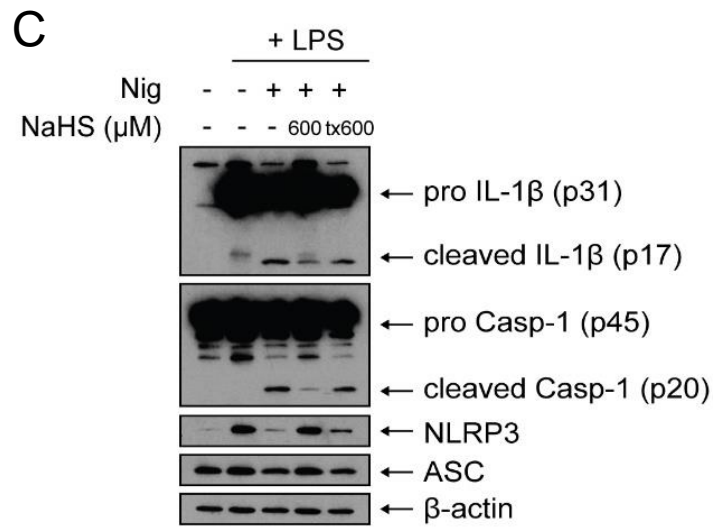
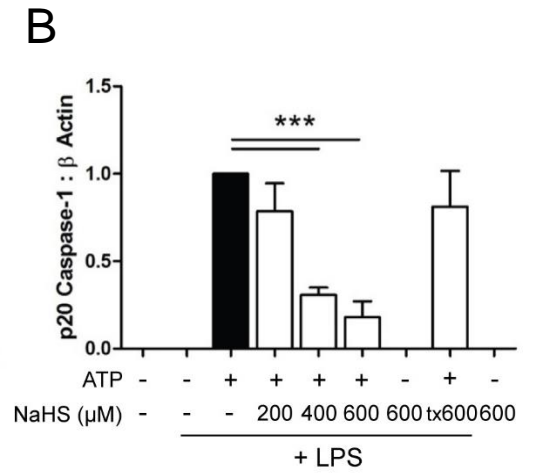
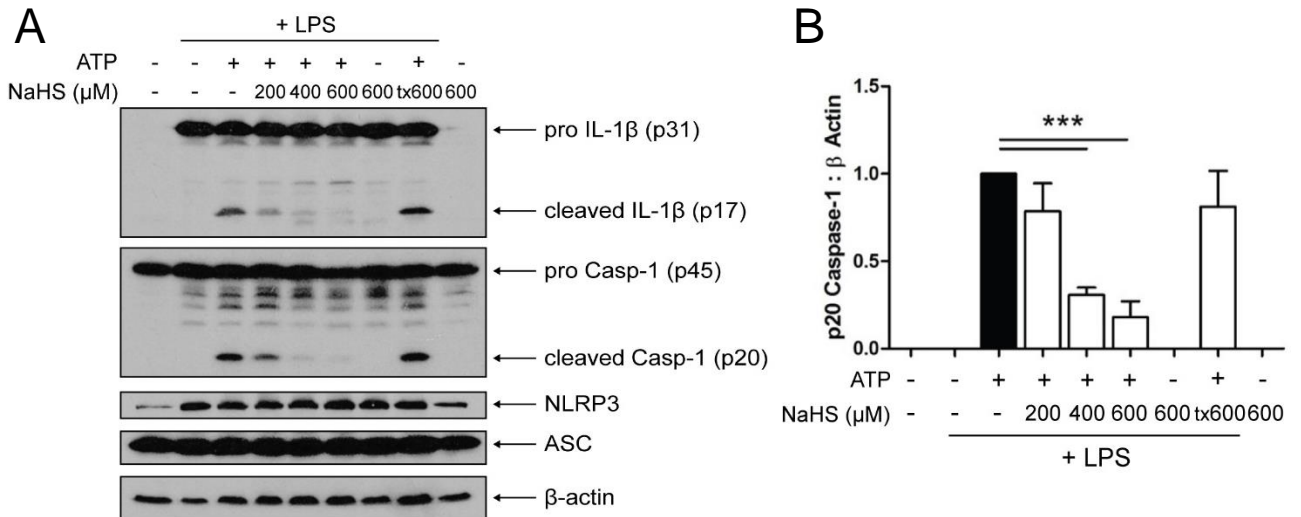


Figure 5.4 The H₂S donor NaHS exerts an inhibitory effect on NLRP3 inflammasome mediated IL-1 β and IL-18 secretion, and caspase-1 activation in BMDMs.

(A) Immunoblot analysis of lysates from BMDMs primed with LPS (1 μ g/ml, 4 h) followed by treatment with varying concentrations of NaHS (0, 200, 400 or 600 μ M, 30 min) or time-expired NaHS (tx-NaHS) (600 μ M, 30 min), before stimulation with ATP (5mM, 30 min).

(B) Quantification of p20 caspase-1 subunit : β -actin as treated in **A**. Results are from 3 repeated experiments.

(C) Immunoblot analysis of lysates from BMDMs primed with LPS (1 μ g/ml, 4 h) followed by treatment with NaHS (600 μ M, 30 min) or tx-NaHS (600 μ M, 30 min), before stimulation with nigericin (10 μ M, 1 h).

(D) Quantification of p20 caspase-1 subunit : β -actin as treated in **C**. Results are from 3 repeated experiments.

(E) Toxicity of NaHS and txNaHS (600 μ M) on BMDMs primed with LPS (1 μ g/ml, 4 h), as determined by the MTT assay. 1% Triton-X (T-X) was used as a positive control.

*** $P < 0.001$. Immunoblots in **A** and **C** are representative of 3 repeated experiments. Data in **B** and **D** is from 3 repeated experiments as indicated for **A** and **C** (mean \pm SD, n=3, one-way ANOVA with Dunnett's post-test against controls), and data in **E** is from 3 repeated experiments (mean \pm SEM, n=3).

5.5 NaHS and slow-releasing H₂S donors FW1256 and GYY4137 inhibits NLRP3 inflammasome activation in BMDMs

To determine whether slow-releasing H₂S donors can also inhibit NLRP3 inflammasome activation in BMDMs, BMDMs were treated with various doses of NaHS (30 min), FW1256 (1 h) or GYY4137 (1 h) after LPS priming and prior to NLRP3 inflammasome activation by ATP. NaHS and FW1256 dose-dependently inhibited IL-1 β and IL-18 release in BMDMs with the half-maximal inhibitory concentration (IC₅₀) of NaHS for IL-1 β and IL-18 being 73.6 μ M and 65.2 μ M respectively (Fig 5.5A & B), and IC₅₀ of FW1256 for IL-1 β and IL-18 being 215.9 μ M and 118.5 μ M respectively (Fig 5.5C & D). GYY4137 however only caused a statistically significant ($P < 0.05$) decrease of IL-1 β but not IL-18 at a concentration of 600 μ M (Fig 5.5E & F). These findings imply that amongst these three H₂S donors, NaHS displayed the highest potency in inhibiting NLRP3 inflammasome activation followed by FW1256 and GYY4137 respectively. This is expected given that the rate of release of H₂S has previously been shown to be the highest for NaHS, followed by FW1256 and then GYY4137 (Feng et al., 2015).

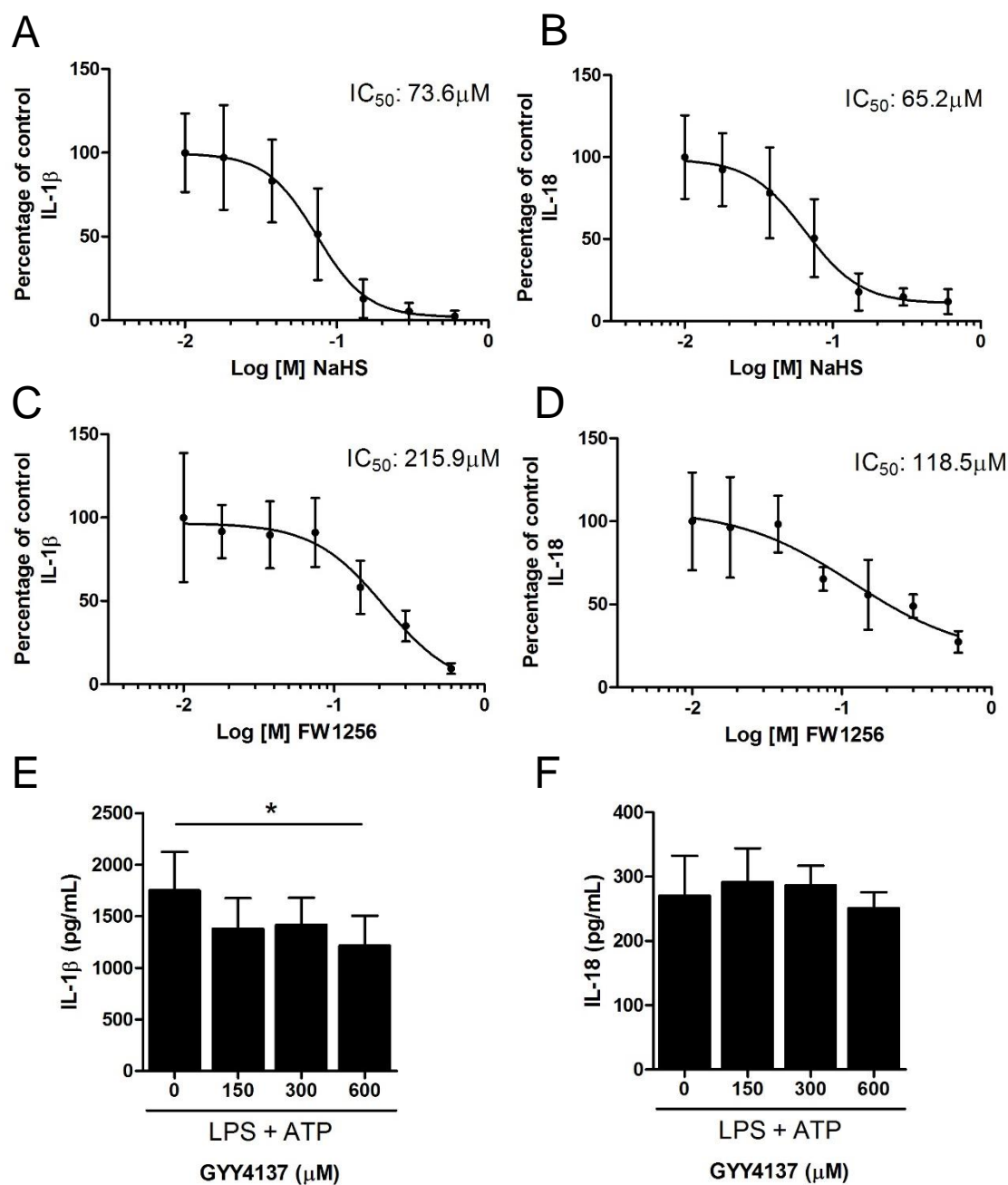


Figure 5.5 NaHS, FW1256 and GYY4137 induced Inhibition of IL-1 β and IL-18 from NLRP3 inflammasome activated BMDMs.

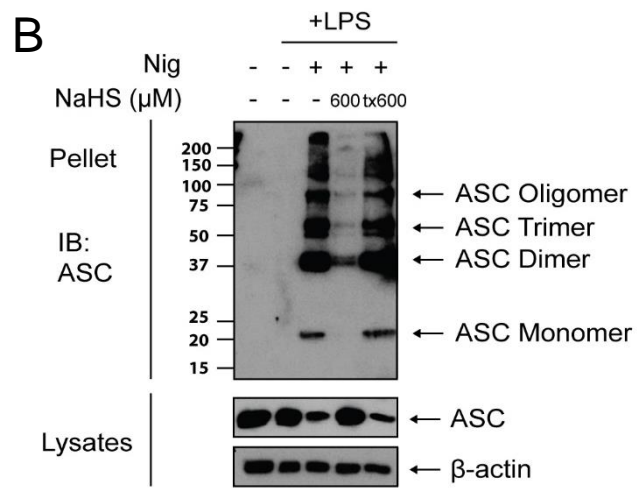
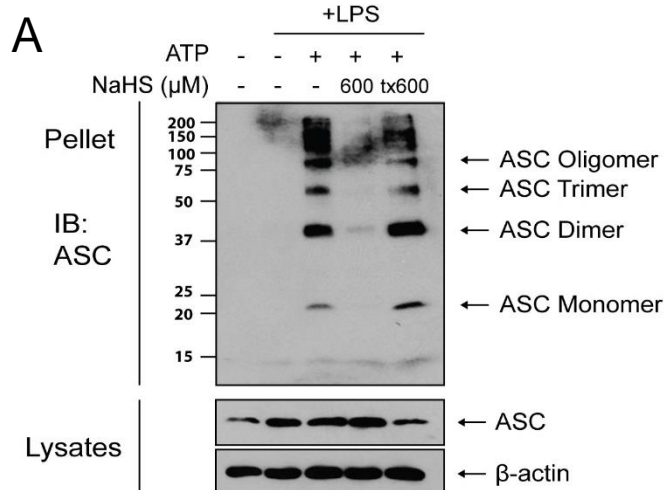
(A-B) Production of IL-1 β and IL-18 from BMDMs primed with LPS (1 $\mu g/ml$, 4 h) followed by treatment with either NaHS (18 - 600 μM , 30 min); (C-D) FW1256 (18 - 600 μM , 1 h); or (E-F) GYY4137 (150 - 600 μM , 1 h) before stimulation with ATP (5mM, 30 min).

Data is from 3 repeated experiments. * $P < 0.05$. Data is from 3 repeated experiments (mean \pm SD, $n=4-8$, one-way ANOVA with Dunnett's post-test against controls). Nonlinear regression analysis was performed for dose response curves, and the curve of Log [M] NaHS or Log [M] FW1256 versus the normalized response is presented.

5.6 Exogenous H₂S inhibits NLRP3 inflammasome-mediated pyroptosome formation in BMDMs

Pyroptosis is a form of cell death that occurs as a result of inflammasome activation. In conjunction with pyroptosis, a pyroptosome, which is a supramolecular assembly of ASC dimers must first be formed (Fernandes-Alnemri et al., 2007). Chemically cross-linking ASC in the cell pellet with disuccinimidyl suberate (DSS) allows for the detection of ASC aggregation by immunoblotting and is thus an indication of pyroptosome formation. To determine whether NaHS inhibits NLRP3 inflammasome-mediated pyroptosome formation, LPS primed BMDMs were treated with NaHS (600 μM) prior to NLRP3 inflammasome activation with either ATP or nigericin. Under these conditions, NaHS inhibited the presence of ASC aggregation as evidenced by decreased ASC laddering visualized by immunoblotting (Fig 5.6A & B).

Using detection via immunofluorescent staining, BMDMs primed with LPS and stimulated with nigericin resulted in the formation of ASC specks. Consistent with published findings (Proell et al., 2013) only one ASC speck was apparent per cell (Fig 5.6C). Treatment of macrophages with NaHS prior to nigericin stimulation significantly reduced ASC speck formation ($P < 0.001$), consistent with that observed from the ASC cross-linking assay (Fig 5.6B - D). Hence, the present data shows that NaHS inhibits NLRP3 inflammasome-mediated pyroptosome formation in BMDMs.



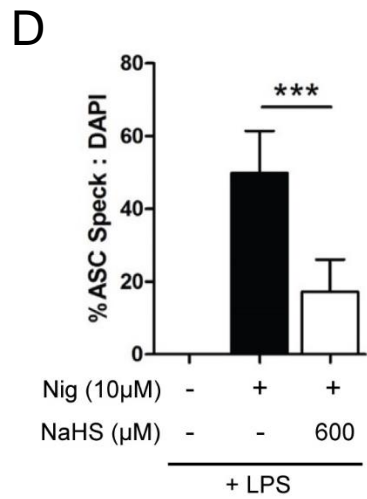
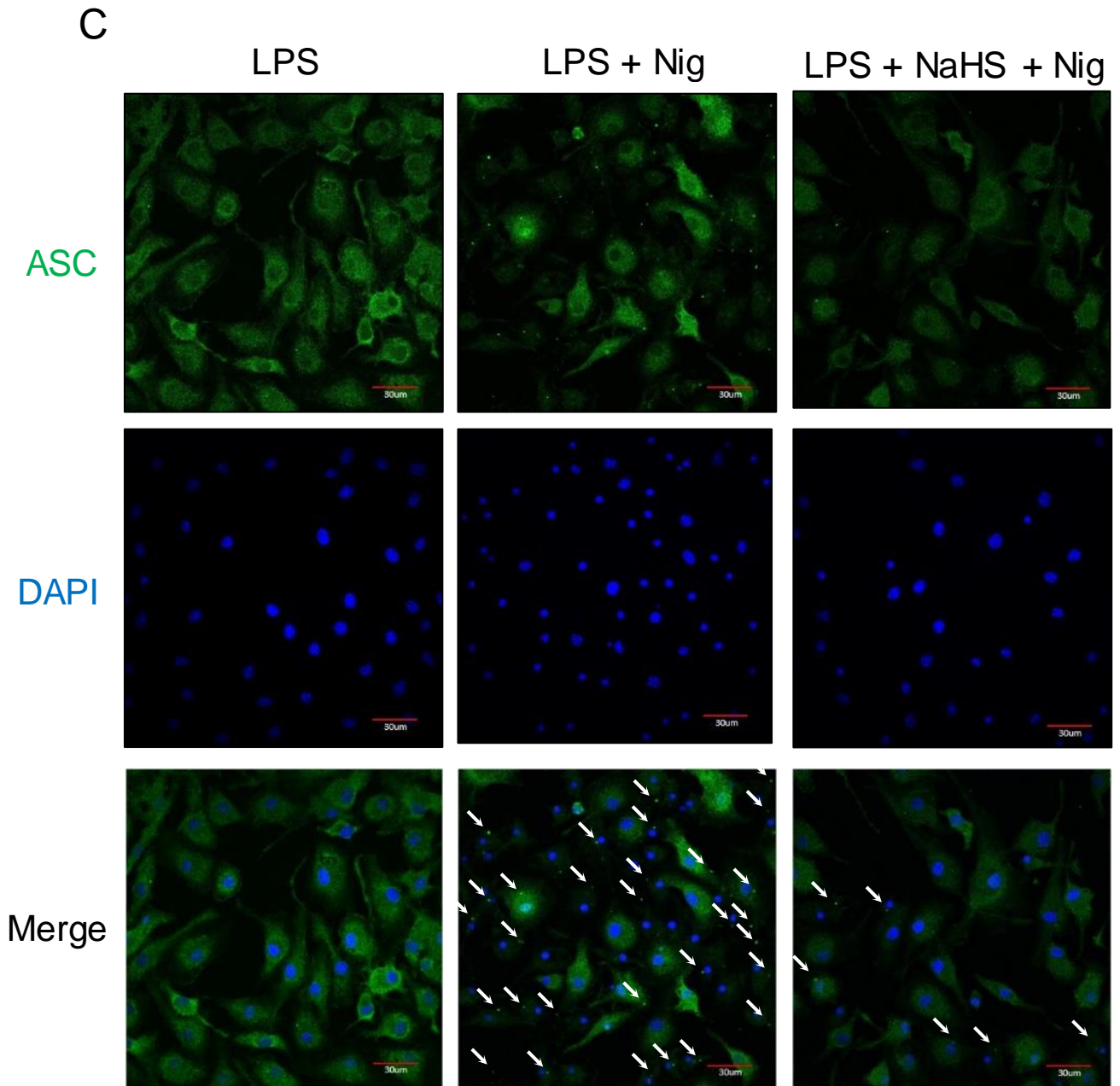


Figure 5.6 The H₂S donor NaHS inhibits NLRP3 inflammasome mediated pyroptosome formation in BMDMs.

(A) ASC oligomerization in BMDMs primed with LPS (1 µg/ml, 4 h), followed by treatment with NaHS or time-expired NaHS (tx600) (600 µM, 30 min), before being stimulated with ATP (5mM, 30 min).

(B) ASC oligomerization in BMDMs primed with LPS (1 µg/ml, 4 h), followed by treatment with NaHS or time-expired NaHS (tx600) (600 µM, 30 min), before being stimulated with nigericin (10 µM, 1 h).

(C) Immunofluorescence microscopy of BMDMs treated as in **B**. Cells were stained for ASC (green) and nuclei (blue; DNA-binding dye DAPI). Arrowheads indicate ASC specks. Scale bars, 30 µm.

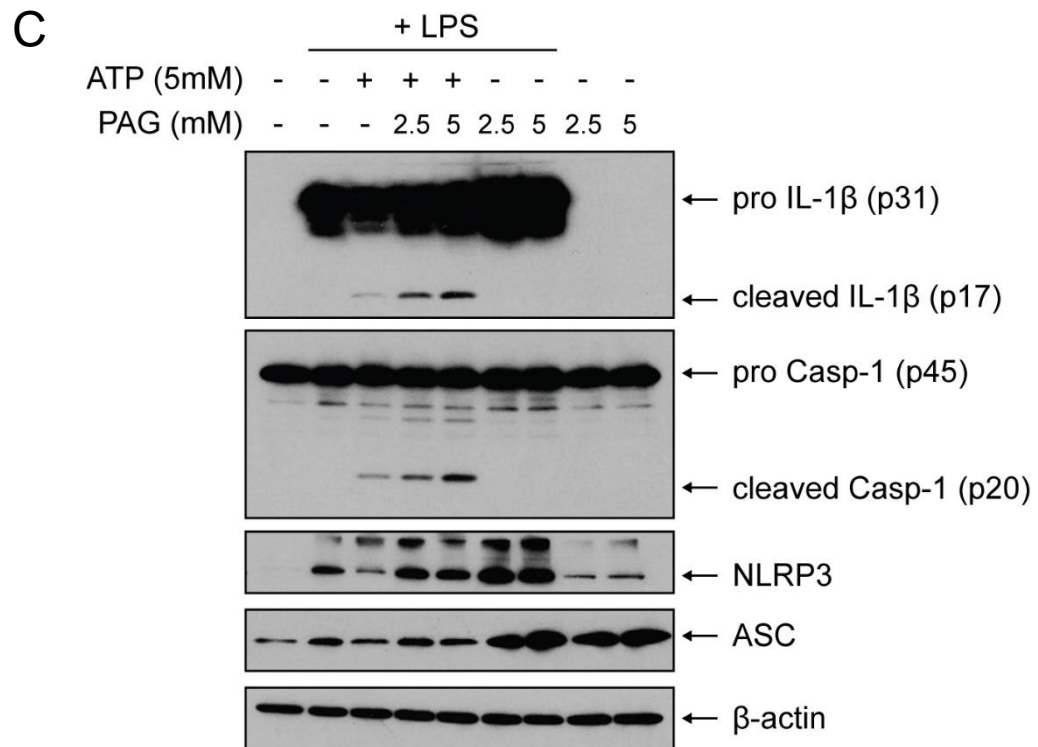
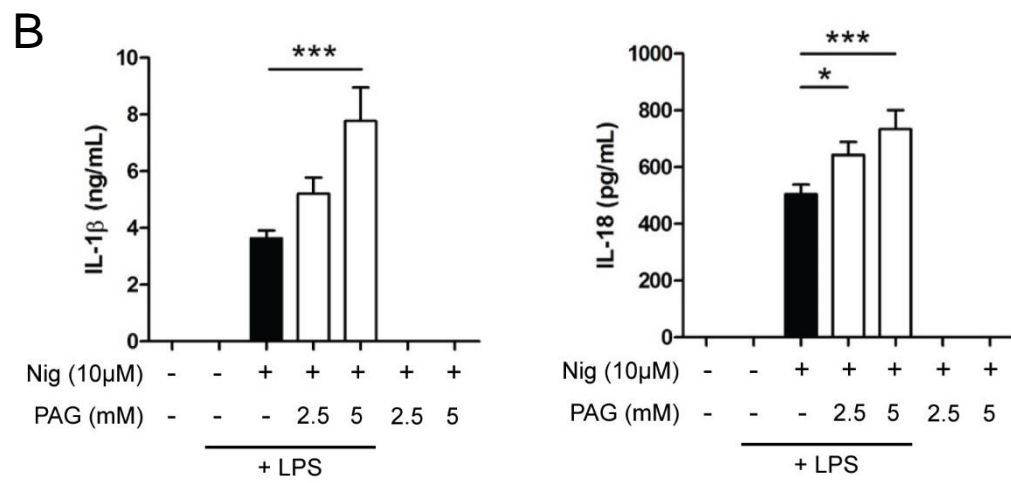
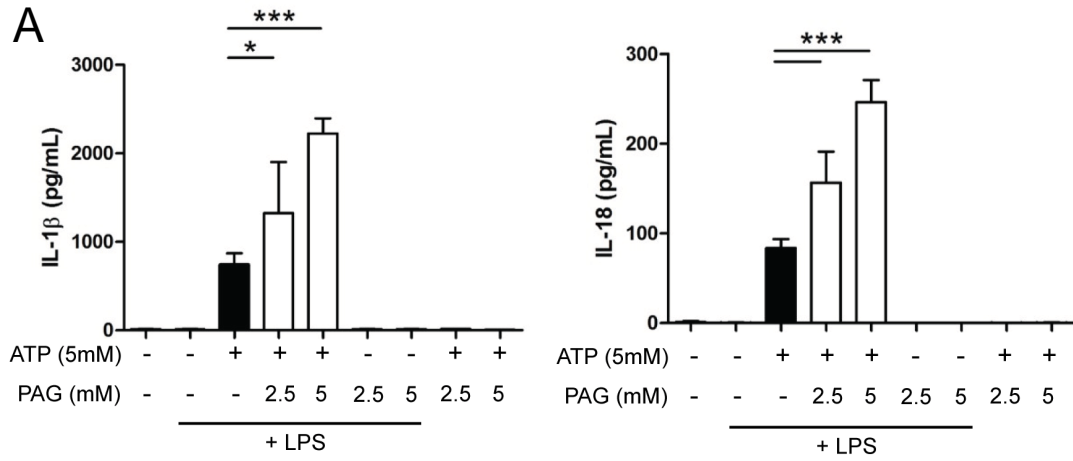
(D) Percentage of BMDMs containing ASC specks. Data is from 2 repeated experiments, with 7 frames taken in each experiment and at least 800 cells counted in total.

*** $P < 0.001$. Immunoblots in **A** and **B** are representative of 3 repeated experiments, and quantification in **D** is from 2 repeated experiments, with 7 frames taken in each experiment and at least 800 cells counted in total. (Mean \pm SD, one-way ANOVA with Dunnett's post-test against controls)

5.7 The CSE inhibitor, DL-PAG, exacerbates NLRP3 inflammasome activation

Since exogenous H₂S inhibited NLRP3 inflammasome activation and pyroptosome formation, it was clearly of interest to determine whether endogenous H₂S had similar activity. Macrophage H₂S production is at least partially dependent on CSE enzyme activity (Dufton et al., 2012). To study the role of endogenous CSE, BMDMs were exposed to the irreversible CSE inhibitor, DL-PAG, for 24 h prior to LPS priming and subsequent ATP or nigericin stimulation. DL-PAG concentration dependently exacerbated NLRP3 inflammasome activation as evidenced by increased amounts of IL-1 β and IL-18 secreted from LPS-primed BMDMs, stimulated with either ATP or nigericin (Fig 5.7A & B). Immunoblot analysis further confirmed that PAG increased cleaved IL-1 β (p17) and caspase-1 (p20) from LPS-primed BMDMs stimulated with ATP (Fig 5.7C). Since DL-PAG treatment was started 24 h prior to LPS priming, it was important to determine whether DL-PAG increased pro IL-1 β expression during the LPS priming step leading to increased cleaved and secreted IL-1 β . Immunoblotting confirmed that DL-PAG treatment (24 h) prior to LPS priming (4 h) did not affect pro IL-1 β , NLRP3, ASC and pro Caspase-1 expression levels (Fig 5.7D).

However, it should be noted that further experiments are needed to validate the data. Such experiments should perhaps utilise alternative approaches to target macrophage CSE activity such as siRNA-mediated silencing of CSE in BMDMs, as well as the use of BMDMs derived from CSE^{-/-} mice. However, such mice were not available in the laboratory at the time of these experiments.



D

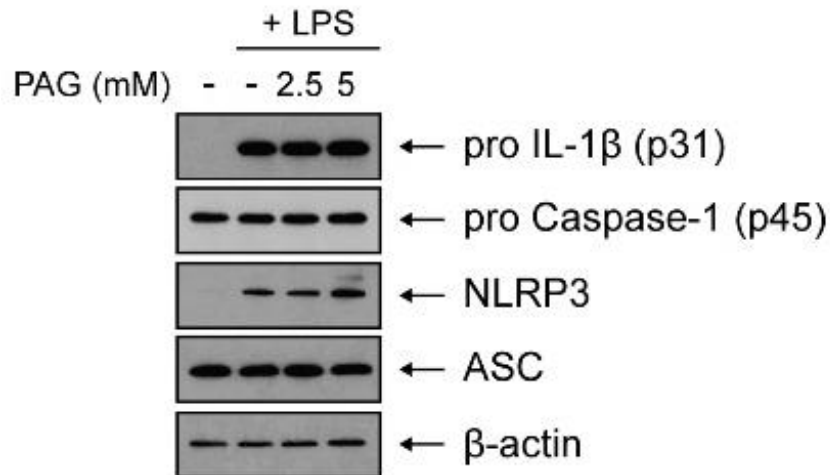


Figure 5.7 DL-PAG exacerbates NLRP3 inflammasome mediated IL-1 β and IL-18 secretion, and caspase-1 activation in BMDMs.

(A) Secreted IL-1 β and IL-18 from BMDMs treated with 2 doses of DL-PAG (24 h), before being primed with LPS (1 μ g/ml, 4 h), followed by stimulation with ATP (5mM, 30 min) (mean \pm SD, n=3).

(B) Secreted IL-1 β and IL-18 from BMDMs treated with 2 doses of DL-PAG (24 h), before being primed with LPS (1 μ g/ml, 4 h), followed by stimulation with nigericin (10 μ M, 1 h) (mean \pm SEM, n=6).

(C) Immunoblot analysis of lysates from BMDMs treated as in **A**.

(D) Immunoblot analysis of lysates from BMDMs treated with DL-PAG (24 h), before being primed with LPS (1 μ g/ml, 4 h).

* $P < 0.05$, *** $P < 0.001$. Data in **A** is from 3 repeated experiments (mean \pm SD, n=3, one-way ANOVA with Dunnett's post-test against controls). Data in **B** is from 6 repeated experiments (mean \pm SEM, n=6, one-way ANOVA with Dunnett's post-test against controls). Immunoblot in **C** and **D** is representative of 3 repeated experiments.

5.8 Development and optimization of an *in vitro* NLRP3 inflammasome reconstitution system in HEK293T cells

Having established that exogenous H₂S inhibits NLRP3 inflammasome activation, the mechanism of action by which this occurs was examined. Since the activation of the NLRP3 inflammasome involves interaction of NLRP3, ASC and pro Caspase-1, we hypothesized that H₂S might inhibit the interplay between these proteins. To study the interaction of these 3 NLRP3 inflammasome components, overexpression plasmids encoding for mouse NLRP3, mouse ASC, mouse pro Caspase-1 and mouse pro IL-1 β were constructed. Co-expressing these 4 plasmids together in HEK293T cells resulted in the secretion of IL-1 β from these cells (Fig 5.8A), which was not apparent in untransfected HEK293T cells (Fig 5.8B).

The *in vitro* NLRP3 inflammasome reconstitution assay has been reported in the literature prior to this present study (Bryan et al., 2009; Wu et al., 2014b; Yu et al., 2014). Of these studies, only two reported the concentrations of overexpressing plasmids used (summarised in Table 5.1). These studies both utilised concentrations of pro IL-1 β , NLRP3, ASC and pro Caspase-1 overexpressing plasmids in the approximate ratio 1 : 0.1 : 0.1 : 0.05. Thus, optimisation of the *in vitro* NLRP3 reconstitution system in the present study was carried out using an identical ratio of overexpressing plasmids. Co-expression of the 4 plasmids was carried out in 10⁶ HEK293T cells plated in 6 well cell culture plates in the presence of pro IL-1 β (1000ng). For all conditions, a negative control with the NLRP3 component excluded was used. IL-1 β secreted from this system was then measured by ELISA.

When pro IL-1 β (500ng to 1000ng) was over-expressed, the presence of NLRP3 was inconsequential as evidenced by similar amounts of secreted IL-1 β by the negative controls (c.f. with NLRP3) (Fig 5.8A). This suggested that pro Caspase-1 was able to trigger IL-1 β secretion in the absence of a fully reconstituted NLRP3 inflammasome. In order to verify whether pro Caspase-1 was necessary for the secretion of IL-1 β in this system, the 4 plasmids were co-expressed at the highest concentration of IL-1 β (1000ng), with or without pro Caspase-1 (50ng). The absence of pro Caspase-1 abrogated IL-1 β secretion, thereby confirming that pro Caspase-1 was required for IL-1 β secretion (Fig 5.8B).

Lowering the concentrations of the 4 plasmids showed that pro IL-1 β (250ng) in the absence of NLRP3 secreted less IL-1 β (c.f. with NLRP3). Thus, it would appear that pro IL-1 β was in excess at concentrations above 250ng. When titres of pro IL-1 β were further reduced (between 31 to 125ng), secreted IL-1 β was not detected (Fig 5.8A). Hence, all further optimisation experiments for plasmid concentrations were carried out using pro IL-1 β (250ng), NLRP3 (25ng), ASC (25ng) and pro Caspase-1 (12.5ng).

It is conceivable that high concentrations of pro Caspase-1 might trigger a non inflammasome-mediated IL-1 β secretion. To assess this possibility the concentration of pro Caspase-1 was reduced and IL-1 β secretion determined with or without NLRP3 in the presence of the other 3 plasmids. Under these conditions, in the absence of NLRP3, pro Caspase-1 concentration dependently reduced IL-1 β secretion (Fig 5.8C), suggesting that pro Caspase-1 at high concentrations was able to cleave pro IL-1 β indiscriminately even in the absence of a fully reconstituted NLRP3 inflammasome in this system.

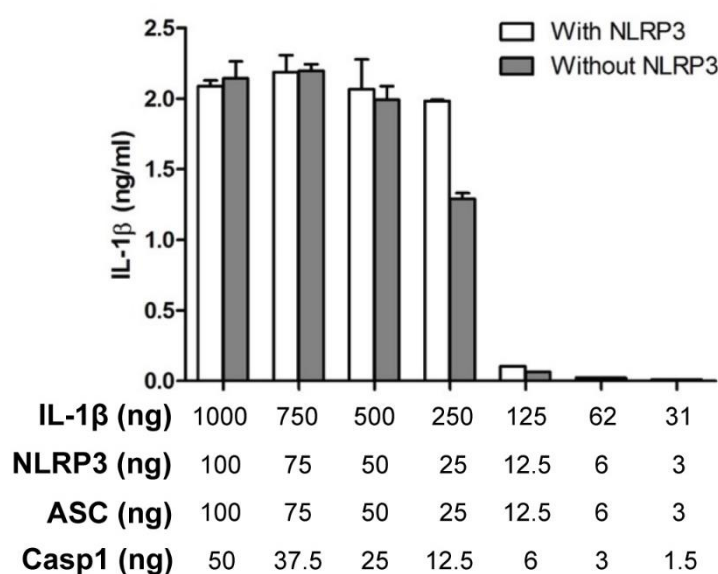
To determine a suitable concentration of pro Caspase-1, pro Caspase-1 was titrated (1.5ng to 25ng) while maintaining the titres of the other 3 plasmids constant at IL-1 β (250ng), NLRP3 (25ng) and ASC (25ng). Pro Caspase-1 (3ng) was the lowest possible titre for this system to function since at pro Caspase-1 (1.5ng), no secreted IL-1 β was detected (Fig 5.8C). As further experiments using this system were scaled down to the 12 well cell culture plate format, the titres of the plasmids were halved to a final titre of pro IL-1 β (125ng), NLRP3 (12.5ng), ASC (12.5ng) and pro Caspase-1 (1.5ng) for all subsequent experiments. Finally, the absence of any component (NLRP3, ASC or pro Caspase-1) prevented the maturation and secretion of IL-1 β (Fig 5.8D), showing that each component of the NLRP3 inflammasome was required for this system to function.

In summary, characterisation of the *in vitro* NLRP3 inflammasome reconstitution system in HEK293T revealed the optimal titres of each overexpressing plasmids required for the system to function. In addition, this system required all components of the NLRP3 inflammasome without which no mature and secreted IL-1 β was formed.

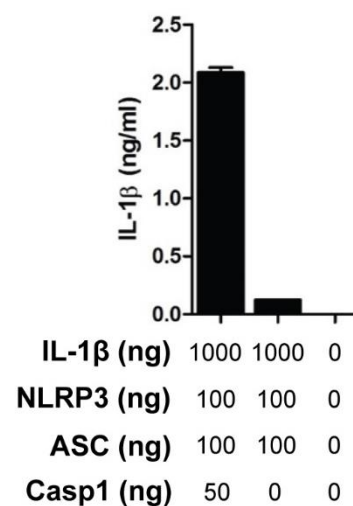
Table 5.1 Previously reported In vitro NLRP3 inflammasome reconstitution assay conditions

No.	Pro IL-1 β (ng)	NLRP3 (ng)	ASC (ng)	Pro Casp-1 (ng)	Reference
1	200	25	20	10	(Lo et al., 2013)
2	1000	150	150	50	(Mishra et al., 2013)

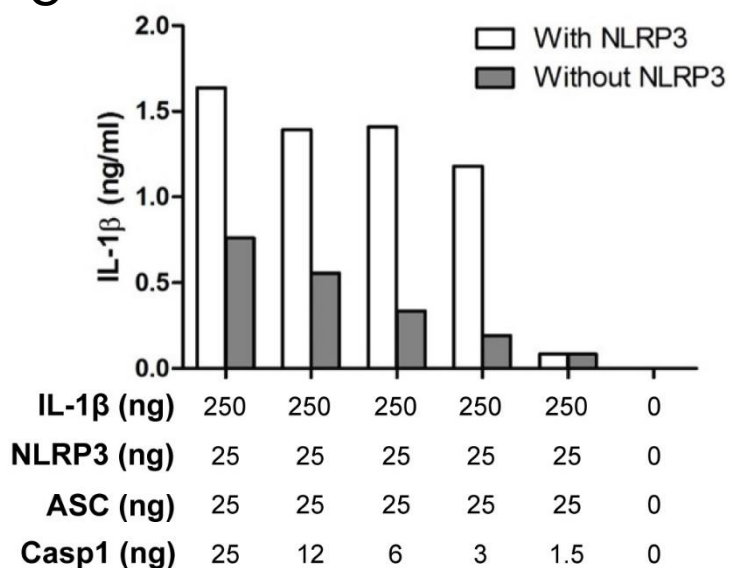
A



B



C



D

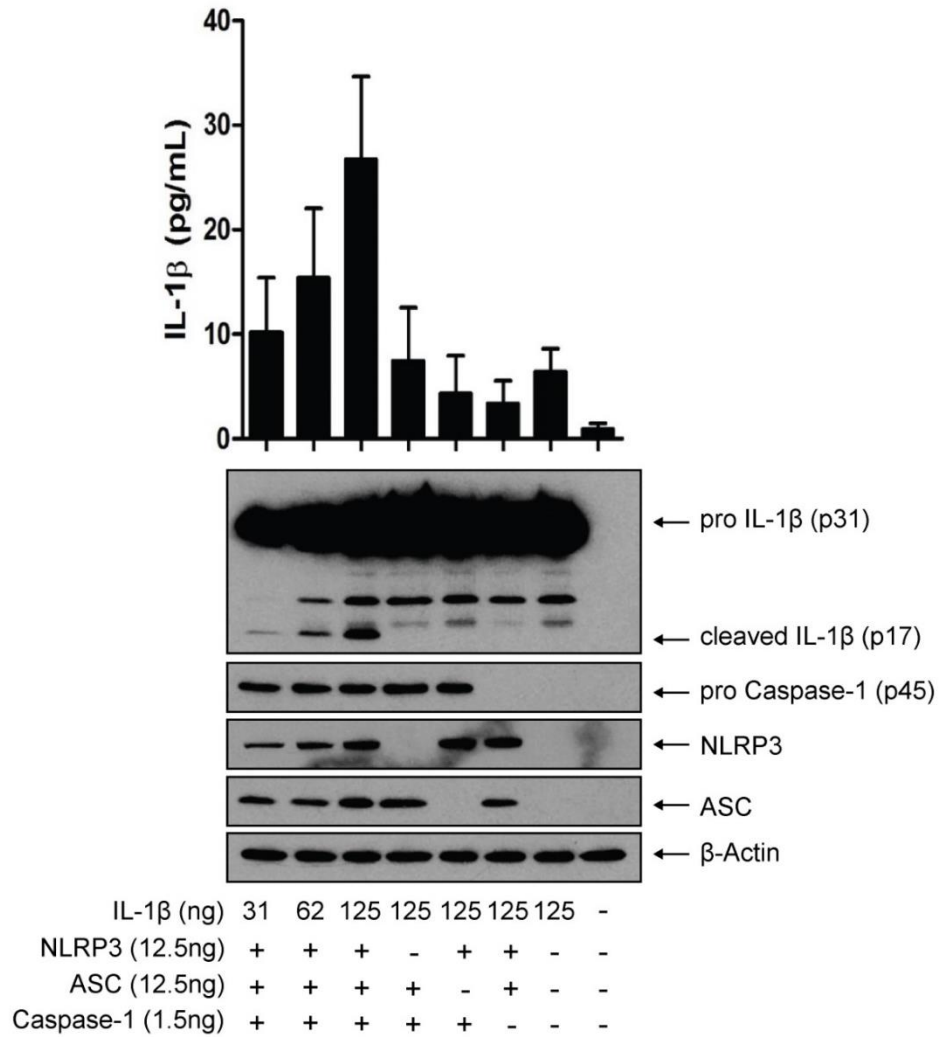


Figure 5.8 In vitro NLRP3 inflammasome reconstitution assay in HEK293T cells.

(A-C) Secreted IL-1β from HEK293T cells plated at a density of 1×10^6 cells in 6 well plates, overexpressed with plasmids encoding for mouse pro IL-1β, NLRP3, ASC and pro Caspase-1 as per the indicated doses for 24 h.

(D) Secreted IL-1β and protein expression from HEK293T cells plated at a density of 2.5×10^5 cells in 12 well plates, overexpressed with plasmids encoding for mouse pro IL-1β, NLRP3, ASC and pro Caspase-1 as per the indicated doses and combinations, for 24 h.

Data in **A** to **C** is from 1 experiment. Immunoblot in **D** is representative of 3 experiments, and ELISA data in **D** is from 3 repeated experiments (mean \pm SD, n=3).

5.9 Exogenous H₂S interferes with plasmid expression when administered concurrently during plasmid transfection

To determine whether exogenous H₂S downregulates secreted IL-1 β in the *in vitro* NLRP3 inflammasome reconstitution system, HEK293T cells were treated with either NaHS or GYY4137 concurrently with the transfection of over-expressing plasmids. 24 h later, secreted IL-1 β was assayed by ELISA. Initial observations showed that NaHS (125 μ M) and GYY4137 (500 μ M) significantly downregulated secreted IL-1 β from this system (Fig 5.9A & B). However, when individual plasmids were expressed together with treatment of NaHS (125 μ M, 24 h), the presence of NaHS downregulated pro IL-1 β , NLRP3, ASC and pro Caspase-1 protein levels (Fig 5.9C). These findings suggest that exogenous H₂S may affect the transfection efficiency, transcription and/or translation of the overexpressing plasmids when administered concurrently during plasmid transfection. To eliminate this confounding factor, H₂S would have to be administered only after the expression of the NLRP3 components.

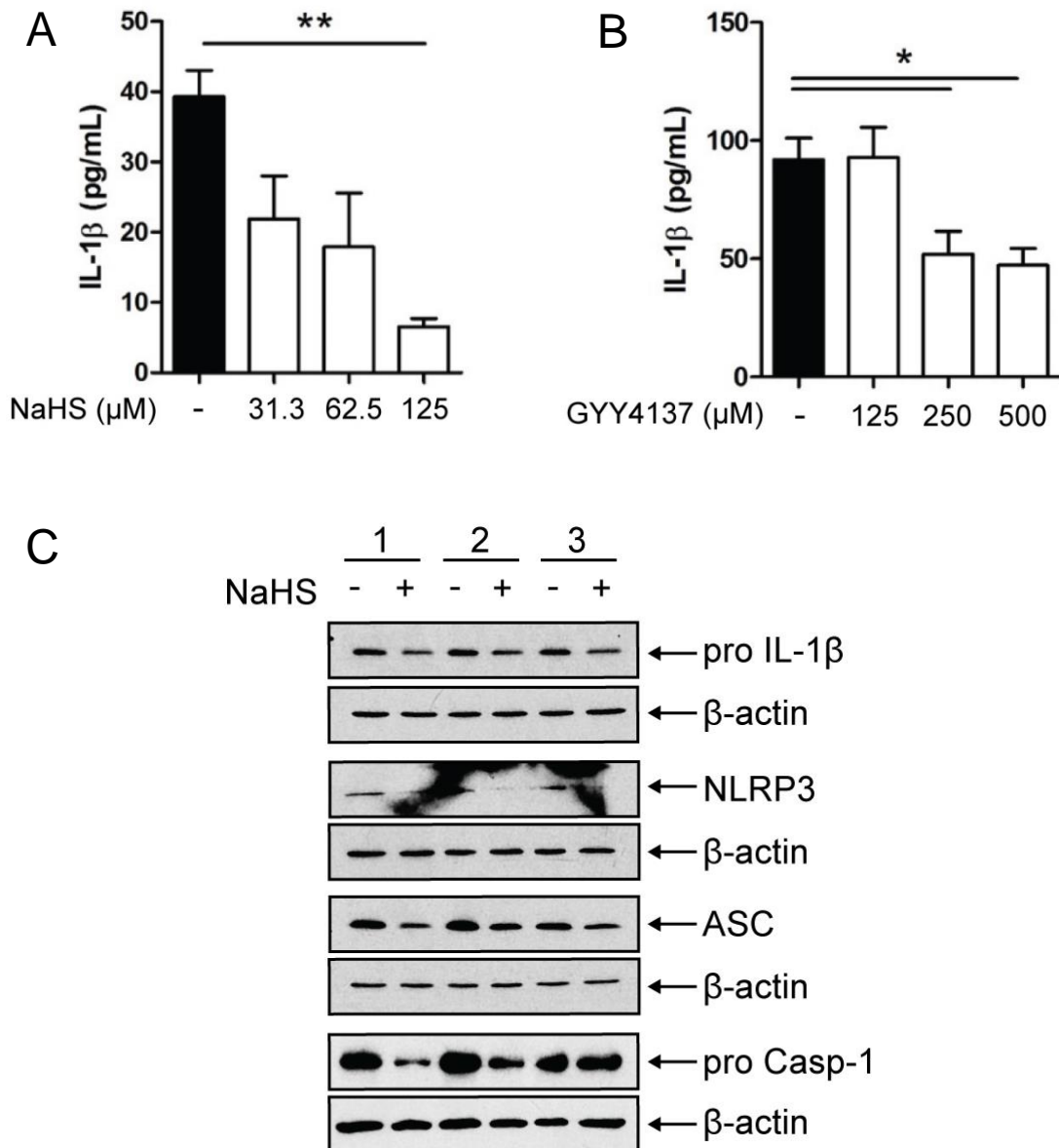


Figure 5.9 Exogenous H₂S interferes with the *in vitro* NLRP3 inflammasome reconstitution assay in HEK293T cells.

(A) Secreted IL-1β from HEK293T cells co-transfected with pro IL-1β (125ng), NLRP3 (12.5ng), ASC (12.5ng), and pro Caspase-1 (1.5ng) overexpression plasmids, together with the co-treatment of varying concentrations of NaHS (24 h).

(B) Secreted IL-1β from HEK293T cells co-transfected as in **A**, and co-treated with varying concentrations of GYY4137 (24 h).

(C) Immunoblot analysis of lysates of HEK293T cells transfected with either pro IL-1β (125ng), NLRP3 (12.5ng), ASC (12.5ng), or pro Caspase-1 (1.5ng) overexpression plasmids simultaneously with treatment of NaHS (125μM, 24 h).

* $P < 0.05$, ** $P < 0.01$. Data in **A** and **B** is from 3 repeated experiments (mean \pm SEM, $n=3$, one-way ANOVA with Dunnett's post-test against controls). Immunoblot in **C** comprises of 3 repeated experiments.

5.10 CSE overexpression inhibits IL-1 β secretion in the *in vitro* NLRP3 inflammasome reconstitution assay

Given that exogenous H₂S affects plasmid expression in the *in vitro* NLRP3 inflammasome reconstitution assay, the concurrent treatment with H₂S donors during plasmid transfection would not be suitable. As such, we reasoned that, if a CSE overexpressing plasmid was co-transfected together with pro IL-1 β and the NLRP3 inflammasome components, H₂S would be generated from CSE after all NLRP3 inflammasome components are expressed in HEK293T cells. Hence, the H₂S generated would not interfere with plasmid expression. This was under the assumption that the overexpression of all co-transfected plasmids would occur at identical rates since all the plasmids were constructed from identical pcDNA3.1(+) vector constructs with identical promoters.

When co-transfected together with pro IL-1 β and the NLRP3 inflammasome components, CSE significantly reduced ($P < 0.05$) secreted IL-1 β from this system (Fig 5.10A). Immunoblotting confirmed that in the presence of CSE, cleaved IL-1 β in the lysates of these cells was also reduced (Fig 5.10B). This suggested that CSE overexpression inhibits the maturation and secretion of IL-1 β in the *in vitro* NLRP3 inflammasome reconstitution assay.

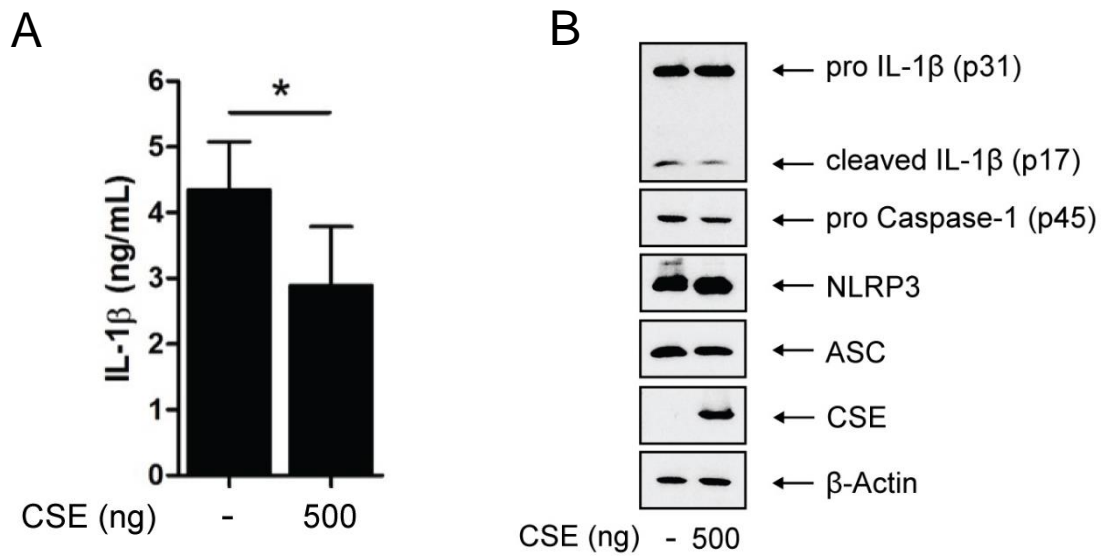


Figure 5.10 CSE overexpression inhibits IL-1 β secretion in the *in vitro* NLRP3 inflammasome reconstitution assay.

(A) Secreted IL-1 β from HEK293T cells co-transfected with pro IL-1 β (125ng), NLRP3 (12.5ng), ASC (12.5ng), pro Caspase-1 (1.5ng), and mouse CSE (500ng) overexpression plasmid for 48 h.

(B) Immunoblot analysis of lysates of HEK293T cells transfected as in **A**.

* $P < 0.05$. Data in **A** is from 6 transfections, and is representative of 3 repeated experiments (mean \pm SD, $n=6$ Mann-Whitney U test, two-tailed). Immunoblot in **B** is representative of 3 repeated experiments.

5.11 Treatment of NLRP3 but not ASC with exogenous H₂S downregulates IL-1 β secretion in the *in vitro* NLRP3 inflammasome reconstitution assay

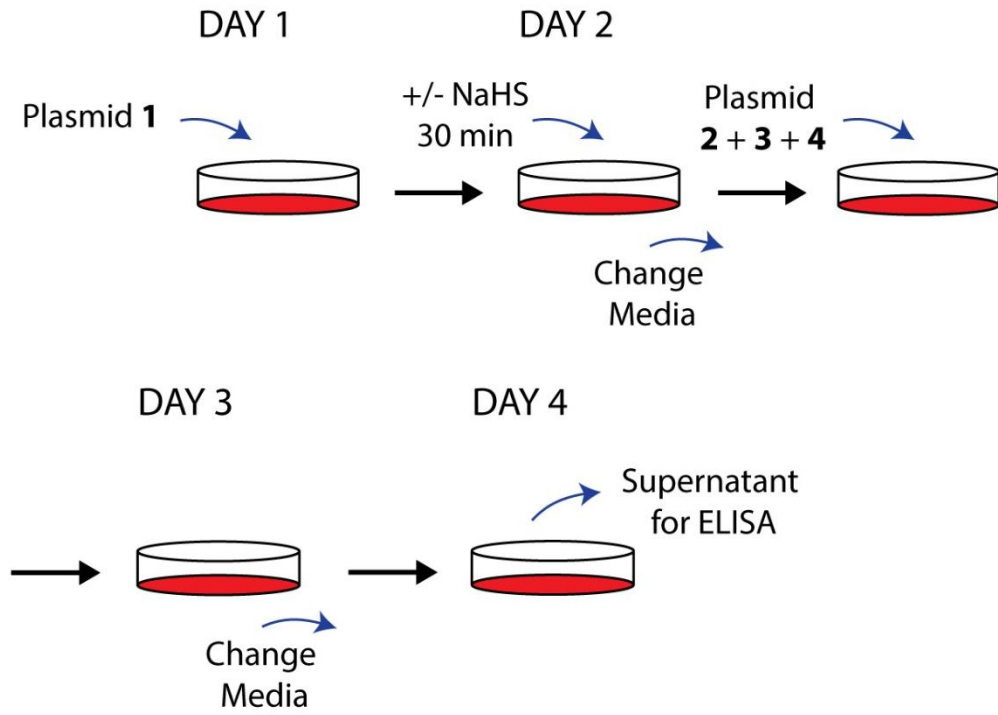
The pathways which lead to activation of the NLRP3 inflammasome in BMDMs are complex with many proteins and receptors playing a part. These include, but are not restricted to, the P2X7 receptor (Ferrari et al., 2006) and pannexin (Pelegrin and Surprenant, 2006) by which mediate ATP and nigericin signalling; proteins regulating K⁺ efflux out of the cell (Muñoz-Planillo et al., 2013); proteins involved in mitochondria ROS (mtROS) (Heid et al., 2013) and mitochondria DNA (mtDNA) (Shimada et al., 2012) mediated NLRP3 inflammasome activation signalling; as well as the calcium sensing pathway (Lee et al., 2012). These individual pathways all contribute to the final step of NLRP3 inflammasome activation which is the formation of the NLRP3 inflammasome protein complex. To isolate and study the effect of H₂S on the formation of this protein complex in the absence of any upstream pathways, the reconstituted *in vitro* NLRP3 inflammasome system in HEK293T cells was used as HEK293T cells do not inherently possess the NLRP3 inflammasome complex (Fig 5.8D).

H₂S modifies protein receptors and enzymes post-translationally (reviewed in Table 1) and in so doing, modify their activities. Hence, we hypothesized that H₂S may be inhibiting the NLRP3 inflammasome by modifying one or more components of the NLRP3 inflammasome protein complex. To test this hypothesis, NLRP3 or ASC was overexpressed in HEK293T cells (24 h) before treatment with NaHS (600 μ M, 30 min). Thereafter the cell culture media was changed to remove any remaining NaHS and cells were transfected with the remaining components of the NLRP3 inflammasome

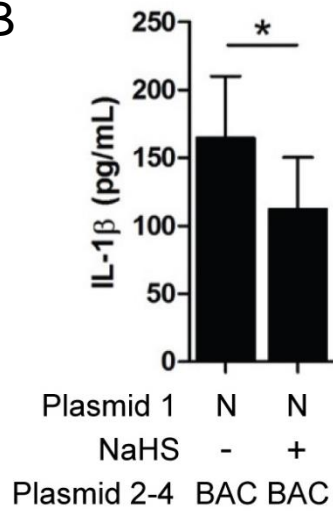
(ie. NLRP3 or ASC, and pro Caspase-1) together with pro IL-1 β for 24 h. On the third day, the cell culture media was changed, and subsequently assayed for secreted IL-1 β by ELISA the next day (Day 4). A cartoon schematic of the transfection regimen is shown in Fig 5.11A. It was observed that treatment of NLRP3 but not ASC with NaHS resulted in the downregulation of secreted IL-1 β from the *in vitro* NLRP3 inflammasome reconstitution system (Fig 5.11B & C).

Since NaHS treatment may conceivably cause a false positive result by interfering with plasmid overexpression using this treatment regimen, control experiments were undertaken in which HEK293T cells were either subjected to overexpression with NLRP3 (24 h) followed by treatment with NaHS (600 μ M, 30 min), or treated with NaHS (600 μ M, 30 min) prior to overexpression with pro IL-1 β , ASC or pro Caspase-1 (24 h). Immunoblot analysis revealed that the plasmid transfection and H₂S treatment regimen used in this study did not interfere with plasmid overexpression (Fig 5.11D).

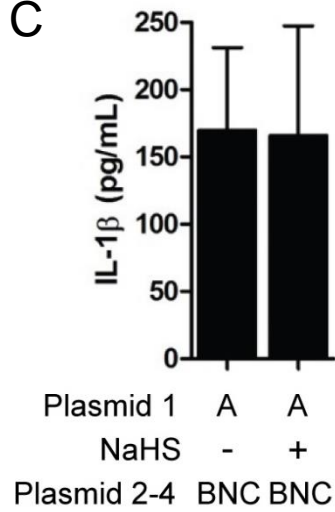
A



B



C



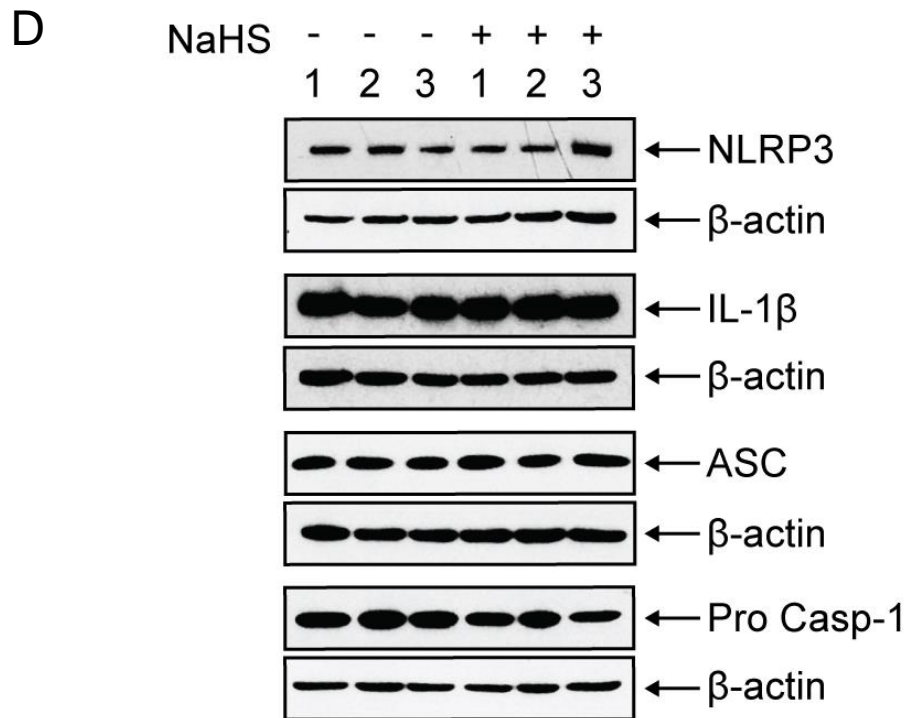


Figure 5.11 Exogenous H₂S reacts with NLRP3 but not ASC in the *in vitro* NLRP3 inflammasome reconstitution assay.

(A) Cartoon schematic of overexpression plasmid transfection and NaHS treatment regimen in HEK293T cells. Plasmid A denotes the first plasmid transfected on Day 1 (ie. NLRP3 or ASC). Plasmid B, C, D denotes the remaining three plasmids to be transfected on Day 2 after treatment of cells with NaHS (600μM, 30 min).

(B-C) Secreted IL-1β from HEK293T cells transfected with overexpressing plasmids in the sequence as shown in **A**. Either NLRP3 (N) or ASC (A) overexpressing plasmid was transfected on Day 1 (24 h). On Day 2, cells were then treated with NaHS (600μM, 30 min) followed by a change of media. Following which, cells were co-transfected with plasmids BAC or BNC (24 h). On Day 3, cell culture media was changed, and assayed for IL-1β by ELISA on Day 4.

B: IL-1β (125ng); N: NLRP3 (12.5ng); A: ASC (12.5ng); C: Caspase-1 (1.5ng)

(D) Immunoblot analysis of lysates from HEK293T cells: (a) Transfected with NLRP3 (12.5ng) overexpressing plasmid (24 h) before being treated with NaHS (600μM, 30 min); or (b) treated with NaHS (600μM, 30 min) followed by a change of media, before being transfected with pro IL-1β (125ng), ASC (12.5ng) or pro Caspase-1 (1.5ng) overexpressing plasmid (24 h). Data shows 3 repeats.

* $P < 0.05$. Data in **B** and **C** is from 6-9 transfections, and is representative of 3 repeated experiments (mean ± SD, n=6-9 Mann-Whitney *U* test, two-tailed). Immunoblot in **D** comprises of 3 repeated experiments.

5.12 Exogenous H₂S disrupts NLRP3 – ASC protein protein interaction

Since treatment of NLRP3 with NaHS, but not ASC, downregulated the secretion of IL-1 β in the *in vitro* NLRP3 inflammasome activation system, we next hypothesized that this effect may be due to inhibition of the interaction between NLRP3 and ASC. To test the hypothesis, a hemagglutinin (HA) - tagged NLRP3 overexpressing plasmid was synthesized for a co-immunoprecipitation (co-IP) assay. To facilitate the co-IP assay, the NLRP3 overexpressing plasmid was modified to include a HA epitope tag on the N terminus of the protein.

The co-IP assay showed that overexpression of HA-NLRP3 (24 h) followed by ASC (24 h) resulted in the interaction of these 2 proteins (Fig 5.12A). However, treatment of HA-NLRP3 overexpressed cells with NaHS (600 μ M, 30 min) prior to ASC overexpression disrupted the NLRP3 – ASC interaction (P < 0.01) (Fig 5.12A & B). Taken together with the prior observation that treatment of NLRP3, but not ASC, with NaHS downregulating the secretion of IL-1 β in the *in vitro* NLRP3 inflammasome activation system, the present findings suggest that the disruption of NLRP3 – ASC interaction by H₂S is a potential mechanism of action by which NaHS inhibits NLRP3 inflammasome activation.

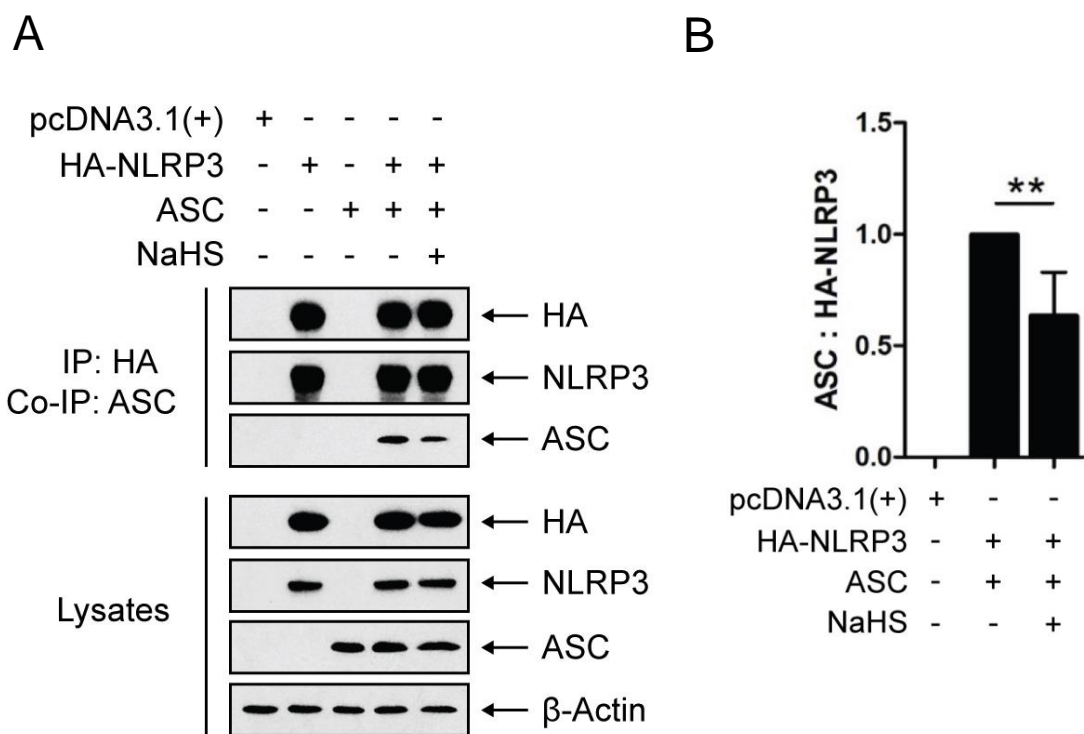


Figure 5.12 Exogenous H₂S disrupts NLRP3-ASC protein protein binding.

(A) Co-immunoprecipitation (co-IP) assay of HA-NLRP3 (1 μ g plasmid) with ASC (1 μ g plasmid), with or without NaHS treatment (600 μ M, 30 min). HA-NLRP3 was first transfected in HEK293T cells for 24 h. Transfected cells were next treated with NaHS followed by a change of media. Cells were then transfected with ASC for another 24 h, before cell lysates were being immunoprecipitated using an antibody against the HA-antigen.

(B) Quantification of ASC : HA-NLRP3 co-IP experiment as treated in **A**.

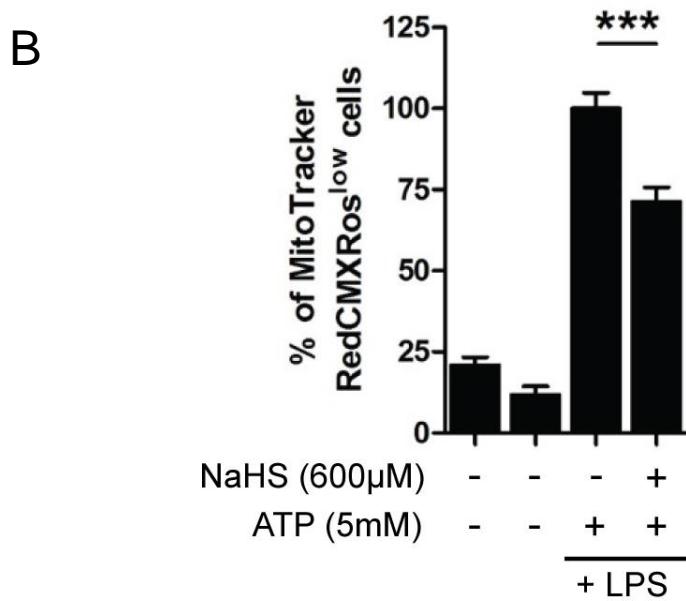
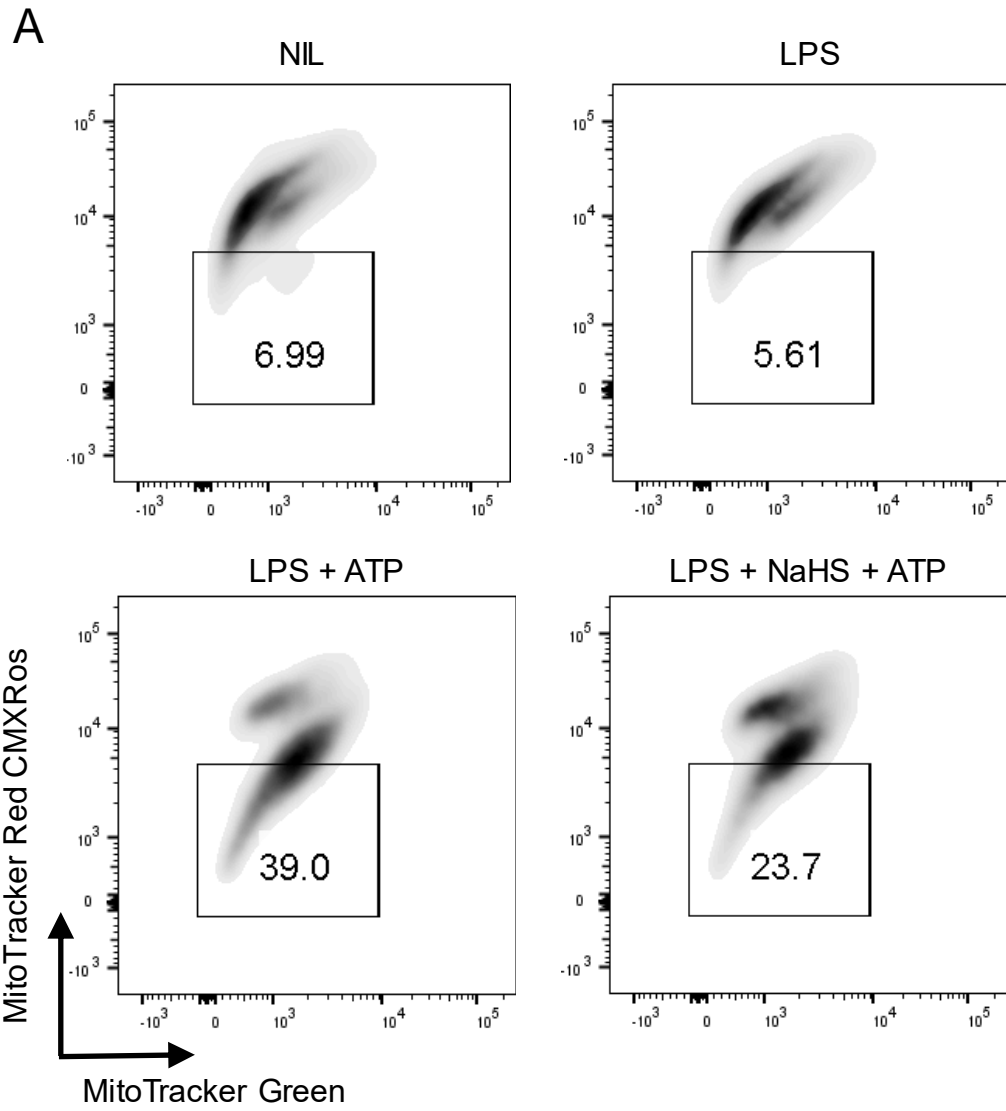
** $P < 0.01$. Immunoblot in **A** is representative of 4 repeated experiments. Data in **B** is from 4 repeated experiments (mean \pm SD, $n=4$, one-way ANOVA with Dunnett's post-test against controls).

5.13 Exogenous H₂S protects mitochondrial integrity and reduces mitochondrial ROS production in BMDMs during NLRP3 inflammasome activation

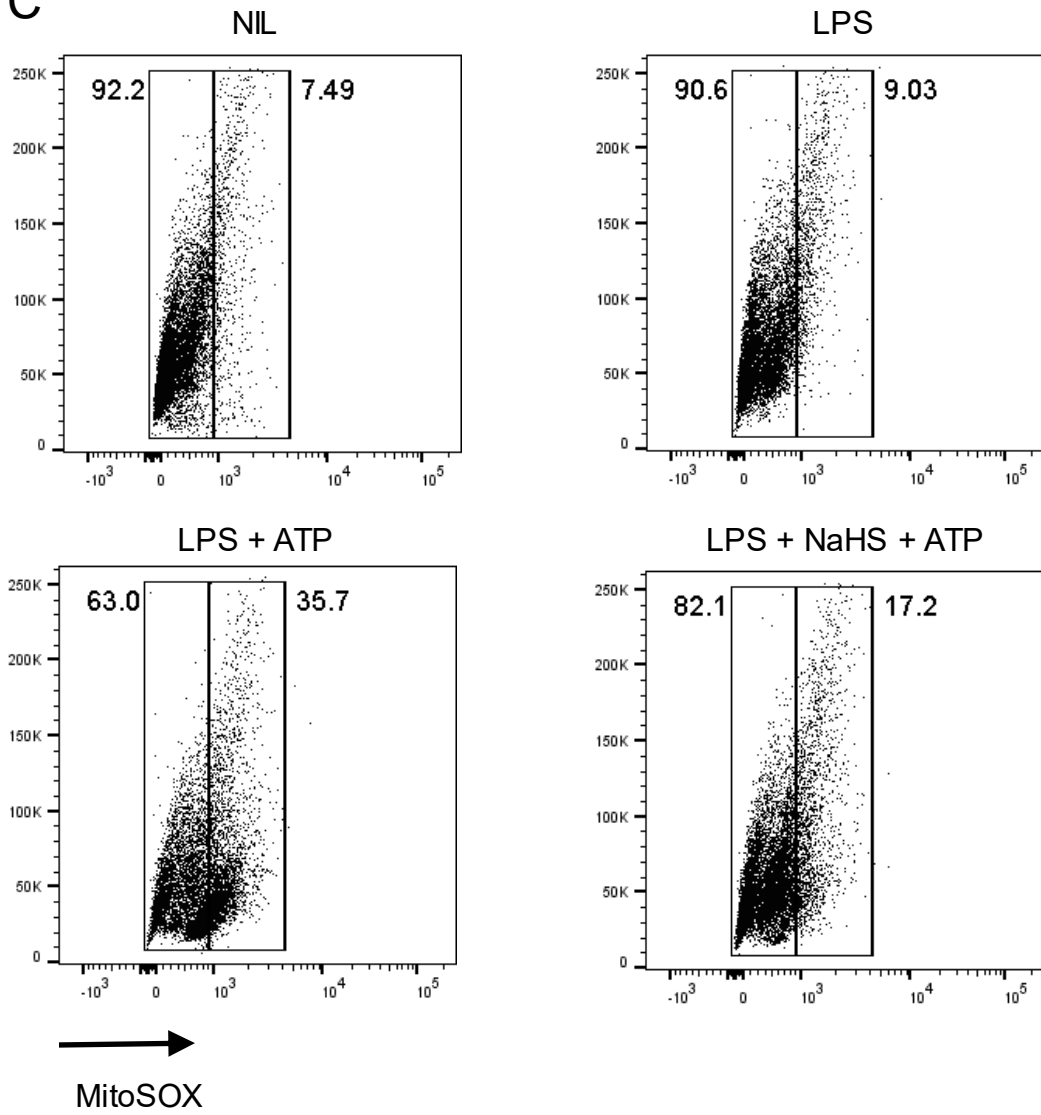
Treatment of HA-NLRP3 and ASC overexpressed HEK293T cells with NaHS (600 μ M) inhibited NLRP3 – ASC interaction by approximately 36% (Fig 5.12B). This is consistent with the extent of downregulation of secreted IL-1 β (approximately 32%) when NLRP3 overexpressed cells were treated with NaHS (600 μ M) before overexpression with pro IL-1 β and the other components of the NLRP3 inflammasome (Fig 5.11B). However, the extent of the downregulation of NLRP3 – ASC interaction and IL-1 β secretion from the overexpression system in HEK293T cells is not similar quantitatively to the downregulation of secreted IL-1 β (approximately 95%) observed in BMDMs treated with NaHS (600 μ M) (Fig 5.3B). This may imply that, in BMDMs, NaHS inhibits NLRP3 inflammasome activation by additional mechanisms in addition to an effect on NLRP3 – ASC interaction.

The role of the mitochondria and mtROS in the activation of the NLRP3 inflammasome has been established in prior studies (Heid et al., 2013; Zhou et al., 2011). It was therefore of interest to determine whether NaHS may inhibit NLRP3 inflammasome activation by a protective effect on the mitochondria. As such, the integrity of the mitochondria as well as mtROS production were assessed in BMDMs treated with LPS and ATP, in the presence or absence of NaHS (600 μ M). Following LPS and NaHS treatment, these cells were co-stained with Mitotracker red CMXRos and Mitotracker green dyes. The red dye is selective towards the mitochondrial inner transmembrane potential while the green dye is selective for mitochondria regardless of mitochondrial membrane

potential (Nakahira et al., 2011). Together, co-staining revealed showed that NLRP3 inflammasome activation by ATP resulted in an increase in non-intact mitochondria in these cells which were partially rescued (approximately 25% decrease) by treatment with NaHS (600 μ M) ($P < 0.001$) (Fig 5.13A & B). Consistent with the observed pattern of mitochondria integrity, measurement of mtROS production from these cells by the mitochondrial superoxide indicator, MitoSOX, showed that NaHS (600 μ M) significantly ($P < 0.001$) decreased mtROS production in NLRP3 inflammasome activated BMDMs (approximately 37% decrease) (Fig 5.13C & D). These data suggest that NaHS protects mitochondrial integrity concomitant with downregulated mtROS production from NLRP3 inflammasome activated BMDMs.



C



D

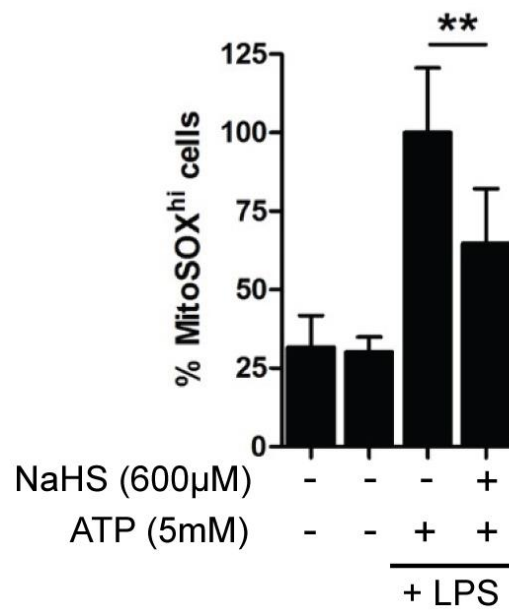


Figure 5.13 Exogenous H₂S decreased mitochondrial damage and mitochondrial ROS production induced during NLRP3 inflammasome activation.

(A) Flow cytometry analysis of BMDMs primed with LPS (1µg/ml, 4 h) followed by treatment with NaHS (600µM, 30 min), before stimulation with ATP (5mM, 30 min). Cells were stained with MitoTracker Red CMXRos and MitoTracker Green (15 min, 37°C) prior to ATP treatment.

(B) Percentage of MitoTracker CMXRos^{low} BMDMs as treated in **A**. (mean ± SEM, n=3, one-way ANOVA with Dunnett's post-test against controls).

(C) Flow cytometry analysis of BMDMs as treated in **A**. Cells were stained with MitoSOX (20 min, 37°C) after ATP treatment.

(D) Percentage of MitoSOX^{hi} BMDMs as treated in **C**.

** $P < 0.01$, *** $P < 0.001$. Data is from 3 repeated experiments (mean ± SD, n=6, one-way ANOVA with Dunnett's post-test against controls).

5.14 Exogenous H₂S does not affect cytoplasmic mitochondrial DNA levels in BMDMs during NLRP3 inflammasome activation

A further possible mechanism which may mediate NLRP3 inflammasome activation is the translocation of mtDNA into the cytoplasm. It has been reported that oxidized mtDNA translocates to the cytoplasm and colocalizes with NLRP3, activating the inflammasome. In this reported study, mtDNA directly induced NLRP3 inflammasome activation as macrophages lacking mtDNA had severely attenuated IL-1 β production (Shimada et al., 2012).

In the current study, mtDNA present in the cytoplasm of BMDMs treated with LPS and ATP, with or without NaHS (600 μ M) treatment was therefore measured by qPCR. Whilst stimulation of LPS primed BMDMs with ATP gradually increased IL-1 β secretion over time (up to 30 min) (Fig 5.14A), the presence of mtDNA in the cytoplasm did not increase concurrently (Fig 5.14B). In addition, treatment of these cells with NaHS (600 μ M) prior to ATP stimulation did not significantly reduce mtDNA levels in the cytoplasm although IL-1 β secretion was attenuated (Fig 5.14A & B). Hence, the data suggests that downregulation of secreted IL-1 β by NaHS from NLRP3 inflammasome activated BMDMs was not attributed to a reduction in cytoplasmic mtDNA.

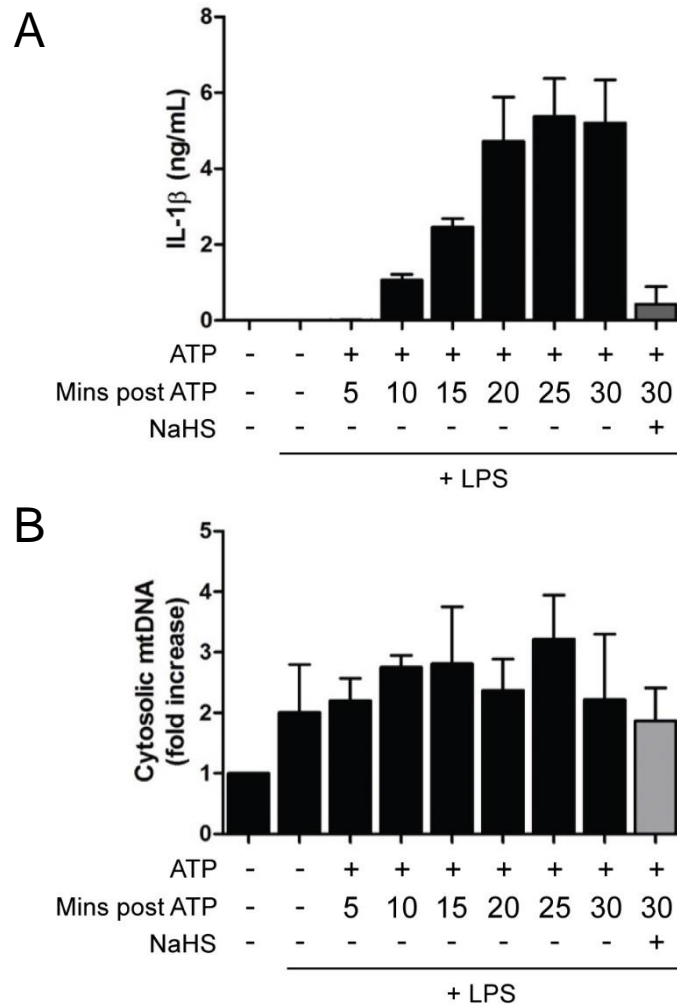


Figure 5.14 NaHS does not reduce cytoplasmic mtDNA in NLRP3 inflammasome activated BMDMs.

(A) Secreted IL-1 β from BMDMs primed with LPS (1 μ g/ml, 4 h) followed by stimulation with ATP (5mM, up to 30 min), with or without treatment with NaHS (600 μ M, 30 min) prior to ATP stimulation. Data is from at least 2 repeated experiments (mean \pm SD).

(B) Quantitative PCR (qPCR) analysis of cytoplasmic mtDNA in BMDMs treated as in **A**. Data in **A** is from 2 repeated experiments (mean \pm SD, n=4), and data in **B** is from at least 3 repeated experiments (mean \pm SD, n=3-8).

5.15 The slow-releasing H₂S donor GYY4137 reduces IL-1 β levels in LPS sepsis mice

It was previously shown that the slow-releasing H₂S donor, FW1256, reduces IL-1 β in the blood plasma and peritoneal cavity of mice with LPS-induced sepsis (Huang et al., 2016a). To evaluate whether another slow-releasing H₂S donor might also downregulate IL-1 β levels *in vivo*, GYY4137 (100mg/kg, i.p.) was administered to wild-type C57BL/6 mice 1 h prior to LPS injection (10mg/kg, i.p.). GYY4137-treated mice exhibited significantly ($P < 0.05$) lower levels of IL-1 β detected in the peritoneal lavage and the blood plasma 2 hr and 6 h respectively after LPS injection (Fig 5.15). While such observations do not directly show the inhibition of the NLRP3 inflammasome *in vivo* by exogenous H₂S, the data does suggest that exogenous H₂S also reduces secreted IL-1 β in an inflammatory condition *in vivo*, of which the NLRP3 inflammasome is required for its release out of the cell.

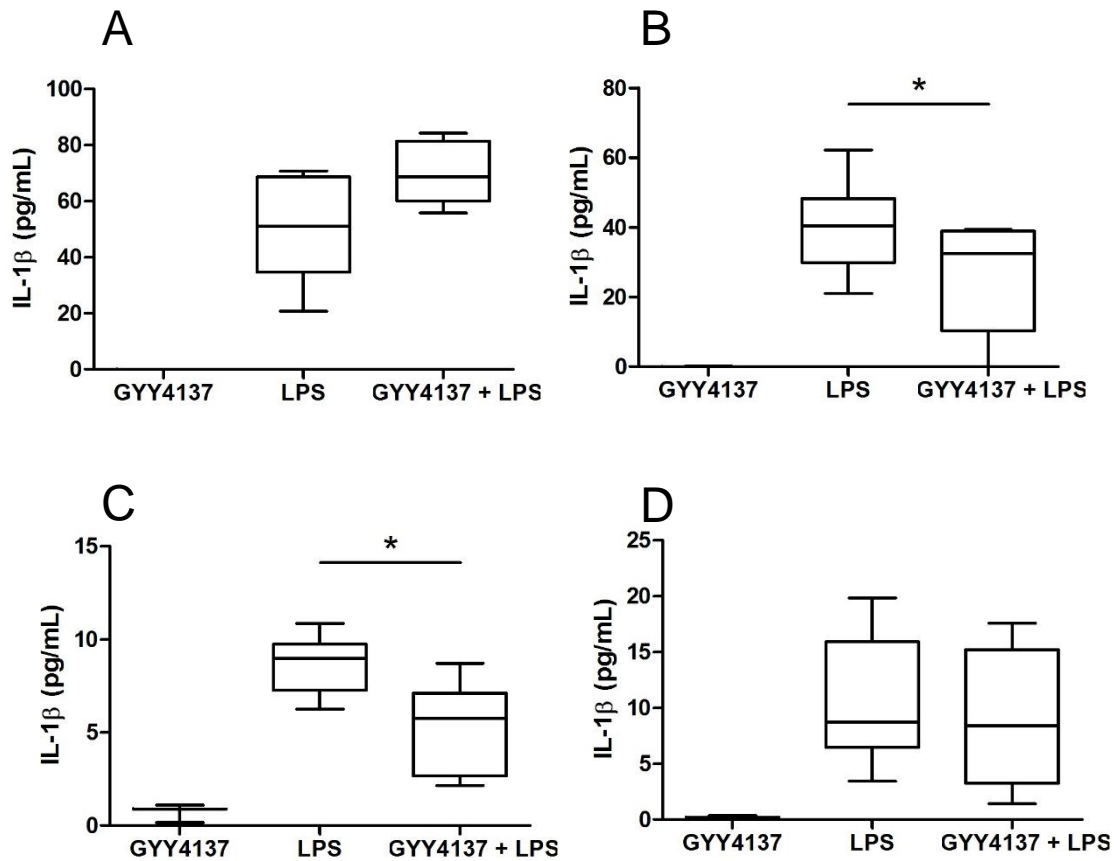


Figure 5.15 GYY4137 reduced IL-1 β in the mouse model of LPS induced septic shock.

(A) IL-1 β levels at 2 h in the blood plasma,

(B) IL-1 β levels at 2 h in the peritoneal lavage,

(C) IL-1 β levels at 6 h in the blood plasma,

(D) IL-1 β levels at 6 h in the peritoneal lavage, after intraperitoneal (i.p.) injection with LPS (10 mg/kg of body weight), with or without 1 h i.p. injection of GYY4173 (100 mg/kg of body weight) prior to LPS injection.

* P < 0.05 (Box and whiskers plot showing median with the 25th and 75th percentiles, whiskers represent smallest and largest values, one-way ANOVA with Dunnett's post-test against controls). N=3 mice in GYY4137 only group; n=5 in LPS or GYY4137 + LPS groups in **A** and **B**, and n=11 mice in LPS or GYY4137 + LPS groups in **C** and **D**.

5.16 Discussion

The NLRP3 inflammasome is a critical nexus between the intracellular synthesis and release of IL-1 β and IL-18 in response to pathogens as well as sterile inflammatory stimuli. However, anomalous NLRP3 inflammasome activation in inflammatory conditions such as gout (Kingsbury et al., 2011), diabetes (Lee et al., 2013) and atherosclerosis (Li et al., 2016b) contribute to undesirable symptoms stemming from the effects of increased IL-1 β and IL-18, which can be detrimental to the host. As such, it is of interest to identify possible molecular mechanisms by which NLRP3 inflammasome activation can be inhibited, paving the way for the continual development of therapeutics.

At the time when this present study was undertaken, two out of the three known gasotransmitters had been observed to inhibit NLRP3 inflammasome activation. Exogenous NO from the NO donor S-nitroso-N-acetylpenicillamine (SNAP), and endogenous NO synthesized by iNOS, reportedly inhibited NLRP3 inflammasome activation in macrophages (Hernandez-Cuellar et al., 2012; Mao et al., 2013). In *M. tuberculosis* infected mice, IFN- γ and iNOS modulated the pathology as well as IL-1 β secretion in these mice. Investigation of the effect of NO on *M. tuberculosis*-infected macrophages revealed that IFN- γ stimulated NO in these macrophages suppressed NLRP3 inflammasome mediated IL-1 β secretion, thereby implicating endogenous NO in the control of the inflammatory response by IL-1 β during persistent *M. tuberculosis* infections (Mishra et al., 2013). The other gasotransmitter, CO, negatively regulated NLRP3 inflammasome activation in macrophages when delivered in a gaseous state (Jung et al., 2015). To the best of our current knowledge, the effects of H₂S in regulating NLRP3 inflammasome activation in macrophages and the

mechanism of action by which this occurs have not been reported in the scientific literature. Recent reports have however shown that Na₂S also exerted cardioprotective effects by inhibiting NLRP3 inflammasome formation in the heart after Ischemia-Reperfusion injury in mice. This inhibitory effect was mediated through signalling pathways requiring microRNA 21 (miR-21) (Toldo et al., 2014). In addition, NaHS prevented ozone-induced emphysema and lung inflammation by regulating the NLRP3-caspase-1, p38 mitogen-activated protein kinase (MAPK), and Akt pathways (Li et al., 2016a). NaHS also attenuated high glucose-induced NLRP3 activation in H9c2 cardiac cells (Huang et al., 2016b).

Previously, H₂S has been shown to inhibit NFκB activation in macrophages (Huang et al., 2016a; Oh et al., 2006). As NFκB activation is the first (i.e. 'priming') step in NLRP3 inflammasome activation in macrophages, we sought to differentiate any possible inhibitory effects of NaHS between the 'priming' and the 'activation' step. Thus, BMDMs were only treated with NaHS after the initial 'priming' step with LPS stimulation. When using such a treatment protocol, NaHS did not significantly change TNFα production and NLRP3, ASC or pro Caspase-1 expression (Fig 5.3B & C; 5.4A & C), thereby providing evidence that NaHS did not interfere with the 'priming' step. NaHS however decreased IL-6 secretion from ATP stimulated BMDMs only at the maximum dose (600μM) used in the present study (Fig 5.3B). This observation is not unexpected given that as compared to TNFα, H₂S has been previously seen to be more potent in inhibiting IL-6 secretion from macrophages (Huang et al., 2016a; Rios et al., 2015).

In the present study, NaHS at concentrations up to 600 μ M were first utilised, with the highest dose (600 μ M) being used subsequently in the later part of the study. Although this concentration of NaHS was not toxic towards BMDMs using the present experimental conditions (Fig 5.4E), we acknowledge that such a high concentration is not feasible for therapeutic applications in humans. Drawing reference from similar studies of the use of exogenous gasotransmitters to inhibit NLRP3 inflammasome activation *in vitro*, it is apparent that comparable concentrations of donor compounds were used. For example, the NO donor SNAP was used at concentrations of up to 500 μ M (Hernandez-Cuellar et al., 2012; Mishra et al., 2013) and 1mM (Mao et al., 2013), while CO was used at a concentration of 250 parts per million (ppm) (Jung et al., 2015). As a benchmark, the National Institute for Occupational Safety and Health (NIOSH) established 200 ppm of CO as an exposure ceiling based on the risk of cardiovascular effects [NIOSH 1992]. Whilst recognizing that these studies are essential for providing a proof-of-concept that gasotransmitters can elicit a biological effect in the absence of cytotoxicity, it is not surprising that high concentrations of gasotransmitters are required under experimental conditions. This also highlights the point that in order to realize the therapeutic potential of gasotransmitters, development of donor compounds that exhibit high specificity and potency towards the intended cellular and molecular targets is essential.

Although the present study has focused largely on the ability of exogenous H₂S in downregulating NLRP3 inflammasome activation, the irreversible CSE inhibitor, DL-PAG, was found to conversely exacerbate NLRP3 inflammasome activation (Fig 5.7). This suggested that endogenous

H₂S could also control NLRP3 inflammasome activation. However, investigating the extent of NLRP3 inflammasome activation in CSE^{-/-} macrophages from CSE^{-/-} mice or siRNA mediated knock-down macrophages will be necessary and crucial for further validation.

The inhibition of NLRP3 activation and pyroptosome formation by exogenous H₂S has been established in the present study. Two mechanisms of action by which H₂S mediates this inhibitory effect was proposed. Firstly, by means of an *in vitro* NLRP3 inflammasome functional assay, it was ascertained that H₂S interfered with the function of the NLRP3 inflammasome when the NLRP3 component was treated with NaHS. The disruption of NLRP3 inflammasome function was not evident when ASC was treated with NaHS (Fig 5.11B & C), suggesting that H₂S reacts preferentially to NLRP3 post-translationally. The co-immunoprecipitation assay between NaHS treated NLRP3, and ASC further confirms that the binding of NLRP3 to ASC was perturbed by H₂S (Fig 5.12A & B). As H₂S is known to post-translationally modify proteins by S-sulfhydration, we further hypothesized that H₂S could possibly be sulfhydrating a cysteine residue in the pyrin domain of NLRP3, which is involved in ASC binding. Examination of the amino acid sequence in the pyrin domain of NLRP3 (residues 1 – 91) revealed 2 cysteine residues (Cys6 and Cys36), of which Cys6 is involved in disulfide bonding with Cys104 [UniProt ID: Q8R4B8]. To determine if Cys36 is crucial for NLRP3 – ASC binding, future functional assay and co-IP experiments involving a mutated form of NLRP3, harbouring an amino acid substitution at residue 36 could be performed. In addition, analysis of NLRP3 Cys36 residue by mass spectrometry after NaHS treatment would also reveal whether S-sulfhydration indeed occurs

at Cys36. In the present study, assays for the detection of S-sulfhydration (ie. modified biotin-switch assay and the detection of S-sulfhydration by red maleimide) was not performed as NLRP3 contains cysteine residues outside of the pyrin domain. Except for Cys104, the other cysteine residues are not known to be involved in disulfide bonding and hence could also be sulfhydrated by H₂S. As the sulfhydration of these residues are likely to be inconsequential towards disrupting NLRP3 – ASC binding, S-sulfhydration detection assays may detect the sulfhydration of cysteine residues outside of the pyrin domain, rendering such data inconclusive.

The presence of mtROS is closely related to NLRP3 inflammasome activation. However, whether mtROS is required in NLRP3 inflammasome activation and the precise mechanism by which mtROS activates the NLRP3 inflammasome remains unclear (Yu and Lee, 2016). The current scientific opinion appears to be divided with regard to whether mtROS activates the NLRP3 inflammasome (Heid et al., 2013; Hu et al., 2010; Kim et al., 2014; Nakahira et al., 2011; Zhong et al., 2016; Zhong et al., 2013; Zhou et al., 2011), is only involved in the ‘priming’ signal (Bauernfeind et al., 2011; Won et al., 2015), or is not required for NLRP3 inflammasome activation (Muñoz-Planillo et al., 2013). In the present study, H₂S protected mitochondrial integrity and reduced mtROS production in NLRP3 inflammasome activated BMDMs (Fig 5.13). This was suggested to be the second mechanism of action by which H₂S inhibited NLRP3 inflammasome activation in BMDMs. Although the present study revealed a novel role of H₂S in reducing mitochondria damage and mtROS production which is concomitant with NLRP3 inflammasome activation

in BMDMs, the exact mechanism of action by which this occurs remains unknown, of which further studies are warranted.

H₂S is generally known to exert its toxicity in cells by inhibiting cytochrome c oxidase in the mitochondria. However, H₂S can also act as a substrate for the mitochondrial respiratory chain (Cooper and Brown, 2008), and also confers antioxidant protective effects (Xie et al., 2016). Several studies have shed light on the protective roles of H₂S on the mitochondria in different cell types. In the neuroblastoma cell line SH-SY5Y, NaHS suppressed rotenone-induced mitochondrial membrane potential dissipation and cell death, which was attenuated by the selective blocker of mitochondrial ATP-sensitive potassium (mitoK_{ATP}) channel, 5-hydroxydecanoate. This suggested that the protective effect of NaHS on the mitochondria in this study was mediated by its interaction with the mitoK_{ATP} channel (Hu et al., 2009). Such an interaction could be plausible given that H₂S has been shown to open the K_{ATP} channel in vascular smooth muscle cells (Zhao et al., 2001). H₂S also protected mitochondria function in human umbilical vein endothelial cells (HUVECs) subject to oxidative stress by H₂O₂, albeit via a mechanism that was not fully understood (Wen et al., 2013). In smooth muscle cells and aorta tissue from mice, the absence of CSE reduced mtDNA copy number, inhibited expressions of mitochondrial transcription factor A and mitochondrial marker genes *mt-CO1*, *CytB* and *Atp6*, which were all reversed upon treatment of the cells with NaHS (Li and Yang, 2015). In HepG2 human liver cancer cells and HEK293T cells, NaHS induced S-sulfhydration of the α subunit (ATP5A1) of ATP synthase, thereby stimulating its enzymatic activity (Modis et al., 2016). Hence, it is plausible that H₂S could be acting on specific components in the mitochondria

in the present study, thereby conferring its protective effects on mitochondrial integrity, reducing mtROS production, and conceivably also maintaining a functional level of mitochondria energetics. Further studies investigating the interaction of H₂S with the aforementioned targets in the mitochondria could be carried out in NLRP3 inflammasome activated BMDMs. In addition, given that NLRP3-mitochondria co-localization occurs during inflammasome activation (Zhou et al., 2011) via the mitochondria-associated adaptor molecule, mitochondrial antiviral-signaling protein (MAVS) (Subramanian et al., 2013), studying whether H₂S affects MAVS-mitochondria co-localization during inflammasome activation could provide insight into the formulation of a more detailed mechanism of action.

Two mechanisms of action by which H₂S inhibited NLRP3 inflammasome activation were proposed in the present study. Given the breadth of targets that H₂S acts on intracellularly and the extensive plexus of molecular networks leading to NLRP3 inflammasome activation, we are inclined to speculate that H₂S may be exerting an inhibitory effect by several other unknown mechanisms. Moreover, the magnitude of effect of H₂S on the two mechanisms proposed in this study (Fig 5.11 - 5.13) did not correspond with the extent of downregulation of IL-1 β and Caspase-1 activation (Fig 5.3 & 5.4) observed in NLRP3 inflammasome activated BMDMs. This incongruence suggests that either the two mechanisms of action by which H₂S inhibited NLRP3 inflammasome activation worked together in an additive or synergistic manner in BMDMs, or that there exists other unknown mechanisms of action.

One molecular pathway downstream of ATP or nigericin stimulation that leads to NLRP3 inflammasome activation is K⁺ efflux from the cell. K⁺ efflux has

been reported to be a unifying trigger of NLRP3 activation (Muñoz-Planillo et al., 2013). Hence, the K⁺ protein channel could conceivably be also a target of H₂S under the current experimental conditions. The tripartite-motif protein 30 (TRIM30), being another player in the NLRP3 inflammasome activation molecular network, could potentially be an H₂S target given that TRIM30 negatively regulates NLRP3 inflammasome activation by regulating ROS production (Hu et al., 2010).

Another step that is crucial in regulating NLRP3 activation involves ubiquitination. ATP signaling was first shown to induce the deubiquitination of NLRP3, thereby activating the NLRP3 inflammasome (Juliana et al., 2012; Lopez-Castejon et al., 2013). The mechanism for the deubiquitination of NLRP3 was later found to be mediated by the deubiquitinating enzyme BRCC3 (Py et al., 2013). Moreover, it was later elucidated that the assembly of the NLRP3 inflammasome also required the ubiquitination of ASC by the linear ubiquitination assembly complex (LUBAC) which consists of HOIL-1L, HOIP and Sharpin (Gurung et al., 2015; Rodgers et al., 2014). Whether H₂S interferes with ubiquitination or deubiquitination of the NLRP3 inflammasome complex is unknown, and may be of value for further investigation.

Dissecting the inhibitory effects of H₂S on NFκB activation and NLRP3 inflammasome activation *in vivo* poses a great challenge. Whilst the 'priming' step involving NFκB activation and the NLRP3 inflammasome activation step can be precisely dissociated *in vitro* in BMDMs by sequential stimulation of LPS followed by ATP or nigericin, these two steps occur dynamically *in vivo* during inflammation. Specifically quantifying NLRP3 inflammasome activated cells *ex vivo* was initially thought possible using a flow cytometric method to assess

inflammsome formation (Sester et al., 2015) in peritoneal macrophages obtained from LPS sepsis mice. As the published method allows for the detection of ASC specks in inflammasome activated cells, this theoretically could allow for the identification and quantification of NLRP3 inflammasome activated macrophages in LPS sepsis mice, with or without H₂S intervention. We were however unable to replicate the flow cytometry gating strategies detailed in the publication despite several optimization attempts. At present we have no explanation for our inability to reproduce this work. As such, this particular strategy was not further pursued. Nevertheless, the data presented in the current mouse model of LPS induced septic shock showed that the slow-releasing H₂S donor GYY4137 downregulated IL-1 β levels in these mice (Fig 5.15). Similarly, another slow-releasing H₂S donor FW1256 was previously shown to also reduce IL-1 β in the blood plasma and peritoneum of LPS sepsis mice (Huang et al., 2016a). When taking into consideration the *in vitro* studies showing that H₂S inhibits NLRP3 inflammasome activation in BMDMs in the present study, it is highly suggestive that H₂S also inhibits NLRP3 activation in addition to NF κ B activation *in vivo*. It must however be noted that *in vivo*, dendritic cells also possess the NLRP3 inflammasome and contributes to IL-1 β secretion (Ghiringhelli et al., 2009). Hence, the likelihood that the reported *in vivo* IL-1 β levels could be attributed from both macrophages and dendritic cells should not be ruled out.

In conclusion, the present study has shown for the first time that exogenous H₂S inhibits NLRP3 inflammasome activation in primary mouse macrophages. The study has also presented two possible mechanistic explanations of how this occurs. Though the use of NaHS is unlikely to be

therapeutically feasible, this study offers a proof-of-concept showing that H₂S from both fast and slow-releasing H₂S donors are able to inhibit NLRP3 inflammasome activation. With the continual discovery of newer H₂S releasing donors, such compounds as compared to NaHS, could potentially be used to reduce IL-1 β and IL-18 levels in inflammatory conditions at a much smaller dose.

CHAPTER 6: OVERVIEW AND FUTURE PERSPECTIVES

6.1 Summary of findings

The aim of this project was to investigate the role of endogenous H₂S producing enzymes and exogenous H₂S in regulating the release of pro-inflammatory cytokines from mouse macrophages.

In the first part of the study, CSE, an endogenous H₂S producing enzyme present in macrophages, was permanently knocked-out in a RAW264.7 mouse macrophage cell line using a CRISPR gene editing tool. Among a panel of pro-inflammatory mediators assayed (TNF α , IL-6, pro IL-1 β , iNOS and COX-2), loss of CSE downregulated iNOS and COX-2 expression at the protein level in these cells (c.f. CSE^{+/+} cells) by a molecular mechanism which was independent of NF κ B. Since exogenous H₂S, via a fast releasing H₂S donor (NaHS), inhibited the production of pro-inflammatory mediators (TNF α and IL-6) in LPS-stimulated wild-type RAW264.7 cells, further examination of this response was conducted in CSE^{-/-} RAW264.7 cells. Interestingly, absence of CSE did not significantly affect the downregulation of pro-inflammatory mediators caused by NaHS in RAW264.7 cells stimulated with LPS. Since CRISPR gene editing allows for the generation of stable knock-out cell lines, a future extension of this project might involve knocking out additional endogenous H₂S producing enzyme, 3-MST, hence generating a 3-MST knockout, and a CSE and 3-MST double-knockout cell line. Having determined that CBS may not be present in mouse macrophages in the present study (Fig 3.2E), the knocking down of CBS would not be necessary.

A previous study showed that the slow-releasing H₂S donor, GYY4137, was more effective than NaHS in decreasing the release of pro-inflammatory mediators from macrophages (Whiteman et al., 2010). We therefore sought, in

the second part of the study, to identify and characterize a novel slow-releasing H₂S donor which was more effective (c.f. NaHS and GYY4137) as an inhibitor of the release of pro-inflammatory mediators from LPS-stimulated macrophages. In this work, we identified FW1256 as a novel H₂S releasing compound which inhibited the production of pro-inflammatory mediators (TNF α , IL-6, NO, PGE₂, pro IL-1 β , iNOS and COX-2) in RAW264.7 cells and primary BMDMs by inhibition of NF κ B activation. FW1256 also downregulated TNF α , IL-1 β , NO and PGE₂ in a mouse model of LPS induced septic shock *in vivo*.

Having determined that exogenous H₂S inhibited the synthesis of pro IL-1 β in RAW264.7 cells, we thereafter explored the possibility that H₂S also inhibited NLRP3 inflammasome activation. NLRP3 inflammasome activation is responsible for maturation of pro IL-1 β into its secretable form. In this work, for the first time, we showed that NaHS inhibited NLRP3 inflammasome activation in primary BMDMs, as evidenced by a decrease in IL-1 β and IL-18 secretion, caspase-1 activation and pyroptosis in these cells. Treatment of BMDMs with DL-PAG prior to NLRP3 inflammasome activation conversely exacerbated IL-1 β and IL-18 secretion as well as caspase-1 activation, suggesting that endogenous H₂S may also have a role to play in controlling NLRP3 inflammasome activation. *In vivo*, it was observed that GYY4137 reduced IL-1 β levels in the mouse model of LPS induced sepsis, an effect similar to that observed in LPS-evoked sepsis in mice treated with FW1256. An examination of the molecular mechanisms by which NaHS inhibited NLRP3 inflammasome activation revealed that this agent reduced NLRP3 – ASC binding in HEK293T cells overexpressed with NLRP3 and ASC, protected mitochondrial integrity and reduced mitochondrial ROS production in BMDMs during NLRP3

inflammasome activation, but did not downregulate the accumulation of cytoplasmic mtDNA in these cells. Together, these findings suggest that NaHS likely inhibits NLRP3 inflammasome activation by multiple molecular mechanisms.

6.2 Future perspectives on the therapeutic applications of H₂S donors

The 'evolution' of H₂S from a noxious toxic gas found in sewers and swamps to a gasotransmitter with physiological and potential clinical relevance has occurred rapidly over the last two decades. The presence and perhaps more importantly, the perception, of its toxicity may well prove to be a formidable challenge for the development of H₂S donor compounds suitable for clinical applications. Major concerns related to H₂S toxicity is the concentration of donor used and the rate of release of H₂S gas therefrom which factors together play a major part in determining the final concentration of this gas inside cells. A paradigm shift in the way pharmacologists consider H₂S delivery is the identification of slow-releasing H₂S donors. The prototype of this class is GYY4137 which releases H₂S gas in low concentrations over a longer period of time c.f. the fast releasing H₂S donors such as NaHS or Na₂S. Reasonably, such donors may reduce H₂S mediated toxicity and thus increase the effective therapeutic window for this compound. GYY4137 has demonstrated therapeutic potential both *in vitro* and *in vivo* in a myriad of animal disease models in the absence of any overt toxicity (Rose et al., 2015). This has shaped the idea that slow-releasing H₂S donors may be the mainstay of so called 'H₂S therapeutics'. The trend of exploring slow-releasing sustained H₂S donors for biomedical applications in recent years has also led to the development of H₂S releasing nanofibrous coating for dermal wound regeneration (Wu et al., 2016).

The present work introduces an additional slow-releasing H₂S donor, FW1256, as an 'improved version' of GYY4137 in inhibiting the production of pro-inflammatory mediators in macrophages. Although non-toxic under the experimental conditions in this study, FW1256 is anti-proliferative and apoptotic

towards MCF7 and SKOV3 cancer cell lines (Feng et al., 2015). Hence, caution should be exercised and its toxicity ascertained when evaluating the effect of FW1256 in normal i.e. non-cancer cell types. However, GYY4137 is shown to be toxic towards cancer cell types but not normal cells (Lee et al., 2011). As such, there is a possibility that FW1256, or perhaps a derivative thereof, might possess such characteristic. If so, such a compound may perhaps have the ability to reduce pro-inflammatory mediator release and at the same time, eradicate cancerous cells during cancer therapy. Such an application however warrants further in-depth studies given that tumour-associated macrophages (TAMs) that reside inside tumours exhibit phenotypic heterogeneity and diverse functional capabilities under the influence of the tumour microenvironment (Petty and Yang, 2017). Given that the presence of TAMs is associated with poor prognosis in patients with several cancer types (Heusinkveld and van der Burg, 2011), and that TAMs suppress CD8+ T cell activation and killing of tumour cells by producing anti-inflammatory cytokines, understanding how H₂S would affect TAMs as well as the generation of pro-inflammatory cytokines for the recruitment of CD8+ T cell into the tumour site would be crucial (Petty and Yang, 2017). The anti-inflammatory effect of H₂S donors like FW1256 may perhaps also be counter-productive in cancer therapy when used in conjunction with treatments involving immunotherapy.

Moving forward, future strategies could also be undertaken to improve the delivery of FW1256 and its potential derivatives to target macrophages specifically, hence increasing its potency *in vivo* and possibly reducing its toxicity towards other cells. Drug delivery systems for intracellular delivery to macrophages have been developed in recent years, particularly for the

treatment of bacterial infections (Pei and Yeo, 2016). Such delivery systems include the use of liposomes (Wagner and Vorauer-Uhl, 2011), polymeric nanoparticles (Makadia and Siegel, 2011), chitosan (Bernkop-Schnürch and Dünnhaupt, 2012), and nanogels (Schmitt et al., 2010). To specifically target drug delivery towards macrophages, the coupling of cell-interactive ligands that target receptors prevalent on the surface of macrophages could be done to FW1256. On the surface of macrophages are an array of receptors such as mannose receptors (CD206) (Martinez-Pomares, 2012), folic acid receptors (Low et al., 2008) and Fc-receptors (Guilliams et al., 2014). Due to the prevalence of CD206 receptors on macrophages, mannose has been a ligand of choice for the delivery of drugs to macrophages (Azad et al., 2014). In addition, folate receptors are upregulated on the surface of activated macrophages (Low et al., 2008). Hence, both mannose and folate could be chemically linked to FW1256 in future studies, thereby enhancing its delivery to macrophages *in vivo*. In tandem, steps could be undertaken to study the bioavailability of FW1256 *in vivo* by characterizing its rate of absorption and metabolic clearance *in vivo*. Understanding the bioavailability of the drug would enable determining the optimum dose required, as well as further optimization for the best delivery route of the drug.

For H₂S donors to be perceived as a safe and viable therapeutic option by the scientific community and the pharmaceutical industry, several fundamental questions and uncertainties about H₂S signalling need to be addressed in greater detail. Firstly, upon administration of a slow-releasing H₂S donor, it still remains unclear whether the compound is being taken up by the cell prior to its release of H₂S intracellularly, or whether the release of H₂S

occurs extracellularly prior to diffusion into the cell. To date, no H₂S specific receptor is known. However, what is clear is that the anionic sulfide (HS⁻) anion channel exists in *Clostridium difficile* (Czyzewski and Wang, 2012). The relevance of a HS⁻ anion channel in H₂S signalling may be significant given that H₂S is a weak acid in equilibrium and dissociates to the HS⁻ anion and H⁺ ion at a pH close to physiological pH (approximately pH 6.9) (Kabil et al., 2014; Olson, 2012), with approximately 80% of H₂S dissociated to the HS⁻ anion (Iciek et al., 2015). A plausible hypothesis is that the effects elicited by H₂S may in fact also be mostly contributed by the HS⁻ anion. In mammals, the existence of such an anion channel thus far has only been reported in human erythrocytes, in the form of an anion exchange protein (AE1) mediating Cl⁻/HS⁻ exchange (Jennings, 2013).

A second, major challenge is the ability to quantitate both the concentration and subcellular localization of H₂S within cells. The development of H₂S intracellular fluorescent probes in recent years has led to significant progress in addressing this question (Feng and Dymock, 2015). In addition, the development of H₂S donors has led to the generation of a novel H₂S releasing compound (AP39) which specifically targets mitochondria (Szczesny et al., 2014). This approach may pave the way for the development of more organelle-specific H₂S releasing donors in the future. Latest research on H₂S fluorescent probes have taken a step further to harness the potential of these probes towards detecting H₂S generated from H₂S releasing donors in subcellular organelles such as the mitochondria and nucleus (Chen et al., 2016), as well as the mitochondria and lysosome (Montoya and Pluth, 2016). As such, it could be said that we are only just starting to achieve a depth of understanding about

the intracellular distribution of H₂S which will be needed if H₂S is to be used therapeutically.

Utilising a gas known for its toxicity in the clinic is undoubtedly a risky strategy. One approach which some pharmacologists have taken is to develop H₂S-releasing anti-inflammatory chimeras drugs. Such chimeras reported in recent studies include ATB-346 (H₂S-releasing derivative of naproxen) (De Cicco et al., 2016), NBS-1120 (H₂S and NO-releasing derivative of aspirin) (Kodela et al., 2015), AVT-18A (H₂S and NO-releasing derivative of sulindac) (Kashfi et al., 2015) amongst others. These H₂S releasing chimeras demonstrated equal or superior effectiveness in reducing inflammation as compared to the parent NSAID, with the additional benefit of significantly lesser gastrointestinal bleeding – a side effect associated with long term NSAID use. One example of an H₂S-releasing anti-inflammatory chimera that has thus far been successful in clinical trials is ATB-346. As the lead drug of Antibe Therapeutics for the treatment of osteoarthritis, ATB-346 had a successful completion of a Phase 2 clinical trial in August 2016 (Antibe, 2016).

6.3 Future perspectives on the intracellular signalling mediated by H₂S.

One of the modes by which H₂S elicits intracellular signalling is through protein post-translational modification via S-sulfhydrylation, which forms persulfides (-SSH) at cysteine residues, or polysulfides (H₂S_{*n*}). Such modifications cause a conformational change in the protein structure thereby changing its enzymatic activity and/or ability to bind with other interacting proteins. As demonstrated in the present study, we proposed that the inhibition of NLRP3 inflammasome activation by H₂S was mediated by an effect of H₂S to reduce NLRP3 – ASC protein-protein binding.

A misconception regarding persulfide formation is that H₂S interacts directly with free thiols (-SH) to form a persulfide (-SSH). This is not possible due to thermodynamic constraints (Filipovic, 2015). Instead, H₂S non-enzymatically interacts with sulfenic acids (-SOH), or -SR groups to yield persulfides. Given that protein S-sulfenylation (the reversible conversion of protein thiols to sulfenic acids via oxidation) occurs in more than 1000 proteins in the cell (Yang et al., 2014), it is conceivable that persulfide formation by H₂S occurs via a 2 step process, involving initially S-sulfenylation. Another mechanism by which H₂S may cause persulfide formation at cysteine residues in proteins in a non-enzymatic manner is via the formation of sulfane sulfur (S⁰), which is also known as “zero valent sulfur”, “sulfur-bonded sulfur”, or more technically defined as “thiosulfoxide sulfur or any sulfur atom which can tautomerize to the thiosulfoxide form” (Toohey and Cooper, 2014). Compounds that contain sulfane sulfur have a reactive sulfur atom in a 0 or -1 oxidation state, that is bounded to another sulfur atom (Iciek et al., 2015).

Besides modifying protein structure, persulfides and polysulfides may also function as H₂S reservoirs, from which H₂S can be released in the presence of reductants like glutathione (GSH) (Ishigami et al., 2009). It is believed that free H₂S in plasma exists in concentrations of less than 1 μM (Zhang et al., 2014b). Coupled with the finding that sulfur chains present in Na₂S₃ and Na₂S₄ preparations was more than 300 times more potent in activating the transient receptor potential ankyrin 1 (TRPA1) channel as compared to H₂S (Kimura et al., 2013), sulfane sulfur present in polysulfides instead of free H₂S may be the sulfide species that contributes significantly to sulfide-mediated intracellular signalling (Greiner et al., 2013). Polysulfides can be generated from H₂S in the presence of oxygen (Nielsen et al., 2011). The HS⁻ anion (which is generated from NaHS) can react with sulfane sulfur, thereby producing polysulfides with varying numbers of sulfurs up to 8 sulfurs, at which cyclization of sulfur occurs and separates from the polysulfide chain (Toohey, 2011). As such, if indeed the active signalling molecule is sulfane sulfur instead of H₂S, then perhaps the required concentration of the active moiety to elicit a biological effect may be only a fraction of the concentration of NaHS required to cause the same biological effect.

In conclusion, it is perhaps simplistic to suggest that the mechanisms governing H₂S-mediated signalling are simply via H₂S gas generated from H₂S-releasing donors. H₂S in the gaseous form could be the starting molecule and/or an intermediate in a complex chain of sulfur-containing molecular reactions. Fundamental to this intricate web of chemical reactions is elemental sulfur (S) which might exist as several different species intracellularly. To elucidate the exact mechanism involved would require new detection tools and

methods to locate and quantitate sulfane sulfur producing species such as persulfides, disulfides, thio analogues and sulfur chains intracellularly.

REFERENCES

- Abe, K., and Kimura, H. (1996). The possible role of hydrogen sulfide as an endogenous neuromodulator. *J Neurosci* 16, 1066-1071.
- Ahmad, A., Gerö, D., Olah, G., and Szabo, C. (2016a). Effect of endotoxemia in mice genetically deficient in cystathionine- γ -lyase, cystathionine- β -synthase or 3-mercaptopyruvate sulfurtransferase. *Int J Mol Med* 38, 1683-1692.
- Ahmad, A., Olah, G., Szczesny, B., Wood, M.E., Whiteman, M., and Szabo, C. (2016b). AP39, A Mitochondrially Targeted Hydrogen Sulfide Donor, Exerts Protective Effects in Renal Epithelial Cells Subjected to Oxidative Stress in Vitro and in Acute Renal Injury in Vivo. *Shock* 45, 88-97.
- Ahmad, A., and Szabo, C. (2016). Both the H₂S biosynthesis inhibitor aminooxyacetic acid and the mitochondrially targeted H₂S donor AP39 exert protective effects in a mouse model of burn injury. *Pharmacol Res* 113, 348-355.
- Akagi, R. (1982). Purification and characterization of cysteine aminotransferase from rat liver cytosol. *Acta Med Okayama* 36, 187-197.
- Aktan, F. (2004). iNOS-mediated nitric oxide production and its regulation. *Life Sci* 75, 639-653.
- Antibe, T. (2016). Antibe Therapeutics Announces Successful Phase 2 Trial of ATB-346 in Osteoarthritis (<http://www.antibetherapeutics.com/2016/08/08/antibe-therapeutics-announces-successful-phase-2-trial-of-atb-346-in-osteoarthritis/>).
- Asimakopoulou, A., Panopoulos, P., Chasapis, C.T., Coletta, C., Zhou, Z., Cirino, G., Giannis, A., Szabo, C., Spyroulias, G.A., and Papapetropoulos, A. (2013). Selectivity of commonly used pharmacological inhibitors for cystathionine beta synthase (CBS) and cystathionine gamma lyase (CSE). *Br J Pharmacol* 169, 922-932.
- Austyn, J.M., and Gordon, S. (1981). F4/80, a monoclonal antibody directed specifically against the mouse macrophage. *Eur J Immunol* 11, 805-815.
- Azad, A.K., Rajaram, M.V., and Schlesinger, L.S. (2014). Exploitation of the Macrophage Mannose Receptor (CD206) in Infectious Disease Diagnostics and Therapeutics. *J Cytol Mol Biol* 1.
- Badiei, A., Rivers-Auty, J., Ang, A.D., and Bhatia, M. (2013). Inhibition of hydrogen sulfide production by gene silencing attenuates inflammatory activity of LPS-activated RAW264.7 cells. *Appl Microbiol Biotechnol* 97, 7845-7852.
- Barakat, A., Al-Majid, A.M., Al-Najjar, H.J., Mabkhot, Y.N., Javaid, S., Yousuf, S., and Choudhary, M.I. (2014). Zwitterionic pyrimidinium adducts as antioxidants with therapeutic potential as nitric oxide scavenger. *Eur J Med Chem* 84, 146-154.

Baroja-Mazo, A., Martín-Sánchez, F., Gomez, A.I., Martínez, C.M., Amores-Iniesta, J., Compan, V., Barberà-Cremades, M., Yagüe, J., Ruiz-Ortiz, E., Antón, J., *et al.* (2014). The NLRP3 inflammasome is released as a particulate danger signal that amplifies the inflammatory response. *Nat Immunol* 15, 738-748.

Barr, L.A., Shimizu, Y., Lambert, J.P., Nicholson, C.K., and Calvert, J.W. (2015). Hydrogen sulfide attenuates high fat diet-induced cardiac dysfunction via the suppression of endoplasmic reticulum stress. *Nitric Oxide* 46, 145-156.

Bartholomew, T.C., Powell, G.M., Dodgson, K.S., and Curtis, C.G. (1980). Oxidation of sodium sulphide by rat liver, lungs and kidney. *Biochem Pharmacol* 29, 2431-2437.

Bauernfeind, F., Bartok, E., Rieger, A., Franchi, L., Nunez, G., and Hornung, V. (2011). Cutting edge: reactive oxygen species inhibitors block priming, but not activation, of the NLRP3 inflammasome. *J Immunol* 187, 613-617.

Beauchamp, R.O., Bus, J.S., Popp, J.A., Boreiko, C.J., and Andjelkovich, D.A. (1984). A critical review of the literature on hydrogen sulfide toxicity. *Crit Rev Toxicol* 13, 25-97.

Beinert, H., Holm, R.H., and Münck, E. (1997). Iron-sulfur clusters: nature's modular, multipurpose structures. *Science* 277, 653-659.

Benavides, G.A., Squadrito, G.L., Mills, R.W., Patel, H.D., Isbell, T.S., Patel, R.P., Darley-Usmar, V.M., Doeller, J.E., and Kraus, D.W. (2007). Hydrogen sulfide mediates the vasoactivity of garlic. *Proc Natl Acad Sci U S A* 104, 17977-17982.

Bergsbaken, T., and Cookson, B.T. (2007). Macrophage activation redirects yersinia-infected host cell death from apoptosis to caspase-1-dependent pyroptosis. *PLoS Pathog* 3, e161.

Bernkop-Schnürch, A., and Dünnhaupt, S. (2012). Chitosan-based drug delivery systems. *Eur J Pharm Biopharm* 81, 463-469.

Beltowski, J. (2015). Hydrogen sulfide in pharmacology and medicine--An update. *Pharmacol Rep* 67, 647-658.

Bhatia, M., Sidhapuriwala, J.N., Ng, S.W., Tamizhselvi, R., and Moochhala, S.M. (2008). Pro-inflammatory effects of hydrogen sulphide on substance P in caerulein-induced acute pancreatitis. *J Cell Mol Med* 12, 580-590.

Blanco, P., Palucka, A.K., Pascual, V., and Banchereau, J. (2008). Dendritic cells and cytokines in human inflammatory and autoimmune diseases. *Cytokine Growth Factor Rev* 19, 41-52.

Bos, E.M., Wang, R., Snijder, P.M., Boersema, M., Damman, J., Fu, M., Moser, J., Hillebrands, J.L., Ploeg, R.J., Yang, G., *et al.* (2013). Cystathionine γ -lyase protects against renal ischemia/reperfusion by modulating oxidative stress. *J Am Soc Nephrol* 24, 759-770.

- Bryan, N.B., Dorfleutner, A., Rojanasakul, Y., and Stehlik, C. (2009). Activation of inflammasomes requires intracellular redistribution of the apoptotic speck-like protein containing a caspase recruitment domain. *J Immunol* 182, 3173-3182.
- Burguera, E.F., Meijide-Failde, R., and Blanco, F.J. (2016). Hydrogen Sulfide and Inflammatory Joint Diseases. *Curr Drug Targets*.
- Cacanyiova, S., Berenyiova, A., and Kristek, F. (2016). The role of hydrogen sulphide in blood pressure regulation. *Physiol Res* 65, S273-S289.
- Chang, T., Untereiner, A., Liu, J., and Wu, L. (2010). Interaction of methylglyoxal and hydrogen sulfide in rat vascular smooth muscle cells. *Antioxid Redox Signal* 12, 1093-1100.
- Chang, Y.P., Ka, S.M., Hsu, W.H., Chen, A., Chao, L.K., Lin, C.C., Hsieh, C.C., Chen, M.C., Chiu, H.W., Ho, C.L., *et al.* (2015). Resveratrol inhibits NLRP3 inflammasome activation by preserving mitochondrial integrity and augmenting autophagy. *J Cell Physiol* 230, 1567-1579.
- Chen, J., Zhao, M., Jiang, X., Sizovs, A., Wang, M.C., Provost, C.R., Huang, J., and Wang, J. (2016). Genetically anchored fluorescent probes for subcellular specific imaging of hydrogen sulfide. *Analyst* 141, 1209-1213.
- Chen, Y., Smith, M.R., Thirumalai, K., and Zychlinsky, A. (1996). A bacterial invasin induces macrophage apoptosis by binding directly to ICE. *EMBO J* 15, 3853-3860.
- Chen, Y.H., Yao, W.Z., Geng, B., Ding, Y.L., Lu, M., Zhao, M.W., and Tang, C.S. (2005). Endogenous hydrogen sulfide in patients with COPD. *Chest* 128, 3205-3211.
- Collart, M.A., Baeuerle, P., and Vassalli, P. (1990). Regulation of tumor necrosis factor alpha transcription in macrophages: involvement of four kappa B-like motifs and of constitutive and inducible forms of NF-kappa B. *Mol Cell Biol* 10, 1498-1506.
- Cooper, C.E., and Brown, G.C. (2008). The inhibition of mitochondrial cytochrome oxidase by the gases carbon monoxide, nitric oxide, hydrogen cyanide and hydrogen sulfide: chemical mechanism and physiological significance. *J Bioenerg Biomembr* 40, 533-539.
- Czyzewski, B.K., and Wang, D.N. (2012). Identification and characterization of a bacterial hydrosulphide ion channel. *Nature* 483, 494-497.
- d'Emmanuele di Villa Bianca, R., Sorrentino, R., Maffia, P., Mirone, V., Imbimbo, C., Fusco, F., De Palma, R., Ignarro, L.J., and Cirino, G. (2009). Hydrogen sulfide as a mediator of human corpus cavernosum smooth-muscle relaxation. *Proc Natl Acad Sci U S A* 106, 4513-4518.
- De Cicco, P., Panza, E., Ercolano, G., Armogida, C., Sessa, G., Pirozzi, G., Cirino, G., Wallace, J.L., and Ianaro, A. (2016). ATB-346, a novel hydrogen

sulfide-releasing anti-inflammatory drug, induces apoptosis of human melanoma cells and inhibits melanoma development in vivo. *Pharmacol Res* 114, 67-73.

De Stefano, D., Maiuri, M.C., Iovine, B., Ialenti, A., Bevilacqua, M.A., and Carnuccio, R. (2006). The role of NF-kappaB, IRF-1, and STAT-1alpha transcription factors in the iNOS gene induction by gliadin and IFN-gamma in RAW 264.7 macrophages. *J Mol Med (Berl)* 84, 65-74.

Dinarello, C.A. (2009). Immunological and inflammatory functions of the interleukin-1 family. *Annu Rev Immunol* 27, 519-550.

Diwakar, L., and Ravindranath, V. (2007). Inhibition of cystathionine-gamma-lyase leads to loss of glutathione and aggravation of mitochondrial dysfunction mediated by excitatory amino acid in the CNS. *Neurochem Int* 50, 418-426.

Duewell, P., Kono, H., Rayner, K.J., Sirois, C.M., Vladimer, G., Bauernfeind, F.G., Abela, G.S., Franchi, L., Nunez, G., Schnurr, M., *et al.* (2010). NLRP3 inflammasomes are required for atherogenesis and activated by cholesterol crystals. *Nature* 464, 1357-1361.

Dufton, N., Natividad, J., Verdu, E.F., and Wallace, J.L. (2012). Hydrogen sulfide and resolution of acute inflammation: A comparative study utilizing a novel fluorescent probe. *Sci Rep* 2, 499.

Duprez, L., Wirawan, E., Vanden Berghe, T., and Vandenabeele, P. (2009). Major cell death pathways at a glance. *Microbes Infect* 11, 1050-1062.

Eliopoulos, A.G., Dumitru, C.D., Wang, C.C., Cho, J., and Tschlis, P.N. (2002). Induction of COX-2 by LPS in macrophages is regulated by Tpl2-dependent CREB activation signals. *EMBO J* 21, 4831-4840.

Elrod, J.W., Calvert, J.W., Morrison, J., Doeller, J.E., Kraus, D.W., Tao, L., Jiao, X., Scalia, R., Kiss, L., Szabo, C., *et al.* (2007). Hydrogen sulfide attenuates myocardial ischemia-reperfusion injury by preservation of mitochondrial function. *Proc Natl Acad Sci U S A* 104, 15560-15565.

Elsheikh, W., Blackler, R.W., Flannigan, K.L., and Wallace, J.L. (2014). Enhanced chemopreventive effects of a hydrogen sulfide-releasing anti-inflammatory drug (ATB-346) in experimental colorectal cancer. *Nitric Oxide* 41, 131-137.

Farrugia, G., and Szurszewski, J.H. (2014). Carbon monoxide, hydrogen sulfide, and nitric oxide as signaling molecules in the gastrointestinal tract. *Gastroenterology* 147, 303-313.

Faustin, B., Lartigue, L., Bruey, J.M., Luciano, F., Sergienko, E., Bailly-Maitre, B., Volkman, N., Hanein, D., Rouiller, I., and Reed, J.C. (2007). Reconstituted NALP1 inflammasome reveals two-step mechanism of caspase-1 activation. *Mol Cell* 25, 713-724.

Feng, W., and Dymock, B.W. (2015). Fluorescent Probes for H₂S Detection and Quantification. *Handb Exp Pharmacol* 230, 291-323.

Feng, W., Teo, X., Novera, W., Ramanujulu, P.M., Dong, L., Huang, D., Moore, P.K., Deng, L.W., and Dymock, B.W. (2015). Discovery of new H₂S releasing phosphordithioates and 2,3-dihydro-2-phenyl-2-sulfanylenebenzo[d][1,3,2]oxazaphospholes with improved antiproliferative activity. *J Med Chem*.

Fernandes-Alnemri, T., and Alnemri, E.S. (2008). Assembly, purification, and assay of the activity of the ASC pyroptosome. *Methods Enzymol* 442, 251-270.

Fernandes-Alnemri, T., Wu, J., Yu, J.W., Datta, P., Miller, B., Jankowski, W., Rosenberg, S., Zhang, J., and Alnemri, E.S. (2007). The pyroptosome: a supramolecular assembly of ASC dimers mediating inflammatory cell death via caspase-1 activation. *Cell Death Differ* 14, 1590-1604.

Fernandes-Alnemri, T., Yu, J.W., Datta, P., Wu, J., and Alnemri, E.S. (2009). AIM2 activates the inflammasome and cell death in response to cytoplasmic DNA. *Nature* 458, 509-513.

Ferrari, D., Pizzirani, C., Adinolfi, E., Lemoli, R.M., Curti, A., Idzko, M., Panther, E., and Di Virgilio, F. (2006). The P2X₇ receptor: a key player in IL-1 processing and release. *J Immunol* 176, 3877-3883.

Filipovic, M.R. (2015). Persulfidation (S-sulfhydration) and H₂S. *Handb Exp Pharmacol* 230, 29-59.

Fink, S.L., and Cookson, B.T. (2006). Caspase-1-dependent pore formation during pyroptosis leads to osmotic lysis of infected host macrophages. *Cell Microbiol* 8, 1812-1825.

Franchi, L., Kamada, N., Nakamura, Y., Burberry, A., Kuffa, P., Suzuki, S., Shaw, M.H., Kim, Y.G., and Núñez, G. (2012). NLRC4-driven production of IL-1 β discriminates between pathogenic and commensal bacteria and promotes host intestinal defense. *Nat Immunol* 13, 449-456.

Franchi, L., and Núñez, G. (2008). The Nlrp3 inflammasome is critical for aluminium hydroxide-mediated IL-1 β secretion but dispensable for adjuvant activity. *Eur J Immunol* 38, 2085-2089.

Franklin, B.S., Bossaller, L., De Nardo, D., Ratter, J.M., Stutz, A., Engels, G., Brenker, C., Nordhoff, M., Mirandola, S.R., Al-Amoudi, A., *et al.* (2014). The adaptor ASC has extracellular and 'prionoid' activities that propagate inflammation. *Nat Immunol* 15, 727-737.

Fu, M., Zhang, W., Wu, L., Yang, G., Li, H., and Wang, R. (2012). Hydrogen sulfide (H₂S) metabolism in mitochondria and its regulatory role in energy production. *Proc Natl Acad Sci U S A* 109, 2943-2948.

Ghiringhelli, F., Apetoh, L., Tesniere, A., Aymeric, L., Ma, Y., Ortiz, C., Vermaelen, K., Panaretakis, T., Mignot, G., Ullrich, E., *et al.* (2009). Activation of the NLRP3 inflammasome in dendritic cells induces IL-1beta-dependent adaptive immunity against tumors. *Nat Med* 15, 1170-1178.

Ghonime, M.G., Shamaa, O.R., Das, S., Eldomany, R.A., Fernandes-Alnemri, T., Alnemri, E.S., Gavrilin, M.A., and Wewers, M.D. (2014). Inflammasome priming by lipopolysaccharide is dependent upon ERK signaling and proteasome function. *J Immunol* 192, 3881-3888.

Ginhoux, F., and Guilliams, M. (2016). Tissue-Resident Macrophage Ontogeny and Homeostasis. *Immunity* 44, 439-449.

Goodwin, L.R., Francom, D., Dieken, F.P., Taylor, J.D., Warenycia, M.W., Reiffenstein, R., and Dowling, G. (1989). Determination of sulfide in brain tissue by gas dialysis/ion chromatography: postmortem studies and two case reports. *Journal of analytical toxicology* 13, 105-109.

Greiner, R., Palinkas, Z., Basell, K., Becher, D., Antelmann, H., Nagy, P., and Dick, T.P. (2013). Polysulfides link H₂S to protein thiol oxidation. *Antioxid Redox Signal* 19, 1749-1765.

Guilliams, M., Bruhns, P., Saeys, Y., Hammad, H., and Lambrecht, B.N. (2014). The function of Fcγ receptors in dendritic cells and macrophages. *Nat Rev Immunol* 14, 94-108.

Guo, H., Callaway, J.B., and Ting, J.P. (2015). Inflammasomes: mechanism of action, role in disease, and therapeutics. *Nat Med* 21, 677-687.

Gurung, P., Lamkanfi, M., and Kanneganti, T.D. (2015). Cutting edge: SHARPIN is required for optimal NLRP3 inflammasome activation. *J Immunol* 194, 2064-2067.

Guzmán, M.A., Navarro, M.A., Carnicer, R., Sarría, A.J., Acín, S., Arnal, C., Muniesa, P., Surra, J.C., Arbonés-Mainar, J.M., Maeda, N., *et al.* (2006). Cystathionine beta-synthase is essential for female reproductive function. *Hum Mol Genet* 15, 3168-3176.

Halle, A., Hornung, V., Petzold, G.C., Stewart, C.R., Monks, B.G., Reinheckel, T., Fitzgerald, K.A., Latz, E., Moore, K.J., and Golenbock, D.T. (2008). The NALP3 inflammasome is involved in the innate immune response to amyloid-beta. *Nat Immunol* 9, 857-865.

Hamelet, J., Maurin, N., Fulchiron, R., Delabar, J.M., and Janel, N. (2007). Mice lacking cystathionine beta synthase have lung fibrosis and air space enlargement. *Exp Mol Pathol* 83, 249-253.

Hanaoka, K., Sasakura, K., Suwanai, Y., Toma-Fukai, S., Shimamoto, K., Takano, Y., Shibuya, N., Terai, T., Komatsu, T., Ueno, T., *et al.* (2017). Discovery and Mechanistic Characterization of Selective Inhibitors of H₂S-producing Enzyme: 3-Mercaptopyruvate Sulfurtransferase (3MST) Targeting Active-site Cysteine Persulfide. *Sci Rep* 7, 40227.

- Harbrecht, B.G. (2006). Therapeutic use of nitric oxide scavengers in shock and sepsis. *Curr Pharm Des* 12, 3543-3549.
- Harper, K.A., and Tyson-Capper, A.J. (2008). Complexity of COX-2 gene regulation. *Biochem Soc Trans* 36, 543-545.
- Heid, M.E., Keyel, P.A., Kamga, C., Shiva, S., Watkins, S.C., and Salter, R.D. (2013). Mitochondrial reactive oxygen species induces NLRP3-dependent lysosomal damage and inflammasome activation. *J Immunol* 191, 5230-5238.
- Held, T., Barakat, A.Z., Mohamed, B.A., Paprotta, I., Meinhardt, A., Engel, W., and Adham, I.M. (2011). Heat-shock protein HSPA4 is required for progression of spermatogenesis. *Reproduction* 142, 133-144.
- Heneka, M.T., Kummer, M.P., Stutz, A., Delekate, A., Schwartz, S., Vieira-Saecker, A., Griep, A., Axt, D., Remus, A., Tzeng, T.C., *et al.* (2013). NLRP3 is activated in Alzheimer's disease and contributes to pathology in APP/PS1 mice. *Nature* 493, 674-678.
- Hernandez-Cuellar, E., Tsuchiya, K., Hara, H., Fang, R., Sakai, S., Kawamura, I., Akira, S., and Mitsuyama, M. (2012). Cutting edge: nitric oxide inhibits the NLRP3 inflammasome. *J Immunol* 189, 5113-5117.
- Herrera, B.S., Coimbra, L.S., da Silva, A.R., Teixeira, S.A., Costa, S.K., Wallace, J.L., Spolidorio, L.C., and Muscara, M.N. (2015). The H2S-releasing naproxen derivative, ATB-346, inhibits alveolar bone loss and inflammation in rats with ligature-induced periodontitis. *Med Gas Res* 5, 4.
- Heusinkveld, M., and van der Burg, S.H. (2011). Identification and manipulation of tumor associated macrophages in human cancers. *J Transl Med* 9, 216.
- Hildebrandt, T.M., and Grieshaber, M.K. (2008). Three enzymatic activities catalyze the oxidation of sulfide to thiosulfate in mammalian and invertebrate mitochondria. *FEBS J* 275, 3352-3361.
- Hillegass, J.M., Miller, J.M., MacPherson, M.B., Westbom, C.M., Sayan, M., Thompson, J.K., Macura, S.L., Perkins, T.N., Beuschel, S.L., Alexeeva, V., *et al.* (2013). Asbestos and erionite prime and activate the NLRP3 inflammasome that stimulates autocrine cytokine release in human mesothelial cells. *Part Fibre Toxicol* 10, 39.
- Hiscott, J., Marois, J., Garoufalidis, J., D'Addario, M., Roulston, A., Kwan, I., Pepin, N., Lacoste, J., Nguyen, H., Bensi, G., *et al.* (1993). Characterization of a functional NF-kappa B site in the human interleukin 1 beta promoter: evidence for a positive autoregulatory loop. *Mol Cell Biol* 13, 6231-6240.
- Hornung, V., Bauernfeind, F., Halle, A., Samstad, E.O., Kono, H., Rock, K.L., Fitzgerald, K.A., and Latz, E. (2008). Silica crystals and aluminum salts activate the NALP3 inflammasome through phagosomal destabilization. *Nat Immunol* 9, 847-856.

Hosoki, R., Matsuki, N., and Kimura, H. (1997). The possible role of hydrogen sulfide as an endogenous smooth muscle relaxant in synergy with nitric oxide. *Biochem Biophys Res Commun* 237, 527-531.

Hu, L.F., Lu, M., Wu, Z.Y., Wong, P.T., and Bian, J.S. (2009). Hydrogen sulfide inhibits rotenone-induced apoptosis via preservation of mitochondrial function. *Mol Pharmacol* 75, 27-34.

Hu, L.F., Wong, P.T., Moore, P.K., and Bian, J.S. (2007). Hydrogen sulfide attenuates lipopolysaccharide-induced inflammation by inhibition of p38 mitogen-activated protein kinase in microglia. *J Neurochem* 100, 1121-1128.

Hu, Y., Mao, K., Zeng, Y., Chen, S., Tao, Z., Yang, C., Sun, S., Wu, X., Meng, G., and Sun, B. (2010). Tripartite-motif protein 30 negatively regulates NLRP3 inflammasome activation by modulating reactive oxygen species production. *J Immunol* 185, 7699-7705.

Huang, C.W., Feng, W., Peh, M.T., Peh, K., Dymock, B.W., and Moore, P.K. (2016a). A novel slow-releasing hydrogen sulfide donor, FW1256, exerts anti-inflammatory effects in mouse macrophages and in vivo. *Pharmacol Res* 113, 533-546.

Huang, C.W., and Moore, P.K. (2015). H₂S Synthesizing Enzymes: Biochemistry and Molecular Aspects. *Handb Exp Pharmacol* 230, 3-25.

Huang, Z., Zhuang, X., Xie, C., Hu, X., Dong, X., Guo, Y., Li, S., and Liao, X. (2016b). Exogenous Hydrogen Sulfide Attenuates High Glucose-Induced Cardiotoxicity by Inhibiting NLRP3 Inflammasome Activation by Suppressing TLR4/NF- κ B Pathway in H9c2 Cells. *Cell Physiol Biochem* 40, 1578-1590.

Iciek, M., Kowalczyk-Pachel, D., Bilska-Wilkosz, A., Kwiecień, I., Górny, M., and Włodek, L. (2015). S-sulfhydration as a cellular redox regulation. *Biosci Rep* 36.

Ikeda, K., Marutani, E., Hirai, S., Wood, M.E., Whiteman, M., and Ichinose, F. (2015). Mitochondria-targeted hydrogen sulfide donor AP39 improves neurological outcomes after cardiac arrest in mice. *Nitric Oxide* 49, 90-96.

Ishigami, M., Hiraki, K., Umemura, K., Ogasawara, Y., Ishii, K., and Kimura, H. (2009). A source of hydrogen sulfide and a mechanism of its release in the brain. *Antioxid Redox Signal* 11, 205-214.

Jennings, M.L. (2013). Transport of H₂S and HS(-) across the human red blood cell membrane: rapid H₂S diffusion and AE1-mediated Cl(-)/HS(-) exchange. *Am J Physiol Cell Physiol* 305, C941-950.

Jo, Y.S., Choi, M.R., Song, S.Y., Kim, M.S., Yoo, N.J., and Lee, S.H. (2016). Frameshift Mutations of HSPA4 and MED13 in Gastric and Colorectal Cancers. *Pathol Oncol Res* 22, 769-772.

- Johnson, D.C., Dean, D.R., Smith, A.D., and Johnson, M.K. (2005). Structure, function, and formation of biological iron-sulfur clusters. *Annu Rev Biochem* 74, 247-281.
- Jourdan, T., Godlewski, G., Cinar, R., Bertola, A., Szanda, G., Liu, J., Tam, J., Han, T., Mukhopadhyay, B., Skarulis, M.C., *et al.* (2013). Activation of the Nlrp3 inflammasome in infiltrating macrophages by endocannabinoids mediates beta cell loss in type 2 diabetes. *Nat Med* 19, 1132-1140.
- Ju, Y., Untereiner, A., Wu, L., and Yang, G. (2015). H₂S-induced S-sulfhydration of pyruvate carboxylase contributes to gluconeogenesis in liver cells. *Biochim Biophys Acta* 1850, 2293-2303.
- Juliana, C., Fernandes-Alnemri, T., Kang, S., Farias, A., Qin, F., and Alnemri, E.S. (2012). Non-transcriptional priming and deubiquitination regulate NLRP3 inflammasome activation. *J Biol Chem* 287, 36617-36622.
- Jung, S.S., Moon, J.S., Xu, J.F., Ifedigbo, E., Ryter, S.W., Choi, A.M., and Nakahira, K. (2015). Carbon monoxide negatively regulates NLRP3 inflammasome activation in macrophages. *Am J Physiol Lung Cell Mol Physiol* 308, L1058-1067.
- Kabil, O., Motl, N., and Banerjee, R. (2014). HS and its role in redox signaling. *Biochim Biophys Acta*.
- Kabil, O., Vitvitsky, V., Xie, P., and Banerjee, R. (2011). The quantitative significance of the transsulfuration enzymes for H₂S production in murine tissues. *Antioxidants & redox signaling* 15, 363-372.
- Kaneko, Y., Kimura, Y., Kimura, H., and Niki, I. (2006). I-Cysteine Inhibits Insulin Release From the Pancreatic β -Cell Possible Involvement of Metabolic Production of Hydrogen Sulfide, a Novel Gasotransmitter. *Diabetes* 55, 1391-1397.
- Karwi, Q.G., Whiteman, M., Wood, M.E., Torregrossa, R., and Baxter, G.F. (2016). Pharmacological postconditioning against myocardial infarction with a slow-releasing hydrogen sulfide donor, GYY4137. *Pharmacol Res* 111, 442-451.
- Kashfi, K., Chattopadhyay, M., and Kodela, R. (2015). NOSH-sulindac (AVT-18A) is a novel nitric oxide- and hydrogen sulfide-releasing hybrid that is gastrointestinal safe and has potent anti-inflammatory, analgesic, antipyretic, anti-platelet, and anti-cancer properties. *Redox Biol* 6, 287-296.
- Kashfi, K., and Olson, K.R. (2013). Biology and therapeutic potential of hydrogen sulfide and hydrogen sulfide-releasing chimeras. *Biochem Pharmacol* 85, 689-703.
- Katsnelson, M.A., Rucker, L.G., Russo, H.M., and Dubyak, G.R. (2015). K⁺ efflux agonists induce NLRP3 inflammasome activation independently of Ca²⁺ signaling. *J Immunol* 194, 3937-3952.

Kauppinen, R.A., Sihra, T.S., and Nicholls, D.G. (1987). Aminoxyacetic acid inhibits the malate-aspartate shuttle in isolated nerve terminals and prevents the mitochondria from utilizing glycolytic substrates. *Biochim Biophys Acta* 930, 173-178.

Kerur, N., Veetil, M.V., Sharma-Walia, N., Bottero, V., Sadagopan, S., Otageri, P., and Chandran, B. (2011). IFI16 acts as a nuclear pathogen sensor to induce the inflammasome in response to Kaposi Sarcoma-associated herpesvirus infection. *Cell Host Microbe* 9, 363-375.

Khare, S., Dorfleutner, A., Bryan, N.B., Yun, C., Radian, A.D., de Almeida, L., Rojanasakul, Y., and Stehlik, C. (2012). An NLRP7-containing inflammasome mediates recognition of microbial lipopeptides in human macrophages. *Immunity* 36, 464-476.

Kim, J.B., Han, A.R., Park, E.Y., Kim, J.Y., Cho, W., Lee, J., Seo, E.K., and Lee, K.T. (2007). Inhibition of LPS-induced iNOS, COX-2 and cytokines expression by poncirin through the NF-kappaB inactivation in RAW 264.7 macrophage cells. *Biol Pharm Bull* 30, 2345-2351.

Kim, S.R., Kim, D.I., Kim, S.H., Lee, H., Lee, K.S., Cho, S.H., and Lee, Y.C. (2014). NLRP3 inflammasome activation by mitochondrial ROS in bronchial epithelial cells is required for allergic inflammation. *Cell Death Dis* 5, e1498.

Kimura, H. (2014). The physiological role of hydrogen sulfide and beyond. *Nitric Oxide*.

Kimura, Y., Mikami, Y., Osumi, K., Tsugane, M., Oka, J., and Kimura, H. (2013). Polysulfides are possible H₂S-derived signaling molecules in rat brain. *FASEB J* 27, 2451-2457.

Kimura, Y., Toyofuku, Y., Koike, S., Shibuya, N., Nagahara, N., Lefer, D., Ogasawara, Y., and Kimura, H. (2015). Identification of H₂S₃ and H₂S produced by 3-mercaptopyruvate sulfurtransferase in the brain. *Sci Rep* 5, 14774.

Kingsbury, S.R., Conaghan, P.G., and McDermott, M.F. (2011). The role of the NLRP3 inflammasome in gout. *J Inflamm Res* 4, 39-49.

Klose, C.S., and Artis, D. (2016). Innate lymphoid cells as regulators of immunity, inflammation and tissue homeostasis. *Nat Immunol* 17, 765-774.

Kodela, R., Chattopadhyay, M., Velázquez-Martínez, C.A., and Kashfi, K. (2015). NOSH-aspirin (NBS-1120), a novel nitric oxide- and hydrogen sulfide-releasing hybrid has enhanced chemo-preventive properties compared to aspirin, is gastrointestinal safe with all the classic therapeutic indications. *Biochem Pharmacol* 98, 564-572.

Kolaczowska, E., and Kubes, P. (2013). Neutrophil recruitment and function in health and inflammation. *Nat Rev Immunol* 13, 159-175.

Kondo, K., Bhushan, S., King, A.L., Prabhu, S.D., Hamid, T., Koenig, S., Murohara, T., Predmore, B.L., Gojon, G., Wang, R., *et al.* (2013). H₂S protects against pressure overload-induced heart failure via upregulation of endothelial nitric oxide synthase. *Circulation* 127, 1116-1127.

Krishnan, N., Fu, C., Pappin, D.J., and Tonks, N.K. (2011). H₂S-Induced sulfhydrylation of the phosphatase PTP1B and its role in the endoplasmic reticulum stress response. *Sci Signal* 4, ra86.

Latz, E., Xiao, T.S., and Stutz, A. (2013). Activation and regulation of the inflammasomes. *Nat Rev Immunol* 13, 397-411.

Lawrence, T. (2009). The nuclear factor NF-kappaB pathway in inflammation. *Cold Spring Harb Perspect Biol* 1, a001651.

Lee, G.S., Subramanian, N., Kim, A.I., Aksentijevich, I., Goldbach-Mansky, R., Sacks, D.B., Germain, R.N., Kastner, D.L., and Chae, J.J. (2012). The calcium-sensing receptor regulates the NLRP3 inflammasome through Ca²⁺ and cAMP. *Nature* 492, 123-127.

Lee, H.H., Han, M.H., Hwang, H.J., Kim, G.Y., Moon, S.K., Hyun, J.W., Kim, W.J., and Choi, Y.H. (2015). Diallyl trisulfide exerts anti-inflammatory effects in lipopolysaccharide-stimulated RAW 264.7 macrophages by suppressing the Toll-like receptor 4/nuclear factor-κB pathway. *Int J Mol Med* 35, 487-495.

Lee, H.M., Kim, J.J., Kim, H.J., Shong, M., Ku, B.J., and Jo, E.K. (2013). Upregulated NLRP3 inflammasome activation in patients with type 2 diabetes. *Diabetes* 62, 194-204.

Lee, Z.W., Zhou, J., Chen, C.S., Zhao, Y., Tan, C.H., Li, L., Moore, P.K., and Deng, L.W. (2011). The slow-releasing hydrogen sulfide donor, GYY4137, exhibits novel anti-cancer effects in vitro and in vivo. *PLoS One* 6, e21077.

Levinsohn, J.L., Newman, Z.L., Hellmich, K.A., Fattah, R., Getz, M.A., Liu, S., Sastalla, I., Leppla, S.H., and Moayeri, M. (2012). Anthrax lethal factor cleavage of Nlrp1 is required for activation of the inflammasome. *PLoS Pathog* 8, e1002638.

Lewy, M., Shapiro, H., Thaïss, C.A., and Elinav, E. (2017). NLRP6: A Multifaceted Innate Immune Sensor. *Trends Immunol.*

Li, F., Zhang, P., Zhang, M., Liang, L., Sun, X., Li, M., Tang, Y., Bao, A., Gong, J., Zhang, J., *et al.* (2016a). Hydrogen Sulfide Prevents and Partially Reverses Ozone-Induced Features of Lung Inflammation and Emphysema in Mice. *Am J Respir Cell Mol Biol* 55, 72-81.

Li, L., Bhatia, M., Zhu, Y.Z., Zhu, Y.C., Ramnath, R.D., Wang, Z.J., Anuar, F.B., Whiteman, M., Salto-Tellez, M., and Moore, P.K. (2005). Hydrogen sulfide is a novel mediator of lipopolysaccharide-induced inflammation in the mouse. *FASEB J* 19, 1196-1198.

- Li, L., Rossoni, G., Sparatore, A., Lee, L.C., Del Soldato, P., and Moore, P.K. (2007). Anti-inflammatory and gastrointestinal effects of a novel diclofenac derivative. *Free Radic Biol Med* 42, 706-719.
- Li, L., Salto-Tellez, M., Tan, C.H., Whiteman, M., and Moore, P.K. (2009). GYY4137, a novel hydrogen sulfide-releasing molecule, protects against endotoxic shock in the rat. *Free Radic Biol Med* 47, 103-113.
- Li, L., Whiteman, M., Guan, Y.Y., Neo, K.L., Cheng, Y., Lee, S.W., Zhao, Y., Baskar, R., Tan, C.H., and Moore, P.K. (2008). Characterization of a novel, water-soluble hydrogen sulfide-releasing molecule (GYY4137): new insights into the biology of hydrogen sulfide. *Circulation* 117, 2351-2360.
- Li, S., and Yang, G. (2015). Hydrogen Sulfide Maintains Mitochondrial DNA Replication via Demethylation of TFAM. *Antioxid Redox Signal* 23, 630-642.
- Li, W.L., Hua, L.G., Qu, P., Yan, W.H., Ming, C., Jun, Y.D., Yuan, L.D., and Nan, N. (2016b). NLRP3 inflammasome: a novel link between lipoproteins and atherosclerosis. *Arch Med Sci* 12, 950-958.
- Libermann, T.A., and Baltimore, D. (1990). Activation of interleukin-6 gene expression through the NF-kappa B transcription factor. *Mol Cell Biol* 10, 2327-2334.
- Lien, H.W., Yang, C.H., Cheng, C.H., Liao, Y.F., Han, Y.S., and Huang, C.J. (2013). Zinc finger protein 219-like (ZNF219L) and Sox9a regulate synuclein- γ 2 (*sncgb*) expression in the developing notochord of zebrafish. *Biochem Biophys Res Commun* 442, 189-194.
- Lin, S., Visram, F., Liu, W., Haig, A., Jiang, J., Mok, A., Lian, D., Wood, M.E., Torregrossa, R., Whiteman, M., *et al.* (2016). GYY4137, a Slow-Releasing Hydrogen Sulfide Donor, Ameliorates Renal Damage Associated with Chronic Obstructive Uropathy. *J Urol* 196, 1778-1787.
- Lin, V.S., Lippert, A.R., and Chang, C.J. (2013). Cell-trappable fluorescent probes for endogenous hydrogen sulfide signaling and imaging H₂O₂-dependent H₂S production. *Proc Natl Acad Sci U S A* 110, 7131-7135.
- Lipinski, C.A., Lombardo, F., Dominy, B.W., and Feeney, P.J. (2001). Experimental and computational approaches to estimate solubility and permeability in drug discovery and development settings. *Adv Drug Deliv Rev* 46, 3-26.
- Liu, K.L., Chen, H.W., Wang, R.Y., Lei, Y.P., Sheen, L.Y., and Lii, C.K. (2006). DATS reduces LPS-induced iNOS expression, NO production, oxidative stress, and NF-kappaB activation in RAW 264.7 macrophages. *J Agric Food Chem* 54, 3472-3478.
- Liu, Y., Yang, R., Liu, X., Zhou, Y., Qu, C., Kikuri, T., Wang, S., Zandi, E., Du, J., Ambudkar, I.S., *et al.* (2014). Hydrogen Sulfide Maintains Mesenchymal Stem Cell Function and Bone Homeostasis via Regulation of Ca Channel Sulfhydration. *Cell Stem Cell*.

- Liu, Z., Han, Y., Li, L., Lu, H., Meng, G., Li, X., Shirhan, M., Peh, M.T., Xie, L., Zhou, S., *et al.* (2013). The hydrogen sulfide donor, GYY4137, exhibits anti-atherosclerotic activity in high fat fed apolipoprotein E(-/-) mice. *Br J Pharmacol* 169, 1795-1809.
- Lo, Y.H., Huang, Y.W., Wu, Y.H., Tsai, C.S., Lin, Y.C., Mo, S.T., Kuo, W.C., Chuang, Y.T., Jiang, S.T., Shih, H.M., *et al.* (2013). Selective inhibition of the NLRP3 inflammasome by targeting to promyelocytic leukemia protein in mouse and human. *Blood* 121, 3185-3194.
- Lopez-Castejon, G., Luheshi, N.M., Compan, V., High, S., Whitehead, R.C., Flitsch, S., Kirov, A., Prudovsky, I., Swanton, E., and Brough, D. (2013). Deubiquitinases regulate the activity of caspase-1 and interleukin-1 β secretion via assembly of the inflammasome. *J Biol Chem* 288, 2721-2733.
- Low, P.S., Henne, W.A., and Doorneweerd, D.D. (2008). Discovery and development of folic-acid-based receptor targeting for imaging and therapy of cancer and inflammatory diseases. *Acc Chem Res* 41, 120-129.
- Maclea, K.N., Sikora, J., Kožich, V., Jiang, H., Greiner, L.S., Kraus, E., Krijt, J., Overdier, K.H., Collard, R., Brodsky, G.L., *et al.* (2010). A novel transgenic mouse model of CBS-deficient homocystinuria does not incur hepatic steatosis or fibrosis and exhibits a hypercoagulative phenotype that is ameliorated by betaine treatment. *Mol Genet Metab* 101, 153-162.
- Maeda, Y., Aoki, Y., Sekiguchi, F., Matsunami, M., Takahashi, T., Nishikawa, H., and Kawabata, A. (2009). Hyperalgesia induced by spinal and peripheral hydrogen sulfide: evidence for involvement of Cav3.2 T-type calcium channels. *Pain* 142, 127-132.
- Makadia, H.K., and Siegel, S.J. (2011). Poly Lactic-co-Glycolic Acid (PLGA) as Biodegradable Controlled Drug Delivery Carrier. *Polymers (Basel)* 3, 1377-1397.
- Mani, S., Li, H., Untereiner, A., Wu, L., Yang, G., Austin, R.C., Dickhout, J.G., Lhotak, S., Meng, Q.H., and Wang, R. (2013). Decreased endogenous production of hydrogen sulfide accelerates atherosclerosis. *Circulation* 127, 2523-2534.
- Mao, K., Chen, S., Chen, M., Ma, Y., Wang, Y., Huang, B., He, Z., Zeng, Y., Hu, Y., Sun, S., *et al.* (2013). Nitric oxide suppresses NLRP3 inflammasome activation and protects against LPS-induced septic shock. *Cell Res* 23, 201-212.
- Mardakheh, F.K., Self, A., and Marshall, C.J. (2016). RHO binding to FAM65A regulates Golgi reorientation during cell migration. *J Cell Sci* 129, 4466-4479.
- Mariathasan, S., Weiss, D.S., Newton, K., McBride, J., O'Rourke, K., Roose-Girma, M., Lee, W.P., Weinrauch, Y., Monack, D.M., and Dixit, V.M. (2006). Cryopyrin activates the inflammasome in response to toxins and ATP. *Nature* 440, 228-232.

- Martin, G.R., McKnight, G.W., Dickey, M.S., Coffin, C.S., Ferraz, J.G., and Wallace, J.L. (2010). Hydrogen sulphide synthesis in the rat and mouse gastrointestinal tract. *Dig Liver Dis* 42, 103-109.
- Martinez-Pomares, L. (2012). The mannose receptor. *J Leukoc Biol* 92, 1177-1186.
- Martinon, F., Burns, K., and Tschopp, J. (2002). The inflammasome: a molecular platform triggering activation of inflammatory caspases and processing of proIL-beta. *Mol Cell* 10, 417-426.
- Martinon, F., Petrilli, V., Mayor, A., Tardivel, A., and Tschopp, J. (2006). Gout-associated uric acid crystals activate the NALP3 inflammasome. *Nature* 440, 237-241.
- Mathai, J.C., Missner, A., Kügler, P., Saparov, S.M., Zeidel, M.L., Lee, J.K., and Pohl, P. (2009). No facilitator required for membrane transport of hydrogen sulfide. *Proc Natl Acad Sci U S A* 106, 16633-16638.
- Medzhitov, R., and Horng, T. (2009). Transcriptional control of the inflammatory response. *Nat Rev Immunol* 9, 692-703.
- Meng, G., Zhu, J., Xiao, Y., Huang, Z., Zhang, Y., Tang, X., Xie, L., Chen, Y., Shao, Y., Ferro, A., *et al.* (2015). Hydrogen Sulfide Donor GYY4137 Protects against Myocardial Fibrosis. *Oxid Med Cell Longev* 2015, 691070.
- Mishra, B.B., Rathinam, V.A., Martens, G.W., Martinot, A.J., Kornfeld, H., Fitzgerald, K.A., and Sasseti, C.M. (2013). Nitric oxide controls the immunopathology of tuberculosis by inhibiting NLRP3 inflammasome-dependent processing of IL-1beta. *Nat Immunol* 14, 52-60.
- Modis, K., Ju, Y., Ahmad, A., Untereiner, A.A., Altaany, Z., Wu, L., Szabo, C., and Wang, R. (2016). S-Sulfhydration of ATP synthase by hydrogen sulfide stimulates mitochondrial bioenergetics. *Pharmacol Res* 113, 116-124.
- Mohamed, B.A., Barakat, A.Z., Zimmermann, W.H., Bittner, R.E., Mühlfeld, C., Hünlich, M., Engel, W., Maier, L.S., and Adham, I.M. (2012). Targeted disruption of Hspa4 gene leads to cardiac hypertrophy and fibrosis. *J Mol Cell Cardiol* 53, 459-468.
- Montoya, L.A., and Pluth, M.D. (2016). Organelle-Targeted H₂S Probes Enable Visualization of the Subcellular Distribution of H₂S Donors. *Anal Chem* 88, 5769-5774.
- Mosser, D.M., and Edwards, J.P. (2008). Exploring the full spectrum of macrophage activation. *Nat Rev Immunol* 8, 958-969.
- Mustafa, A.K., Gadalla, M.M., Sen, N., Kim, S., Mu, W., Gazi, S.K., Barrow, R.K., Yang, G., Wang, R., and Snyder, S.H. (2009). H₂S signals through protein S-sulfhydration. *Sci Signal* 2, ra72.

Mustafa, A.K., Sikka, G., Gazi, S.K., Steppan, J., Jung, S.M., Bhunia, A.K., Barodka, V.M., Gazi, F.K., Barrow, R.K., Wang, R., *et al.* (2011). Hydrogen sulfide as endothelium-derived hyperpolarizing factor sulfhydrates potassium channels. *Circ Res* 109, 1259-1268.

Muñoz-Planillo, R., Kuffa, P., Martínez-Colón, G., Smith, B.L., Rajendiran, T.M., and Núñez, G. (2013). K⁺ efflux is the common trigger of NLRP3 inflammasome activation by bacterial toxins and particulate matter. *Immunity* 38, 1142-1153.

Módis, K., Coletta, C., Erdélyi, K., Papapetropoulos, A., and Szabo, C. (2013). Intramitochondrial hydrogen sulfide production by 3-mercaptopyruvate sulfurtransferase maintains mitochondrial electron flow and supports cellular bioenergetics. *FASEB J* 27, 601-611.

Nagahara, N. (2013). Regulation of mercaptopyruvate sulfurtransferase activity via intrasubunit and intersubunit redox-sensing switches. *Antioxid Redox Signal* 19, 1792-1802.

Nagahara, N., Ito, T., Kitamura, H., and Nishino, T. (1998). Tissue and subcellular distribution of mercaptopyruvate sulfurtransferase in the rat: confocal laser fluorescence and immunoelectron microscopic studies combined with biochemical analysis. *Histochem Cell Biol* 110, 243-250.

Nagy, P., Pálinkás, Z., Nagy, A., Budai, B., Tóth, I., and Vasas, A. (2014). Chemical aspects of hydrogen sulfide measurements in physiological samples. *Biochim Biophys Acta* 1840, 876-891.

Nakahira, K., Haspel, J.A., Rathinam, V.A., Lee, S.J., Dolinay, T., Lam, H.C., Englert, J.A., Rabinovitch, M., Cernadas, M., Kim, H.P., *et al.* (2011). Autophagy proteins regulate innate immune responses by inhibiting the release of mitochondrial DNA mediated by the NALP3 inflammasome. *Nat Immunol* 12, 222-230.

Neacsu, P., Mazare, A., Schmuki, P., and Cimpean, A. (2015). Attenuation of the macrophage inflammatory activity by TiO₂ nanotubes via inhibition of MAPK and NF- κ B pathways. *Int J Nanomedicine* 10, 6455-6467.

Nielsen, R.W., Tachibana, C., Hansen, N.E., and Winther, J.R. (2011). Trisulfides in proteins. *Antioxid Redox Signal* 15, 67-75.

Oh, G.S., Pae, H.O., Lee, B.S., Kim, B.N., Kim, J.M., Kim, H.R., Jeon, S.B., Jeon, W.K., Chae, H.J., and Chung, H.T. (2006). Hydrogen sulfide inhibits nitric oxide production and nuclear factor-kappaB via heme oxygenase-1 expression in RAW264.7 macrophages stimulated with lipopolysaccharide. *Free Radic Biol Med* 41, 106-119.

Okabe, Y., and Medzhitov, R. (2016). Tissue biology perspective on macrophages. *Nat Immunol* 17, 9-17.

- Olson, K.R. (2012). A practical look at the chemistry and biology of hydrogen sulfide. *Antioxid Redox Signal* 17, 32-44.
- Pan, J., and Carroll, K.S. (2013). Persulfide reactivity in the detection of protein s-sulfhydration. *ACS Chem Biol* 8, 1110-1116.
- Pan, L.L., Liu, X.H., Gong, Q.H., Wu, D., and Zhu, Y.Z. (2011). Hydrogen sulfide attenuated tumor necrosis factor- α -induced inflammatory signaling and dysfunction in vascular endothelial cells. *PLoS One* 6, e19766.
- Park, C.M., Macinkovic, I., Filipovic, M.R., and Xian, M. (2015). Use of the "tag-switch" method for the detection of protein S-sulfhydration. *Methods Enzymol* 555, 39-56.
- Patel, P., Vatish, M., Heptinstall, J., Wang, R., and Carson, R.J. (2009). The endogenous production of hydrogen sulphide in intrauterine tissues. *Reprod Biol Endocrinol* 7, 10.
- Paul, B.D., Sbodio, J.I., Xu, R., Vandiver, M.S., Cha, J.Y., Snowman, A.M., and Snyder, S.H. (2014). Cystathionine gamma-lyase deficiency mediates neurodegeneration in Huntington's disease. *Nature* 509, 96-100.
- Paul, B.D., and Snyder, S.H. (2015). Protein sulfhydration. *Methods Enzymol* 555, 79-90.
- Peeters, P.M., Perkins, T.N., Wouters, E.F., Mossman, B.T., and Reynaert, N.L. (2013). Silica induces NLRP3 inflammasome activation in human lung epithelial cells. *Part Fibre Toxicol* 10, 3.
- Pei, Y., and Yeo, Y. (2016). Drug delivery to macrophages: Challenges and opportunities. *J Control Release* 240, 202-211.
- Pelegrin, P., Barroso-Gutierrez, C., and Surprenant, A. (2008). P2X7 receptor differentially couples to distinct release pathways for IL-1 β in mouse macrophage. *J Immunol* 180, 7147-7157.
- Pelegrin, P., and Surprenant, A. (2006). Pannexin-1 mediates large pore formation and interleukin-1 β release by the ATP-gated P2X7 receptor. *EMBO J* 25, 5071-5082.
- Peng, B., Chen, W., Liu, C., Rosser, E.W., Pacheco, A., Zhao, Y., Aguilar, H.C., and Xian, M. (2014). Fluorescent probes based on nucleophilic substitution-cyclization for hydrogen sulfide detection and bioimaging. *Chemistry* 20, 1010-1016.
- Perregaux, D., and Gabel, C.A. (1994). Interleukin-1 β maturation and release in response to ATP and nigericin. Evidence that potassium depletion mediated by these agents is a necessary and common feature of their activity. *J Biol Chem* 269, 15195-15203.
- Petty, A.J., and Yang, Y. (2017). Tumor-associated macrophages: implications in cancer immunotherapy. *Immunotherapy* 9, 289-302.

Pfeffer, M., and Ressler, C. (1967). Beta-cyanoalanine, an inhibitor of rat liver cystathionase. *Biochem Pharmacol* 16, 2299-2308.

Polhemus, D.J., Li, Z., Pattillo, C.B., Gojon, G., Giordano, T., and Krum, H. (2015). A novel hydrogen sulfide prodrug, SG1002, promotes hydrogen sulfide and nitric oxide bioavailability in heart failure patients. *Cardiovasc Ther* 33, 216-226.

Proell, M., Gerlic, M., Mace, P.D., Reed, J.C., and Riedl, S.J. (2013). The CARD plays a critical role in ASC foci formation and inflammasome signalling. *Biochem J* 449, 613-621.

Py, B.F., Kim, M.S., Vakifahmetoglu-Norberg, H., and Yuan, J. (2013). Deubiquitination of NLRP3 by BRCC3 critically regulates inflammasome activity. *Mol Cell* 49, 331-338.

Queiroz, T.M., Mendes-Júnior, L.G., Guimarães, D.D., França-Silva, M.S., Nalivaiko, E., and Braga, V.A. (2014). Cardiorespiratory effects induced by 2-nitrate-1,3-dibuthoxypropan are reduced by nitric oxide scavenger in rats. *Auton Neurosci* 181, 31-36.

Rafi, M.M., Yadav, P.N., and Rossi, A.O. (2007). Glucosamine inhibits LPS-induced COX-2 and iNOS expression in mouse macrophage cells (RAW 264.7) by inhibition of p38-MAP kinase and transcription factor NF-kappaB. *Mol Nutr Food Res* 51, 587-593.

Ran, F.A., Hsu, P.D., Wright, J., Agarwala, V., Scott, D.A., and Zhang, F. (2013). Genome engineering using the CRISPR-Cas9 system. *Nat Protoc* 8, 2281-2308.

Reiffenstein, R.J., Hulbert, W.C., and Roth, S.H. (1992). Toxicology of hydrogen sulfide. *Annu Rev Pharmacol Toxicol* 32, 109-134.

Rinaldi, L., Gobbi, G., Pambianco, M., Micheloni, C., Mirandola, P., and Vitale, M. (2006). Hydrogen sulfide prevents apoptosis of human PMN via inhibition of p38 and caspase 3. *Lab Invest* 86, 391-397.

Rios, E.C., Szczesny, B., Soriano, F.G., Olah, G., and Szabo, C. (2015). Hydrogen sulfide attenuates cytokine production through the modulation of chromatin remodeling. *Int J Mol Med* 35, 1741-1746.

Rodgers, M.A., Bowman, J.W., Fujita, H., Orazio, N., Shi, M., Liang, Q., Amatya, R., Kelly, T.J., Iwai, K., Ting, J., *et al.* (2014). The linear ubiquitin assembly complex (LUBAC) is essential for NLRP3 inflammasome activation. *J Exp Med* 211, 1333-1347.

Rose, P., Dymock, B.W., and Moore, P.K. (2015). GYY4137, a novel water-soluble, H₂S-releasing molecule. *Methods Enzymol* 554, 143-167.

Roy, A., Khan, A.H., Islam, M.T., Prieto, M.C., and Majid, D.S. (2012). Interdependency of cystathione γ -lyase and cystathione β -synthase in

hydrogen sulfide-induced blood pressure regulation in rats. *Am J Hypertens* 25, 74-81.

Sachdev, P.S. (2005). Homocysteine and brain atrophy. *Prog Neuropsychopharmacol Biol Psychiatry* 29, 1152-1161.

Saha, S., Chakraborty, P.K., Xiong, X., Dwivedi, S.K., Mustafi, S.B., Leigh, N.R., Ramchandran, R., Mukherjee, P., and Bhattacharya, R. (2016). Cystathionine β -synthase regulates endothelial function via protein S-sulfhydration. *FASEB J* 30, 441-456.

Schmitt, F., Lagopoulos, L., Käuper, P., Rossi, N., Busso, N., Barge, J., Wagnières, G., Laue, C., Wandrey, C., and Juillerat-Jeanneret, L. (2010). Chitosan-based nanogels for selective delivery of photosensitizers to macrophages and improved retention in and therapy of articular joints. *J Control Release* 144, 242-250.

Searcy, D.G., and Lee, S.H. (1998). Sulfur reduction by human erythrocytes. *Journal of Experimental Zoology* 282, 310-322.

Sekiguchi, F., Miyamoto, Y., Kanaoka, D., Ide, H., Yoshida, S., Ohkubo, T., and Kawabata, A. (2014). Endogenous and exogenous hydrogen sulfide facilitates T-type calcium channel currents in Cav3.2-expressing HEK293 cells. *Biochem Biophys Res Commun* 445, 225-229.

Sen, N., Paul, B.D., Gadalla, M.M., Mustafa, A.K., Sen, T., Xu, R., Kim, S., and Snyder, S.H. (2012). Hydrogen sulfide-linked sulfhydration of NF-kappaB mediates its antiapoptotic actions. *Mol Cell* 45, 13-24.

Sen, U., Basu, P., Abe, O.A., Givwimani, S., Tyagi, N., Metreveli, N., Shah, K.S., Passmore, J.C., and Tyagi, S.C. (2009). Hydrogen sulfide ameliorates hyperhomocysteinemia-associated chronic renal failure. *Am J Physiol Renal Physiol* 297, F410-419.

Sester, D.P., Thygesen, S.J., Sagulenko, V., Vajjhala, P.R., Cridland, J.A., Vitak, N., Chen, K.W., Osborne, G.W., Schroder, K., and Stacey, K.J. (2015). A novel flow cytometric method to assess inflammasome formation. *J Immunol* 194, 455-462.

Shakhov, A.N., Collart, M.A., Vassalli, P., Nedospasov, S.A., and Jongeneel, C.V. (1990). Kappa B-type enhancers are involved in lipopolysaccharide-mediated transcriptional activation of the tumor necrosis factor alpha gene in primary macrophages. *J Exp Med* 171, 35-47.

Sharif, O., Bolshakov, V.N., Raines, S., Newham, P., and Perkins, N.D. (2007). Transcriptional profiling of the LPS induced NF-kappaB response in macrophages. *BMC Immunol* 8, 1.

Sharma, D., and Kanneganti, T.D. (2016). The cell biology of inflammasomes: Mechanisms of inflammasome activation and regulation. *J Cell Biol* 213, 617-629.

- Shen, X., Kolluru, G.K., Yuan, S., and Kevil, C.G. (2015). Measurement of H₂S in vivo and in vitro by the monobromobimane method. *Methods Enzymol* 554, 31-45.
- Shen, X., Pattillo, C.B., Pardue, S., Bir, S.C., Wang, R., and Kevil, C.G. (2011). Measurement of plasma hydrogen sulfide in vivo and in vitro. *Free Radic Biol Med* 50, 1021-1031.
- Shibuya, N., Koike, S., Tanaka, M., Ishigami-Yuasa, M., Kimura, Y., Ogasawara, Y., Fukui, K., Nagahara, N., and Kimura, H. (2013). A novel pathway for the production of hydrogen sulfide from D-cysteine in mammalian cells. *Nat Commun* 4, 1366.
- Shibuya, N., Mikami, Y., Kimura, Y., Nagahara, N., and Kimura, H. (2009a). Vascular endothelium expresses 3-mercaptopyruvate sulfurtransferase and produces hydrogen sulfide. *J Biochem* 146, 623-626.
- Shibuya, N., Tanaka, M., Yoshida, M., Ogasawara, Y., Togawa, T., Ishii, K., and Kimura, H. (2009b). 3-Mercaptopyruvate sulfurtransferase produces hydrogen sulfide and bound sulfane sulfur in the brain. *Antioxid Redox Signal* 11, 703-714.
- Shimada, K., Crother, T.R., Karlin, J., Dagvadorj, J., Chiba, N., Chen, S., Ramanujan, V.K., Wolf, A.J., Vergnes, L., Ojcius, D.M., *et al.* (2012). Oxidized mitochondrial DNA activates the NLRP3 inflammasome during apoptosis. *Immunity* 36, 401-414.
- Sidhapuriwala, J., Li, L., Sparatore, A., Bhatia, M., and Moore, P.K. (2007). Effect of S-diclofenac, a novel hydrogen sulfide releasing derivative, on carrageenan-induced hindpaw oedema formation in the rat. *Eur J Pharmacol* 569, 149-154.
- Sims, J.E., and Smith, D.E. (2010). The IL-1 family: regulators of immunity. *Nat Rev Immunol* 10, 89-102.
- Smith, D.E., Mendes, M.I., Kluijtmans, L.A., Janssen, M.C., Smulders, Y.M., and Blom, H.J. (2012). A liquid chromatography mass spectrometry method for the measurement of cystathionine β -synthase activity in cell extracts. *J Chromatogr B Analyt Technol Biomed Life Sci* 911, 186-191.
- Sparatore, A., Perrino, E., Tazzari, V., Giustarini, D., Rossi, R., Rossoni, G., Erdmann, K., Erdman, K., Schröder, H., and Del Soldato, P. (2009). Pharmacological profile of a novel H₂S-releasing aspirin. *Free Radic Biol Med* 46, 586-592.
- Steegborn, C., Clausen, T., Sondermann, P., Jacob, U., Worbs, M., Marinkovic, S., Huber, R., and Wahl, M.C. (1999). Kinetics and inhibition of recombinant human cystathionine gamma-lyase. Toward the rational control of transsulfuration. *J Biol Chem* 274, 12675-12684.

- Subramanian, N., Natarajan, K., Clatworthy, M.R., Wang, Z., and Germain, R.N. (2013). The adaptor MAVS promotes NLRP3 mitochondrial localization and inflammasome activation. *Cell* 153, 348-361.
- Sun, Q., Collins, R., Huang, S., Holmberg-Schiavone, L., Anand, G.S., Tan, C.H., van-den-Berg, S., Deng, L.W., Moore, P.K., Karlberg, T., *et al.* (2009). Structural basis for the inhibition mechanism of human cystathionine gamma-lyase, an enzyme responsible for the production of H₂S. *J Biol Chem* 284, 3076-3085.
- Sun, S.C. (2011). Non-canonical NF- κ B signaling pathway. *Cell Res* 21, 71-85.
- Suzuki, K., Olah, G., Modis, K., Coletta, C., Kulp, G., Gerö, D., Szoleczky, P., Chang, T., Zhou, Z., Wu, L., *et al.* (2011). Hydrogen sulfide replacement therapy protects the vascular endothelium in hyperglycemia by preserving mitochondrial function. *Proc Natl Acad Sci U S A* 108, 13829-13834.
- Szczesny, B., Módis, K., Yanagi, K., Coletta, C., Le Trionnaire, S., Perry, A., Wood, M.E., Whiteman, M., and Szabo, C. (2014). AP39, a novel mitochondria-targeted hydrogen sulfide donor, stimulates cellular bioenergetics, exerts cytoprotective effects and protects against the loss of mitochondrial DNA integrity in oxidatively stressed endothelial cells in vitro. *Nitric Oxide* 41, 120-130.
- Tak, P.P., and Firestein, G.S. (2001). NF- κ B: a key role in inflammatory diseases. *J Clin Invest* 107, 7-11.
- Takeuchi, O., and Akira, S. (2010). Pattern recognition receptors and inflammation. *Cell* 140, 805-820.
- Tang, G., Zhang, L., Yang, G., Wu, L., and Wang, R. (2013). Hydrogen sulfide-induced inhibition of L-type Ca²⁺ channels and insulin secretion in mouse pancreatic beta cells. *Diabetologia* 56, 533-541.
- Taoka, S., and Banerjee, R. (2001). Characterization of NO binding to human cystathionine beta-synthase: possible implications of the effects of CO and NO binding to the human enzyme. *J Inorg Biochem* 87, 245-251.
- Toldo, S., Das, A., Mezzaroma, E., Chau, V.Q., Marchetti, C., Durrant, D., Samidurai, A., Van Tassell, B.W., Yin, C., Ockaili, R.A., *et al.* (2014). Induction of microRNA-21 with exogenous hydrogen sulfide attenuates myocardial ischemic and inflammatory injury in mice. *Circ Cardiovasc Genet* 7, 311-320.
- Toohey, J.I. (2011). Sulfur signaling: is the agent sulfide or sulfane? *Anal Biochem* 413, 1-7.
- Toohey, J.I., and Cooper, A.J. (2014). Thiosulfoxide (sulfane) sulfur: new chemistry and new regulatory roles in biology. *Molecules* 19, 12789-12813.

- Truong, D.H., Mihajlovic, A., Gunness, P., Hindmarsh, W., and O'Brien, P.J. (2007). Prevention of hydrogen sulfide (H₂S)-induced mouse lethality and cytotoxicity by hydroxocobalamin (vitamin B_{12a}). *Toxicology* 242, 16-22.
- Vallabhapurapu, S., and Karin, M. (2009). Regulation and function of NF- κ B transcription factors in the immune system. *Annu Rev Immunol* 27, 693-733.
- Van de Louw, A., and Haouzi, P. (2013). Ferric Iron and Cobalt (III) compounds to safely decrease hydrogen sulfide in the body? *Antioxid Redox Signal* 19, 510-516.
- Vandiver, M.S., Paul, B.D., Xu, R., Karuppagounder, S., Rao, F., Snowman, A.M., Ko, H.S., Lee, Y.I., Dawson, V.L., Dawson, T.M., *et al.* (2013). Sulfhydration mediates neuroprotective actions of parkin. *Nat Commun* 4, 1626.
- Vladimer, G.I., Weng, D., Paquette, S.W., Vanaja, S.K., Rathinam, V.A., Aune, M.H., Conlon, J.E., Burbage, J.J., Proulx, M.K., Liu, Q., *et al.* (2012). The NLRP12 inflammasome recognizes *Yersinia pestis*. *Immunity* 37, 96-107.
- Wagner, A., and Vorauer-Uhl, K. (2011). Liposome technology for industrial purposes. *J Drug Deliv* 2011, 591325.
- Wallace, J.L., Blackler, R.W., Chan, M.V., Da Silva, G.J., Elsheikh, W., Flannigan, K.L., Gamaniek, I., Manko, A., Wang, L., Motta, J.P., *et al.* (2015). Anti-inflammatory and cytoprotective actions of hydrogen sulfide: translation to therapeutics. *Antioxid Redox Signal* 22, 398-410.
- Wallace, J.L., Caliendo, G., Santagada, V., and Cirino, G. (2010). Markedly reduced toxicity of a hydrogen sulphide-releasing derivative of naproxen (ATB-346). *Br J Pharmacol* 159, 1236-1246.
- Wallace, J.L., Caliendo, G., Santagada, V., Cirino, G., and Fiorucci, S. (2007). Gastrointestinal safety and anti-inflammatory effects of a hydrogen sulfide-releasing diclofenac derivative in the rat. *Gastroenterology* 132, 261-271.
- Wallace, J.L., and Wang, R. (2015). Hydrogen sulfide-based therapeutics: exploiting a unique but ubiquitous gasotransmitter. *Nat Rev Drug Discov* 14, 329-345.
- WALLACH, D.P. (1961). Studies on the GABA pathway. I. The inhibition of gamma-aminobutyric acid-alpha-ketoglutaric acid transaminase in vitro and in vivo by U-7524 (amino-oxyacetic acid). *Biochem Pharmacol* 5, 323-331.
- Wang, R. (2014). Gasotransmitters: growing pains and joys. *Trends Biochem Sci* 39, 227-232.
- Warenycia, M.W., Goodwin, L.R., Benishin, C.G., Reiffenstein, R.J., Francom, D.M., Taylor, J.D., and Dieken, F.P. (1989). Acute hydrogen sulfide poisoning. Demonstration of selective uptake of sulfide by the brainstem by measurement of brain sulfide levels. *Biochem Pharmacol* 38, 973-981.

Watanabe, M., Osada, J., Aratani, Y., Kluckman, K., Reddick, R., Malinow, M.R., and Maeda, N. (1995). Mice deficient in cystathionine beta-synthase: animal models for mild and severe homocyst (e) inemia. *Proceedings of the National Academy of Sciences* 92, 1585-1589.

Weischenfeldt, J., and Porse, B. (2008). Bone Marrow-Derived Macrophages (BMM): Isolation and Applications. *CSH Protoc* 2008, pdb.prot5080.

Weisser, S.B., McLarren, K.W., Kuroda, E., and Sly, L.M. (2013). Generation and characterization of murine alternatively activated macrophages. *Methods Mol Biol* 946, 225-239.

Wen, Y.D., Wang, H., Kho, S.H., Rinkiko, S., Sheng, X., Shen, H.M., and Zhu, Y.Z. (2013). Hydrogen sulfide protects HUVECs against hydrogen peroxide induced mitochondrial dysfunction and oxidative stress. *PLoS One* 8, e53147.

Whiteman, M., Li, L., Rose, P., Tan, C.H., Parkinson, D.B., and Moore, P.K. (2010). The effect of hydrogen sulfide donors on lipopolysaccharide-induced formation of inflammatory mediators in macrophages. *Antioxid Redox Signal* 12, 1147-1154.

Whiteman, M., and Winyard, P.G. (2011). Hydrogen sulfide and inflammation: the good, the bad, the ugly and the promising. *Expert Rev Clin Pharmacol* 4, 13-32.

Won, J.H., Park, S., Hong, S., Son, S., and Yu, J.W. (2015). Rotenone-induced Impairment of Mitochondrial Electron Transport Chain Confers a Selective Priming Signal for NLRP3 Inflammasome Activation. *J Biol Chem* 290, 27425-27437.

Wu, C.Y., Lin, C.T., Wu, M.Z., and Wu, K.J. (2011). Induction of HSPA4 and HSPA14 by NBS1 overexpression contributes to NBS1-induced in vitro metastatic and transformation activity. *J Biomed Sci* 18, 1.

Wu, H., Krishnakumar, S., Yu, J., Liang, D., Qi, H., Lee, Z.W., Deng, L.W., and Huang, D. (2014a). Highly selective and sensitive near-infrared-fluorescent probes for the detection of cellular hydrogen sulfide and the imaging of H₂S in mice. *Chem Asian J* 9, 3604-3611.

Wu, J., and Chen, Z.J. (2014). Innate immune sensing and signaling of cytosolic nucleic acids. *Annu Rev Immunol* 32, 461-488.

Wu, J., Li, Y., He, C., Kang, J., Ye, J., Xiao, Z., Zhu, J., Chen, A., Feng, S., Li, X., *et al.* (2016). Novel H₂S Releasing Nanofibrous Coating for In Vivo Dermal Wound Regeneration. *ACS Appl Mater Interfaces*.

Wu, Y.H., Kuo, W.C., Wu, Y.J., Yang, K.T., Chen, S.T., Jiang, S.T., Gordy, C., He, Y.W., and Lai, M.Z. (2014b). Participation of c-FLIP in NLRP3 and AIM2 inflammasome activation. *Cell Death Differ* 21, 451-461.

Wu, Z., Peng, H., Du, Q., Lin, W., and Liu, Y. (2015). GYY4137, a hydrogen sulfide-releasing molecule, inhibits the inflammatory response by suppressing

the activation of nuclear factor-kappa B and mitogen-activated protein kinases in Cocksackie virus B3-infected rat cardiomyocytes. *Mol Med Rep* 11, 1837-1844.

Xie, Z.Z., Liu, Y., and Bian, J.S. (2016). Hydrogen Sulfide and Cellular Redox Homeostasis. *Oxid Med Cell Longev* 2016, 6043038.

Xie, Z.Z., Shi, M.M., Xie, L., Wu, Z.Y., Li, G., Hua, F., and Bian, J.S. (2014). Sulfhydration of p66Shc at cysteine59 mediates the antioxidant effect of hydrogen sulfide. *Antioxid Redox Signal* 21, 2531-2542.

Yang, G., Wu, L., Jiang, B., Yang, W., Qi, J., Cao, K., Meng, Q., Mustafa, A.K., Mu, W., Zhang, S., *et al.* (2008). H₂S as a physiologic vasorelaxant: hypertension in mice with deletion of cystathionine gamma-lyase. *Science* 322, 587-590.

Yang, G., Zhao, K., Ju, Y., Mani, S., Cao, Q., Puukila, S., Khaper, N., Wu, L., and Wang, R. (2013). Hydrogen sulfide protects against cellular senescence via S-sulfhydration of Keap1 and activation of Nrf2. *Antioxid Redox Signal* 18, 1906-1919.

Yang, J., Gupta, V., Carroll, K.S., and Liebler, D.C. (2014). Site-specific mapping and quantification of protein S-sulphenylation in cells. *Nat Commun* 5, 4776.

Yang, Z., Zhuang, L., Szatmary, P., Wen, L., Sun, H., Lu, Y., Xu, Q., and Chen, X. (2015). Upregulation of heat shock proteins (HSPA12A, HSP90B1, HSPA4, HSPA5 and HSPA6) in tumour tissues is associated with poor outcomes from HBV-related early-stage hepatocellular carcinoma. *Int J Med Sci* 12, 256-263.

Yap, S., Naughten, E.R., Wilcken, B., Wilcken, D.E., and Boers, G.H. (2000). Vascular complications of severe hyperhomocysteinemia in patients with homocystinuria due to cystathionine beta-synthase deficiency: effects of homocysteine-lowering therapy. *Semin Thromb Hemost* 26, 335-340.

Yu, J., Nagasu, H., Murakami, T., Hoang, H., Broderick, L., Hoffman, H.M., and Horng, T. (2014). Inflammasome activation leads to Caspase-1-dependent mitochondrial damage and block of mitophagy. *Proc Natl Acad Sci U S A* 111, 15514-15519.

Yu, J.W., and Lee, M.S. (2016). Mitochondria and the NLRP3 inflammasome: physiological and pathological relevance. *Arch Pharm Res* 39, 1503-1518.

Zhang, D., Macinkovic, I., Devarie-Baez, N.O., Pan, J., Park, C.M., Carroll, K.S., Filipovic, M.R., and Xian, M. (2014a). Detection of protein S-sulfhydration by a tag-switch technique. *Angew Chem Int Ed Engl* 53, 575-581.

- Zhang, J., Sio, S.W., Moochhala, S., and Bhatia, M. (2010). Role of hydrogen sulfide in severe burn injury-induced inflammation in mice. *Mol Med* 16, 417-424.
- Zhang, J.M., and An, J. (2007). Cytokines, inflammation, and pain. *Int Anesthesiol Clin* 45, 27-37.
- Zhang, L., Li, S., Hong, M., Xu, Y., Wang, S., Liu, Y., Qian, Y., and Zhao, J. (2014b). A colorimetric and ratiometric fluorescent probe for the imaging of endogenous hydrogen sulphide in living cells and sulphide determination in mouse hippocampus. *Org Biomol Chem* 12, 5115-5125.
- Zhang, R., Sun, Y., Tsai, H., Tang, C., Jin, H., and Du, J. (2012). Hydrogen sulfide inhibits L-type calcium currents depending upon the protein sulfhydryl state in rat cardiomyocytes. *PLoS One* 7, e37073.
- Zhang, X., Edwards, J.P., and Mosser, D.M. (2009). The expression of exogenous genes in macrophages: obstacles and opportunities. *Methods Mol Biol* 531, 123-143.
- Zhao, F.L., Fang, F., Qiao, P.F., Yan, N., Gao, D., and Yan, Y. (2016). AP39, a Mitochondria-Targeted Hydrogen Sulfide Donor, Supports Cellular Bioenergetics and Protects against Alzheimer's Disease by Preserving Mitochondrial Function in APP/PS1 Mice and Neurons. *Oxid Med Cell Longev* 2016, 8360738.
- Zhao, K., Ju, Y., Li, S., Altaany, Z., Wang, R., and Yang, G. (2014). S-sulfhydration of MEK1 leads to PARP-1 activation and DNA damage repair. *EMBO Rep* 15, 792-800.
- Zhao, W., Zhang, J., Lu, Y., and Wang, R. (2001). The vasorelaxant effect of H₂S as a novel endogenous gaseous K(ATP) channel opener. *EMBO J* 20, 6008-6016.
- Zheng, Y., Luo, N., Mu, D., Jiang, P., Liu, R., Sun, H., Xiong, S., Liu, X., Wang, L., and Chu, Y. (2013). Lipopolysaccharide regulates biosynthesis of cystathionine gamma-lyase and hydrogen sulfide through Toll-like receptor-4/p38 and Toll-like receptor-4/NF-kappaB pathways in macrophages. *In Vitro Cell Dev Biol Anim* 49, 679-688.
- Zhong, Z., Umemura, A., Sanchez-Lopez, E., Liang, S., Shalapour, S., Wong, J., He, F., Boassa, D., Perkins, G., Ali, S.R., *et al.* (2016). NF- κ B Restricts Inflammasome Activation via Elimination of Damaged Mitochondria. *Cell* 164, 896-910.
- Zhong, Z., Zhai, Y., Liang, S., Mori, Y., Han, R., Sutterwala, F.S., and Qiao, L. (2013). TRPM2 links oxidative stress to NLRP3 inflammasome activation. *Nat Commun* 4, 1611.
- Zhou, R., Yazdi, A.S., Menu, P., and Tschopp, J. (2011). A role for mitochondria in NLRP3 inflammasome activation. *Nature* 469, 221-225.

Zhu, X.Y., Liu, S.J., Liu, Y.J., Wang, S., and Ni, X. (2010). Glucocorticoids suppress cystathionine gamma-lyase expression and H₂S production in lipopolysaccharide-treated macrophages. *Cell Mol Life Sci* 67, 1119-1132.

Łowicka, E., and Belkowski, J. (2007). Hydrogen sulfide (H₂S) - the third gas of interest for pharmacologists. *Pharmacol Rep* 59, 4-24.